

CHARACTERIZATION AND PREDICTION OF PROTEIN SOLUTION STABILITY BY RHEOLOGICAL METHODS

zur Erlangung des akademischen Grades eines
DOKTORS DER INGENIEURWISSENSCHAFTEN (Dr.-Ing.)

der Fakultät für Chemieingenieurwesen und Verfahrenstechnik des
Karlsruher Instituts für Technologie (KIT)

genehmigte
DISSERTATION

von
Dipl.-Ing. Marie-Therese Schermeyer
geboren in Merzig

Referent: Prof. Dr. Jürgen Hubbuch
Korreferent: Prof. Dr. med. Christian Pylatiuk
Tag der mündlichen Prüfung: 26. Juli 2017



This document is licensed under the Creative Commons Attribution – Share Alike 3.0 DE License (CC BY-SA 3.0 DE): <http://creativecommons.org/licenses/by-sa/3.0/de/>

Danksagung

Diese Arbeit entstand mit Hilfe der fachlichen und seelischen Unterstützung zahlreicher Menschen. Einen besonderen Dank gilt hierbei folgenden Personen:

Prof. Jürgen Hubbuch danke ich für die Möglichkeit diese Dissertation in seiner Arbeitsgruppe anzufertigen. Vor allem danke ich ihm für das mir entgegengebrachte Vertrauen, seine fachliche und persönliche Förderung und die uneingeschränkte Unterstützung meiner Ideen.

Prof. Christian Pylatiuk danke ich für die Übernahme des Korreferats. Außerdem danke ich ihm für die tolle Zusammenarbeit und fachliche Unterstützung.

Dank gilt auch Bas Kokke und Michel Eppink. Projektpartner wie man sie sich wünscht - kooperativ, unterstützend und immer für eine Diskussion zu haben.

Dem BMBF danke ich für die finanzielle Unterstützung meines Projekts im Rahmen von "EuroTransBio".

Bedanken möchte ich mich ganz herzlich bei Prof. Norbert Willenbacher für die Zurverfügungstellung des Rheometers. Außerdem danke ich Claude Oelschlaeger für die Beantwortung meiner zahlreichen Fragen als Rheologie-Greenhorn.

Vielen Dank an die gesamte Arbeitsgruppe des MAB. Ihr alle tragt zu einer kameradschaftlichen und offenen Atmosphäre bei. Besonders danken möchte ich den Studenten, die ich während meiner Promotion betreuen durfte: Hannah, Philipp, Jonas, Anna, Patrizia, Jonathan und Sandra. Ihr alle habt meine Arbeit wesentlich vorangetrieben.

Für die Unterstützung im Labor und den unermüdlichen Einsatz, bedanke ich mich bei unseren Ingenieuren. Besonderer Dank gilt Kristina für die Durchführung unzähliger Experimente.

Dank geht an Marion Krenz, Iris Perner-Nochta, Michael Wörner und Margret Meixner, die es schaffen uns Doktoranden bestmöglich von Papierarbeit und administrativen Aufgaben fern zu halten. Auch den IT Jungs, vor allem Simon Woll und Jan Müller, möchte ich für den tollen und professionellen IT Service danken.

Besonders bedanken möchte ich mich bei meinen Kollegen Pascal Baumann, Sven Amrhein, Katharina Bauer und Carsten Radtke.

Pascal danke ich für die fruchtbare Zusammenarbeit, die vielen konstruktiven Diskussionen und Ideen-Findungs-Gespräche.

Sven, deine uneingeschränkte Hilfsbereitschaft und Geduld haben mich aus so mancher Programmier-Sackgasse geführt. Du hast, und das im wörtlichen Sinne, wesentlich dazu beigetragen, dass meine Arbeit so aussieht wie sie aussieht. Danke auch für die vielen amüsanten und zerstreuenden Kaffee- und Bierrunden.

Katha, du bist und bleibst meine Lieblingsbürokollegin. Vielen Dank für deine direkte Art, die vielen ernsten und lustigen Bürogespräche und natürlich die tolle fachliche Zusammenarbeit.

Besonderer Dank geht an Carsten. Ich bin froh, dass ich mit dir solch einen aufrichtigen, ehrlichen und vor Kreativität sprühenden Menschen kennen lernen durfte. Du bist einfach ein toller Freund.

Unglaublichen Rückhalt gaben mir meine Freunde und Familie. Ich bedanke mich ganz herzlich für eure uneingeschränkte, wertvolle Unterstützung. Ohne euch wäre diese Arbeit nicht entstanden, so mancher Stein auf dem Weg zu schwer gewesen und vor allem wäre ich nicht der Mensch der ich jetzt bin.

Von ganzem Herzen danke ich meinem Mann Hans. Du bist mein ehrlichster Kritiker, mein bester Motivator und mein größter Halt - Vielen Dank!

Es ist nicht das Wissen, sondern das Lernen,
nicht das Besitzen, sondern das Erwerben,
nicht das Dasein, sondern das Hinkommen,
was den größten Genuß gewährt.

Carl Friedrich Gauss

Contents

1	Abstract	1
2	German Abstract: Zusammenfassung	7
3	Introduction	13
3.1	Molecular Characteristics of Proteins	14
3.2	Conformational and Colloidal Stability of Proteins in Solution	16
3.3	Analytical Methods to Characterize and Predict Protein Solution Stability	24
3.4	Rheology of Viscoelastic Fluids	28
4	Research Proposal	35
5	Comprehensive Overview of Publications & Manuscripts	39
6	Implementation of a Microfluidic Device	45
6.1	Introduction	47
6.2	Materials and Methods	49
6.3	Results	54
6.4	Discussion	60
6.5	Concluding Remarks	63
6.6	Acknowledgments	64
6.7	References	64
7	Squeeze Flow Rheometry as a Novel Tool	67
7.1	Introduction	69
7.2	Materials and Methods	72
7.3	Results	76
7.4	Discussion	84
7.5	Conclusions	89
7.6	Acknowledgments	90
7.7	References	90

8	Studies on the Stability Enhancing Effect of the Cherry-Tag™	95
8.1	Introduction	97
8.2	Materials and Methods	99
8.3	Results and Discussion	103
8.4	Conclusions	118
8.5	Acknowledgments	119
8.6	References	122
9	Analytical Toolbox for the Description of mAb Solution Stability	127
9.1	Introduction	129
9.2	Materials and Methods	132
9.3	Results and Discussion	136
9.4	Conclusions	163
9.5	Acknowledgments	164
9.6	References	169
10	Tracer Particle Screening for Microrheological Measurements	177
10.1	Introduction	179
10.2	Materials and Methods	181
10.3	Results	185
10.4	Discussion	192
10.5	Conclusions	197
10.6	Acknowledgments	198
10.7	References	198
11	Conclusion and Outlook	205
12	Comprehensive Reference List	209
13	Abbreviations	235
A	Curriculum Vitae	

Abstract

New insights in the field of biotechnology allow the understanding of processes in the body down to the smallest detail and to intervene in the event of deviation. One type of intervention is the treatment of diseases with recombinant proteins, such as antibodies or enzymes. The efficacy of these biopharmaceutical active substances makes it possible to treat diseases which have hitherto been difficult to deal with, such as malign neoplasm or multiple sclerosis. The more complex the mode of action of the drug applied, the more complex is the biomolecule of choice. This complexity has an impact on the processability, formulation and application of biopharmaceuticals. In particular, the colloidal and conformational solution stability is a challenge during their shelf life. Protein solution instabilities can cause process delays or in a worst case scenario life-threatening immune reactions in the patient's body and are thus important to control.

The solution stability is dependent on the molecular properties and the environmental conditions. A high-impact parameter is the protein concentration. To save process costs and to simplify drug administration, the concentration of the target molecule is maximally increased during processing and formulation. The increase in protein concentration to highly concentrated conditions does not only affect protein stability itself but also increases the possible number of stability-influencing parameters. Due to the reduced distance between the molecules at high concentrations long- as well as short-range forces do have an impact on the protein solution behavior. The complex interplay of the resulting interactions are difficult to depict. Additionally, as a result of the increased number of molecules in solution, the two-dimensional protein interactions occurring in an ideal dilute solution become multidimensional, so that a characterization by conventional predicting methods reaches its limits. Due to the lack of an established predicting analytical tool it is therefore common practice to store the molecules of interest under varying solution conditions over a period of 12-24 months and analyze the samples for protein unfolding or aggregation, afterwards. This method is precise and ensures the safety of

the patient but is time and cost intensive. Furthermore, with the help of this method, only knowledge about the stability range is gained, but no information is available on the mechanisms of protein-protein or protein-solvent interactions. Thus the transfer of the results to other molecules or solution conditions is limited. Novel analytical methods are demanded, which enable a better characterization of protein solution behavior and parameters which allow a direct prediction of protein solution stability even in the highly concentrated regime. A promising method for analyzing complex fluids such as highly concentrated protein solutions is rheology.

Rheology is the science of fluent materials and describes the flow behavior and the deformation of matter. According to rheology, experimental objects can be divided according to their elasticity and their viscosity. In the case of an ideally elastic body, the extent of the deformation is directly proportional to the applied stress, and the body moves back into its initial position after applied force. An ideally viscous body reacts to an effective force with a time-delayed deformation and the deformation is irreversible. Protein solutions behave viscoelastic. This means that after application of a force, they only partially relax and accordingly demonstrate partially elastic, partially viscous behavior. The viscoelastic properties of protein solutions depend on the size and number of molecules in solution, their flexibility, the degree of cross-linking, and the degree of molecule-molecule and molecule-solvent interactions. The changes in the viscoelastic behavior of fluids can be described very precisely by the measurable storage and loss moduli (G' and G''). In contrast to industrial branches such as the food or cosmetics industry, the characterization of the viscoelastic behavior of protein solutions has not yet been established in the biopharmaceutical industry.

The aim of this thesis is therefore to investigate the potential of rheology for the biopharmaceutical process and formulation development. Focusing on the characterization of the viscoelastic behavior of highly concentrated protein solutions. In addition, the determined rheological parameters were evaluated for their suitability to predict the long-term stability of these complex fluids. To refine the predictive approach, in a next step, the rheological measurements were combined with results of orthogonal analyzing tools. Furthermore, the microrheological technique was optimized by a tracer particle screening. Prior to the rheological characterization, handling and standard analytics for studying highly concentrated protein solutions were optimized. In the first part of the thesis an analytical microfluidic device is presented, which enables the automated determination of protein concentration by means of UV absorption. Commercially available devices for the determination of protein concentration are limited either by high-throughput compatibility or the measuring range. For the exact determination of the protein concentration,

highly concentrated protein solutions must therefore be diluted several times. The time consuming dilution procedure can lead to unacceptable standard deviations especially when handling small sample volumes. It is for this reason that a disposable silicone chip was developed for automated high-throughput measurements at microliter scale. The device allows the direct measurement of UV absorption in a wide protein concentration range by the use of microfluidic channels, which enable a layer thickness of less than 1 mm. The device was validated according to ICH guidelines and the application was demonstrated by a case study on an automated liquid handling station. The use of the device allows high-throughput absorption measurements in a protein concentration range of around 0.1-100 mg/ml with an accuracy of 99.2 %.

As a second preparatory step a robot-based method for generating protein phase diagrams was adapted to the handling of highly concentrated protein solutions. The protein phase diagrams generated in this way were used to compare the long-term stability behavior of studied proteins with the rheological measurements. With this automated platform more than 20 phase diagrams with different protein types, protein concentrations, additives types and concentrations, and changing pH values could be screened.

The main focus of this work was the rheological characterization and the interpretation of obtained viscoelastic properties of protein solutions under varying process and formulation conditions. For the comparatively weak viscoelastic protein solutions, oscillating experiments were performed in the high-frequency range for the determination of the rheological parameters. In this respect, G' and G'' were determined over a frequency ramp with oscillatory squeeze flow.

Within the framework of this work, a rheological screening of the model protein lysozyme from chicken egg white in a concentration range of 100-225 mg/ml and varying solution conditions was carried out. This screening initially served to evaluate suitable viscoelastic key parameters. The viscoelastic moduli G' and G'' were determined over a frequency range of 100-40000 rad/sec and the crossover point of the two resulting curves calculated. The frequency value of the detected crossover point, ω_{CO} , was selected to be correlated with the protein phase behavior. It was shown that highly concentrated protein solutions show a characteristic viscoelastic behavior which is sensitive towards changing solution conditions. Furthermore, the ω_{CO} values of all samples, determined directly after sample preparation (t_0), could successfully be correlated with the phase behavior of lysozyme after 40 days of incubation (t_{40}). The large-scale screening allowed to draw a solubility limit for lysozyme based on ω_{CO} values at 20000 rad/sec. The calculated ω_{CO} limit provides the prerequisite for the prediction of the long-term solution stability of lysozyme, with only one rheological measurement, conducted directly after sample preparation.

In a next step, the predictive rheological approach was combined with molecular dynamics (MD) simulations. The MD simulations used in this work provide information on the surface characteristics of the proteins being studied and can therefore explain the long-term behavior of protein samples predicted by the rheological approach. For this purpose, a case study with Glutathione-S-Transferase was performed in its pure form and fused with a potentially stabilizing tag (Cherry-TagTM) under varying solution conditions. The rheological characterization allowed a precise prediction of the colloidal and conformational solution stability of both studied proteins. The rheological screening revealed the strong solubility-enhancing nature of the Cherry-TagTM. In combination with the results of the MD simulations, the solubility increase could be attributed to a pronounced change in the protein surface charge and protein surface hydrophobicity caused by the Cherry-TagTM.

Monoclonal antibodies and antibody related species belong to a quickly expanding field of application in the pharmaceutical industry. Due to the complexity and size, the long-term stability of this molecule class is classified as particularly critical. This challenging situation is aggravated by the fact that new application forms require antibody titers of more than 100 mg/ml. In order to confront these challenges, the study of viscoelasticity was transferred to antibodies under process-relevant conditions. It was shown that viscoelastic measurements are very sensitive to changes in the solution conditions of antibody formulations and that the parameter ω_{CO} enables the prediction of the colloidal stability of the antibody under investigation. The rheological analysis was also linked with established, orthogonal methods for the characterization of the protein surface, the protein mobility and thermal stability studies. The application of the resulting analytical toolbox ensures a precise prediction of the protein solution stability and is therefore an important contribution to the rapid development of stable and safe antibody formulations.

The mechanical high-frequency rheology used for the above listed screenings is not common in the pharmaceutical industry and a corresponding device is currently not commercially available. Therefore, parallel to the mechanical measurements the optimization of the microrheological technique was expedited. In the case of microrheological measurements, the parameters G' and G'' are determined by means of dynamic light scattering. To gain reproducible, correct results it is required that the tracer particles do not interact with the proteins in solution. Therefore, the surface characteristic and the interaction tendency of four different potential tracer particles were investigated under changing buffer conditions. It was found that the choice of the tracer particle has a significant influence on the rheological results. An internally developed polystyrene particle with a modified

surface turned out to be the only suitable tracer particle for the microrheological measurements of protein solutions tested. With this particle type, a high measurement accuracy and a good correlation with the results of mechanical rheometers could be achieved.

In summary, the emphases of this work have been extensively studied to obtain a comprehensive picture of the viscoelastic properties of highly concentrated protein solutions. In particular, the sensitivity of viscoelastic parameters against changing protein solution conditions has been demonstrated and a rheological parameter, ω_{CO} , has been introduced that allows predictive statements about the solubility of proteins in highly complex solutions. The introduced and validated parameter, particularly in combination with further analytical methods used here, enables a fast and reliable characterization of viscoelastic fluids and can thus also be applied in other research disciplines.

German Abstract: Zusammenfassung

Neue Erkenntnisse im Bereich der Biotechnologie ermöglichen es Vorgänge im Körper bis ins kleinste Detail zu verstehen und bei Abweichungen regulierend einzugreifen. Eine Art des Eingreifens ist die Behandlung von Krankheiten mit rekombinanten Proteinen, wie Antikörpern oder Enzymen. Die Wirksamkeit dieser biopharmazeutischen Wirkstoffe ermöglicht die Behandlung von bisher schwer zu therapierenden Erkrankungen wie maligne Neoplasie oder multiple Sklerose. Je komplexer der Wirkmechanismus des eingesetzten Medikaments ist, desto komplexer ist das Biomolekül welches zum Einsatz kommt. Diese Komplexität hat Auswirkungen auf die Prozessierbarkeit des Biopharmazeutikums. Insbesondere die kolloidale und konformelle Stabilität des Zielmoleküls ist eine Herausforderung während des Herstellungsprozesses, des Aufreinigungsprozesses und der Formulierung. Proteinlösungsinstabilitäten können Prozessverzögerungen oder im schlimmsten Fall lebensbedrohliche Immunreaktionen im Körper des Patienten verursachen und sind daher wichtig zu kontrollieren.

Die Stabilität des Biomoleküls ist abhängig von der Beschaffenheit des Moleküls an sich sowie den Umgebungsbedingungen. Ein Lösungsparameter mit hohem Einfluss ist die Proteinkonzentration. Um die Prozesskosten zu senken und die Verabreichung des Medikaments zu erleichtern, wird die Konzentration des Zielmoleküls während der Verarbeitung und der Formulierung maximal erhöht. Die Erhöhung der Proteinkonzentration hin zu hochkonzentrierten Bedingungen hat nicht nur Auswirkungen auf die Protein-stabilität sondern erhöht auch die mögliche Anzahl von Mechanismen, die diese beeinflussen. Der Parameterraum vergrößert sich mit dem zunehmenden Einfluss von hauptsächlich attraktiven kurzreichweitigen Wechselwirkungen. Zusätzlich werden, durch die Erhöhung der Molekülzahl, die in idealer Lösung vorliegenden zweidimensionalen Protein-Wechselwirkungen mehrdimensional, sodass eine Charakterisierung mittels herkömmlicher prädiktiver Analysemethoden an ihre Grenzen stößt. Um die Lösungsstabilität von hochkonzentrierten Proteinlösungen und Formulierungen sicherzustellen ist es wegen

fehlender prädiktiver Methoden gängige Praxis, das Molekül von Interesse unter variierenden Lösungsbedingungen über eine Zeit von 12-24 Monaten zu lagern und daraufhin auf Entfaltung oder Aggregation zu analysieren. Diese Methode ist zeit- und kostenintensiv. Mit Hilfe dieser Methode wird außerdem ausschließlich Wissen über den Stabilitätsbereich gewonnen, allerdings keine Informationen über den Mechanismus dahinter, welcher für die Übertragbarkeit der Ergebnisse auf andere Moleküle oder Lösungsbedingungen von Bedeutung wäre. Es werden innovative, neuartige Methoden gefordert, welche das Verhalten von Proteinen in hochkonzentrierten Bereich besser charakterisieren können. Außerdem gilt es Parameter zu evaluieren, die eine Vorhersage der Lösungsstabilität auch im hochkonzentrierten Bereich ermöglichen. Eine vielversprechende Methode zur Analyse komplexer Flüssigkeiten, wie hochkonzentrierte Proteinlösungen, ist die Rheologie.

Rheologie ist die Lehre der fließenden Stoffe und beschreibt damit das Fließverhalten und die Verformung von Materie. Nach der Lehre der Rheologie werden Versuchsobjekte nach ihrer Elastizität beziehungsweise ihrer Viskosität unterteilt. Bei einem ideal elastischen Körper ist das Ausmaß der Deformation direkt proportional zur eingesetzten Spannung und der Körper bewegt sich nach der Krafteinwirkung in seine Ausgangslage zurück. Ein ideal viskoser Körper reagiert auf eine Krafteinwirkung mit einer zeitlich verzögerten Deformation und die Verformung ist irreversibel. Proteinlösungen verhalten sich viskoelastisch. Das bedeutet, dass sie nach Aufbringung einer Kraft nur unvollständig relaxieren, also teilweise elastisches, teilweise viskoses Verhalten aufweisen. Die viskoelastischen Eigenschaften von Fluiden sind von der Größe und Anzahl der Moleküle in Lösung, deren Flexibilität, Vernetzungs- und Interaktionsgrad abhängig. Die Änderungen des viskoelastischen Verhaltens von Fluiden können sehr genau durch das Speicher- und das Verlustmodul (G' und G'') beschrieben werden. Im Gegensatz zu Industriezweigen wie der Lebensmittel- oder Kosmetikindustrie ist die Charakterisierung des viskoelastischen Verhaltens von Proteinlösungen in der biopharmazeutischen Industrie noch nicht etabliert.

Ziel dieser Arbeit war es deshalb, das Potenzial der Rheologie für die biopharmazeutische Prozess- und Formulierungsentwicklung zu untersuchen. Hierbei lag der Fokus auf der Charakterisierung des viskoelastischen Verhaltens hochkonzentrierter Proteinlösungen. Darüber hinaus wurden die ermittelten rheologischen Parameter auf ihre Eignung zur Vorhersage der Langzeitstabilität von Proteinlösungen geprüft. Um den prädiktiven Ansatz zu verfeinern, wurden in einem nächsten Schritt die rheologischen Messungen mit Ergebnissen orthogonaler Analytikmethoden kombiniert. Darüber hinaus wurde die Mikrorheologische Technik durch ein Tracer-Partikel-Screening optimiert.

Vorbereitend zur rheologischen Charakterisierung, wurde die Handhabung und Standar-

danalytik von hochkonzentrierte Proteinlösungen optimiert. Der erste Teil dieser Arbeit beschreibt die Entwicklung eines analytischen Mikrofluidik-Chips der die automatisierte Messung der Proteinkonzentration mittels UV Absorption ermöglicht. Bei kommerziell erhältlichen Geräten, für die Bestimmung der Proteinkonzentration, ist entweder die Hochdurchsatzkompatibilität oder der Messbereich limitierender Faktor. Für die exakte Bestimmung der Proteinkonzentration, müssen daher hochkonzentrierte Proteinlösungen um ein vielfaches verdünnt werden, was bei geringem Probenvolumen zu hohen Abweichungen und Zeitverlust führen kann. Daher wurde in der vorliegenden Arbeit für die automatisierte Hochdurchsatzmessung im Mikrolitermaßstab ein Silikon-Chip entwickelt, der die direkte Bestimmung der Absorption von hochkonzentrierten Proteinlösungen zulässt. Der Chip wurde nach ICH Guidelines validiert und die Anwendung mit Hilfe einer Fallstudie demonstriert. Die Verwendung des Chips ermöglicht Absorptionsmessungen im 96-well kompatiblen Maßstab in einem Protein-Konzentrationsbereich von 0.1-100 mg/ml mit einer Genauigkeit von 99.2 %.

Als zweiter vorbereitender Schritt wurde ein Roboter-basiertes Verfahren zur Generierung von Proteinphasendiagrammen auf hochkonzentrierte Proteinlösungen angepasst. Die so erzeugten Proteinphasendiagramme wurden verwendet, um das Langzeitstabilitätsverhalten der Proteine mit den rheologischen Messungen zu vergleichen. Diese Methodik wurde zur Herstellung von mehr als 20 Phasendiagrammen mit variierender Proteinart, Proteinkonzentration, Additivart und Konzentration sowie variierendem pH-Wert verwendet.

Der Schwerpunkt dieser Dissertation liegt in der rheologischen Charakterisierung und der Interpretation der erhaltenen viskoelastischen Eigenschaften von Proteinlösungen unter wechselnden Prozess- und Formulierungsbedingungen. Für die schwach viskoelastischen Proteinlösungen wurden für die Ermittlung der rheologischen Parameter Oszillationsversuche im Hochfrequenzbereich durchgeführt. Hierbei wurden G' und G'' über einen Frequenzrampe bei oszillierender Quetschströmung ermittelt.

Im Rahmen dieser Arbeit wurde für die Definition geeigneter viskoelastischer Parameter zunächst ein rheologisches Screening mit dem Modellprotein Lysozym aus Hühnerei in einem Konzentrationsbereich von 100-225 mg/ml unter variierenden Lösungsbedingungen durchgeführt. Mit Hilfe dieses Screenings konnte gezeigt werden, dass hochkonzentrierte Proteinlösungen ein für Polymere charakteristisches viskoelastisches Verhalten aufweisen. Des Weiteren wurde der ω_{CO} Wert aller vermessenen Proben zum Zeitpunkt t_0 berechnet und erfolgreich mit dem Phasenverhalten von Lysozym nach 40 Tagen Inkubationszeit (t_{40}) korreliert. Das groß angelegte Screening ermöglichte es eine Löslichkeitsgrenze für Lysozym basierend auf den ω_{CO} Werten zu ziehen. Der ermittelte ω_{CO} Grenzwert schafft

die Voraussetzung die Langzeit-Lösungsstabilität von Lysozym, mit nur einer rheologischen Messung, direkt nach Probenpräparation bestimmen zu können.

In einem nächsten Schritt wurde der prädiktive rheologische Ansatz mit Molekuldynamik (MD)-Simulationen kombiniert. Die in dieser Arbeit eingesetzten MD-Simulationen geben Aufschluss über die Oberflächencharakteristik der untersuchten Proteine und können somit die Langzeit-Lösungsstabilität, welche durch den rheologischen Ansatz vorhergesagt wurde, begründen. Hierzu wurde eine Fallstudie mit Glutathione-S-Transferase in ihrer Reinform und fusioniert mit einem potentiell löslichkeitserhöhenden Tag (Cherry-TagTM) unter variierenden Lösungsbedingungen durchgeführt. Die rheologische Charakterisierung der beiden Proteine ermöglichte eine präzise Vorhersage der kolloidalen und konformellen Lösungsstabilität. Das rheologische Screening gab Aufschluss über den stark löslichkeitserhöhenden Charakter des verwendeten Cherry-TagsTM. In Kombination mit den Ergebnissen der MD-Simulation, konnte die Löslichkeitserhöhung auf eine starke Änderung der Oberflächenladung und der Oberflächenhydrophobizität, hervorgerufen durch den Cherry-Tag, zurückgeführt werden.

Monoklonale Antikörper und ihre Untergruppen besitzen das am schnellsten wachsende Anwendungsfeld in der pharmazeutischen Industrie. Durch die Komplexität und die Größe dieser Moleküle wird deren Langzeitstabilität als besonders kritisch eingestuft. Erschwerend kommt hinzu, dass neue Applikationsformen Antikörpertiter von mehr als 100 mg/ml in der Endformulierung voraussetzen. Um diesen Herausforderungen entgegenzutreten, wurde die Untersuchung der Viskoelastizität auf Antikörper unter prozessrelevanten Bedingungen übertragen. Es konnte gezeigt werden, dass viskoelastische Messungen sehr sensitiv gegenüber Änderungen der Lösungsbedingungen von Antikörperformulierungen sind, und dass der vorgestellte Parameter ω_{CO} die kolloidale Stabilität des untersuchten Antikörpers exakt vorhersagen kann. Die rheologische Analytik wurde zudem mit etablierten, orthogonalen Methoden zur Charakterisierung der Proteinoberfläche, der Proteinmobilität und thermischen Stabilitätsuntersuchungen verknüpft. Die Anwendung der so entstandene analytische Toolbox gewährleistet eine präzise Vorhersage der Proteinlösungsstabilität und ist somit ein wichtiger Beitrag für die schnelle Entwicklung stabiler und sicherer Formulierungen von Biopharmazeutika.

Die Anwendung mechanische Hochfrequenz-Rheologie, die für die oben aufgeführten Screenings verwendet wurde, ist in der pharmazeutischen Industrie nicht etabliert, und eine entsprechendes Gerät ist derzeit nicht im Handel erhältlich. Daher wurde parallel zur Verwendung der mechanischen Rheologie die Optimierung der mikrorheologischen Technik vorangetrieben. Bei mikrorheologischen Messungen werden die Parameter G' und G'' mittels dynamischer Lichtstreuung bestimmt. Um reproduzierbare, korrekte Ergebnisse

zu erzielen, ist es erforderlich, dass die Tracerpartikel nicht mit den Proteinen in Lösung wechselwirken. In einer Studie wurden daher die Oberflächencharakteristik und die Interaktionsneigung vier unterschiedlicher Tracerpartikel untersucht. Festgestellt wurde, dass die Wahl des Tracerpartikels einen großen Einfluss auf die rheologischen Ergebnisse hat. Ein intern hergestelltes Polystyrolpartikel mit modifizierter Oberfläche stellte sich als einzig geeigneter Tracerpartikel für die rheologische Untersuchung von in dieser Studie untersuchten Proteinlösungen heraus. Mit diesem konnte eine hohe Messgenauigkeit und eine gute Korrelation mit den Ergebnissen mechanischer Rheometer erreicht werden. Zusammenfassend wurde in der vorliegenden Arbeit ein umfassendes Bild der viskoelastischen Eigenschaften von hochkonzentrierten Proteinlösungen gewonnen. Im Speziellen konnte eine ausführliche Charakterisierung hochkonzentrierter Proteinlösungen erreicht und ein rheologischer Parameter, ω_{CO} eingeführt werden, der prädiktive Aussagen über die Lösungsstabilität der hochkomplexen Lösungen zulässt. Der eingeführte und validierte Parameter ermöglicht, gerade in Kombination mit weiteren hier verwendeten analytischen Verfahren, eine schnelle und sichere Charakterisierung von viskoelastischen Fluiden und kann so auch in anderen Forschungsdisziplinen Anwendung finden.

Introduction

Biotechnology as a name was first used by Károly Ereky, an Hungarian Engineer from 1919. He used the term to describe the process by which raw materials could be biologically upgraded into socially useful products [1, 2]. Ereky did research in the field of agricultural biotechnology. However, its definition has been valid for an ever-growing field of application [3, 4]. The revolution of the medical use of biotechnology started when Watson and Crick deciphered the DNA in 1953 [5]. Only 20 years later the research group around Paul Berg from Stanford University succeeded to produce the first recombinant DNA [6]. New techniques for manipulating the expression gene and manufacturing gene products paved the way for the commercial production of recombinant biopharmaceutical products [7, 8]. In 1978 Genentech, the first biotech company, succeeded in isolating a gene which decodes human insulin [9]. They managed to insert the gene in a cloning vector which can be placed and transcribed by the easy to handle bacterium *Escherichia coli*. This technical achievement and the pioneering role of this company led to an incredible increase in the share price from \$35 to \$89 within 20 minutes during Genentech's stock market entry two years later [10]. Tax relief as well as the support of stock market speculators and private investors allowed the creation of about 700 biotechnology companies in the following years [11]. The economical success and the better understanding of molecular biology laid the foundation for a still increasing biopharmaceutical market. Nowadays, the biopharmaceutical products range from small, fairly simple proteins, such as insulin or growth hormones, antibodies and their subclasses, to complex structured viruses or virus like particles[12, 13].

Essentially, four steps are required for the manufacture of these drug products. First, the feedstock must be prepared so that it can serve as a source of food for the target microorganisms (upstream processing). Then the host cell is multiplied and the desired compound, i.e. the target molecule is expressed during the fermentation (biotransformation). As a third step, the drug substance must be purified over a large number of

orthogonal process steps so that it can be administered as drug product to humans after the final formulation (fourth step) [14]. In order to reduce process costs and to enable new forms of application, ever higher protein titers are processed and formulated [15, 16]. In order to ensure the quality of the product, the manufacture and purification are subject to strict rules [13]. Special attention is given here to the stability and the associated activity of the molecule [17, 18]. The stability of a molecule in highly concentrated solutions is considered to be a critical factor as the influencing parameters change constantly during the course of the biopharmaceutical process [19, 20] and poses new challenges for process engineers [21, 22]. Not only the mechanical stress, triggered by pumping or shearing, but also the environmental conditions that change over the different process steps can lead to a decreased solution stability in form of protein aggregation or unfolding [23, 24]. Furthermore, the increase in protein concentration also increases the number of possible interaction mechanisms, which further increases the complexity of the protein behavior. The impact of molecular characteristics and the forces and interaction mechanisms involved are discussed in more detail in section 3.1 and 3.2, respectively. In the last decades analytical strategies were developed to identify, control and manipulate the protein solution behavior. An overview of established analytical techniques for the characterization and identification of protein solution behavior is given in section 3.3. Unfortunately, there is so far no methodology that can describe and predict the stability of the protein solution in the highly concentrated regime. To counter this problem, novel analytical methods have to be found and evaluated. This work focuses on the evaluation of rheological methods and their potential for describing the solution behavior of highly concentrated protein formulations. Section 3.4 discusses the science of soft matter, focusing on rheological methods that can be applied to biopharmaceutical substances.

3.1 Molecular Characteristics of Proteins

Proteins are macromolecules, which can be assigned to a variety of tasks in the human body. The processes range from signal processing over immunological responses to catalytic reactions [25]. The specificity of each molecule is enabled by a unique sequence of 21 proteinogenic amino acids adapted to the particular function [26]. The sequence of the amino acids as a polypeptide is encoded in the DNA or RNA. This allows the production of proteins by recombinant genetic engineering. The amino acids differ in their side chains. These have basic, acidic, nonpolar hydrophobic or polar hydrophobic properties [27, 28]. These properties allow the assembly of the amino acids into ordered structures

3.1 Molecular Characteristics of Proteins

(2D structure) and their further structural formation towards the 3D structure specific for each protein [29]. Electrostatic interactions, hydrophobic forces, van der Waals forces and hydrogen bonds between the side chains of the polypeptide are responsible for the correct folding of the protein [30]. In order to avoid contact with water, amino acids with hydrophobic side chains are mostly found in the center of the protein [31]. The resulting hydrophobic interactions in the protein core stabilize its 3D structure. Amino acids with hydrophilic side chains interact positive with the surrounding aqueous solution and thus stabilize the molecule with respect to intermolecular interactions [32]. The hydrophilic character of side chains is an intrinsic property of pH dependent charge. The charge of the amino acids is determined by the terminal carboxyl (COOH) and amine (NH_2) groups as well as by titratable amino acid residues [33]. The number of these amino acids as well as their distribution on the protein surface are crucial for the protein polarity and thus for their solution colloidal stability. In Figure 3.1 the charge distribution of three proteins, namely IgG1, Glutathion-S-Transferase and lysozyme from chicken egg-white at pH 7 are illustrated. Positive charges are colored in blue, whereas negative charges are colored in red. The figure also shows geometric differences of the proteins. Lysozyme and Glutathion-S-Transferase, composed of two identical subunits, are globular proteins with a molecular mass of 14 kDa and 52 kDa, respectively [34]. Whereas the monoclonal antibody with a molecular mass of 145 kDa exhibits the characteristic y-shape. The geometry of the protein has an impact on the charge distribution and hydrophobicity of the proteins. It is also decisive for the accessibility of certain surface patches.

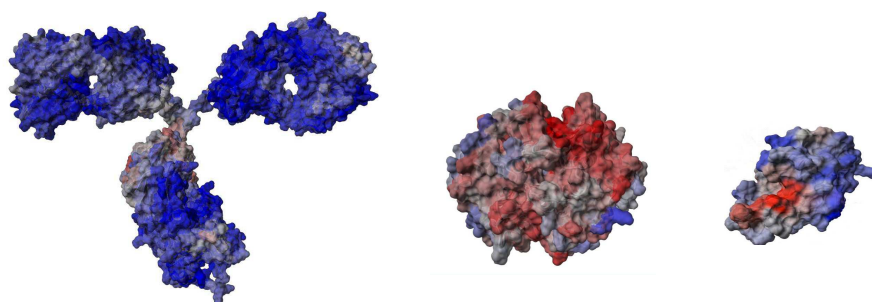


Figure 3.1: Illustration of the 3D structure of IgG1, Glutathion-S-Transferase and lysozyme from chicken egg white at pH 7. The protein surface is colored according to its surface charge distribution. Positive charges are colored in blue, negative charges are colored in red. Molecular graphics were created with YAZARA and POVRay.

The native state of the protein is energetically the most stable conformation. But is only exiguously more stable as the undesired unfolded or partly unfolded conformational state [35]. Because of this narrow range of stability, small changes in the chemical surrounding can lead to structural changes. The sensitivity of the proteins towards their colloidal and conformational stability poses a major challenge for the biopharmaceutical process and formulation development.

3.2 Conformational and Colloidal Stability of Proteins in Solution

The conservation of the native structure as well as the solubility of proteins are dictated by basic chemical and physical principles. After the differentiation between protein unfolding and protein aggregation this section will address these principles and describe the forces of impact (section 3.2.1 and 3.2.2). How these forces are triggered and which solution parameters influence them will be explained afterwards (section 3.2.3).

3.2.1 Definition of Protein Unfolding

Protein unfolding describes the elongation of the superordinate 3D structure of a protein into a structural disordered polypeptide chain [36, 37]. As a result of the unfolding, the protein loses its activity and thus also its pharmacological effect [37]. Depending on the protein, the unfolding process can proceed via one or more intermediate stages. In recent years kinetic and equilibrium data have provided extensive information on protein unfolding pathways [38, 39]. In addition, the molten globule state was investigated more closely [40]. The molten globule state is a non-native compact stage with a formed 2D but a non-developed 3D structure. Lysozyme from chicken egg white which was used in this study as a model protein develops such a molten globule state in strongly acidic conditions [41, 42].

3.2.2 Definition of Protein Aggregation

In this work protein aggregation include all forms of protein assembly, whether they are amorphous or fibrillar [43], soluble or insoluble, native or non-native, in the form of crystals or precipitates [44].

3.2 Conformational and Colloidal Stability of Proteins in Solution

Protein aggregation has a decisive influence on over 40 diseases, in terms of their outbreak, course and mortality. The negative impact of protein aggregates could be shown for common diseases such as Alzheimer's disease, Huntington disease and Parkinson's disease [43, 45]. In addition to the serious health consequences and when administered as a drug product, the uncontrolled assembly of proteins during processing, formulation and storage are considered as a bottleneck in the biopharmaceutical industry [46–48]. Negative consequences come in the form of yield losses or process delays due to clogged filters or the abrupt increase of protein viscosity. Especially in the highly concentrated regime, the mechanisms of protein aggregation are not sufficiently investigated, so that targeted process manipulation is not possible nowadays.

Depending on the protein structure and the solution conditions, macromolecules can accumulate over different reaction pathways [43]. The aggregation nucleus can arise from an assembly of native, elongated or partially unfolded, as well as completely unfolded proteins. Additionally one can distinguish between homogeneous (protein-protein) and heterogeneous (protein-non-proteinogenic species) nucleation polymerization [49, 50]. The resulting protein aggregates may be covalently (e.g., disulfide bonds, thiol binding), or non-covalently (e.g. hydrophobic and electrostatic interactions) linked. The initial states and binding forms of the protein aggregate are crucial for its reversibility and degree of order. To illustrate the different aggregation pathways, these are shown in simplified form in Figure 3.2.

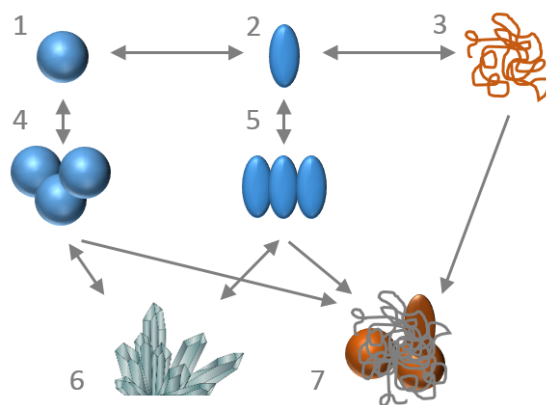


Figure 3.2: Theoretical pathways of protein aggregation. Double arrows symbolize equilibrium reactions. Whereas single arrows symbolize irreversible aggregation steps. 1= native structure, 2=intermediate state, 3=unfolded state, 4=aggregate, 5=intermediate aggregate, 6=crystal, 7=precipitate.

Thermodynamic studies have shown that most aggregation processes proceed through the intermediate state. The aggregation of the intermediates is promoted by the exposure of hydrophobic side chains and the higher flexibility of the molecules [51, 52].

3.2.3 Physical and Chemical Principles of Protein Interactions

The forces that influence the protein itself as well as the protein solution behavior can be divided into attractive and repulsive forces. Attractive interactions lead to a stabilization within the molecule and induce the assembly of the proteins in solution. Repulsive interactions lead to a higher flexibility of the molecule, i.e. a conformational destabilization, but enhance the colloidal stability. Van der Waals forces, hydrogen bonds and hydrophobic interactions are counted among the attractive interactions. Electrostatic forces induced by the repulsion of uniformly charged electron double layers, on the other hand, are repulsive [53, 54].

Van der Waals forces combine Keeson interactions, Debey interactions and London forces. They can be described as a universal weak attractive interaction of electromagnetic origin [55]. Keeson interactions describe the interaction of two dipoles. The Debey interactions also known as dipole-induced dipole forces occur between a dipole and a polar molecule, whereas London forces, which are the dominant dispersion interactions, describe the attractive forces between two polarized molecules.

Another important factor of protein stability are hydrogen bonds, which can be formed in between peptide groups and amino acid side chains. Their contribution to protein stability was found to be significant with a strength of about 1 kcal mol^{-1} per bond [56]. The studies on hydrogen bonds are focused on investigations at the molecular level. How hydrogen bonds may link proteins in the native state and if they contribute to the colloidal stability of proteins by strengthening the hydration layer is not totally understood [57].

Hydrophobic interactions are used to describe the gain in free energy which occurs when non-polar residues of proteins associate in an aqueous environment in order to reduce the surface area in contact with water [58]. Hydrophobic interactions are governed by entropy and not enthalpy features, since the attraction of hydrophobic groups counteracts the undesirable entropy loss of water in the presence of non-polar groups [59]. Hydrophobic interactions are the strongest, non-covalent, non-electrostatic binding forces [60]. A number of hydrophobic scales have been developed in the last decades to be able to assign molecular residues dependent on their hydrophobic character [58, 61, 62]. The deviations

of the results of different research groups demonstrate that hydrophobic forces and induced interactions are not yet fully understood.

Most of the amino acids on the protein surface are able to be protonated or deprotonated. Dependent on the solution pH, their number and distribution on the protein surface electrolytic double layers develop. The interaction of two electrolytic double layers is associated with an increase of the free energy. The resulting repulsive electrostatic interactions play a major role in protein-protein association and desolvation on the molecular level [63, 64].

The DLVO (Derjaguin-Landau-Verwey-Overbeek) theory presented more than 50 years ago combines the forces which have an impact on the protein in solution by introducing the potential of mean force [65]. In the last decades the DLVO theory was optimized by extending the potential of mean force by specific ion effects [66], the impact of the hydration layer on the protein surface and anisotropic interactions [53]. Notwithstanding the improvements of the DLVO theory, the division of forces dependent on their reach is still valid [65]. Van der Waals, hydrogen bonds and hydrophobic interactions can be classified as short-range interactions. Electrostatic repulsion is mainly referred to as a long-range interaction. It has to be taken into account that the range of electrostatic interactions depends on the degree of ionization and the background electrolyte concentration. The distance over which the forces show an effect is of crucial importance when protein-protein interactions are compared by ideally dilute and highly concentrated solution, as the distance of the molecules to each other changes. At highly concentrated conditions the reduced distance between the molecules allow, that additionally to long-range interactions, short-range interactions influence the protein monodispersity [15, 21]. That implies that analytical results of ideally dilute protein solutions can not be easily transferred to highly concentrated conditions and that the interplay of short and long-range interactions have to be taken into account when characterizing these solutions. Additionally to the listed forces the molecular crowding effect can affect the protein solution stability [67, 68]. Molecular crowding describes the influence of excluded volume in extremely high concentrated protein solutions and the concomitant impact on protein conformational and colloidal stability. Molecular crowding is expected to stabilize the native state of molecules and supports the assembly of functional protein networks. As the impact of molecular crowding on protein solution stability has only be recently addressed, experimental results are rare and most theoretical explanations are speculative [69].

3.2.4 Influencing Parameters

The behavior of proteins in aqueous solutions depends strongly on intrinsic and extrinsic properties. The description of protein-specific intrinsic properties such as shape, surface charge and hydrophobicity can be found in section 3.1. This section discusses the forces of impact which are caused by the physical and chemical solution properties.

Protein concentration

Proteins are soluble up to a specific molecule content. This limit is defined as the solubility line and is specific for every protein and also dependent on the surrounding solution [70].

This work focuses on the characterization and prediction of protein solution stability in the highly concentrated regime, where the molecule density in solution plays a decisive role (see also 3.2.3). Under highly concentrated conditions the molecule density increases to an extent that not only long-range but also short-range forces do have an impact on the protein-protein interactions. Not only the distance between the molecules decreases but also the rate of molecule collisions increases. The increased molecule density has most often a negative impact on the solution colloidal stability but was found to stabilize the compact native state of the protein [15, 71]. Thus, aggregation of proteins which was triggered solely by a protein concentration increase is most often reversible [72, 73].

Short-range interactions include specific ionic bonds and hydrophobic interactions of specific patches on protein surfaces. These directed interactions can lead not only to the assembly of the molecules in the form of disordered aggregates, but also to an ordered network-like structure. This network formation can have a stabilizing effect on the solubility of the protein [74]. This fascinating behavior could already be observed with a series of monoclonal antibodies which could be concentrated up to 400 mg/ml [75]. Unfortunately, little is known about the exact causes and conditions under which stabilizing networks are created, so that a targeted manipulation is not possible yet.

Temperature

The stability of a protein is a sensitive balance between enthalpic and entropic terms, derived from the physico-chemical difference between the native and non-native state of the polypeptide [76]. By increasing the temperature the total energy of the system increases what directly effects the protein colloidal and conformational stability in solution. With increasing temperature the diffusion of dissolved particles, i.e. the movement of proteins in solution, accelerates. The increased Brownian movement increases the probability of molecule collisions, which in turn leads to an increased aggregation propensity.

3.2 Conformational and Colloidal Stability of Proteins in Solution

The increase of the temperature above 40°C usually leads to an irreversible conformational change of proteins. Above this temperature limit, stabilizing disulfide bridges are weakened and endothermic oxidation processes can occur. The accompanied exposition of hydrophobic amino acids result in non-reversible aggregation [77].

If the temperature of protein solutions is lowered, the stability of the proteins is first increased by their slowed diffusion (up to approx. 4°C). This effect is important for the storage of biopharmaceutical formulations. When the temperature falls below the freezing point of water, the colloidal stability decreases. On the one hand due to the ever lower available liquid volume (crystallization of water molecules) on the other hand due to the formation of solid-liquid interfaces. Proteins with a hydrophobic character adsorb on the developed solid surfaces, what leads to aggregate formation. On a molecular level cold denaturation can occur. Cold denaturation is caused by specific interactions of protein non-polar groups with water. In contrast to studies at room or accelerated temperatures it was found that hydration of these groups is thermodynamically favorable at cold temperatures. The exposition of non polar compounds of the protein core leads to protein unfolding [78]. In general cold denaturation is reversible [71] unlike most high-temperature denaturations. In this work temperature was solely used to accelerate processes like protein aggregation or unfolding to be able to study the protein solution behavior in a short time period. For all other experiments the temperature was kept constant to limit the parameters of impact.

pH

The protonation or deprotonation of the proteinogenic amino acid residues is dependent on their pK_a value and the pH of the surrounding solution [79]. Thereby, the pH has a great impact on the charge distribution and net charge of a protein. The isoelectric point (pI) defines the pH where the protein net charge is 0 [80]. This does not imply that all amino acids of the protein are uncharged; rather, it means that the sum of all charges is 0. In Figure 3.3 the net charge curves of three proteins with different pIs are shown. The charge curves were calculated on the basis of zeta potential measurements, which are explained in more detail in chapter 3.3.

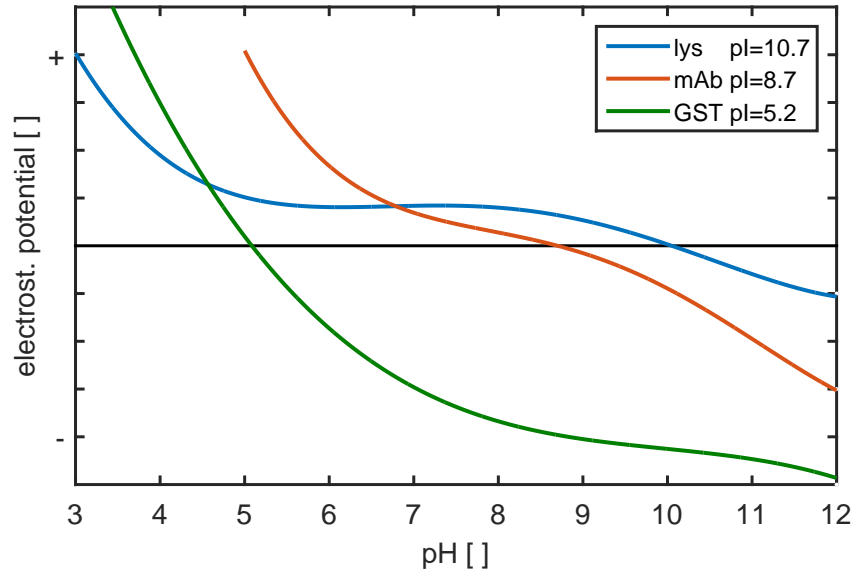


Figure 3.3: Net charge curves of lysozyme, a monoclonal antibody and Glutathione-S-Transferase in a pH range from 3 - 12.

Since the electrostatic potential at the pI is lowest, only weak or no repulsive electrostatic interactions occur at this pH. Here, attractive short-range interactions, such as hydrophobic or van der Waals interactions, contribute to the aggregation tendency of the protein. The further apart the solution pH and the pI are, the stronger the net charge of the protein and thus the repulsive interactions. The electrostatic repulsion which stabilizes the protein colloidal stability also impact the protein conformation. Equally charged amino acids in the protein core repel each other, which firstly impacts the protein flexibility and at extreme acid or basic conditions lead to protein unfolding [28]. Thus, the selection of buffer pH should always take both conformational and colloidal stability aspects into account.

Co-solutes

Co-solutes correspond to molecules which are dissolved in solution with the protein of interest. Either their presence is process related or they are added to the solution in a targeted stabilizing manner. In order to delineate this huge subject, only co-solutes are discussed in this section whose stabilizing or destabilizing effects on proteins have been studied in this work (salts, polymers, amino acids).

Salt molecules dissociate in aqueous solution into positive (cations) and negative (anions) ions. The impact of salt on the protein solution stability is firstly dependent on

the salt concentration. At low salt concentrations, the salt ions stabilize the protein via nonspecific electrostatic interactions. This phenomenon was found to be only dependent on the ionic strength [81]. When increasing the salt concentration the differences between salt types become more and more pronounced. The differing effect of the ions on protein stability is generally referred to as salting-in and salting-out effect [82, 83]. Salting-in describes the specific and unspecific binding of the ions to charged amino acid residues of the protein [84, 85]. The related chaotropic salts have a positive effect on the colloidal stability but a negative impact on the conformational stability of the protein in solution. Ions with salting-out character, also known as kosmotropes, are strongly hydrated in solution and thus have a negative influence on the protecting hydration shell of the protein [82]. They increase the aggregation propensity, however, have a stabilizing effect on the 3D structure of the proteins in solution. Dependent on their salting-out character salt ions can be classified according to the Hofmeister series (anions: $\text{SCN}^- > \text{ClO}_4^- > \text{I}^- > \text{ClO}_3^- > \text{Br}^- > \text{NO}_3^- > \text{Cl}^- > \text{CH}_3\text{CO}_2^- > \text{HPO}_4^{2-} > \text{SO}_4^{2-}$, cations: guanidinium $> \text{Ca}^{2+} > \text{Mg}^{2+} > \text{Li}^+ > \text{Na}^+ > \text{K}^+ > \text{NH}_4^+$) [86, 87]. Whereby anions are known to have a stronger impact on the protein behavior than cations [85]. In the highly concentrated regime the impact of common salts on the protein solution stability can not be generalized. Especially specific electrostatic interactions or hydration effects, triggered by the addition of salt, can lead to a stabilization or destabilization dependent on the protein under investigation [15, 16]. In this work three different salts (NaCl , Na_2SO_4 , $(\text{NH}_4)_2\text{SO}_4$) were chosen to study their impact on the protein solution stability in the highly concentrated regime.

Polymers, like polyethylene glycol, are neutral, hydrophilic additives which have a stabilizing, neutral or destabilizing character on the protein dependent on their molecular mass [88]. High molecular mass polymers induce depletion attraction leading to attractive protein-protein interactions [89]. This effect can be explained by the concentration gradient which occurs when the relatively large polymer molecules are excluded from the protein vicinity. The resulting polymer concentration gradient causes the attraction of the water molecules from the gap between the proteins towards the polymer and thus to attractive protein-protein interactions [90, 91]. The strength of this effect decreases with decreasing polymer chain length. The presence of low molecular weight polymer molecules can mitigate attractive protein-protein interactions due to shielding effects [88].

Amino acids, such as glycine, belong to the group of osmolytes and have a generally stabilizing effect on proteins in solution. Several theories have been published which describe the stabilizing influence of the small organic compounds. One theory assumes that the direct interaction of the osmolyte with the polypeptide backbone lead to structural

stabilization of the protein [92–94]. Other studies disprove this specific interaction theory and found higher structured water in the presence of osmolytes, which also has a stabilizing impact on the protein solution stability [95–97].

The impact of the physico-chemical solution conditions on protein stability is so complex, that no general valid model exists, which can describe all interaction mechanisms [98–100]. The challenge of this work is therefore to establish analytical methods and to validate potential parameters which are sensitive enough to depict changes in the protein behavior which are caused by the factors listed above, also for the characterization of highly concentrated protein solutions. Only with the exact characterization of those interaction parameters conclusions can be drawn on the conformational and colloidal long-term solution stability of proteins.

3.3 Analytical Methods to Characterize and Predict Protein Solution Stability

The solution stability of a biopharmaceutical molecule must be ensured throughout its shelf life to guarantee stable process, storage and application conditions. Analytical methods allow, on the one hand, the detection of conformational changes of the protein and its aggregation (section 3.3.1). On the other hand, several scientific groups are working on the better understanding and analysis of the forces that cause the state change of the proteins in solution (section 3.3.2). The characterization of the influencing forces and the related alteration of the solution bulk properties are intended to allow the prediction of protein solution stability. This chapter gives a brief overview of established analytical techniques, shows their limitations and the associated need for the development of novel methods.

3.3.1 Analysis of Protein Conformational Changes and Aggregation

The conformational change of the protein in solution can be analyzed either directly or indirectly. Fourier transform infrared spectroscopy is a direct, very precise measurement method [22]. The spectra analysis allows the determination of the protein 2D structure and thus also the detection of its change in unfolding processes. Indirect methods, like activity assays are based on color reactions which are coupled to the catalytic activity of the proteins in solution [101, 102]. The implementation of the activity assays is only

possible at specific solution conditions such as ideally dilute solutions. These methods are limited to detect protein unfolding and associated non-native, non reversible protein aggregation [103, 104].

Techniques which are capable of detecting all forms of visible protein aggregates are mostly based on optical evaluation procedures. High-resolution cameras enable a simple method to differentiate between different types of aggregation, namely precipitation, crystallization, gelation and skin formation [88]. Soluble aggregates with an average size of 1-100 nm, however are not visible by eye and have to be measured via light scattering techniques. With static light scattering measurements the molecular mass of a particle in solution can be determined whereas dynamic light scattering (DLS) provides insights into the hydrodynamic radii of particles and particle size distributions [105–107]. The further development of dynamic light scattering instruments enable also the detection of particles in highly concentrated and turbid solutions by cross-correlation or high angle measurements [108]. The non-invasive dynamic light scattering techniques determine the time-dependent fluctuations in the intensity of scattered light that occur due to the Brownian motion of particles dispersed in solution. The time-dependent fluctuation enables the determination of the Diffusion coefficient, which in turn can be directly correlated to the hydrodynamic radius of the protein. The relationship between the diffusion coefficient and the hydrodynamic radius is described by the well known Stokes-Einstein equation [72].

In order to screen the solution stability of proteins under varying solution conditions, protein phase diagrams can be prepared. Within a phase diagram, two or more influencing parameters, such as protein and additive concentration, are varied. When solution equilibrium is reached, the individual samples of the phase diagram can be examined for aggregation or conformational changes, using the analytical methods described above. The resulting phase diagrams provide information about the solubility range of the protein in the selected screening window. Baumgartner et al. published an automated method for the preparation of protein phase diagrams in a 96-well micro scale format. In this study, this technique was adapted to highly concentrated protein solutions [88]. The resulting protein phase diagrams were used to validate predicted long-term stability results (see Chapter 6, Chapter 7 and Chapter 8). The method is precise but also very time-consuming since the analysis of the individual wells and the associated scoring can only take place after the solution equilibrium is reached. According to FDA guidelines, pharmacological active proteins must be stable at least for 12-24 months to be approved for human administration [109].

To accelerate the conformational and colloidal changes of proteins in solution energy in

form of increased temperature can be imported into the system. While running a temperature ramp, both the melting temperature (T_m) and the aggregation temperature (T_{agg}) can be depicted by fluorescence and static light scattering measurements, respectively [110]. In several studies, it was shown that the T_m and T_{agg} values can be correlated with the long-term stability of identical samples also in the highly concentrated regime [99, 108]. Other research groups stated, that a direct correlation between the thermal stability and the long-term stability of protein solutions is not always given [100]. These findings indicate that the temperature has to be treated as an additional parameter, and that the direct correlation is not readily possible.

The selection of the expedient screening area for the preparation of protein phase diagrams or thermal stability tests requires experience or follows the principle of trial and error. In addition, the listed methods can accurately describe the physico-chemical state of the proteins in solution but do not contain any information on the causes that led to the analyzed behavior of the protein under investigated conditions. In order to facilitate the prediction of the protein behavior in solution and thus enable a targeted manipulation of the process and formulation conditions, analytical methods are necessary which can identify the inter- and extra-molecular forces and interaction mechanisms.

3.3.2 Characterizing Analytics

To investigate the molecular surface properties *in silico* and experimental techniques can be applied. Experimental methods, such as the determination of the ζ - potential [111] or the surface tension [112], enable the description of protein net surface charge or surface hydrophobicity, respectively. In order to be able to determine more precisely the structural features, charge distribution or the position of the hydrophobic patches [58] on the protein surface, computational methods are necessary. *In silico* methods include Molecular dynamics (MD) and Monte Carlo (MC) simulations as well as Quantitative Structure Activity Relationship (QSAR) studies. They were successfully applied for protein drug design [113], to predict protein structures [114] and protein stability [112] in ideal dilute solutions.

For the description of the unfolding or aggregation tendency of a protein in solution not only the molecular characteristics but also the resulting intrinsic and extrinsic interactions are of importance. To assess the various interactions, thermodynamic properties like the diffusion coefficient [115], the osmotic pressure [116] or the solution viscosity [117] can be determined. The deviation of these parameters from the ideal behavior describes the

sum of all influencing interactions, also known as potential of mean force. The potential of mean force can be semi quantitatively related to the second virial coefficient (B_{22}), preferably determined by self interaction chromatography [118]. The parameter is a well documented approach to predict optimal crystallization conditions [119–121] and the aggregation propensity of proteins [118, 122, 123] in ideal dilute solutions. In recent years, a number of studies clearly demonstrated the limits of the predicting potential of the B_{22} . It was revealed that an insufficient correlation of the B_{22} and protein solution behavior is given when the aggregation of the proteins is driven by the conformational change of the molecule [27] or the aggregation kinetics are extremely slow [124]. Additionally, the B_{22} implies only information on two dimensional protein-protein interactions as it is measured in the ideal diluted state. In the highly concentrated regime the interaction mechanisms are far more complex (see also 3.2.3). Multidimensional interactions, the increasing impact of short-range interactions and protein network formation aggravate the transferability of parameters, like the B_{22} , measured in the ideal diluted state to highly concentrated protein solutions. Saito et al. [125], Scherer et al. [126] and Saluja et al. [127] demonstrated that there is only an insufficient correlation of the B_{22} and protein solution stability when screening highly concentrated protein solutions.

So far, there is no method approved by the authorities to reliably predict the stability of highly concentrated protein solutions. Nowadays, the selection of the ideal process solution conditions, as well as the formulation development is very time and cost intensive. Thus, the biopharmaceutical industry demands the development of a novel method which is capable to describe the protein behavior in the highly concentrated regime. This method should meet the following requirements:

- highly sensitive
 - to depict also the weak short-range interactions
- non invasive
 - to not influence the solution properties during the measurement
- low volume consumption (μL scale)
 - to fulfill the requirements in the early development and enable the measurement of costly formulations
- output of one single valuing parameter
 - to be competitive to B_{22} measurements

A method not yet established in the biopharmaceutical industry, which has the potential to meet the listed criteria, is the complex rheology. Complex rheology implies the rheological characterization of soft matter with regard to its viscoelastic properties. The next

section deals with the investigation of viscoelastic parameters and the role of rheological measurements in the biopharmaceutical industry.

3.4 Rheology of Viscoelastic Fluids

3.4.1 Principles of Rheology

Rheology is the science of deformation and flow. This definition includes fluid dynamics, hydraulics and solid state mechanics. Rheology is used to measure fluid properties, understand structure-property relations and to predict flow behavior of complex liquids under processing conditions [128–130]. In a physical stressful environment there are four ways how a material under investigation can react on an acting force.

1. The load is directly transferred to the forces which bond the atomic components or molecules. This rheological behavior is typical for rigid materials like ceramics or crystals.
2. The load lead to significant changes of the materials' shape. This behavior can be observed with non crystalline polymers.
3. The material flows away from the load and deforms semi-permanently as with viscoelastic materials.
4. The load forces the material to flow away and to deform permanently (plastics).

The first behavior describes ideal elastic materials. They will remember the deformation indefinitely and return to its initial state. Based on Hook's law the stress (σ), which acts on an ideal elastic material, and strain (γ) are directly and simply proportional to each other [131].

$$E = \frac{\sigma}{\gamma} \quad (3.1)$$

If this equation is applied to stress caused by shearing (τ), the relation to the shear modulus (G) is obtained.

$$G = \frac{\tau}{\gamma} \quad (3.2)$$

Following Newton's law, a perfect liquid material will stop deforming instantaneously when stress is removed and never recover to its previous state. Here, the shear rate ($\dot{\gamma}$)

3.4 Rheology of Viscoelastic Fluids

is proportional to the shear stress (τ) with the constant of proportionality η (dynamic viscosity):

$$\tau = \eta \cdot \dot{\gamma} \quad (3.3)$$

Protein solutions behave like a combination of a Newtonian fluid and an Hookean solid. They can partly store the energy which is applied whereas the other part dissipates. Additionally, they exhibit a pronounced time (t) dependence and belong therefore to the viscoelastic materials (Equation 3.4) [132]. For viscoelastic fluids the relation between stress and strain can be interpreted as a linear combination of a Newtonian element and a Hookean element (Maxwell model, Figure 3.4). This model is only valid in the linear viscoelastic range [131]. As in this work only rheological tests in the linear viscoelastic range are performed, the behavior of viscoelastic fluids in the non-linear region will not be discussed.

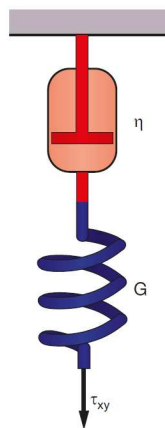


Figure 3.4: Schematic diagram of a Maxwell model.

$$G(t) = \frac{\tau(t)}{\gamma_0} \quad (3.4)$$

Dynamic rheological tests in the linear viscoelastic range are best suited to study the viscoelastic properties of protein solutions. The most common test is oscillation [131]. When a viscoelastic material is subjected to a sinusoidal load, a constant state is obtained in the linear viscoelastic range, in which the resulting load is also sinusoidal, has the same radial frequency (ω) but is phase shifted by the angle δ . This relationship can be described by:

$$\gamma(t) = \gamma_0 \cdot \sin(\omega \cdot t) \quad (3.5)$$

and

$$\tau(t) = \tau_0 \cdot \sin(\omega \cdot t + \delta) \quad (3.6)$$

The resulting shear modulus takes the complex form of

$$G^* = \frac{\tau(t)}{\gamma(t)} = \frac{\tau_0 \cdot e^{i\delta}}{\gamma_0} = \frac{\tau_0}{\gamma_0(\cos\delta + i\sin\delta)} \quad (3.7)$$

The complex shear modulus, G^* , is formed by an elastic component, the storage modulus (G') that is in phase with the strain input and the viscous component, the loss modulus (G'').

$$G^* = G' + iG'' \quad (3.8)$$

with

$$G' = \frac{G(\omega\lambda)^2}{1 + (\omega\lambda)^2} \quad (3.9)$$

and

$$G'' = \frac{G\omega\lambda}{1 + (\omega\lambda)^2} \quad (3.10)$$

G' is the measure of the deformation energy stored by the sample during the shear process. G'' is the measure of the energy which dissipates [131]. To characterize the viscoelastic behavior frequency sweep measurements can be performed. Here, G' and G'' are detected over an applied frequency ramp at a set amplitude. At low frequencies, representing large time scales, the viscoelastic material responds like a viscous fluid. At high frequency values, representing short time scales, the material responds like a perfect Hookean solid. Between these extremes, the material behave viscoelastic. At a material specific frequency value, the two curves of G' and G'' cross each other. At frequencies below this crossover point, the material is a viscoelastic fluid. The particles in solution can follow the applied movement and relax in the given time frame. Above the crossover point, the material behaves like a viscoelastic solid. Here, the time frame up to the forced movement change is so short that the viscoelastic fluid can not completely relax. The energy introduced into the system is thus stored until the next frequency step so that the behavior appears predominantly elastic [133, 134]. In Figure 3.5 the characteristic curve shapes of G' and G'' are plotted over the radial frequency. The relaxation processes of complex fluids such as protein solutions can extend over 8-12 decades in frequency. In order to obtain as complete a rheological characterization of a substance as possible, it is necessary to determine the viscoelastic characteristics such as G' and G'' in a wide frequency range [135]. Furthermore, protein solutions exhibit very small relaxation times

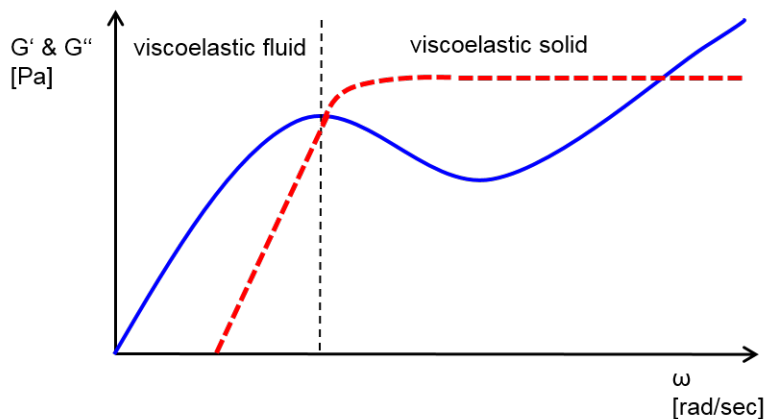


Figure 3.5: Characteristic curve shape of G' and G'' over a wide frequency range, determined by frequency sweep measurements.

[136]. In order to be able to detect the weakly viscoelastic behavior of protein solutions, it is therefore necessary to measure in the kilo- to megahertz frequency region. Conventional mechanical rheometers, such as cone-and-plate rheometers, operate up to 200 Hz and are thus not suitable for the measurement of viscoelastic properties of protein solutions [20]. Additionally, highly concentrated protein solutions react sensitively to ambient conditions, so that the impact of the measurement on the sample should be as low as possible. To avoid shearing and to reach high enough frequencies, the dynamic squeeze flow rheometry can be applied. Here, the sample is squeezed and not sheared during the oscillatory measurement [137]. Since the restoring force of the sample is proportional to the reciprocal of the third power of the sample thickness, low-viscosity samples can also be measured exactly.

For this reason a squeeze-flow rheometer - the Piezo Axial Vibrator (PAV) was used in this work to characterize the viscoelastic behavior of protein solutions. This device is able to measure in a frequency range of 0.5-7 kHz, has a sample volume of 30 μL with a measuring gap of 15 μm and is limited to the linear viscoelastic regime due to a very low voltage and deformation amplitude. The excitation of the sample as well as the stress response of the sample is realized by eight piezoelectric elements. These are arranged in pairs on four sides of a copper tube, which holds the measurement head. The piezoelectric elements are connected to a lock-in amplifier which transfers a constant voltage amplitude to the piezoelectric actuators and records the resulting complex voltage amplitude of the piezo sensors. In order to determine the viscoelastic moduli G' and G'' , a measurement without a sample (blank measurement) and a measurement with a sample is carried out.

The deflection of the probe length of the blank measurement, \hat{x}_0 is equated with the deflection with sample in the measuring gap \hat{x} , whereby the complex spring constant K^* can be calculated. Assuming linear viscoelasticity and no slippage occurs, the complex viscoelastic modulus G^* can be calculated from K^* .

$$K^* = \frac{3\pi}{2} \cdot R \left(\frac{R}{d} \right)^3 \cdot \frac{G^*}{1 + \frac{\varphi\omega^2 d^2}{10G^*}} \quad (3.11)$$

With φ =density, R =radius of the measurement head, d =gap width and ω =radial frequency [138]. The measurement accuracy of the device and the good suitability for low-viscosity complex fluids, has been demonstrated in numerous publications [138–141]. Unfortunately, the device is not commercially available, so this work is also concerned with an alternative rheological technique [127, 142].

Alternatively to mechanical rheometry also dynamic light scattering, diffusive wave spectroscopy or particle tracking techniques can be applied to determine the viscoelastic moduli G' and G'' . These measurement methods are referred to as optical microrheological techniques [143]. All microrheological measurements have a sample volume in μL -scale and the use of so-called tracer particles in common. The tracer particles are used to measure the relation between stress and deformation of the sample. Analogues to mechanical rheometry a stress is applied by the tracer particles and the strain in form of the tracer position is detected. The movement of the tracer particles is induced by Brownian motion and thus very little stress is applied on the probes. Similar to high shear or squeeze flow rheometry, microrheology allows access to short-time dynamics, so that the viscoelastic response of weakly elastic materials like protein solutions can be measured [144]. In this thesis the dynamic light scattering technique is examined more closely. An advantage of the dynamic light scattering technique is that it is already established as an analytical tool in the biopharmaceutical process development. With dynamic light scattering measurements the autocorrelation function (ACF - correlation of a signal with a delayed copy of itself as a function of delay) of the light scattered by the particles is measured. The ACF can be written as a function of the mean square displacement (MSD) of the scattering particles. The MSD is a measure of the mean distance covered by a particle in a given period of time. The viscoelastic moduli can be obtained by calculating the Fourier Transform of the MSD and combining the resulting term with the Stokes Einstein Equation, resulting in:

$$G^*(\omega) = \frac{k_b T}{\pi a (\Delta r^2 (1/\omega)) \Gamma(1 + a(\omega))} \quad (3.12)$$

$$G'(\omega) = G^*(\omega)\cos(\pi a(\omega)/2) \quad (3.13)$$

$$G''(\omega) = G^*(\omega)\sin(\pi a(\omega)/2) \quad (3.14)$$

where Γ denotes the gamma function which is a result of the Fourier Transform of the MSD, k_bT =thermal energy, a =diameter of the particle, $(\Delta r^2(t))$ =MSD and ω =radial frequency [145].

The rapid wide-scale adaption of microrheology techniques is prevented by technical challenges. One challenge is the selection of suitable tracer particles. Besides the concentration and size of the tracer particle, one condition which has to be fulfilled to gain accurate and reproducible results is the inertness of the tracer particles in solution. Interactions of the tracer particles with themselves or with the proteins alter their mobility in solution and therefore distort the rheological results [146, 147]. In the biopharmaceutical sector, tracer particles with different surface properties are used. So far, the interaction with the protein to be investigated has been either neglected or only presumed [146, 148]. The study of tracer particle-protein interaction mechanisms and the corporate thorough evaluation of potential tracer particles is demanded to further push this promising analytical technique for the biopharmaceutical development.

3.4.2 Rheological Characterization of Biopharmaceutical Solutions

In food, cosmetic and ink industry rheology is an established analytical technique to physically characterize raw materials, intermediate and finished products [134, 149, 150]. Dependent on the processing steps rheological parameters are used to design flow processes, predict storage stability, understand and design texture and generally control quality attributes [134, 151–153]. In contrast, the application of the rheological technique is very limited in the biopharmaceutical industry. Only the measurement of the dynamic viscosity is considered as a standard in the process and formulation development. The determination of complex rheological parameters, i.e. the characterization of the viscoelastic properties of protein solutions, is not widely used. In the last decades the viscoelastic characterization of biopharmaceutical solutions focused mainly on the rheology of blood [154] and the investigation of the shear thinning behavior of blood related solutions [132, 155–157]. In the last decade, the implementation and further development of high-frequency and microrheological rheometers as well as the increasing

pressure of the biopharmaceutical industry to develop novel analytical methods for the better characterization of protein solutions expended the knowledge about the viscoelasticity of pharmaceutically relevant protein solutions.

Pioneer work in the area of complex rheology was done by the group of D. Kalonia. In the last 15 years they profoundly studied the viscoelastic properties of protein solutions by determining the storage modulus, G' of various protein solutions at a defined frequency value. Numerous publications demonstrate that G' is influenced by protein stability-relevant parameters such as pH, protein concentration, ionic strength or the amino acid sequence of a protein [15, 20, 136, 158]. Furthermore, the value of G' has been successfully correlated with the strength of the protein-protein interaction [127]. This correlation was confirmed by Neergard et al. who studied the aggregation tendency of highly concentrated antibody solutions [159]. The listed studies demonstrate the great potential of complex rheology to better understand the behavior of proteins in solution. The scientific challenge is to find a direct link between the viscoelastic behavior and the stability of proteins in solution. For this purpose, the relaxation behavior of the protein solutions should be investigated over a wide frequency range and, in addition to the storage modulus G' , the loss modulus G'' must be included in the rheological characterization.

Research Proposal

The processing and formulation of highly concentrated protein solutions gain increasing importance in the biopharmaceutical industry [15, 16]. Advantages of the highly concentrated protein solutions are the associated decreased volume consumption of process related liquids or the possibility of new application forms, like subcutaneous injections. However, a major challenge is to keep the proteins stable in solution since the increased molecular density enhances the aggregation propensity and adversely affects the conformational stability of the target molecules [21, 22]. Aggravating, the effective forces which have an influence on the colloidal and conformational stability of the highly concentrated protein solutions are not yet fully understood. Consequently, there are no methods approved by regulatory authorities that can predict the solution stability of proteins in the highly concentrated regime. Therefore, the targeted manipulation of the solution conditions is not possible nowadays. The ideal solution conditions have to be identified in time-consuming long-term stability tests in trial and error procedures [24].

In recent years, numerous studies have been undertaken to understand the complex relationships between protein-protein interactions, the environmental conditions that influence them, and the associated protein solution stability [15, 106, 119]. *In silico* methods, such as MD simulations, provide insights into the surface characteristics of the proteins in terms of their structure, charge distribution and hydrophobicity [53, 160]. The effects of changing environmental and buffer conditions on the solution stability of proteins could be demonstrated experimentally by means of phase diagrams [88, 161, 162]. In addition, a parameter has been established that can describe the strength and direction of protein-protein interactions. The second virial coefficient, B_{22} maps the potential of mean force [118, 163]. This theoretic potential combines all the interactions which have an influence on the protein under studied conditions. The semi-quantitative parameter B_{22} can solely be experimentally determined in ideal dilute solutions. Studies have shown that the results thus obtained can not be transferred directly to highly concentrated conditions [125,

164]. Here, the interaction mechanisms change due to the increasing impact of forces, like van der Waals or hydrophobic forces, which have no influence on the protein in an ideal dilute solution. In addition, multi-dimensional interactions and complex network formations, which can not be displayed by the B_{22} , can occur [15, 22, 125]. Therefore, a novel analytical method is demanded which can describe the complex behavior of proteins in highly concentrated solutions directly.

Molecules, which behave very similarly in solution as proteins, are synthetically produced polymers. They also form stabilizing networks, react sensitively to changing solution conditions, and behave viscoelastic [135, 139, 165, 166]. Viscoelasticity is a rheological property that describes the complex relaxation behavior of matter which possesses both elastic and viscous properties. Polymer solutions are mainly processed in the food and cosmetics industry. Here, rheology is an established analytical method for quality control, to investigate the sedimentation properties or to predict the long-term stability of the polymer solutions also at highly concentrated conditions [130, 167]. Compared to the rheological characterization of polymer solutions the potential of rheology to characterize biopharmaceutical relevant solutions has by far not been fully exploited.

Compared to conventional analytics applied in the biopharmaceutical industry, rheological methods have the advantage of measuring the bulk properties of the solution and not single protein-protein interactions [130]. They have thus the potential to capture all interactions and network formation that occur in highly concentrated protein solutions. The group of D. Kalonia has already shown that viscoelastic parameters are sensitive to protein solution conditions, such as pH, ionic strength or protein type. In addition, the elastic modulus, G' was correlated successfully with the strength and type of protein-protein interaction [15, 20, 127, 136]. But up to know little is known about the connection between the viscoelastic behavior and protein solution stability.

Accordingly, the question at hand is whether the rheological data correlate with the protein solution behavior directly and if one single rheological parameter can be extracted which is suitable to predict the long-term stability of highly concentrated protein solutions.

To answer the overriding question the focus of this thesis is laid on the rheological characterization of highly concentrated protein solutions and the correlation of determined viscoelastic parameters with the protein solution long-term stability. For this purpose, the viscoelastic properties of a model protein is firstly be investigated. The screening range is chosen in such a way that the sensitivity of the viscoelastic measurements can be validated against changing solution conditions. Rheological parameters which have the potential to predict the long-term solution stability shall be extracted and correlated

directly with the protein solution stability. As a reference protein phase diagrams are prepared in an automated high-throughput format.

The rheological methodology shall then be extended to pharmaceutical relevant solutions, including more complex molecules like monoclonal antibodies or structural manipulated proteins. In order to underline the predictive performance of the developed rheological method, this is to be combined and optimized in a further step with established orthogonal analytical techniques.

In order to ensure the applicability of the complex rheology in the biopharmaceutical industry, it is also the aim of this work to select and optimize potential rheological measurement techniques. Microrheology was found to be effective for the determination of viscoelastic parameters of protein solutions. To gain reproducible and stable results the essential tracer particles have to be selected thoroughly. An important criterion is that the tracer particles do not interact with the proteins or with themselves during the measurement. In this thesis, a screening of tracer particles with different surface properties is attempted in order to generate knowledge about their suitability for microrheological measurements of protein solutions.

In summary, this project aims at the characterization of highly concentrated protein solutions based on complex rheological measurements and the evaluation of this novel method, with regard to the prediction of protein solution stability. The resulting better understanding of protein behavior in highly concentrated solutions is expected to make a significant contribution towards the optimization of the biopharmaceutical process and is a further step towards stable and safe formulations.

Comprehensive Overview of Publications & Manuscripts

This chapter provides an overview of the manuscripts and publications compiled in this thesis. The order of the manuscripts listed is topic-based and not chronologically ordered. The present work can be divided into three main sections.

The first section focuses on the optimization of the concentration measurements of highly concentrated protein solutions. The manuscript *“Implementation of an analytical microfluidic device for the quantification of protein concentrations in a high-throughput format”* describes the development and introduction of a silicone microfluidic chip. This device enables the automated concentration determination of protein solutions in a large concentration range in a high-throughput, 96-well plate compatible format.

The aim of the second part of this work was to better characterize highly concentrated protein solutions and to find a methodology that predicts the long-term stability behavior of these complex fluids. For this, rheological methods were applied. First, the viscoelastic properties of the model protein lysozyme were determined. In the study *“Squeeze flow rheometry as a novel tool for the characterization of highly concentrated protein solutions”* it was shown that the determined rheological parameters are sensitive to stability-influencing parameters such as pH or ionic strength. In addition, a key parameter was identified which could be correlated directly with the colloidal long-term stability of the model protein. This key parameter, ω_{CO} describes the frequency point of the intersection of the rheological parameters G' and G'' .

In the study *“Prediction and characterization of the stability enhancing effect of the Cherry-TagTM in highly concentrated protein solutions by complex rheological measurements and MD simulations”*, aimed in the description of the stability enhancing effect of the Cherry-TagTM. Therefore, the viscoelastic characteristics of native GST and GST fused with the Cherry-TagTM technology were investigated in varying solution conditions. Based on the rheological results their long-term stability was predicted. In addition, the rheological results were linked with MD simulations. With the MD simulation results,

the causes for the predicted stability differences of GST and Cherry-GST were investigated by studying their structure and surface characteristics *in silico*. The combination of rheological measurements and MD simulations revealed a comprehensive micro- and macroscopic characterization of both proteins studied.

The prediction of the colloidal and conformational long-term stability of highly concentrated protein solutions was further refined in the manuscript “*Characterization of highly concentrated antibody solution - A toolbox for the description of long-term solution stability*“. In this study the rheological characterization of protein solutions was combined with established orthogonal analytical methods. The resulting analytical toolbox was used to predict the long-term solution stability of a monoclonal antibody in process- and formulation-relevant conditions. The study demonstrated the strengths and weaknesses of novel and established analytical techniques. In addition, the intelligent combination of the results provided an accurate characterization of the mAb solutions and a good prediction of their colloidal long-term behavior.

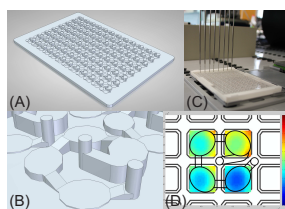
The aim of the third part of this thesis was the optimization of the rheological measurement technique with regard to the applicability in biopharmaceutical laboratories. In addition to the mechanical rheology used for the screenings presented above, microrheology has the potential to be used as a standard analytic as it is based on the well known dynamic light scattering technique. In order to obtain reproducible results, certain criteria must be met. An essential criterion is that the tracer particles used for this measurement technique do not interact with the proteins in solution. In order to ensure this, the measurement quality with the use of different tracers was investigated in the manuscript “*Impact of polymer surface characteristics on the microrheological measurement quality of protein solutions - a tracer particle screening*“. For this purpose, the surfaces of four different particles were characterized and the quality of the microrheological measurements under different solution conditions was tested. The results of this study show which tracer surface characteristics are essential for the measurement quality and can also recommend the use of a surface-modified tracer for the rheological measurement of protein solutions.

Implementation of an analytical microfluidic device for the quantification of protein concentrations in a high-throughput format

Carsten Philipp Radtke*, Marie-Therese Schermeyer*, Yün Claudia Zhai, Jacqueline Göpper and Jürgen Hubbuch

Engineering in Life Sciences 16 (2016): 515-524.

*contributed equally



This work presents the qualification and usage of a disposable measurement device which can be used with conventional microplate photometers to determine protein concentration. The application of the microfluidic device (μ F-device) allows absorption measurements of protein concentrations from around 0.1 to 100 mg/mL with an accuracy of 99.2 % dependent on given protein extinction coefficients. The integrated four measurement chambers of increasing height (100 – 1500 μ m) allow the direct calculation of calibration curves and the determination of protein concentrations independent of used optical path lengths with a sample volume of 36 μ L. This study contains the validation of the analytical μ F-device according to ICH Guidelines as well as a representative case study. A salt gradient screening with chromatography columns in microliter scale performed on a liquid handling station presents the usability of the μ F-device. It is shown that an improvement of the repeatability and accuracy of the chromatograms could be achieved by μ F-device implementation in comparison to photometric measurements performed in microtiter plates.

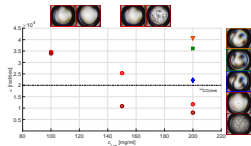
Squeeze flow rheometry as a novel tool for the characterization of highly concentrated protein solutions

Marie-Therese Schermeyer, Heike Sigloch, Katharina C. Bauer, Claude Oelschlaeger and Jürgen Hubbuch

Biotechnology and Bioengineering 113 (2016): 576-87.

This study aims at defining rheological parameters for the characterization of highly concentrated protein solutions. As a basis for comparing rheological behavior with protein solution characteristics the protein phase behavior of lysozyme from chicken egg white

with concentrations up to 225 mg/mL, changing pH values and additive concentrations was studied in a microbatch scale format.



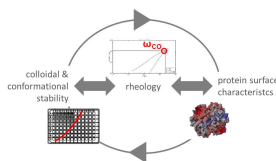
Oscillatory frequency sweep measurements of samples with exactly the same conditions were conducted immediately after preparation (t_0). The protein solutions behave viscoelastic and show a characteristic curve shape of the storage modulus (G') and the loss modulus (G''). The measured rheological parameters were sensitive concerning solution composition, protein concentration and solution inner structure. We succeeded to correlate protein phase behavior with the defined rheological key parameter ω_{CO} . This point represents the frequency value of the intersection point from G' and G'' . In our study lysozyme expressed a ω_{CO} threshold value of 20000 rad/sec as a lower limit for stable protein solutions. The predictability of lysozyme aggregation tendency and crystallization by means of squeeze flow rheometry is shown.

Prediction and characterization of the stability enhancing effect of the Cherry-Tag™ in highly concentrated protein solutions by complex rheological measurements and MD simulations

Pascal Baumann*, Marie-Therese Schermeyer*, Hannah Burghardt, Cathrin Dürr, Jonas Gärtner and Jürgen Hubbuch

International Journal of Pharmaceutics (2017), submitted

*contributed equally



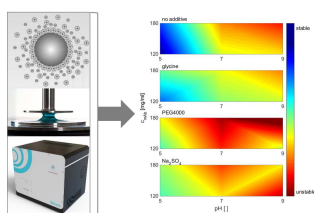
Protein solution stability needs to be engineered and monitored throughout production and storage. In contrast to the gold standard of long-term storage experiments applied in industry, novel experimental and *in silico* molecular dynamics tools for predicting protein solution stability can be applied within several minutes or hours. Here, a rheological approach in combination with molecular dynamics simulations are presented, for determining and predicting long-term phase behavior of highly concentrated protein solutions. A diversity of liquid phase conditions, including salt type, ionic strength, pH and protein concentration are tested in a Glutathione-S-Transferase (GST) case study, in combination with the enzyme with and without the solubility-enhancing Cherry-Tag™. The rheological characterization of GST and Cherry-GST solutions enabled a fast and efficient prediction

of protein instabilities without the need of long-term protein phase diagrams. Finally, the strong solubility enhancing properties of the Cherry-TagTM were revealed by investigating protein surface properties in MD simulations. The tag highly altered the overall surface charge and hydrophobicity of GST, making it less accessible to alteration by the chemical surrounding.

Characterization of highly concentrated antibody solution - A toolbox for the description of long-term solution stability

Marie-Therese Schermeyer, Anna K. Wöll, Bas Kokke, Michel Eppink and Jürgen Hub-
buch

mAbs (2017), accepted manuscript

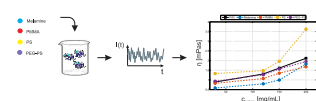


For a better understanding of highly concentrated solutions, this work combines established and novel analytical tools to characterize the impact of solution properties on the stability of highly concentrated mAb formulations. In this study monoclonal antibody solutions in a concentration range of 50 - 200 mg/ml at pH 5 - 9 with and without glycine, PEG4000 and Na_2SO_4 were analyzed. To determine the monomer content analytical SEC runs were performed. ζ -potential measurements were conducted to analyse the electrophoretic properties within different solutions. The melting and aggregation temperatures were determined with the help of fluorescence and static light scattering measurements. Additionally, rheological measurements were conducted to study the solution viscosity and the viscoelastic behavior of the mAb solutions. The so determined analytical parameters were scored and merged as an analytical toolbox. The resulting scoring was then successfully correlated with long-term storage (40 days of incubation) experiments. The study indicates that the sensitivity of complex rheological measurements in combination with the applied techniques allow reliable statements about the impact of solution properties such as protein concentration, ionic strength and pH shift on the strength of protein-protein interaction and solution colloidal stability.

Impact of polymer surface characteristics on the microrheological measurement quality of protein solutions - a tracer particle screening

Katharina C. Bauer*, Marie-Therese Schermeyer*, Jonathan Seidel and Jürgen Hubbuch
International Journal of Pharmaceutics 505 (2016): 246-54.

*contributed equally



In the present work a screening of melamine, PMMA, polystyrene and surface modified polystyrene as tracer particles for conduction of microrheological measurements were investigated at various protein solution conditions. The sur-

face characteristics of the screened tracer particles were evaluated by zeta potential measurements. Furthermore each tracer particle was used to determine the dynamic viscosity of lysozyme solutions by microrheology and compared to a standard. The results indicate that the selection of the tracer particle had a strong impact on the quality of the microrheological measurement dependent on pH and additive type. Surface modified polystyrene was the only tracer particle that yielded good microrheological results for all tested conditions. The study indicated that the electrostatic surface charge of the tracer particle had a minor impact than its hydrophobicity. This characteristic was the crucial surface property that needs to be considered for the selection of a suitable tracer particle to achieve high measurement accuracy.

Implementation of an analytical microfluidic device for the quantification of protein concentrations in a high-throughput format

Carsten Philipp Radtke¹, Marie-Therese Schermeyer¹, Yün Claudia Zhai, Jacqueline Göpper and Jürgen Hubbuch

Institute of Engineering in Life Sciences, Section IV: Biomolecular Separation Science, Karlsruhe Institute of Technology (KIT), 76131 Karlsruhe, Germany

¹ *These authors contributed equally to this work.*

Abstract

Nowadays the performance of experiments in automated microliter scale format are common practice in the biopharmaceutical process development. The increased number of experiments, reduced sample volumes and usage of robotic platforms require the adjustment of photometric measurements to determine the protein concentration. This work presents the qualification and usage of a disposable measurement device which can be used with conventional microplate photometers. The application of the microfluidic device (μ F-device) allows absorption measurements of protein concentrations from around 0.1 to 100 mg/mL with an accuracy of 99.2 % dependent on given protein extinction coefficients. The integrated four measurement chambers of increasing height (100 – 1500 μ m) allow the direct calculation of calibration curves and the determination of protein concentrations independent of used optical path lengths with a sample volume of 36 μ L. This study contains the validation of the analytical μ F-device according to ICH Guidelines as well as a representative case study. A salt gradient screening with chromatography columns in microliter scale performed on a liquid handling station presents the usability of the μ F-device. It is shown that an improvement of the repeatability and accuracy of the chromatograms could be achieved by μ F-device implementation in comparison to photometric measurements performed in microtiter plates.

Keywords: *absorption measurement; high protein concentration; high throughput experimentation; microfluidic*

6.1 Introduction

The market of biopharmaceuticals is steadily growing especially the commercialization of monoclonal antibody drug substances [168]. This trend requires the development of new process steps as well as the optimization of established ones. The purification development of the complex molecules is regarded as the most cost and time intensive step due to high investment and material costs [169]. To face these disadvantages the downstream development focusses on statistically based design of experiments [170] as well as automated sample handling and analysis [171] at an early phase. At this early phase of product development only a low amount of target molecules are available. To gain the highest amount of information out of the given low sample volume the execution of high throughput screening procedures in microliter scale is the method of choice [172, 173]. Many process steps are already established in an automated microscale format, like microliter scale chromatography [174] or precipitation screenings [175]. Unfortunately they are not used to their full potential due to limited integrated analytical methods. Implemented analytical methods are often time consuming, do need high sample volumes and are not specialized to the extended determination range tested in the high throughput format. One of the most important parameters to be tested is the product yield and the impurity concentration. The method of choice to determine these parameters are photometric measurements. Dependent on the tested process step, the concentrations to be determined vary from around 0.01 mg/mL to more than 100 mg/mL. Thus, the analytical method has to cover a wide concentration range. Since conventional photometric methods do not cover this range the samples have to be diluted. The dilution of the samples increase the inaccuracy of the measurement and requires a rough knowledge of the initial concentration of the molecule to be measured. Aggravating this situation in some cases, not only one specific type of molecule has to be quantified but also samples with different types of molecules, with varying extinction coefficients and concentrations. One example is the determination of target molecule and impurity concentrations of fractions collected from chromatography runs. The selection of the optimal dilution requires previous knowledge of expected protein content to avoid measurement inaccuracy for one type of the molecules to be determined. Every photometric detector has a specific absorption limit depending on given device properties. Based on the Lambert Beer Law, the absorption

A and therefore the maximum measurable protein concentration c is linearly dependent on the extinction coefficient ϵ_λ and the path length d of the measurement cell.

$$A = c * \epsilon_\lambda * d \tag{6.1}$$

The extinction coefficient ϵ_λ is dependent on the amino acids on the protein surface which absorb light at the set wave length and therefore specific for every protein. The parameter which can be manipulated by the developers is the path length d . The linear relation of d to A led to the implementation of novel instruments with lower or flexible path lengths. One example therefore is the Nanodrop spectrophotometer series from Thermo Scientific (Waltham, USA) [176]. With these tools one to eight sample drops with a volume of $2 \mu\text{L}$ are contained by surface tension between two planar surfaces. The instruments can generate path lengths between 1 and 0.05 mm. The low sample consumption, easy usage and the relatively high protein concentration which can be measured directly, explain the sales volume of these instruments. The Solo VPE from C. Technologies Inc. (Bridgewater, USA) is able to change the optical path length from 0.01 mm to 15 mm via a movable optical fiber (FibretteTM). From the variable path length data the slope m can be calculated ($m = \Delta A / \Delta d$). With m and known ϵ_λ the protein concentration can be determined. Due to many measurement points over a wide path length range the tool is very precise and covers a huge protein concentration range [177]. Disadvantages of described tools are the manual operation and the limited number of samples which can be measured simultaneously (one sample (Nanodrop 2000c and Solo VPE) to eight samples (Nanodrop 8000)). Thus they are hardly automatable nor high throughput compatible. An instrument which meets the high throughput needs of the biopharmaceutical process development is the DropSenseTM 96 UV/VIS droplet reader from Trinean (Gentbrugge, Belgium). This instrument also has a very small sample consumption of $2 \mu\text{L}$ and is equipped with 96-well robotic compatible measurement units. Here the protein absorption is measured in two chambers of differing heights. This two point measurement does not allow the application of the slope technique implemented with the SoloVPE. The microfluidic device (μF -device) presented in the current study is an approach to combine the advantages of the instruments described above. The μF -device and its channel structures are constructed according to the microplate format. The specific design of the channel structures, each with four measurement chambers of different height, allow the application of the slope method for an increased measurement accuracy and a direct four-point calibration of every measured sample. Especially to be

emphasized is the accurate measurement in a wide protein concentration range enabled by the provided path lengths. Furthermore, microplate photometers already implemented in the lab can be used so that no investment in a new instrument has to be done.

6.2 Materials and Methods

6.2.1 Design and manufacturing of the μ F-device

6.2.1.1 Materials

The two component curing silicone Elastosil[®]RT 601 (Wacker Chemie, Burghausen, Germany), a polydimethylsiloxane (PDMS), was used for manufacturing the μ F-device. The replication master for the μ F-device was designed in-house and manufactured by Proform AG (Marly, Switzerland). This master served as inverted structure in the molding cavity and therefore defined the channels of the molded μ F-device. The master was designed according to the microwell plate standard. A total of 96 channel structures are evenly distributed on the master. The inlets of the channel structures are vertical cylinders which are aligned such as wells of a 96-well plate (see figure 6.1).

Connected to the inlet, a circular channel with four oval chambers and a vertical outlet on the end was designed. The four chambers have different heights (100, 600, 1000 and 1500 μ m) and are arranged in the pattern of the wells of a 384-well plate. This allows a simple read out of the chambers in the microplate photometer. To improve the stability and the automated handling of the μ F-device on the liquid handling station (LHS), the silicone μ F-device was placed inside a specially designed, 3D printed cartridge (Sculpteo, Villejuif, France). This cartridge allowed the handling by the robotic manipulator arm of the LHS. The measurement in the microplate photometer was possible through 384 perforations which were arranged evenly according to the microplate standard.

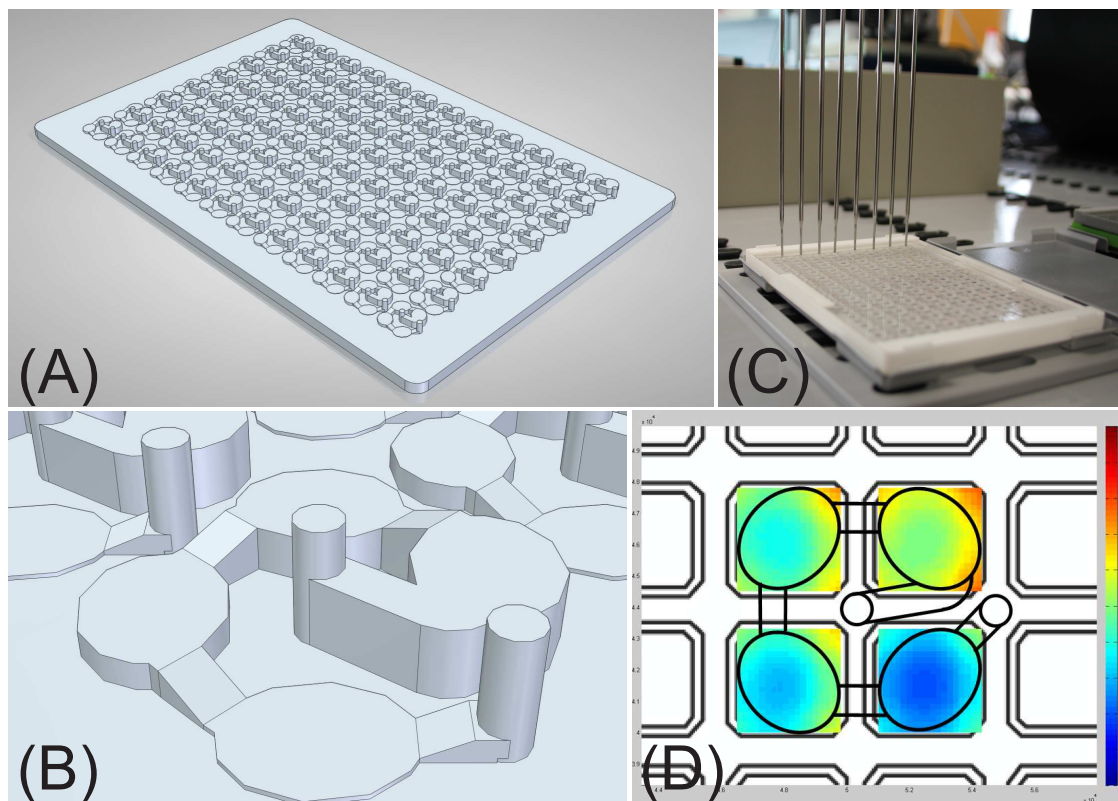


Figure 6.1: (A) CAD model of the replication master for the manufacturing of the μ F-device. (B) Magnified channel structure with the four measuring chambers of varying channel height (100, 600, 1000, and 1500 μm) (C) Photograph of the assembled device on the deck of the liquid handling station. The LHS-tips dispense the samples directly into the channel structures eight at a time. (D) Visualization of the absorption data gained in the four measuring chambers of one channel structure to illustrate the absorption gradient due to the differing channel heights.

6.2.1.2 Methods

The molding process of the μ F-device was executed as described by Waldbaur, Kittelmann, Radtke & Hubbuch [178]. Only the spacer part of the molding tool was replaced. To obtain a clear and plain surface, a flat piece of polished stainless steel was employed instead.

6.2.2 Qualification of the μ F-device

6.2.2.1 Materials

Lysozyme from Chicken egg white was purchased in solid form from Hampton Research (Aliso Viejo, USA). Acetic acid and sodium acetate for buffer preparation were purchased from Merck KGaA (Darmstadt, Germany). Ultrapure water (ISO 3696) was used to prepare all solutions. Protein solutions for μ F-device qualification were prepared in 20 mM acetate buffer at pH 5 with a nominal mass concentration of 50 mg/mL. A buffer exchange of the protein solution with Sephadex media from GE Healthcare (Buckinghamshire, Great Britain) was performed to remove buffer salts or other components present in the purchased protein preparations. The size exclusion chromatography (SEC) column was manually packed with a diameter of 2.5 cm and a bed height of 23 cm. The fractions were concentrated to a protein concentration of 100 mg/mL with the help of 20 mL Vivaspın ultra filtration spin columns (Sartorius, Goettingen, Germany) with a molecular weight cut off of 3000 Da. For liquid handling a Tecan Freedom Evo 200 (Tecan, Crailsheim, Germany) LHS equipped with 1 mL syringes was used. The LHS was equipped with an Infinite® M200 pro plate reader (Tecan, Crailsheim, Germany) and controlled by Magellan 7.1, both provided by Tecan. The LHS was controlled by Evoware 2.5 also provided by Tecan. To compare the absorption results of the μ F-device with an established method, measurements of protein absorption at 280 nm in the Nanodrop 2000 (Thermo Scientific, Waltham, USA) were performed.

6.2.2.2 Methods

The buffer exchange of the lysozyme solution was conducted at an ÄktaPrime plus system from GE Healthcare. A total of 5 mL of lysozyme solution with a concentration of 50 mg/mL was purified. The protein was fractionated in 10 mL Falcon tubes and the

concentration measured with an extinction coefficient of 22 L/(g*cm) with the Nanodrop 2000. The concentration of the dilute protein concentration was performed with Vivaspins and a rotational speed of 8000 rad/sec. A protein dilution series from 100 mg/mL to 0.1 mg/mL with acetate buffer was prepared. The μ F-device was automatically handled and filled on the robotic platform. The absorption at 280 nm of protein solutions and buffer blanks were measured in the μ F-device in quadruplicate. For the calculation of protein concentration the Lambert-Beer Law was applied

$$c = \frac{A}{\epsilon_{\lambda} * d} \quad (6.2)$$

With the absorption A, the concentration c [mg/mL], the extinction coefficient ϵ_{λ} [mL/mg*cm] and the path length d [cm]. Additionally the slope m, which results of the absorptions plotted against the four given path lengths was determined. With this slope the calculation of protein concentrations with increased measurement accuracy became possible.

$$c = \frac{m}{\epsilon_{\lambda}} \quad (6.3)$$

The evaluation of gained results and consequently the validation of the μ F-device followed the International Conference on Harmonisation (ICH) harmonized tripartite guideline Q2(R1) (Validation of analytical procedures: text and methodology) [15]. Following these guidelines the accuracy, repeatability and measuring range of absorption results gained with the developed analytical μ F-device were studied. To prove the precision of the analytical device lysozyme solution with a concentration of 5 mg/mL was prepared and measured in four measurement units of the μ F-device. The deviation of the absorption measurements were calculated. To determine the absorption range of the μ F-device, lysozyme solutions in a concentration range of 0.1 and 100 mg/mL were prepared and measured in quadruplicate.

6.2.3 Case Study

6.2.3.1 Materials

For the chromatography runs the buffer described in section 2.1 was used (Buffer A). By adding 1.25 M sodium chloride (NaCl) (Merck, Darmstadt, Germany) to Buffer A the high salt buffer (Buffer B) was prepared. Purified monoclonal antibody (mAb) solution was provided by Synthron (Nijmegen, Netherlands). Cytochrome C (CytC) was purchased as lyophilized powder from Sigma-Aldrich (St. Louis, USA). The mAb stock solution was buffer exchanged and concentrated to 65 mg/mL by 20 mL Vivaspins with a molecular weight cut off of 50000 Da. For fraction collection, fraction volume determination and UV absorption measurements, half area UV-MTPs were used. For the preparation of high salt buffers and the dilution of elution fractions two 96 deep well square plates (DWP) (VWR, Germany) with a volumetric capacity of 2 mL were used. RoboColumns[®] prepacked with 200 μ L SP Sepharose FF were purchased from Atoll GmbH (Weingarten, Germany). Column chromatography in high throughput experimental mode using RoboColumns[®] was performed on a Tecan Freedom Evo 200 LHS, additionally equipped with a Te-Chrom column carrier.

6.2.3.2 Methods

To prepare the elution buffers, two different troughs with Buffer A and Buffer B were assigned to the robotic platform. These components were mixed automatically in a DWP to achieve four salt gradients with respectively 10 salt steps resulting in different end concentrations. The gained end salt concentrations were 1.25 M, 1 M, 0.75 M and 0.5 M NaCl. CytC was dissolved in acetate buffer and transferred to the mAb solution to reach a starting protein concentration of 60 mg/mL mAb and 3 mg/mL CytC. This solution was transferred to eight Eppendorf Tubes (Eppendorf, Hamburg, Germany) and also placed in designated carriers on the robotic platform. A detailed description of parallelized chromatography performed automated on an LHS has been published by Wiendahl *et al.* [177]. In this case study an exemplary salt gradient screening was performed. Therefore, four gradients of varying slopes were tested to separate mAb molecules from CytC via cation-exchange chromatography (CEX). The salt gradients had a length of ten column volumes respectively 2 mL with different end salt concentrations which resulted in four different salt gradient slopes. For every tested salt gradient twenty elution fractions with a

set volume of 100 μL were collected in half area UV-MTP. After measuring the absorption at 900 and 990 nm to gain information of the precise fraction volumes following the method published by McGown & Hafeman [179] and Lampinen *et al.* [180], 38 μL of the samples were transferred to the presented analytical μF -device. A volume of 20 μL of the samples for the 1:50 dilution and 33 μL for the 1:15 dilution were transferred to DWPs. To reach the respective dilution low salt buffer was added to every sample (980 μL respectively 467 μL), mixed and transferred to a full area UV-MTP. Afterwards the absorption at 280 nm and 410 nm was measured of undiluted samples transferred to the μF -device and diluted samples transferred to the UV-MTPs. Every cation-exchange run was executed and analyzed in duplicate.

6.3 Results

6.3.1 Qualification of the μF -device

According to the ICH Q2 guidelines the μF -device has been tested in regard to accuracy, precision (repeatability), linearity and range. For the qualification a lysozyme solution series from 0.1 – 100 mg/mL was prepared. After the preparation the theoretical lysozyme concentration was verified by fourfold absorption measurements with the Nanodrop 2000. The determined concentration values can be found in figure 6.2.

For qualification the absorption of every sample was determined in four channel structures. Additionally a buffer blank was measured and subtracted from the protein absorption values. The absorption values were plotted against the height of the four measuring chambers synonymous to the optical path length. The resulting values and the zero value were fitted with a linear regression. Values deviating from the regression line by more than 3 % were excluded from the regression of the second fit calculation. Thereupon, the slope m of the optimized regression was calculated for every measured sample. With m and ϵ_{280} (equation 6.3) the concentration could be calculated. In figure 6.2a the described method is exemplarily shown for a protein sample containing 4.9 mg/mL lysozyme. For this measurement the slope m with a value of 10.71 1/cm was calculated which resulted in a protein concentration of 4.87 mg/ml (see equation 6.3). For measurements in the areas of the upper and lower detection limits the concentration can directly be calculated with the application of the Lambert-Beer law (equation 6.2). Here only the highest or lowest channel height was suitable for the exact absorption measurement. For the used

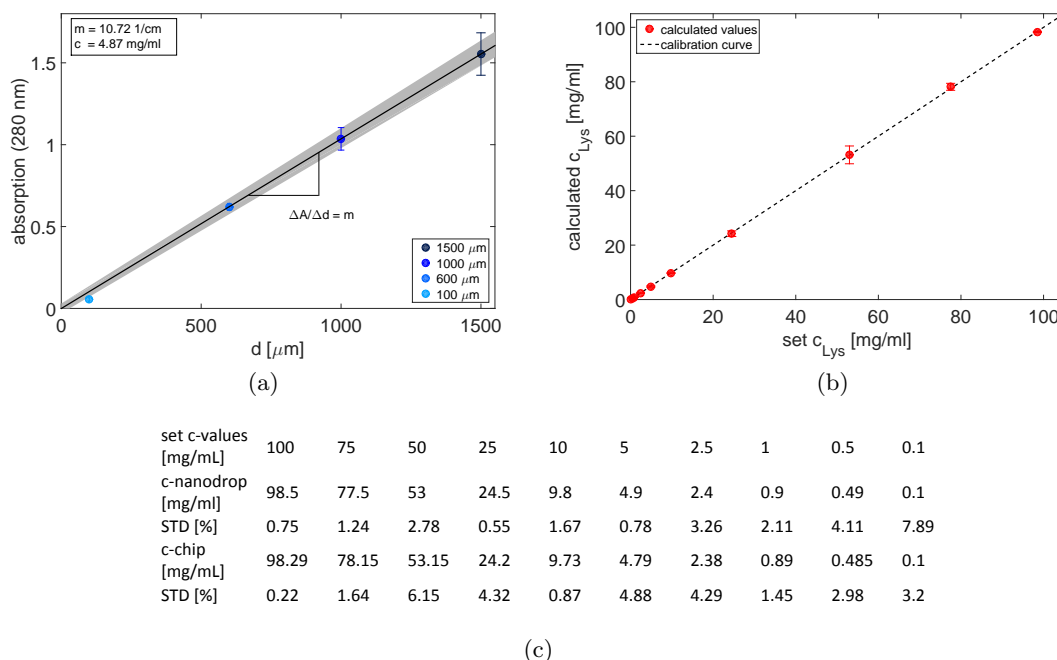


Figure 6.2: (a) Lysozyme absorption values measured in the μ F-device plotted against the channel height. Exemplarily determination of the slope m of the regression line. The reference concentration of this sample measured in Nanodrop 2000 was 4.9 mg/mL. (b) Calculated lysozyme concentrations based on μ F-device absorption data plotted against set concentration values with corresponding standard deviations. (c) Tabular listing of theoretical lysozyme concentrations, concentrations based on Nanodrop measurements and concentrations based on μ F-device measurements with corresponding standard deviations.

photometer the range of detection was between 0.001 and 2.3 OD. Calculated lysozyme concentrations can be found in the tabular listing in figure 6.2c. For the visualization of the gained results, the lysozyme concentrations and related standard deviations determined with the μ F-device are plotted against set concentration values determined by Nanodrop measurements in figure 6.2b.

6.3.2 Case Study

The presented analytical μ F-device enables direct protein absorption measurements in a wide concentration range implementable on a liquid handling station. In order to demonstrate the applicability of the μ F-device it was implemented in a HTE (high throughput

experimentation) process development step. For this, HTE chromatography was performed with a binary protein solution containing mAb with a starting concentration of 65 mg/mL and CytC with a starting concentration of 3 mg/mL. The actual aim of the chromatography screening was to find the optimal salt gradient to separate these two proteins. For this, four gradients of varying slope and end salt concentration were tested in duplicate. Important for the selection of the best suited gradient was the proper determination of protein concentration in the collected elution fractions. The elution fractions were analyzed directly in the channel structures of the μ F-device respectively in four chambers of differing heights and after dilution of the fractions in MTPs for comparison. The absorption values of every single fraction are displayed as round symbols in figure 6.3 and figure 6.4. The absorption values of the mAb and CytC molecules were separated with the help of the also measured absorption at 410 nm wavelength. At this wavelength CytC has a second absorption maximum whereas mAb does not absorb light. With the known absorption ratio of 280 nm and 410 nm of CytC (0.24, data not shown) the detected 280 nm sum signal could be divided in mAb and CytC specific absorption. The absorption values of the 20 elution fractions formed the basis of a nonlinear Gaussian fit for the preparation of chromatograms describing the elution of the molecules. In figure 6.3 the absorption values at 280 nm from mAb and CytC are plotted against the elution volume.

The fitted chromatogram represents the run with the steepest salt gradient with absorption values measured in the measuring chambers from 100 μ m to 1500 μ m path length in the μ F-device. With decreasing channel height the absorption values decreased. The mAb represented by the blue symbols eluted first over an elution volume of 1000 μ L. CytC, represented by the red symbols, starts to elute at around 650 μ L and over an elution volume of 850 μ L. No baseline separation could be achieved. Independent on the chamber height the curve progression was similar. Only the absorption signals of CytC measured with a path length of 100 μ m did not show a significant absorption peak. Depending on the salt gradient slope the chromatograms showed varying resolutions. The plot set in figure 6.4 a-d illustrates the influence of the varying salt gradients on the resolution of the chromatographic runs.

The graphs contain the absorption values measured in the channels at a path length of 1000 μ m and absorption values measured in a UV MTP. For the measurement in the MTP the fractions had to be diluted. Depending on the expected protein content the samples were diluted in a ratio of 1:50 (fraction 1-12) respectively in a ratio of 1:15 (fraction 13-20). The shown absorption values of the MTP are standardized to a dilution

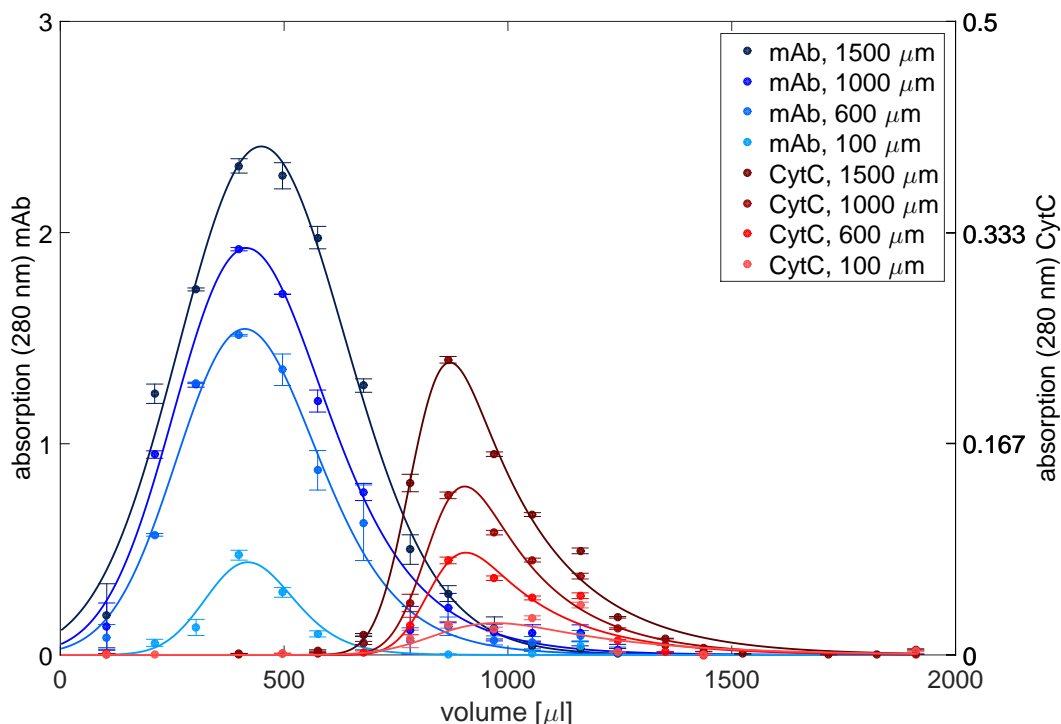


Figure 6.3: Elution profiles of mAb and CytC with a gradient from 0–1.25 mM NaCl in 10 CV. Plotted are absorption values at 280 nm measured in the μ F-device in the four respective measuring chambers with a height of 100, 600, 1000 and 1500 μ m. Absorption values of mAb are plotted as blue circles, absorption values of CytC are plotted as red circles. The absorption values were fitted with a nonlinear Gaussian fit (blue and red lines).

of 1:50. With decreasing slope of the salt gradient the detected elution peaks of both protein types widened. Additionally the elution points were shifted to higher volumes and the resolution of the separation declined. In figure 6.4d the run with the lowest gradient is depicted. Here the elution peak of the mAb overlays the CytC elution peak. The absolute absorption values of the MTP were lower in the order of magnitude of around 75 % in comparison to absorption values measured in the 1000 μ m chamber of the μ F-device. With decreasing slope of the salt gradient the chosen nonlinear Gaussian fit did get less precise independent on measurement device. In figure 6.4a fraction 4, 9 and 13 (F4, F9 and F13) are highlighted in yellow. For these fractions the approach to calculate protein concentrations from μ F-device absorption data is shown for both proteins (figures 6.5a and 6.5b) and compared to the calculated protein concentrations based on MTP absorption data (figure 6.5a).

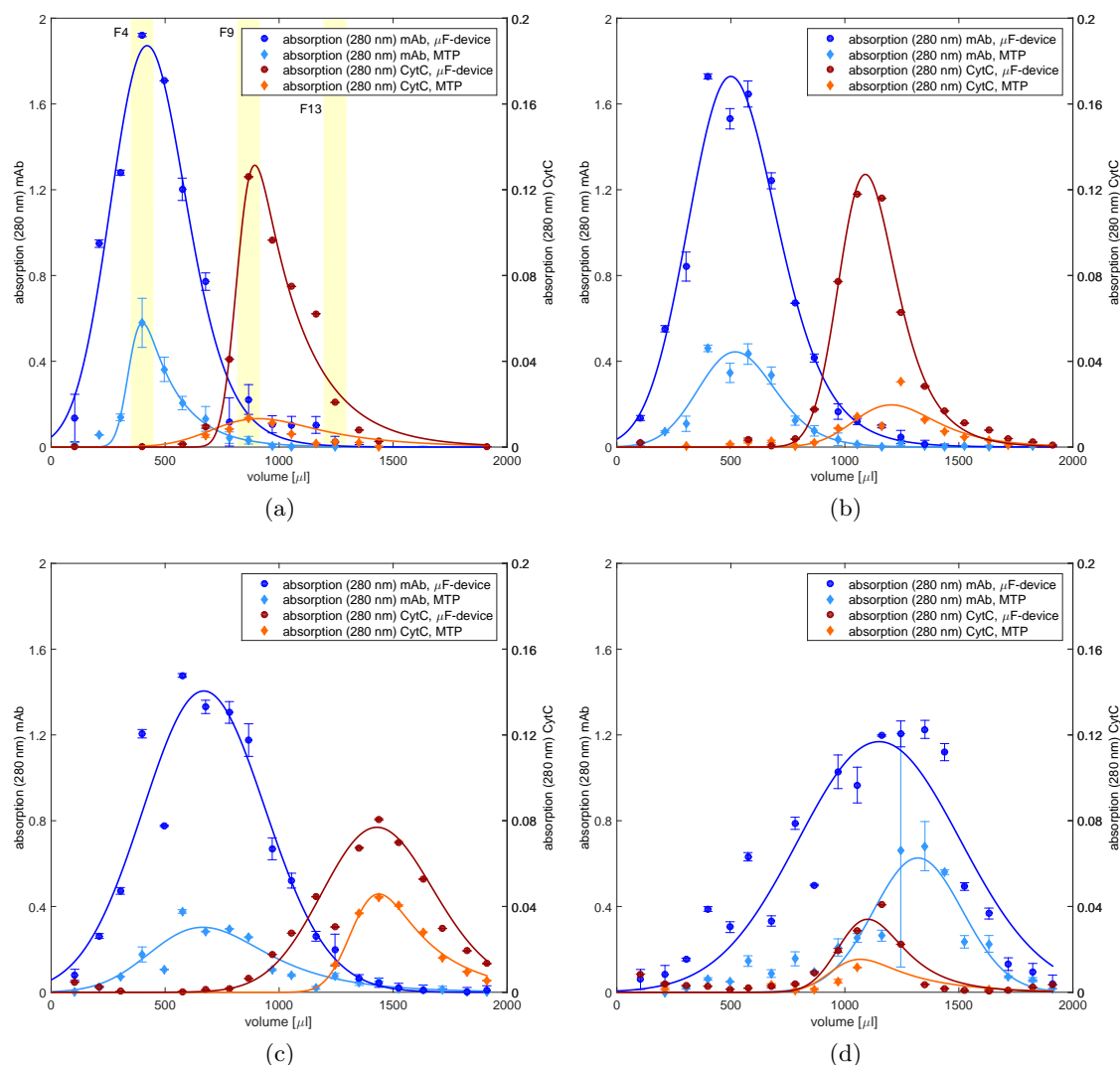


Figure 6.4: Chromatograms of the four screened elution gradients of mAb and CytC absorption values. Illustrated are absorption values with related standard deviations measured in the μ F-device in a measuring chamber height of 1000 μ m and absorption values measured in MTP after dilution. (a) Gradient from 0 – 1.25 mM NaCl in 10 CV, highlighted are fraction 4, 9 and 13 which have been further investigated; (b) gradient from 0 – 1 mM NaCl in 10 CV; (c) gradient from 0 – 0.75 mM NaCl in 10 CV; (d) gradient from 0 – 0.5 mM NaCl in 10 CV.

In figure 6.5a and 6.5b the mAb respectively CytC absorption values of F4, F9 and F13 are plotted against the path lengths of the measuring chambers of the μ F-device.

6.3 Results

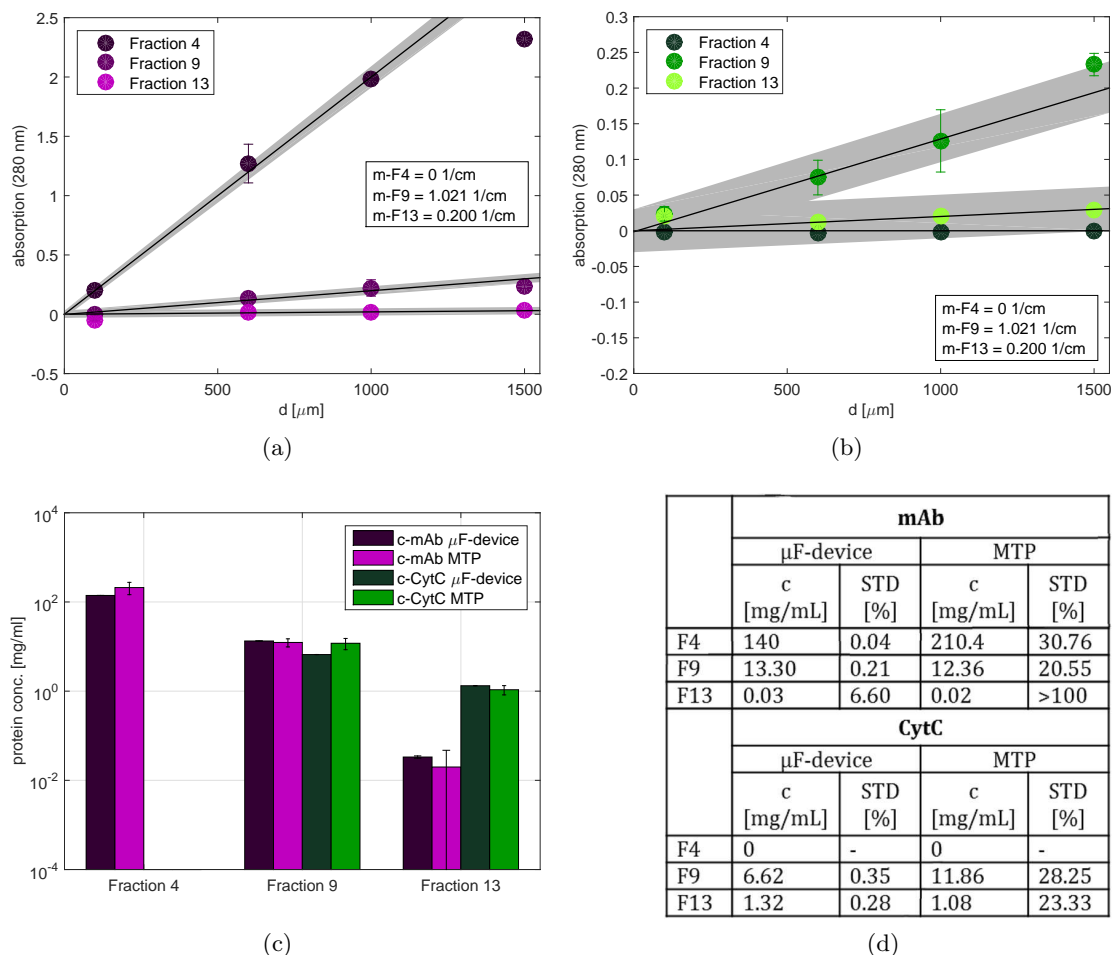


Figure 6.5: Absorption values with related standard deviations of fraction 4, 9 and 13 from mAb (a) and CytC (b) measured in the μF -device plotted against channel height with regression lines and related slope values m . The grey area depicts the allowed deviation of 3 %. (c, d) Protein concentrations with related standard deviations of F4, F9 and F13 calculated based on μF -device absorption values (dark colored) and based on MTP absorption values (light colored). The concentrations based on absorption values measured in the μF -device were calculated with the slope method (equation 6.3).

The regression lines were calculated based on at least 3 measured values of one channel structure in duplicate. Measurement values which deviated from this regression by more than 3 % were not included in the calculation of the slope m . The mAb absorption value for F4 determined with a path length of 1500 μm was eliminated from further calculations due to this deviation as well as the CytC absorption value of F9 which was determined

with a chamber height of 1500 μm and F13 which was determined with a chamber height of 100 μm . This exclusion criteria is illustrated by the grey area in figures 6.5a and 6.5b. The calculated regression coefficients (R2) for shown data all had a value above 0.996. The corresponding protein concentrations were determined following equation 6.3. The protein concentrations of similar fractions were also determined based on absorption measurements conducted in MTPs. The so calculated mAb and CytC concentrations are compared to μF -device results in figure 6.5c. To display the wide protein concentration range of chosen fractions in one plot, a logarithmic scale was selected. The highest mAb concentration could be found in F4 with a value of 140 mg/mL based on data of the μF -device and a standard deviation of 0.04 % and 210 mg/mL based on MTP data with a standard deviation of 30.1 %. In F9 both molecules were present at a comparable concentration. In F13 the lowest mAb concentration was detected with in a value of 0.02 – 0.03 mg/mL. All calculated protein concentrations with associated standard deviations can be found in a tabular listing in figure 6.5d.

6.4 Discussion

6.4.1 Qualification of the μF -device

In this section the validation of the presented analytical tool according to accuracy, repeatability, linearity and range as prescribed by the ICH guideline Q2 (R1) is discussed. The comparison between measured protein concentrations determined with the μF -device and the reference concentration values determined with the Nanodrop 2000 (see figure 6.2) illustrates an excellent consistency. In accordance to ICH guidelines this complies the validation criterion of accuracy. The determined accuracy was 99.02 % in a concentration range of 0.5 – 10 mg/mL (equation 6.3) and 99.92 % in a range of 0.1 – 0.5 mg/mL and 10 – 100 mg/mL Lysozyme. The obtained measurement deviations can be explained by the manual manufacturing of the μF -device and the used silicone material with relatively low stiffness. With known protein concentration the applied slope method and so fitted calibration curve can be used to calculate the extinction coefficient with only one protein sample respectively one starting concentration. Nonetheless, with the fourfold measurement of ten different lysozyme concentrations an excellent repeatability could be determined expressed by an average standard deviation of 3.1 %. The linearity of gained results could be shown both for plotting the absorption values over path length

($R^2 = 0.988$) and plotting calculated concentration over reference concentration values ($R^2 = 0.9998$) (see figure 6.2).

6.4.2 Case Study

The aim of the executed case study was to separate the mAb molecules with a relatively high starting concentration of 65 mg/mL from CytC molecules with a starting concentration of 3 mg/mL. To find an optimal separation with CEX a screening of four salt gradients differing in slope and end salt concentration were performed in microliter scale on a LHS. As assumed the mAb molecules with an isoelectric point (pI) of 7.9 eluted prior to CytC molecules with a pI of 10.4 for all performed runs with the exception of the run presented in figure 6.4d (this phenomenon will be discussed within the next paragraph). The explanation for this elution order can be found in the stronger electrostatic interaction of CytC with negatively charged ligands in comparison with weaker adsorption of mAb molecules on the resin. Thus, a higher salt concentration is necessary to desorb the CytC molecules from the resin what implies a later elution. With decreasing gradient slope the peaks were shifted to later elution volumes. In figure 6.4d it seems that CytC is eluting with the mAb molecules but taking the mass balance of CytC molecules into account, it can be expected that the main peak of CytC elutes outside the set fraction range. The elution of CytC at comparatively low salt concentrations are potentially caused by a specific interaction with the mAb and thus a co-elution of CytC molecules. The best chromatographic resolution could be found with the steepest gradient and an end salt concentration of 1.25 mM NaCl. To further optimize the run with the aim of a baseline separation, a step elution with a step height of 0.4 mM NaCl hold for 5 CV for mAb elution and a second step with 1.25 mM NaCl hold for 4 CV to elute CytC from the column is recommended, based on the results of the gradient screening. In the next paragraph the absorption values of μ F-device measurements will be discussed and compared to MTP absorption measurements. Fractions analyzed with the analytical device have a mean standard deviation of 3.5 % compared to MTP measurements with a mean standard deviation of 8.2 % (see figure 6.3 and 6.4). The higher accuracy of absorption measurements executed with the μ F-device can be explained by direct analysis of all fractionated samples without the need of dilution. In figure 6.3 the absorption measurements of every measuring chamber is plotted. The decrease of absorption values with decreasing path length respectively height of measuring chamber is in good agreement with the Lambert Beer law (equation 6.1). The selected nonlinear Gaussian fit represents

the absorption values very precise. This not only implies that the absorption values can be fitted with a characteristic chromatographic elution curve but also that the absorption values actually represents the eluting protein amount. The CytC peak cannot be depicted well by the fit of results of the 100 μm measuring chamber. Here, the measured absorption values of CytC are close to the buffer blank absorption what may explain the weak fit results. In figure 6.4 the influence of the salt gradient on the elution profile measured in the μF -device and in the MTP is shown. The absolute absorption values of the MTP and the μF -device varied due to divergent path length and the dilution of the fractions for MTP measurements. In principal the curve progressions of chromatograms obtained by absorption results of the μF -device and MTP are comparable as well as elution starting points, absorption maxima and elution end points. Deviations traceable to the measurement system are obtained with CytC peaks and were especially significant at the flattest tested gradient (see figure 6.4d). One explanation may be the chosen dilution rate of 1:50 for the fractions F1-F12. Due to the low amount of CytC in these fractions the error caused by dilution had a higher impact. Contributing to this assumption the comparability of CytC peaks was better for a flatter gradient depicted in figure 6.4c. Here, CytC molecules elute where the fractions have been diluted in a ratio of 1:15 what gives a better precision of the results. In all displayed graphs the measured absorption values oscillate around the fit curve for measurements executed in μF -device and MTP. The oscillatory movement is periodical and due to the practical implementation of the chromatographic run on the LHS. The dispensing of the buffers is not continuous as in common chromatographic runs but subsequently. This potentially cause a longer holding time of the proteins on the column. This phenomenon had an increased impact on fit results with decreasing salt gradient slope. To increase fit accuracy the step size as well as the fraction size should be decreased. To depict the dependencies of specific path length of the measuring chambers on the absorption values the linear relation is shown in figure 6.5a and 6.5b for three exemplarily chosen fractions (F4, F9, and F13). The regression coefficient of 0.996 proves the linearity of the adsorption values gained with different chamber heights. The mAb absorption value of F4 measured in the chamber with a height of 1500 μm was excluded from further calculations due to the exceedance of the determined absorption limit of 2.3 OD. The same reasoning applies to the CytC absorption value of F13 measured in a chamber of 100 μm height. At this point the quantification limit was reached. This explanation does not hold true for the deviation of the CytC absorption value of F9 measured in the 1500 μm chamber height. Here the deviation is potentially due to a measurement error in the channel structure caused by small air bubbles. With the help of the slope of the discussed regression lines the concentra-

tions of mAb and CytC in the respective fractions could be calculated. These calculated concentrations were compared to the concentrations determined with MTP absorption values and are displayed in figure 6.5c. The calculated values represent the expected concentrations of mAb and CytC when taking the related chromatograms of figure 6.4a into account. In direct comparison, deviations between MTP and μ F-device results of more than 60 % were detected for both protein species. One explanation of these high discrepancies can be found in the extent of calculated standard deviations. The standard deviations of determined mean protein concentrations measured in the microfluidic channels had a maximum value of 0.06 mg/mL. The comparatively low standard deviations of these measurements prove the reliability of the developed μ F-device. In contrast, the standard deviations of protein concentrations determined with MTP were between 1.08 and 64.71 mg/mL (20 – >100 %). These standard deviations were so high that the standard deviation error also covered concentrations calculated with μ F-device absorption results. The high standard deviations of the concentrations calculated based on MTP results could be explained with dilution errors, additional required liquid handling steps and the potential formation of a meniscus in the wells of the MTP. The angle of this meniscus is highly dependent on protein concentration and buffer compositions. The consideration of this phenomenon is complex especially when measuring varying concentrations at varying liquid levels during one screening, such as occurred in this case study. The deviations potentially caused by meniscus can be excluded by application of the μ F-device due to the completely filled channel structures. Including the discussed standard deviations the calculated concentrations based on μ F-device and MTP results are comparable and support the statement that the presented μ F-device is applicable for absorption measurements. In the discussed case study the target molecule (mAb) and the impurity (CytC) could be quantified due to the second absorption maximum of Cytochrome C at 410 nm. To distinguish between target molecule and impurities having similar absorption characteristics the spectral method published by Hansen, Skibsted, Staby & Hubbuch [181] and Hansen, Jamali & Hubbuch [182] may be transferred to the presented μ F-device. This possible application will be part of future investigations.

6.5 Concluding Remarks

The presented analytical μ F-device could be validated according to ICH guidelines. In the course of this validation the accuracy, repeatability and linearity was proven for a

concentration range from 0.1 – 100 mg/mL, with lysozyme as model protein. This qualification permits the application of the μ F- device for protein absorption measurements in the biopharmaceutical process development. The case study demonstrated a successful application of the μ F-device on a liquid handling station. The analytical μ F-device was simple to implement in an existing automated development step. Furthermore, the absorption of elution fractions measured with the presented μ F-device resulted in comprehensible characteristic elution profiles. Consequently, the μ F-device presented in this study is a promising alternative or supplement to existing devices combining a wide measurement range with high throughput compatibility.

6.6 Acknowledgments

This research work is part of the project „Molecular Interaction Engineering: From Nature’s Toolbox to Hybrid Technical Systems“, which is funded by the German Federal Ministry of Education and Research (BMBF), funding code 031A095B and the project “Euro Trans Bio”, also funded by the BMBF, funding code 031607B. The authors bear the complete responsibility for the content of this publication. Special thanks go to Gang Wang for the modeling support.

6.7 References

168. Walsh, G. Biopharmaceutical benchmarks 2014. *Nature Biotechnology* **32**, 992–1000 (2014).
169. Lowe, C. R., Lowe, A. R. & Gupta, G. New developments in affinity chromatography with potential application in the production of biopharmaceuticals. *Journal of Biochemical and Biophysical Methods* **49**, 561–574 (2001).
170. Nfor, B. K. *et al.* Rational and systematic protein purification process development: the next generation. *Trends in Biotechnology* **27**, 673–679 (2009).
171. Bhambure, R., Kumar, K. & Rathore, A. S. High-throughput process development for biopharmaceutical drug substances. *Trends in Biotechnology* **29**, 127–135 (2011).
172. Hertzberg, R. P. & Pope, A. J. High-throughput screening: new technology for the 21st century. *Current Opinion in Chemical Biology* **4**, 445–451 (2000).

173. Nfor, B. K. *et al.* Design strategies for integrated protein purification processes: challenges, progress and outlook. *Journal of Chemical Technology & Biotechnology* **83**, 124–132 (2008).
174. Bensch, M., Schulze Wierling, P., von Lieres, E. & Hubbuch, J. High Throughput Screening of Chromatographic Phases for Rapid Process Development. *Chemical Engineering & Technology* **28**, 1274–1284 (2005).
175. Wiendahl, M. *et al.* A novel method to evaluate protein solubility using a high throughput screening approach. *Chemical Engineering Science* **64**, 3778–3788 (2009).
176. Robertson, C. US6628382 B2 (2003).
177. Wiendahl, M. *et al.* High Throughput Screening for the Design and Optimization of Chromatographic Processes – Miniaturization, Automation and Parallelization of Breakthrough and Elution Studies. *Chemical Engineering & Technology* **31**, 893–903 (2008).
178. Waldbaur, A., Kittelmann, J., Radtke, C. P. & Hubbuch, J. Microfluidics on liquid handling stations (μ F-on-LHS): an industry compatible chip interface between microfluidics and automated liquid handling stations. *Lab on a Chip* **13**, 2337–2343 (2013).
179. McGown, E. L. & Hafeman, D. G. *Multichannel Pipettor Performance Verified by Measuring Pathlength of Reagent Dispensed into a Microplate* 1998.
180. Lampinen, J. *et al.* Microplate Based Pathlength Correction Method for Photometric DNA Quantification Assay (1993).
181. Hansen, S. K., Skibsted, E., Staby, A. & Hubbuch, J. A label-free methodology for selective protein quantification by means of absorption measurements. *Biotechnology and bioengineering* **108**, 2661–2669 (11/2011).
182. Hansen, S. K., Jamali, B. & Hubbuch, J. Selective high throughput protein quantification based on UV absorption spectra. *Biotechnology and Bioengineering* **110**, 448–460 (02/2013).
253. Thakkar, S. V. *et al.* An Application of Ultraviolet Spectroscopy to Study Interactions in Proteins Solutions at High Concentrations. *Journal of Pharmaceutical Sciences* **101**, 3051–3061 (09/2012).

Squeeze flow rheometry as a novel tool for the characterization of highly concentrated protein solutions

Marie-Therese Schermeyer¹, Heike Sigloch¹, Katharina C. Bauer¹, Claude Oelschlaeger² and Jürgen Hubbuch¹

¹*Institute of Engineering in Life Sciences, Section IV: Biomolecular Separation Science, Karlsruhe Institute of Technology (KIT), 76131 Karlsruhe, Germany*

²*Institute of Mechanical Process Engineering and Mechanics, Department: Applied Mechanics, Karlsruhe Institute of Technology (KIT), 76131 Karlsruhe, Germany*

Abstract

This study aims at defining rheological parameters for the characterization of highly concentrated protein solutions. As a basis for comparing rheological behavior with protein solution characteristics the protein phase behavior of lysozyme from chicken egg white with concentrations up to 225 mg/mL, changing pH values and additive concentrations was studied in a microbatch scale format. The prepared phase diagrams, scored after 40 days (t_{40}) give insights into the kind and kinetics of the phase transitions that occur. Oscillatory frequency sweep measurements of samples with exactly the same conditions were conducted immediately after preparation (t_0). The protein solutions behave viscoelastic and show a characteristic curve shape of the storage modulus (G') and the loss modulus (G''). The graphs provide information about the cross-linking degree of the respective sample. The measured rheological parameters were sensitive concerning solution composition, protein concentration and solution inner structure. The rheological moduli G' and G'' and especially the ratio of these parameters over a frequency range from 100 to 40000 rad/sec give information about the aggregation tendency of the protein under tested conditions. We succeeded to correlate protein phase behavior with the defined rheological key parameter ω_{CO} . This point represents the frequency value of the intersection point from G' and G'' . In our study lysozyme expressed a ω_{CO} threshold value of 20000 rad/sec as a lower limit for stable protein solutions. The predictability of lysozyme aggregation tendency and crystallization by means of squeeze flow rheometry is shown.

Keywords: *Protein Phase Behavior; Solubility; Formulation; Rheology; Storage and Loss Modulus*

7.1 Introduction

Over the lifespan of a biopharmaceutical molecule - combining development into drug substance and drug product - the molecule has to withstand different fluid phase transitions during processing, while the final formulation and storage buffer ensures a long-term stability of the final product.

Depending on the respective process the target molecule comes into contact with changing buffer conditions. Examples are a potential pH shift due to buffer exchange steps, an increase of the ionic strength as a result of the elution step in cation and anion exchange chromatography or the increase of the protein concentration after polishing operations. The buffer conditions applied influence protein solubility and hence aggregation tendency of the protein, depending on the molecule and the strength of the deviation from ideal conditions Dumetz, Snellinger-O'brien, Kaler & Lenhoff [54], Baumgartner *et al.* [88], and Pelegrine & Gasparetto [183]. While unintentional and irreversible aggregation needs to be avoided, controlled crystallization or precipitation might be a central step in modern processing. Finally one of the most decisive steps in the biopharmaceutical drug development are the formulation and storage of the final drug product. Without a proven long-term storage stability the aim of marketability can not be reached. Aggravating this situation, novel dosage forms like subcutaneous injections require volumes below 1.5 mL Liu, Nguyen, Andya & Shire [184]. To obtain a high enough medication dosage, one has to strongly increase the target molecule concentration in the formulation buffer. Due to the high concentration the agglomeration tendency increases and as a side effect of protein-protein interaction the viscosity increases as well.

It would thus be desirable to know physico-chemical parameters which contain information about the aggregation tendency of the target molecule for a given fluid phase or formulation. In order to address this issue it is state of the art to test the long-term stability of a target molecule via trial and error. The molecule is injected in the potentially appropriate buffer and then placed in a storage compartment until equilibrium is reached. Afterwards the sample is scored as stable or unstable. This method is generally accepted but it is time consuming and requires experience in the selection of appropriate buffers. An apriori prediction of the protein phase behavior would reduce development costs and time. However without a suitable characterization of protein solutions a worthwhile predictability of their phase behavior will never be reached. A better understanding of protein phase behavior in solution is necessary.

In the last decades a considerable amount of research work has been done to understand

protein behavior in varying solution conditions [27, 85, 88, 185]. Due to the complexity of the system one approach has been to study the different physical and chemical parameters, which influence the aggregation process, separately. Step by step different interaction theories and influencing parameters were evaluated [150, 186, 187]. Kumar, Dixit, Zhou & Fraunhofer [21] analyzed the impact of short and long-range forces on protein aggregation under varying conditions. They could show that electrostatic interactions have a main impact on protein-protein interactions under ideal dilute conditions. With increasing protein concentration the impact of hydrophobic forces strengthen [21, 164]. With the theoretical understanding of physical and chemical interaction regimes the second virial coefficient (B_{22}) was introduced. This parameter is measured by static light scattering and reflects the total thermodynamic environment for protein molecules diluted in a given solvent. The parameter characterizes solute-solute and solute-solvent interactions [188]. The B_{22} could be successfully correlated with crystallization slots as well as precipitation points [105, 120, 189, 190]. Unfortunately, that could only be shown for ideal dilute solutions. A direct projection from results gathered in dilute solutions to high concentrated protein solutions can not be easily made. The B_{22} does not take into account short-range interactions between molecules which are almost negligible in dilute solutions but influence the protein behavior with increasing protein concentration. Also not displayed is the exponential increase of the macromolecular crowding effect. This effect describes the reduction of solvent volume around molecules and occurs only in highly concentrated protein solution. This crowding effect can make molecules behave in radically different ways than in dilute solutions especially regarding their interaction behavior [69, 191]. A missing link is thus a method describing both dilute and high concentrated protein solutions towards their phase behavior independently of interaction characteristics.

In order to address this dilemma, the current study analyses the systems flow characteristics, hence the rheology of protein solutions. Advantages of rheological measurements are, that they provide information on solution inner structure as well as implicit flow characteristics and that they are independent of the target molecule concentration. In the cosmetic, food and color industry rheological measurements are performed to analyze the stability of dispersions and emulsions. Rheological standard analytics serve to assure quality criteria with regard to homogeneity, sedimentation characteristics, sensation experience and material haptics [153, 192–194]. Routinely rheologically analyzed materials are polymer solutions [195–198]. Polymers and proteins have some solution characteristics in common: They are complex in structure, form macromolecular networks in crowded solutions and show both viscoelastic behavior. That implies that the material exhibit

both viscous and elastic characteristics when undergoing deformation. The characteristics are represented by the measurable parameters G' (storage modulus) and G'' (loss modulus). G' describes the elastic component of the measured sample, G'' the viscous component of the probe.

In the biotechnological field the information density of rheological measured parameters is comparatively unused. Since the turn of the century the need of an analyzing tool intensified and as a consequence biotech research groups are taking a closer look on the rheological characterization of protein solutions. Rheological measurements revealed a correlation between the viscosity and therefore the injectability of a protein formulation and the strength of protein-protein interactions [199]. With the help of ultrasonic rheological measurements the group around Kalonia could demonstrate that the solution composition and model protein concentration do have a strong impact on the solution rheology [136]. Furthermore, they could show that the rheological parameter G' , measured by frequency sweep measurements, is sensitive to the type and strength of protein-protein interaction [15, 20, 127]. Neergaard & Kalonia [159] could prove a linear correlation of the storage modulus G' with the strength of protein-protein interaction under tested conditions. The knowledge of the protein flow characteristics paves the way for a better understanding of the protein solution characteristics. So far, the missing link is the correlation of the measurable rheological parameters with the most important solution property namely - protein solubility. Such an undertaking is already seen at the polymer industry where rheological parameters are already used to predict long-term storage stability of polymer solutions [131, 139].

To understand the correlation between the rheological characteristics and the aggregation tendency of a protein solution, the molecular flow properties of a liquid containing proteins need to be analyzed. The viscosity of a sample is related to the way and the strength molecules are interacting in the solution and is directly linked to its relaxation time. The relaxation time of the sample is dependent on the temperature, the type of molecule, the solute and solvent concentration. These parameters demonstrably influence the phase behavior of a molecule in the respective solution. The measured relaxation time (τ) is directly linked to observable parameters G' and G'' and the radial frequency (ω):

$$G' \propto \frac{\omega^2 \tau^2}{1 + \omega^2 \tau^2} \quad (7.1)$$

$$G'' \propto \frac{\omega \tau}{1 + \omega^2 \tau^2} \quad (7.2)$$

The moduli shift to lower or higher values, depending on the sample inner structure and specific to the currently set frequency values.

The overriding question to be answered is, whether the rheological data allows a direct correlation to the phase behavior of proteins. To find an answer to this question, we investigated if the above mentioned sensitivity of the moduli shift can be used to rheologically characterize the protein solution with regard to its aggregation tendency. To do so, we first established phase diagrams of the protein lysozyme as a function of protein concentration, pH, salt type and salt concentration. The systems were scored after 40 days (t_{40}) to mark a potential phase shift. Samples with identical conditions were prepared and rheologically characterized at t_0 to see if a correlation exists between the inner structure of a solution and its long-term stability.

7.2 Materials and Methods

Materials

The model protein used in this study was lysozyme from chicken egg white (Hampton Research, Aliso Viejo, CA, USA). It was supplied as a lyophilized powder. The protein has a size of 14,3 kDa, a theoretical pI of 10.7 [200, 201] and an extinction coefficient of $2.2 \text{ l}/(\text{mol} * \text{cm})$. Acetic acid, sodium acetate, citric acid, trisodium citrate, sodium monobasic phosphate, sodium dibasic phosphate, BisTris propane (1,3-bis(tris(hydroxy methyl) methylamino) propane), MOPSO (β -Hydroxy-4-morpholine-propane-sulfonic acid), ammonium sulfate, sodium chloride and sodium hydroxide for titration were purchased from Merck KGaA (Darmstadt, Germany) and Sigma- Aldrich (St. Louis, MO, USA). Ultrapure water (ISO3696) was used to prepare all solutions. For verification measurements viscosity standards (Olbrich, Hemer, Germany) produced in accordance to the premium quality of BS EN ISO/IEC17025 were used. To reduce the residual salt content of the lyophilized protein, the prepared protein solution was buffer exchanged with Sephadex media from GE Healthcare (Buckinghamshire, Great Britain). The column was manually packed with a diameter of 2,5 cm and a bed height of 23 cm. For the concentration of the protein 20 mL Vivaspin ultra filtration spin columns (Sartorius, Göttingen, Germany) with a molecular weight cut off of 3000 Da were used. 96 - well microbatch crystallization plates from Greiner Bio-One (Frickenhausen, Germany) were used for the preparation of protein phase diagrams.

Methods

Sample preparation

Buffers used in this study all had an ionic strength of 100 mM. For the experiments buffers with pH values of 3, consisting of citric acid and trisodium citrate, pH 5, consisting of acetic acid and sodium acetate, pH 7, consisting of MOPSO and pH 9, consisting of BisTris Propane were selected. Lysozyme from chicken egg white was dissolved in the respective buffer with a starting concentration of 150 mg/ml. To get rid of residual salts an SEC method followed. The buffer exchange was conducted at an ÄctaPrime plus system from GE Healthcare. Here 5 mL of lysozyme solution with a concentration of 150 mg/ml was purified with a Sephadex adsorber packed in a constant flow method. The protein was fractionated in 10 mL Falcon tubes and the concentration measured with an extinction coefficient of $2.2 \text{ l}/(\text{mol} * \text{cm})$. The concentration of this dilute protein solution to 250 mg/mL was performed with Vivaspins (Sigma- Aldrich), and a rotational speed of 8000 rad/sec. Subsequently, a protein dilution series with the corresponding buffer was prepared, so that after the addition of the second component, either a high salt or low salt buffer in a ratio of 1:5 (buffer:protein solution), the required final protein concentration could be achieved. The second component was added directly on the liquid handling station or in the case of the rheological measurements manually, immediately before the measurement.

Preparation of protein phase diagrams

The automated method for the preparation of protein phase diagrams was realized with the help of a Tecan robotic platform (Maennedorf, Switzerland). Four different troughs with buffers were assigned to the robotic platform. Two low salt and two high salt buffers. These components were mixed automatically in a buffer plate to achieve six salt concentrations. These solutions and the manually prepared protein samples were mixed in a ratio of 1:5 to achieve the desired 96 different conditions. One crystallization plate consists of two different pH values, protein concentrations from 100-225 mg/mL and salt concentrations from 0-175 mM. The crystallization plates were placed in the Rock Imager from Formulatrix (Bedford, MA, USA), an automated high resolution imaging system for protein crystallization. The plates were marked with a bar code and photographed in specified time intervals. After 40 days every single well was scored as clear, crystallized or precipitated. To verify that the crystals consisted out of protein and not crystallized salt, photographs with ultraviolet light were taken.

Squeeze Flow Rheometry measurements

The elastic portion of a protein solution - comparably low to other materials - requires frequency values in the kilo Hertz region, to reach the interesting area of linear viscoelasticity. Conventional mechanical Rheometers are limited to frequencies up to 100 Hz [202]. Not only a high frequency range is indispensable for a suitable measurement technique but also a low sample volume, acceptable measurement times, low mechanical stress and highly accuracy and reproducibility of the measurement are required. An instrument which fulfills all the requirements is the Piezo Axial Vibrator [138]. The measurement accuracy of this tool is proven for various solutions, even for low viscous samples [139, 141, 202]. It has already been shown, that this tool is also well suited for protein solution measurements [203]. The measurement principle of the Piezo Axial Vibrator (PAV) is based on axial oscillating piezo elements and operates at frequencies between 1 and 6000 Hz. The lower part of the device is surrounded by a double walled cylinder and can be easily tempered by a circulating fluid. A LockIn - amplifier is directly connected to the measurement cell and controls the dynamic squeeze flow excited by four piezo elements. It also processes the response signal four different piezo elements take up. A complete scheme of the instrument is described in the doctoral thesis of L. [138].

All measurements were conducted at a temperature of 20°C and a sample volume of 25 μL. The sample is directly pipetted on the measuring head and the measurement chamber is hermetically closed with a thick stainless steel top plate leaving a circular gap. The gap width d is chosen depending on the viscosity of the sample. In this work we used a relatively narrow gap of 15 μL matching the relatively low viscosity of lysozyme solutions. The principle of the measurement system is based on the measurement of the electronic characteristics of the piezo electrodes without the sample and with the sample in the measurement gap. With the difference in the electronic response of the measurement voltage one can calculate the rheological properties of the sample. First the dynamic displacement \hat{x}_0 is measured. The measurement with exact the same frequency values is conducted with the sample in the measurement chamber. With this measurement the dynamic displacement \hat{x} is measured in accordance with the rheological characteristics of the sample. By formulating the equation of motion and the ratio of $\frac{\hat{x}_0}{\hat{x}}$ the complex compressive rigidity K^* can be calculated:

$$K^* = \frac{3\pi}{2} \cdot R \left(\frac{R}{d} \right)^3 \cdot \frac{G^*}{1 + \frac{\varphi\omega^2 d^2}{10G^*}} \quad (7.3)$$

R is the radius of the plate, d is the gap width, ρ is the density of the squeezed material and ω the radial frequency. With K^* one can calculate G^* and η^* . G^* can be easily divided in its imaginary and real part.

$$G^* = \sqrt{(G')^2 + (G'')^2} \quad (7.4)$$

A detailed derivation of these parameters is described in the doctoral thesis of L. Kirschenmann [138]. For the rheological characterization of protein solutions the loss (G'') and storage moduli (G') were calculated over a frequency range from 100-40000 rad/sec in 22 measurement points. Every measurement was performed in duplicate.

Characterization of viscoelastic materials by means of rheological moduli

G' and G'' are measured over the radial frequency ω for the characterization of the given protein solution. The parameters show a characteristic curve shape that is shifted along the x-axes with changing molecular weight or the formation of intermolecular scaffolds of the tested material. In Figure 7.1 such a characteristic curve shape is illustrated. The graph can be divided in two main parts. The frequency value of the crossover point (ω_{CO}), where $G' \sim G''$, marks the dividing line. The point is metrologically reached when the vibration period τ is as long as the relaxation time λ of the sample. In the frequency area before the intersection occurs the molecules move almost freely in the solution without forming any ordered structure. At lower frequencies the structure of the temporary entanglement network is relatively flexible. Due to the relative motion between the macromolecules deformation energy is transformed into frictional heat and gets lost. The viscous behavior dominates. At high frequencies the structures have less flexibility and therefor a higher rigidity. Due to the limited relative motion the molecules are able to store more deformation energy than gets lost. The elastic behavior dominates. This can be done through a reticular structure the molecules form in the solution. In this work G' and G'' are plotted as a function of the radial frequency in a range of 10 - 100000 rad/sec. The measurement points were fitted with a fourier fit of the second class and the crossover point, here considered as a rheological key parameter, calculated with equating the two Fourier fits and in the following abbreviated with ω_{CO} .

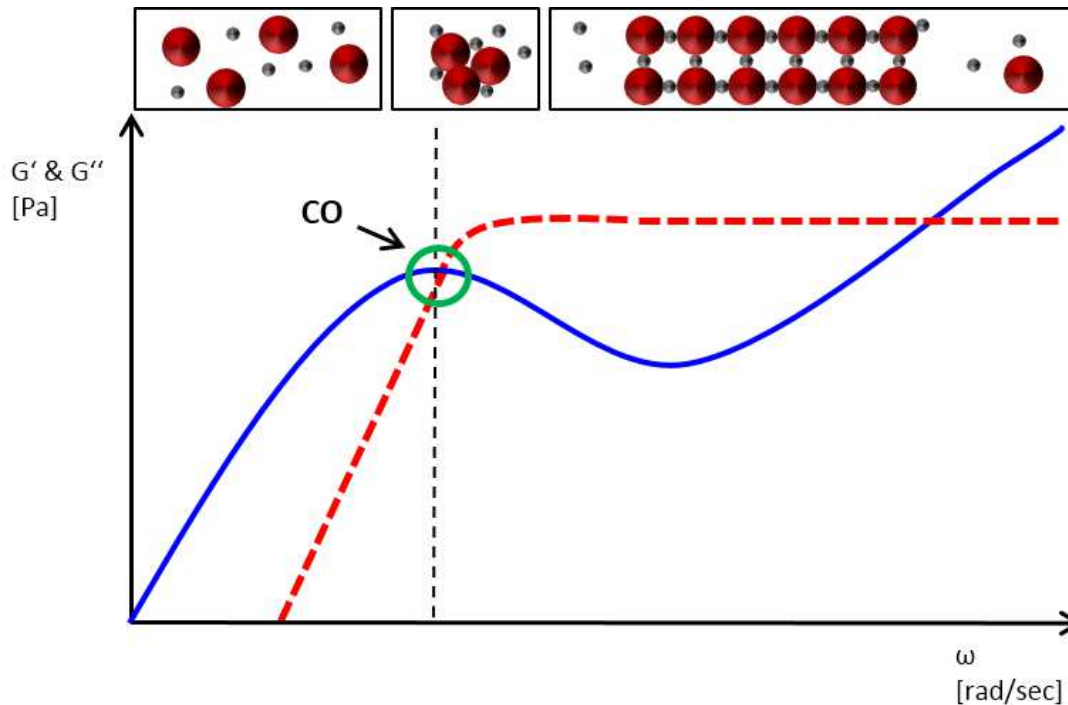


Figure 7.1: Characteristic curve shape of G' and G'' for a viscoelastic material. Subdivision of the graph in soluble, aggregating and scaffold forming protein solutions depending on the applied frequency.

7.3 Results

In order to correlate protein phase behavior (determined after 40 days of incubation, t_{40}) under different fluid phase conditions to the rheological behavior, measured initially after mixing (t_0), a matrix of conditions for protein solutions at different protein concentration, pH and salt content was analyzed.

7.3.1 Protein Phase Diagrams

Protein phase behavior under different fluid phase conditions was evaluated as described above. The phase state of the protein at a pH range from 3 - 9, a protein concentration of 100-225 mg/mL and a sodium chloride concentration of 0-175 mM is shown in Figure 7.2 a.

At pH 5 and pH 7 lysozyme is soluble up to a concentration of 225 mg/mL over the whole

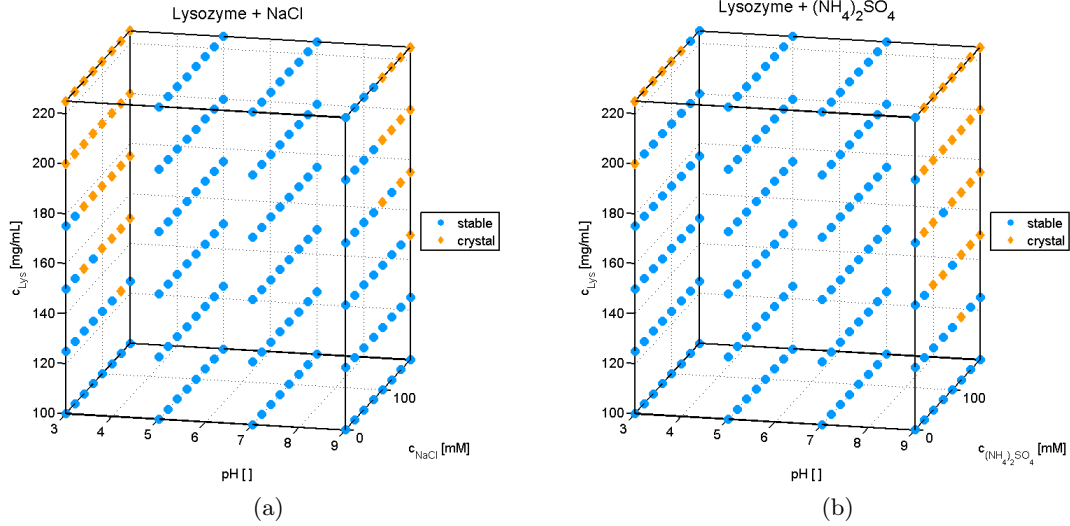


Figure 7.2: Protein phase behavior of lysozyme. At pH values from 3-9, protein concentrations from 100-225 mg/mL and (a) sodium chloride concentrations from 0-175 mM and (b) ammonium sulfate concentrations from 0-175 mM.

tested sodium chloride concentration range. A large crystallization area can be detected at pH 3 starting at a salt concentrations of 100 mM and a protein concentrations of 100 mg/ml. Also at a pH of 9 crystals nucleate starting at a salt concentration of 100 mM and a lysozyme concentration of 125 mg/mL. For pH 9 the samples stayed stable without the addition of sodium chloride.

In order to test if influences based on kosmotropic strength and nature of salt can be seen by the proposed method the addition of ammonium sulfate was investigated. At pH 5 and pH 7 samples remained homogeneous fluids throughout the experiment (Figure 7.2 b). At pH 3 crystals nucleated starting at a lysozyme concentration of 200 mg/mL without salt. Systems at pH 3, a protein concentration of 200 and 225 mg/mL and an ammonium sulfate concentration of 25 mM respectively 125 mM stayed stable over the whole time span of 40 days. At pH 9 crystals were formed at protein concentrations above 125 mg/ml starting at an ammonium sulfate concentration of 25 mM.

7.3.2 Rheological Behavior

To study the general influence of the sample conditions on the rheological parameters G' and G'' frequency sweep measurements were conducted for all systems described above.

The standard deviation of the measurements with the Piezo Axial Vibrator never exceeded 1%. In the following the influence of the protein concentration, the pH value and the type and concentration of salt on the rheological behavior of the protein is represented.

The majority of the measured samples behave linear viscoelastic in the chosen frequency range. The viscous part (G'') of the probe dominates the elastic part (G') up to the first crossover point which is marked as a circle in the shown Figures.

Influence of protein concentration

Protein aggregation is inherently dependent on protein concentration for given fluid conditions. In Figure 7.3 samples of lysozyme with constant pH and sodium chloride concentration of 175 mM with varying protein concentration are shown. With increasing protein concentration the curves of G' and G'' shift closer to each other. That leads to a shift of the crossover point to lower frequency values from ca. 34000 rad/sec to 8000 rad/sec for increasing protein concentrations. The first crossover point of the Figure 7.3 c is physically incorrect and can be neglected. This physically incorrect calculation of G' occurs when the detection limit of the PAV is reached at very low frequency values and samples with a low elastic response, like protein solutions. The incorrect record of the response signal could also be noticed for lysozyme solution with a concentration of 200 mg/ml, at pH 9 and the addition of 175 mM ammonium sulfate.

Influence of pH

Protein-protein interactions and thus protein phase behavior exhibits a high level of sensitivity towards changing pH. The latter is mainly due to a change in electrostatic repulsion, due to varying charge on the protein surface. To evaluate if the resulting change in interaction forces in a protein solution is also depicted by rheological measurements, a range of pH values by otherwise constant conditions are compared. Figure 7.4 compares samples at pH 3, pH 5, pH 7 and pH 9 and constant protein concentration without additional salt. The Figures show clearly that the sample at pH 3 has the lowest ω_{CO} at 11662 rad/sec. The ω_{CO} for samples at pH 5 and pH 7 are located at higher frequency values. These samples have a very low elastic part and behave almost like water. The ω_{CO} for the sample at pH 9 is at 22250 rad/sec and thus the second lowest.

Influence of Salt

Generally different salt types may alter the structure of water and thus also the impact of hydrophobic forces in the system. To evaluate this sodium chloride and ammonium

7.3 Results

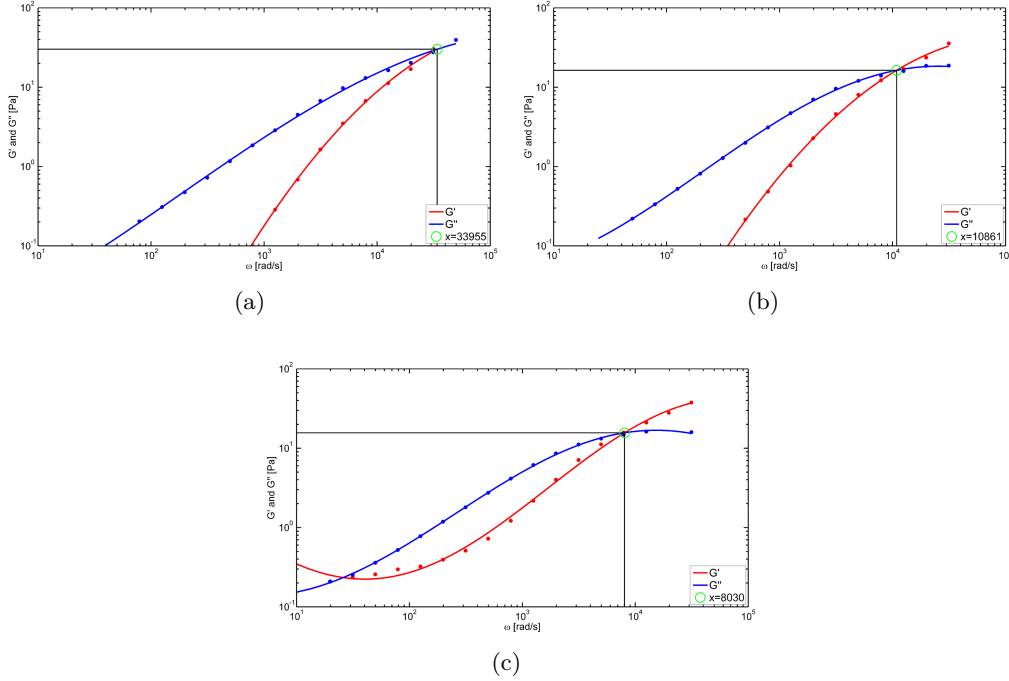


Figure 7.3: Influence of protein concentration on the curve shape of the loss and storage modulus. Shown are the loss and storage modulus from lysozyme at protein concentrations of 100 (a), 150 (b), and 200 mg/mL (c), at pH 3 and a sodium chloride concentration of 175 mM. Recorded at 22 frequency points over a frequency range from 100-40000 rad/sec.

sulfate were added to the system to reach final concentrations of 50 mM and 175 mM. Figure 7.5 a-c and Figure 7.5 d-f show the respective course of G' and G'' under varying salt concentrations. To avoid additional influence of changing protein concentration this was kept constant. For both salts the general trend is comparable. For sodium chloride the ω_{CO} ranges from 11662 rad/sec to 8030 rad/sec for low to high salt, while for ammonium sulfate we see a significant decrease of ω_{CO} from 22250 rad/sec to 5422 rad/sec. A clear exception was found for the system containing 50 mM sodium chloride. Over a wide frequency range G' is above G'' . The curve of G' is parallel to the x-axes up to the second crossover point. G'' describes a shape with a pronounced minimum. With increasing salt concentration this behavior gets lost. The elastic modulus is above the viscous modulus and there is no plateau of G' . The crossover point is at a relatively low frequency value of $\omega_{CO} = 8030$ rad/sec.

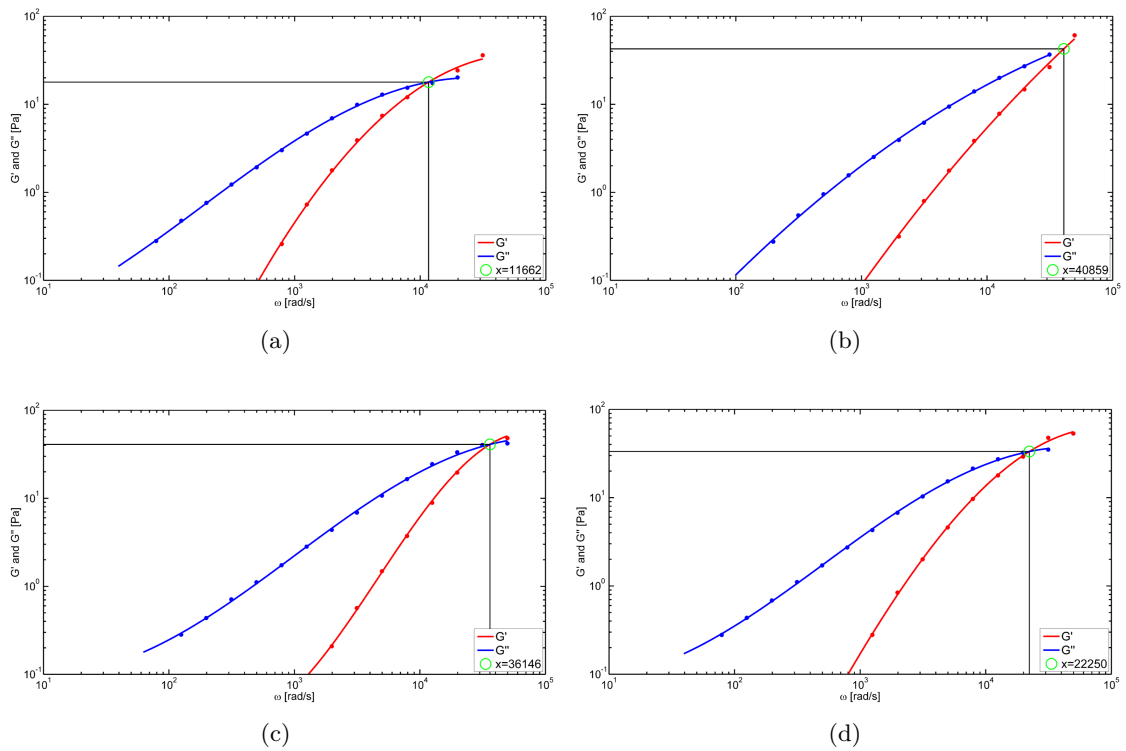


Figure 7.4: Influence of pH on the curve shape of the loss and storage modulus. Shown are the loss and storage modulus from lysozyme at a constant protein concentration of 200 mg/mL, at pH 3 (a), 5 (b), 7 (c) and 9 (d) without salt. Recorded at 22 frequency points over a frequency range from 100-40000 rad/sec.

7.3 Results

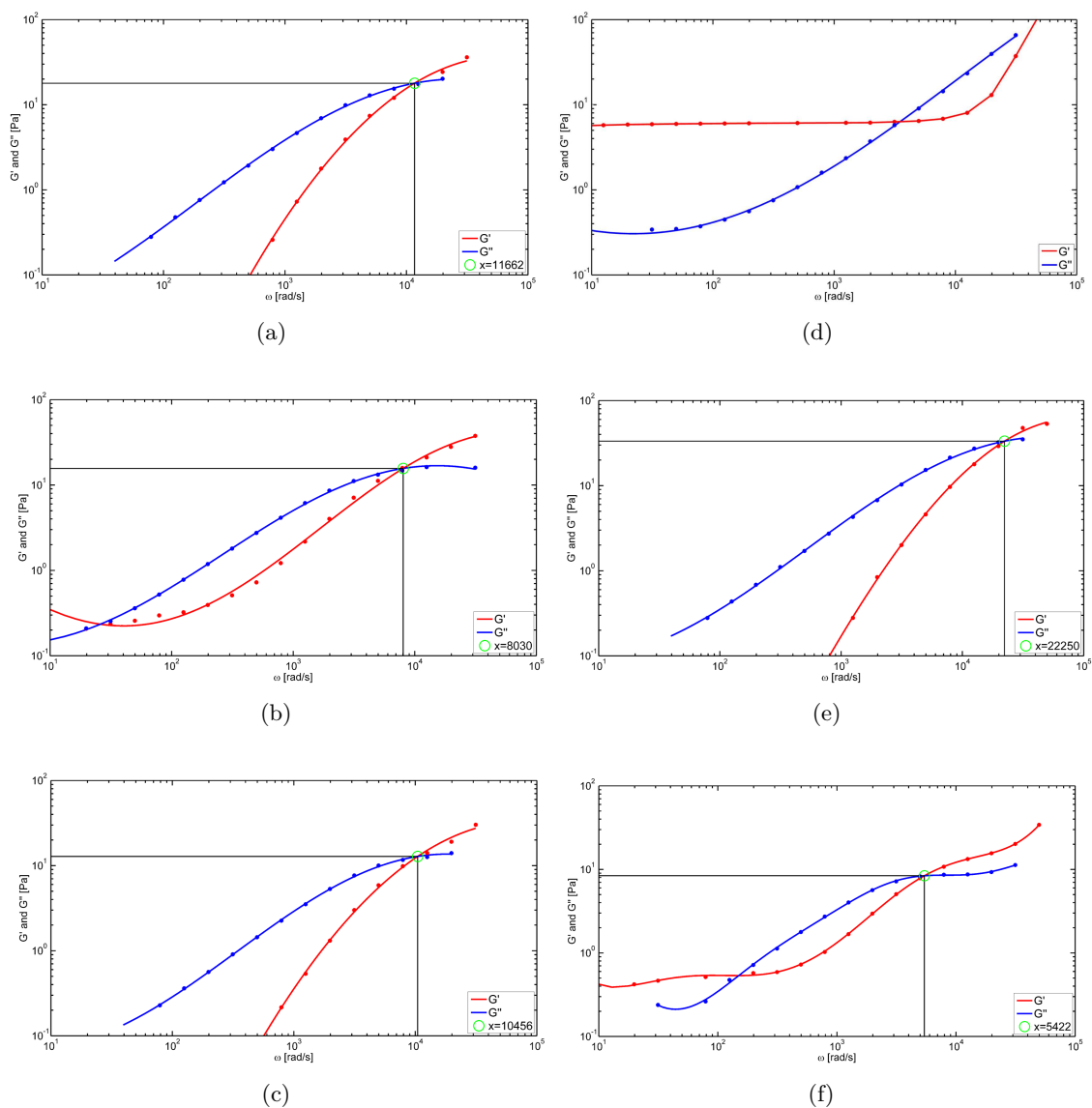


Figure 7.5: Influence of sodium chloride and ammonium sulfate on the curve shape of the loss and storage modulus. Shown are the loss and storage modulus from lysozyme at a constant protein concentration 200 mg/mL, at pH 3 and varying salt concentrations of 0, 50 and 175 mM. Recorded at 22 frequency points over a frequency range from 100-40000 rad/sec. (a) Lysozyme pH 3 200 mg/mL 0 mM NaCl; (b) Lysozyme pH 3 200 mg/mL 50 mM NaCl; (c) Lysozyme pH 3 200 mg/mL 175 mM NaCl; (d) Lysozyme pH 9 200 mg/mL 0 mM AS; (e) Lysozyme pH 9 200 mg/mL 50 mM AS; (f) Lysozyme pH 9 200 mg/mL 175 mM AS

7.3.3 Correlation of ω_{CO} and Protein Phase Behavior

Analyzing the obtained curve shape of G' and G'' for different fluid phase conditions, it becomes apparent, that the measured rheological parameters react sensitive to varying solution compositions. The parameter chosen for this study is the frequency value ω_{CO} for which G' equals G'' . In the next section this parameter will be correlated with the protein phase behavior of identical sample composition.

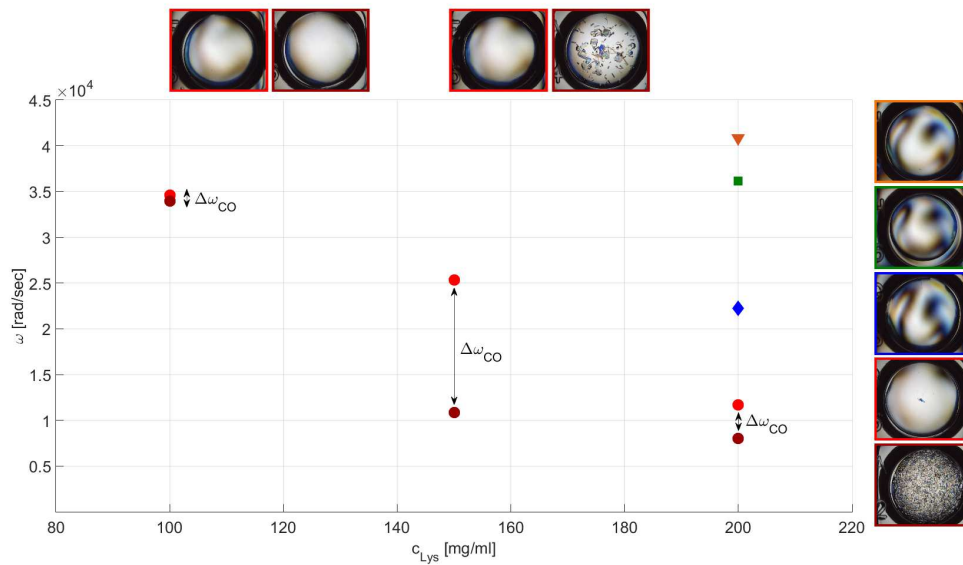


Figure 7.6: Correlation of ω_{CO} and protein phase behavior for selected samples at pH 3 with 175 mM sodium chloride and without salt (dark red and red circles) and varying protein concentrations; at pH 5 (orange triangle), pH 7 (green square) and pH 9 (blue diamond) without salt and a constant protein concentration of 200 mg/mL.

In Figure 7.6 the ω_{CO} of samples at t_0 are juxtaposed to a photograph showing one well of a crystallization plate containing exactly the same sample taken after 40 days of incubation (t_{40}). The ω_{CO} is plotted as a function of the protein concentration. The Figure shows samples with different protein concentrations and differing pH values. For samples at pH 3 containing 175 mM sodium chloride the ω_{CO} falls rapidly from values above 30000 rad/sec to values below 15000 rad/sec as a function of increasing protein concentration. The photographs show that the solubility limit for lysozyme is exceeded somewhere in between 100 and 150 mg/mL at a pH value of 3 and a sodium chloride concentration of 175 mM. Samples at pH 3 without additional salt do have their ω_{CO} at higher frequency values. The solubility line shifts to values in between 150 and 200 mg/mL.

For the comparison of the ω_{CO} values determined for samples with and without salt, $\Delta\omega_{CO}$ has been calculated. $\Delta\omega_{CO}$ is the difference of ω_{CO} values between samples to be compared. In this context the ω_{CO} values without salt minus the ω_{CO} values with added sodium chloride ($\Delta\omega_{CO}=\omega_{CO,1}-\omega_{CO,2}$) at different protein concentrations. The influence of added salt seems to be a function of protein concentration. The ω_{CO} values for samples with a lysozyme concentration of 100 mg/mL without salt and a salt concentration of 175 mM are almost similar ($\Delta\omega_{CO}=616$ rad/sec). Both systems are stable at t_{40} . At a protein concentration of 150 mg/mL the $\Delta\omega_{CO}$ increases to a value of 14480 rad/sec (sample without salt is stable, sample containing 175 mM sodium chloride is unstable at t_{40}) while the values close up to $\Delta\omega_{CO}$ of only 3632 rad/sec at 200 mg/mL (both systems are unstable at t_{40}).

A change of the systems to other pH values with constant protein concentration and ionic strength consequently leads to a change of lysozyme solubility. Lysozyme crystallizes at pH3 and a concentration of 200 mg/mL without any salt. Here the ω_{CO} are situated below 15000 rad/sec. At pH9 close to the pI, lysozyme is soluble at identical conditions and the ω_{CO} is situated above 20000 rad/sec. At pH5 and pH7 the studied model protein is soluble over the whole screened area and the ω_{CO} are situated at very high frequency values. Therefore, at conditions with increasing agglomeration tendency the ω_{CO} is situated at a lower frequency area while the more stable conditions express higher values. Figure 7.7 compares all measured ω_{CO} values of the rheological screening at t_0 with the obtained scoring of the crystallization plates at t_{40} . It becomes apparent that a distinct limit frequency value (ω_{limit}) develops. All examined samples, whose ω_{CO} is situated above ω_{limit} are soluble and exhibit a high long-term stability. Samples where the ω_{CO} is situated below ω_{limit} do agglomerate in form of crystal formation under tested conditions.

The solubility limit of lysozyme is found to be $\omega_{limit} = 20000$ rad/sec under tested conditions.

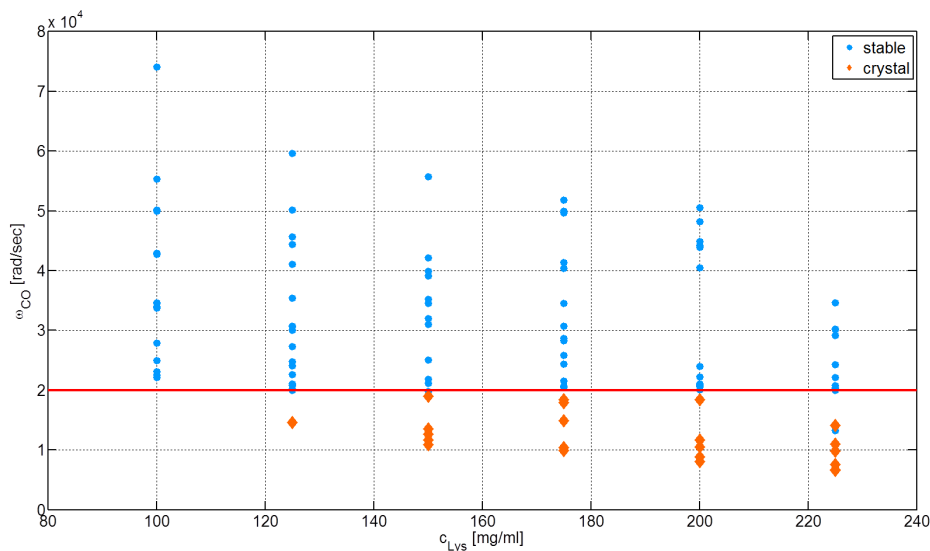


Figure 7.7: ω_{CO} of every measured sample plotted against the protein concentration. The blue circles represent measurement points of soluble samples. The orange diamonds represent measurement points of samples scored as crystallized. The red line symbolizes ω_{limit} for lysozyme under tested conditions.

7.4 Discussion

This work deals with the rheological characterization of protein solutions containing lysozyme from chicken egg white. The primary objective is to find a correlation of the determined rheological parameters and the protein phase behavior. The study of the phase behavior showed that lysozyme is stable over a wide pH and salt range, even in high concentrated solutions. Under the given conditions, only the metastable region where lysozyme crystallizes could be reached. The unstable region where precipitation occurs could not be reached. From a biochemical point of view, the observed behavior of protein solutions and phase transitions as a function of protein concentration, pH and salt type and concentration followed established knowledge.

The rheological data obtained, responded sensitive to the solution parameters pH, protein concentration, salt type and salt concentration. The rheological results demonstrate, that the crossover point is shifted to lower frequency values with an increase of observed agglomeration tendency. Studies with polymer solutions have shown that strongly interacting systems tend to behave more non-Newtonian. They do have a smaller linear viscoelastic region and the crossover point at comparably low frequency values [135,

204]. Dilute and non interacting systems tend to behave more as Newtonian solutions. In this context, it was shown that samples with a smaller region where G'' dominates G' , compared to other samples, do have longer polymer chains and stronger cross-linked structures [204–206]. These molecules can move against each other at lower frequencies, while with increasing frequency, the molecules start to block each other. Therefore, a shift of the cross over point to lower frequency values implies, that the molecules are less flexible and mobile. Extrapolated to protein solutions this means stronger protein-protein interaction and the formation of more or less ordered structures, which leads to aggregation of the protein. For all frequency values equal or higher than defined by ω_{CO} the molecules can not follow the imposed movement. As seen throughout the study, ω_{CO} is specific for every tested system.

Influence of Protein Concentration

The explanation why the ω_{CO} is decreasing with increasing protein concentration seems to be straight forward. If the molecular percentage in solution is relatively low molecules can move freely in solution without significant attractive interaction. The positively charged protein does have a repulsive effect on molecules of the same kind and the proteins present do not form any kind of network structure. Applied energy is only stored to a very small portion and dissipates to a large fraction (see Figure 7.3a). The values of G'' are higher than the values of G' over a wide frequency range. If the protein concentration increases, at constant solution properties, the molecule density in solution is high enough, that the molecules interact due to short-range interactions. Protein samples with higher protein concentrations are able to store more of the energy applied. Only at pH 3 a phase transition occurred due to an increase of the protein concentration up to 200 mg/mL without the addition of salt. This behavior leads to the assumption that the protein is partially unfolded at pH 3. This partial unfolding of lysozyme from chicken egg white at low pH values is also discussed by Haezebrouck *et al.* [207] and Venkataramani, Truntzer & Coleman [208]. The surface of the protein is enlarged due to the partially unfolding. The enlargement of the protein but even more a significant increase of the proteins hydrophobicity induce a limitation of protein movement in the solution and thus a shift of ω_{CO} to lower frequency values, compared to samples at other pH values. The constrained movement could lead to the agglomeration of the proteins as shown in Figure 7.2. Another explanatory approach would be the formation of lattices at pH 3. The lattice formation becomes possible when the meta-stable region (crystallization area) of proteins is reached [209]. The assumed lattice formation increases the ability of the protein solution to store a greater portion of fed energy. So that the determined G' values exceed the G'' values

at lower frequency values and thus the ω_{CO} value decreases. The assumption is backed up by the fact that lysozyme crystallizes and does not precipitate at these conditions.

Influence of pH

With changing pH a decrease of the region where G'' dominates G' for samples at pH 9 and pH 3 compared to samples at pH 5 and pH 7 is obtained (see Figure 7.4). Proteins are polyelectrolytes. The density of their charge, relative to the pKa values of the charged groups on the protein surface, is strongly dependent on the pH and the ionic strength of the solution. Building on thermodynamic theories of polyelectrolytes, three main parameters influencing rheological properties were determined: shape, hydration and electrostatic charge [210]. The primary effect is induced by the resistance of a diffuse electrostatic double layer surrounding the protein. The repulsion of the double layers between different protein molecules is called the secondary effect. The tertiary effect takes the size of the protein into account. The primary effect does not seem to correlate to the findings of this study. Lysozyme does have a pI of 10.7. Samples measured at pH 9 are closest to the point of zero charge. The mentioned primary effect induces a light increase of the hydrodynamic radius of the molecule and a related increase of the flow resistance. However, a protein close to the pI (at pH 9) is in the most compact form and should have the lowest flow resistance and a ω_{CO} at high frequency values. In our studies samples at pH 9 do have a smaller region where G'' is above G' compared to samples at pH 5 and pH 7. Yadav *et al.* [158] could assess the same phenomena with the protein bovine serum albumin (BSA). At a protein concentration of 250 mg/mL measured viscosities of the protein gained, against the electroviscous theory, the highest viscosity values at pH values close to the pI. At equal measurements with ideal diluted protein solution the phenomena was reversed. The measured intrinsic viscosity of the protein was minimal close to the pI and increased on both sides with increasing distance from the pI. It can be concluded from these findings that the rheological behavior of a protein solution at high concentrations is not only influenced by the first and second electroviscous effect but also by short-range interactions. Dynamic light scattering measurements of lysozyme solutions at varying pH values and protein concentrations substantiate the study of S. Yadav (Data not shown). According to these findings the short-range interactions at pH 9 are relatively high. The correlation with the protein phase behavior of lysozyme at pH 9 shows that an addition of a small quantity of salt induces a phase transition. We presume that the salt covers the charged groups of the protein so that short-range interactions induce the decrease of ω_{CO} and due to hydrophobic interactions the agglomeration of the molecule. At pH 5 and pH 7 the positively charged groups of the protein surface induce a repulsive force.

This repulsion is so strong that the protein molecules are not able to interact. They can move against each other up to high frequency values without forming aggregates or networks of higher order. In comparison to pH 5 and pH 7 the region where G'' dominates G' decreases for samples at pH 3 (7.3.2). The ω_{CO} values are situated in a low frequency region. In this case the electroviscous theory holds true. The protein molecule tend to expand as pH moves away from the pI. This increase of the electrostatic double layer leads to a limited flexibility of the protein and an increased agglomeration tendency. One should also take into account the potential lattice formation and a partially unfolding of the protein at pH 3, mentioned already in the previous section. The unfolding posses an increased protein surface and thus an increase of the electroviscous effect, as seen for protein gels and solutions at high protein concentrations [167].

Influence of Salt

Sodium chloride seems to have a strong influence on lysozyme solution even at lower concentrations. Without salt the sample exhibits a long linear elastic region. The molecules can follow the applied motion up to high frequency values. The elastic part of the probe is almost negligible. An amount of 50 mM of sodium chloride seems to change the rheological behavior completely. The region where G'' dominates G' disappears. The elastic part of the probe is larger than the viscous part. It can thus be concluded that the sample may show a nonlinear viscoelastic behavior at the measured frequency range. At the observed region G' is at a constant value over a wide frequency range. Studies on systems containing polymers have shown, that solutions with constant or slowly shifting G' values have a more or less perfectly elastic behavior and comparatively less energy dissipates during applied stress. This effect can be observed with polymers in solution, which are glass like or crystalline but also with polymers which exhibit effects of structured entanglement coupling [135]. The potentially nonlinear viscoelastic behavior of this sample could also be found in biomaterials like blood vessels [211] or cornea [212] which are made of complex protein scaffolds. To reach this rheological region, the protein molecules have to form a structured, cross-linked network. To obtain such a network a unique interplay of charged groups at the protein surface, protein concentration and salt present in solution needs to be met. For the discussed sample this implies a unique interplay of the lysozyme and sodium chloride molecules, which leads to a predominant elastic rheological behavior This approach is supported by the studied phase behavior and especially the kinetic of the crystallization process (data not shown). The homogeneous nucleation took place after ten days. Compared to samples with the same pH and protein concentration, relatively late. The detected crystals are big and do have an ordered 3d structure. The addition

of 175 mM sodium chloride induces an almost direct agglomeration of the protein. Just after two hours, crystals could be detected optically. The crystals were comparatively small and had a 2d structure. Matching, also the rheological characteristic of the sample changed. A crossover point at comparably low frequency values is a strong argument for protein-protein interaction. The ordered network formation, hence a constant G' value over a certain frequency area, as described above, could not be observed. Based on the theoretical considerations from above the amount of salt ions in the solution is so high, that more charged surface groups are shielded, what enables multiple protein-protein interactions. The proteins interact over several surface groups what facilitates a fast crystallization process.

Ammonium sulfate also shows considerable influence, both on protein phase behavior as well as on the rheological behavior of the protein solution. At pH9 the ω_{CO} is shifted to lower frequency values with increasing ammonium sulfate concentration (see Figure 7.5). The curves of G' and G'' are very close to each other at the highest measured salt concentration, what implies, adapting the theory from studies with polymers, a strong interaction of the molecules in solution. The mobility of the protein molecules is restricted by the salt ions due to the well known salting-out effect, so that an agglomeration in form of crystallization takes place (see Figure 7.2). Interestingly this phenomenon does not occur at pH3. Here the salt seems to stabilize the protein. The repulsion between the protein molecules is stronger in ammonium sulfate solutions at low pH than at high pH [213]. This might be explained with the sulfate binding to the positively charged residues of lysozyme at pH3. This binding causes a decrease of the free surface energy of lysozyme compared to the uncomplexed protein. Curtis *et al.* [214] could already show that ion binding alters the surface chemistry of the protein and reverses the lyotropic series in terms of the salting out effect. That implies that the interactions between kosmotropic ion-protein complexes are more repulsive than those of the uncomplexed proteins. The different influence of ammonium sulfate on the aggregation tendency of lysozyme was also detected with the rheological measurements. At pH9, where the aggregation tendency of lysozyme is increased with increasing ammonium sulfate concentration, the ω_{CO} is shifted to lower frequency values. Samples which aggregate do have ω_{CO} values below 20000 rad/sec. At pH3 the ω_{CO} values are shifted to higher frequency regions with increasing ammonium sulfate concentration. The shift of the ω_{CO} strictly follows the aggregation tendency of the protein, whether it is influenced by chaotropic effects or ion binding on the surface of the protein.

As mentioned above the ω_{CO} values of the analyzed systems are very sensitive towards

the aggregation tendency of the protein. This sensitivity is not influenced by the type of interaction that causes the network formation and aggregation of the protein in solution. It is for this reason, that this parameter might be used as an assessment if the protein is stable or not over a wide protein concentration range, pH range and also for different additives and additive concentrations. For the tested conditions it was possible to delimit a crystallization area with measured ω_{CO} values. Samples with ω_{CO} values below 20000 rad/sec did crystallize. Samples with ω_{CO} values above 20000 rad/sec were stable over the tested time period of 40 days.

7.5 Conclusions

The present work shows that a correlation of the protein phase behavior of lysozyme and measurable rheological parameters is possible for the studied system. With the definition of the rheological key parameter ω_{CO} one can make specific statements about the agglomeration tendency of the protein with one single measurement, immediately after sample preparation. Due to the low sample volume needed, analytical measurements are possible even if only very few sample volume is available or if the material costs are very high. That makes the measurement method interesting for early and late stage development. A very important finding is, that rheological measurements can model both electroviscous and short-range effects. That implies that the measurement method is valid for high and low concentrated protein solutions in comparison to the B_{22} value, which is only valid for ideal dilute solutions. Furthermore, it became possible to determine correlations between crystallization kinetics, crystal morphology and the curve shapes of G' and G'' by the characterization of the molecular network structure of the protein in solution. These findings are important for the understanding of the crystallization characteristics of a protein and thus a step further towards targeted phase transition, which can be used as a purification step or a stable storage form of the drug substance.

The prediction of the protein phase behavior is not only interesting for the storage of the protein but also the whole lifespan of the drug substance and drug product, including the development of the Upstream and Downstream process as well as the selection of the right formulation buffer. For this purpose it is important, that the analytical method is applicable at different protein concentrations and buffer conditions. Squeeze Flow rheological measurements and the determination of the ω_{CO} fulfill these requirements. The analytic tool has the potential to reduce biopharmaceutical development time and costs many times over.

7.6 Acknowledgments

The authors would like to acknowledge the financial support by the Federal Ministry of Education and Research (BMBF) - funding code 0316071B. We gratefully acknowledge instrumental support by Norbert Willenbacher, head of the Department of Applied Mechanics, Institute of Mechanical Process Engineering and Mechanics, KIT. Special thanks go to Sven Amrhein, PhD student at the Institute of Engineering in Life Sciences, Section IV: Biomolecular Separation Sciences, for the excellent scientific support.

7.7 References

15. Chari, R., Jerath, K., Badkar, A. V. & Kalonia, D. S. Long- and short-range electrostatic interactions affect the rheology of highly concentrated antibody solutions. *Pharmaceutical research* **26**, 2607–18 (2009).
20. Saluja, A. *et al.* Application of high-frequency rheology measurements for analyzing protein-protein interactions in high protein concentration solutions using a model monoclonal antibody (IgG2). *Journal of Pharmaceutical Sciences* **95** (2006).
21. Kumar, V., Dixit, N., Zhou, L. L. & Fraunhofer, W. Impact of short range hydrophobic interactions and long range electrostatic forces on the aggregation kinetics of a monoclonal antibody and a dual-variable domain immunoglobulin at low and high concentrations. *International Journal of Pharmaceutics*. **421**, 82–93 (2011).
27. Chi, E. & Krishnan, S. Physical stability of proteins in aqueous solution: mechanism and driving forces in nonnative protein aggregation. *Pharmaceutical Research* **20**, 1325–1336 (2003).
54. Dumetz, A. C., Snellinger-O'brien, A. M., Kaler, E. W. & Lenhoff, A. M. Patterns of protein protein interactions in salt solutions and implications for protein crystallization. *Protein science : a publication of the Protein Society* **16**, 1867–77 (2007).
85. Arakawa, T. & Timasheff, S. Mechanism of protein salting in and salting out by divalent cation salts: balance between hydration and salt binding. *Biochemistry*, 5912–5923 (1984).

88. Baumgartner, K. *et al.* Determination of protein phase diagrams by microbatch experiments: Exploring the influence of precipitants and pH. *International Journal of Pharmaceutics* **479**, 28–40 (2015).
112. Galm, L., Amrhein, S. & Hubbuch, J. Predictive approach for protein aggregation: Correlation of protein surface characteristics and conformational flexibility to protein aggregation propensity. *Biotechnology and bioengineering* (2016).
127. Saluja, A. *et al.* Ultrasonic storage modulus as a novel parameter for analyzing protein-protein interactions in high protein concentration solutions: correlation with static and dynamic light scattering measurements. *Biophysical journal* (2007).
131. Metzger, T. G. *Das Rheologiehandbuch* 4th ed., 138–216 (Vincentz Network, Hannover, 2011).
139. Crassous, J. & Régisser, R. Characterization of the viscoelastic behavior of complex fluids using the piezoelastic axial vibrator. *Journal of Rheology* **49(4)**, 851–864 (2005).
150. Rao, M. A. in *Food Rheology and Structure* 1–26 (2014).
167. Clark, A. *Functional Properties of Food Macromolecules* (eds Hill, S., Ledward, D. A. & Mitchell, J.) 77–138 (Springer Science & Business Media, 1998).
183. Pelegri, D. & Gasparetto, C. Whey proteins solubility as function of temperature and pH. *LWT - Food Science and Technology* **38**, 77–80 (02/2005).
184. Liu, J., Nguyen, M. D. H., Andya, J. D. & Shire, S. J. Reversible self-association increases the viscosity of a concentrated monoclonal antibody in aqueous solution. *Journal of Pharmaceutical Sciences* **94**, 1928–40 (2005).
185. Cleland, J. L., Powell, M. F. & Shire, S. J. The development of stable protein formulations: a close look at protein aggregation, deamidation, and oxidation. en. *Critical reviews in therapeutic drug carrier systems* **10**, 307–77 (1993).
186. Teeter, M. M. Water protein interactions : Theory and Experiment. *Annual Review of Biophysics and Biophysical Chemistry* **20**, 577–600 (1991).
187. Naveed, H. & Han, J. J. Structure-based protein-protein interaction networks and drug design. *Quantitative Biology* **1**, 183–191 (2013).
189. Ruppert, S., Sandler, S. I. & Lenhoff, a. M. Correlation between the osmotic second virial coefficient and the solubility of proteins. *Biotechnology progress* **17**, 182–7 (2001).

190. Rakel, N., Galm, L., Bauer, K. & Hubbuch, J. From osmotic second virial coefficient (B₂₂) to phase behavior of a monoclonal antibody. *Biotechnological Process* **31**, 438–451 (2015).
191. Ellis, R. J. Macromolecular crowding : obvious but under appreciated. *TRENDS in Biochemical Sciences* **26**, 597–604 (2001).
192. Davis, S. S. Rheological Properties of Semi Solute Food Stuff - Elasticity and its Role in Quality Control. *Journal of Texture Studies* **4**, 15–40 (1973).
193. Brummer, R. & Godersky, S. Rheological studies to objectify sensations occurring when cosmetic emulsions are applied to the skin. *Colloids and Surfaces A: Physicochemical and Engineering Aspects* **152**, 89–94 (1999).
194. Brummer, R. *Rheology Essentials of Cosmetic and Food Emulsions* 81–124 (2006).
195. Abegg, J.-L., Boiteux, J.-P. & Hourseau, C. US3958581 A (1976).
196. Winnik, F. M. Elements of Polymer Science, 1–50 (1999).
197. Goddard, D. E. & Gruber, J. V. *Principles of Polymer Science and Technology in Cosmetics and Personal Care* 230–434 (Marcel Dekker AG, 1999).
198. Liu, R. C. W., Morishima, Y. & Winnik, F. M. Rheological Properties of Mixtures of Oppositely Charged Polyelectrolytes. A Study of the Interactions between a Cationic Cellulose Ether and a Hydrophobically Modified Poly[sodium 2-(acrylamido)-2-methylpropanesulfonate]. *Polymer Journal* **34**, 340–346 (05/2002).
199. Kanai, S., Liu, J., Patapoff, T. W. & Shire, S. J. Reversible self-association of a concentrated monoclonal antibody solution mediated by Fab-Fab interaction that impacts solution viscosity. *Journal of pharmaceutical sciences* **97**, 4219–27 (10/2008).
200. Huopalahti, R., López-Fandiño, R., Anton, M. & Schade, R. in *Bioactive Egg Compounds* 298 (Springer Science & Business Media, 2007).
201. Abeyrathne, E., Lee, H. & Ahn, D. Sequential separation of lysozyme, ovomucin, ovotransferrin, and ovalbumin from egg white. *Poultry Science* **93**, 1001–1009 (2014).
202. Fritz, G., Pechhold, W., Willenbacher, N. & Wagner, N. J. Characterizing complex fluids with high frequency rheology using torsional resonators at multiple frequencies. *Journal of Rheology* **47**, 303 (02/2003).
204. Macosko, C. W. *Rheology: Principles, Measurements, and Applications* (Wiley-VCH, 1994).

205. Larson, R. *The structure and rheology of complex fluids*. 105–258 (Oxford University Press, New York, 1999).
206. Mewis, J. & Wagner, N. in *Cambridge Series in Chemical Engineering* 36–62 (Cambridge University Press, Cambridge, 2012).
207. Haezebrouck, P. *et al.* An equilibrium partially folded state of human lysozyme at low pH. *Journal of molecular biology* **246**, 382–387 (1995).
209. Muschol, M. & Rosenberger, F. Liquid-liquid phase separation in supersaturated lysozyme solutions and associated precipitate formation/crystallization. *The Journal of Chemical Physics* **107**, 1953 (08/1997).
210. Harding, S. in *Functional properties of food macromolecules* (eds Hill, S., Ledward, D. & Mitchel, J.) 2nd ed., 10–15 (Aspen, 1998).
213. Moretti, J. J., Sandler, S. I. & Lenhoff, A. M. Phase equilibria in the lysozyme-ammonium sulfate-water system. en. *Biotechnology and bioengineering* **70**, 498–506 (12/2000).
214. Curtis, R. a. *et al.* Protein-protein interactions in concentrated electrolyte solutions. *Biotechnology and bioengineering* **79**, 367–80 (2002).
230. Consortium, U. UniProt: a hub for protein information. *Nucleic Acids Research* **43**, 204–212 (2015).
231. Wilkins, M. R. *et al.* Protein identification and analysis tools in the ExPASy server. *Methods in Molecular Biology* **112**, 531–52 (1999).
239. Kuwada, M., Hasumi, H. & Furuse, Y. Purification of Cytochrome b5 from Pig Testis Microsomes by Isoelectric Focusing in an Immobiline pH Gradient. *Protein Expression and Purification* **12**, 420–424 (1998).
240. Brown, W. H. *Organic chemistry* (Brooks/Cole Cengage Learning, 2009).
242. Miklos, A., Sarkar, M., Wang, Y. & Pielak, G. Protein Crowding Tunes Protein Stability. *Journal of the American Chemical Society* **133**, 7116–7120 (2011).
296. Minton, A. P. Influence of macromolecular crowding upon the stability and state of association of proteins: predictions and observations. *Journal of pharmaceutical sciences* **94**, 1668–75 (08/2005).
301. Jezek, J., Rides, M. & Derham, B. Viscosity of concentrated therapeutic protein compositions. *Advanced drug delivery ...* (2011).

Prediction and characterization of the stability enhancing effect of the Cherry-TagTM in highly concentrated protein solutions by complex rheological measurements and MD simulations

Pascal Baumann¹, Marie-Therese Schermeyer¹, Hannah Burghardt, Cathrin Dürr, Jonas Gärtner and Jürgen Hubbuch

Institute of Engineering in Life Sciences, Section IV: Biomolecular Separation Science, Karlsruhe Institute of Technology (KIT), 76131 Karlsruhe, Germany

¹*These authors contributed equally to this work.*

Abstract

Solution stability attributes are one of the key parameters within the production and launching phase of new biopharmaceuticals. Instabilities of active biological compounds can drastically reduce the yield of biopharmaceutical productions, and may induce undesired reactions in patients, such as immunogenic rejections. Protein solution stability thus needs to be engineered and monitored throughout production and storage. In contrast to the gold standard of long-term storage experiments applied in industry, novel experimental and *in silico* molecular dynamics tools for predicting protein solution stability can be applied within several minutes or hours. Here, a rheological approach in combination with molecular dynamics simulations are presented, for determining and predicting long-term phase behavior of highly concentrated protein solutions. A diversity of liquid phase conditions, including salt type, ionic strength, pH and protein concentration are tested in a Glutathione-S-Transferase (GST) case study, in combination with the enzyme with and without solubility-enhancing Cherry-TagTM. The rheological characterization of GST and Cherry-GST solutions enabled a fast and efficient prediction of protein instabilities without the need of long-term protein phase diagrams. Finally, the strong solubility enhancing properties of the Cherry-TagTM were revealed by investigating protein surface properties in MD simulations. The tag highly altered the overall surface charge and hydrophobicity of GST, making it less accessible to alteration by the chemical surrounding.

Keywords: *Protein Phase Behavior; Solution Stability; Rheology; Viscoelasticity; Highly Concentrated Protein Solutions; Cherry-TagTM*

8.1 Introduction

Nowadays, proteins are indispensable as active components of key pharmaceuticals, due to their specificity and potency for the treatment of diverse diseases. Such molecules vary strongly in their size, shape, hydrophobic character and surface charge. Due to the individuality of the biomolecules, their stability and activity in aqueous solution depends on numerous parameters, including pH, ionic strength or protein concentration. The interaction of the different influencing parameters and their effect on the protein phase behavior is highly complex and not totally understood, though the solution stability of proteins is of primary concern during processing, formulation, and storage. As a consequence, the stability of a protein solution has to be proven for the release of the medical product by the regulatory bodies. Therefore, the long-term stability of the protein solutions needs to be tested under selected buffer conditions. Besides long-term stability tests, approaches for the fast prediction of protein phase behavior were developed in the last decades [188, 215]. Such methods include static light scattering for the determination of B_{22} values (protein self-interaction coefficient) or molecular modeling approaches to characterize protein-protein interactions *in silico* [188, 216, 217]. These approaches are able to display solute-solute and solute-solvent interactions. The results obtained with these methods were correlated successfully with protein phase behavior, but for ideally diluted protein solutions only [105, 120]. Short-range interactions or cluster formation, which occur at higher protein concentrations could neither be correctly predicted with B_{22} values [15] nor be included in the *in silico* model.

Whereas low or moderate protein concentrations are process-relevant for many biopharmaceutical unit operations, especially during late stage formulation studies, the focus is shifted to highly concentrated protein solutions. Product concentrations of antibody solutions for clinical applications can be easily above 100 mg/mL [22, 184]. In the last years the toolbox for the determination of protein phase behavior was thus extended to methods for highly concentrated protein solutions, including the traditional approaches of long-term protein phase diagrams [190], as well as less time consuming alternatives such as dynamic light scattering or rheological measurements [22, 127, 208, 218]. The rheological method to characterize protein solution viscoelasticity, as introduced by Saluja *et al.* [127] and extended by our group in 2016 [218] has the advantage of detecting the entire bulk properties of the sample. The sensitivity of the complex rheological analysis allows the identification of short and long-range interactions as well as the study of protein network formation [20].

With the ability to predict protein stability in ideally diluted and highly concentrated regime, the next logical step in the biopharmaceutical work flow is to manipulate protein phase behavior, and characterize such processes with the new tools developed.

Besides choosing stabilizing excipients and buffer conditions [161, 219, 220] also chemical modifications of proteins can be highly beneficial in terms of protein solution stability. Such modifications include glycosylation and PEGylation strategies [221]. Such effects on PEGylated proteins were reported for recombinant human endostatin when conjugated with a 5 kDa PEG chain [222], and human interferon-beta when modified with a 40 kDa PEG chain [223].

Another approach for engineering protein phase behavior and enhancing solubility is fusing an additional protein or peptide tag to the protein of interest. Some of these protein fusions are also commonly used as affinity tags, such as the maltose-binding protein (MBP) [224]. Further examples of solubility enhancing fusion proteins were reviewed, including Thioredoxin (Trx), the phage T7 protein kinase (T7PK), synthetic solubility-enhancing tags (SETs) [225, 226] and many more. In this study the newly developed Cherry-TagTM by Delphi Genetics (Belgium) is used as a potential protein stabilizer. The tag was originally developed for an easy traceability of proteins as it resembles cytochrome c, and can thus be determined in the VIS region. As soon as the fused protein becomes unstable the chromophore function of the protein is lost, enabling a distinction between native and non-native protein species [227]. The thermostability and solubility enhancing properties of the Cherry-TagTM technology was shown in studies involving enterokinase, staphylokinase, and G-CSF [228, 229]. In order to establish the targeted use of the tag in the biopharmaceutical industry, it is necessary to systematically study the stabilizing effect, also under highly concentrated conditions, and over time. To be able to transfer the gained knowledge to other molecule classes it is also indispensable to uncover the basic chemical-physical principles on which the stabilization is based.

To investigate the stability enhancing effect of the Cherry-TagTM a straightforward strategy is presented for predicting the long-term stability of highly concentrated GST and Cherry-GST solutions, with different straight to determine parameters from experimental (rheological) and *in silico* molecular dynamics investigations. The validity of the proposed measurement toolbox is proven by protein phase behavior studies performed in 96-well format in the Rock Imager (Formulatrix, USA) as was proposed by Rakel et al. and Baumgartner et al. [88, 162].

8.2 Materials and Methods

8.2.1 Chemicals & Buffers

The proteins used in this study were Glutathion-S-Transferase (GST - 26 kDa) and GST fused with the Cherry-TagTM (Cherry-GST - 39 kDa). GST has a theoretical pI of 5.2. The pI of GST was calculated based on the amino acid sequence obtained from the UniProt database [230] with the ExPASy ProtParam tool from the Swiss Institute of Bioinformatics [231]. The Cherry-TagTM being a polypeptide with a size of 11 kDa was developed by Delphi Genetics (Belgium). It is expressed in *Escherichia coli* SE1. The nucleic acid sequence of GST was inserted into the StabyExpress T7 kit for the protein of interest alone and into the Cherry Express T7 protein expression kit for the solubility enhanced fusion protein (Delphi Genetics, Belgium). All proteins were produced and purified as described in Baumann et al. [232].

1,3-Bis[tris(hydroxymethyl)methylamino]propane (BisTris propane) was purchased from Molekula (United Kingdom). β -Hydroxy-4-morpholinepropanesulfonic acid (MOPSO) was purchased from AppliChem (Germany). Acetic acid, citric acid, sodium chloride (*NaCl*) and ammonium sulfate ($(NH_4)_2SO_4$) were obtained from Merck KGaA (Germany). Trisodium citrate, sodium acetate, sodium monobasic phosphate and sodium dibasic phosphate were purchased from Sigma-Aldrich (USA). Ultrapure water (ISO3696) was used to prepare all solutions. For verification measurements viscosity standards (Olbrich, Germany) produced in accordance to the premium quality of BS EN ISO/IEC17025 were used.

8.2.2 Disposables & Reaction Vessels

For buffer exchange and ultra-filtration 20 mL Vivaspin ultra filtration spin columns (Sartorius, Germany) with a molecular weight cut off of 10000 Da were employed. The preparation of protein phase diagrams were carried out in 96-well microbatch crystallization plates from Greiner Bio-One (Germany).

8.2.3 Complex Rheology

Protein solutions behave viscoelastic. That implies that the protein solutions exhibit both viscous and elastic characteristics when undergoing deformation [204]. The characteris-

tic viscoelastic response of the samples gives insights of the strength of protein-protein interaction and the development of protein networks. The viscoelastic characteristics of protein solutions can be studied by frequency sweep measurements, where the rheological parameters G' (storage modulus - elastic portion) and G'' (loss modulus - viscous portion) can be calculated over a defined frequency range.

The rheological measurements were performed with the Piezo Axial Vibrator (PAV) Pechhold, Kirschenmann & Groß [233]. The measurement principle of the PAV is based on axial oscillating piezo elements, and operates at frequencies between 1 and 7000 Hz. In this work frequency sweep measurements were conducted over a frequency range of 100 - 5000 Hz in 22 frequency steps. For the rheological characterization of protein solutions the loss (G'') and storage modulus (G') were calculated over the dynamic displacement \hat{x} , the complex compressive rigidity K^* and the equation of motion:

$$K^* = \frac{\frac{3\Pi}{2} R \left(\frac{R}{d}\right)^3 G^*}{1 + \frac{\rho\omega^2 d^2}{10G^*} + \dots} \quad (8.1)$$

R is the radius of the plate, d is the gap width, ρ is the density of the squeezed material, and ω the radial frequency. With K^* one can calculate the complex modulus G^* . G^* can be easily divided in its imaginary and real part:

$$G^* = \sqrt{(G')^2 + (G'')^2} \quad (8.2)$$

A detailed derivation of these parameters is described in the doctoral thesis of Kirschenmann Kirschenmann [138]. The crossover point frequency of G' and G'' , ω_{CO} was used in this study to predict the long-term phase behavior of protein solutions. All measurements were conducted at a temperature of 20°C and a sample volume of 30 μ l. Every measurement was performed in duplicate. The standard deviation of the measurements conducted with the PAV were below 1.5 %.

8.2.4 Preparation of Protein Phase Diagrams

The automated method for the preparation of protein phase diagrams was realized on a robotic work station (Tecan GmbH, Germany). Four different troughs with buffers were

assigned to the robotic platform, including two low salt (without additional salt) and two high salt buffers (2 M salt added). These components were mixed automatically in a buffer plate to achieve six salt concentrations in range of 0 to 2 M salt. These solutions and the manually prepared protein samples (0 to 150 mg/mL) were mixed in a ratio of 1:5 to achieve the desired 96 different conditions. One crystallization plate consisted of two different pH values, protein concentrations from 5-120 mg/mL and salt concentrations from 0 – 400 mM. The crystallization plates were placed in the Rock Imager from Formulatrix (USA), an automated high resolution imaging system for protein crystallization. The plates were marked with a bar code and photographed in specified time intervals. After 40 days every single well was scored as clear, crystallized or precipitated based on the taken pictures.

8.2.5 Molecular Dynamics (MD) Simulations and Molecular Descriptors

For the investigation of 3D structure surface properties of GST and Cherry-GST MD models were generated and characterized. These models served for explaining the solubility enhancing properties of the attached Cherry-TagTM. The amino acid sequence of GST was derived from the RCSB Protein Data Bank [234] using the primary protein structure of the class-mu 26 kDa isozyme from *Schistosoma japonicum* (PDB ID 1DUG). The Cherry-TagTM being resemblant to Cytochrome B5 was modeled using PDB ID 1I8C. For manipulation, visualization, modeling of molecules, and molecular dynamics simulations under defined conditions the Yasara software was used [235]. Seven amino acids were added manually to GST (PDB ID 1DUG) being the linker molecules (Asp-Asp-Asp-Asp-Lys-His-Asn). For the Cherry-TagTM, per contrast, the Cytochrome B5 sequence was applied in its original form. Finally, both structures were linked by peptide bonding between Asn225 of the linker sequence attached to GST and the Ala226 of the Cherry-TagTM structure. Two of the Cherry-GST monomers were assembled to one dimer. For GST without the additional Cherry-TagTM the same procedure was performed except for attachment of the linker and the Cytochrome B5 sequence.

For generating the 3D equilibrium structure the dimers were simulated for 50 ns in Yasara. The energy minimization was carried out using the Amber03 force field [236]. This step serves for folding the newly added amino acids and for modeling interactions of the assembled sub-structures of the protein. As soon as the root mean square deviation (RMSD) of the simulation was constant within 1 Å the simulation was stopped.

In the next step the equilibrium structure of the dimer was prepared for the MD sim-

ulation in varying chemical environment. In a first step the degree of protonation was adjusted structure-based in H++ [237] according to pH and salt concentration and respective pKa values of the amino acids. Following, a simulation cell was formed around the protein-dimer in Yasara guaranteeing 10 Å of distance of all atoms to the periodic simulation box boundaries. The simulation box was filled with water molecules and respective ions depending on salt strength simulated. An energy minimization step followed to result in the final conditions for the MD simulation. The simulation was performed for 10 ps at 298 K, collecting a snapshot of the modeled structure every ps. In the MD analysis the mean structure of 10 frames of the MD simulation were presented as the protein structure.

In a final step the molecular descriptors of the 3D models under different conditions were determined using mantoQSAR, being an in-house developed tool for describing protein properties. These molecular descriptors can be calculated for the entire molecule, patches or plane projections and include information about size, shape, electrostatics and hydrophobicity of the respective molecule under pre-defined conditions (267 descriptors in total). Here, only the total electrostatic potential on the protein surface (sumMapSurfESP), the total hydrophobicity (Kyte and Doolittle hydrophathy scores [61]) on the protein surface (sumMapSurfHyd) and a molecule geometry factor (shapeMaxGeo) were used for identifying the influence of the Cherry-TagTM on protein solubility. The descriptor sumMapSurfESP describes the total charge of a protein with negative algebraic signs representing molecules of anionic and positive algebraic signs proteins of cationic surface characteristics, respectively. The descriptor of protein surface hydrophobicity (sumMapSurfHyd) is based on the hydrophathy scores of all surface amino acids of respective proteins. A negative algebraic sign represents hydrophilic behavior and a positive algebraic sign hydrophobic behavior, respectively. The molecular descriptor shapeMaxGeo is calculated in terms of geometric properties of the protein. Distances are determined between the center of gravity of each molecule to the protein surface at all possible angles in three dimensions. Finally, the maximal measured distance is divided by the mean distance of all angles resulting in values close to 1 for perfectly spherical proteins and values above 1 for proteins of other shapes.

8.3 Results and Discussion

8.3.1 Rheological Characterization of Cherry-GST and GST solutions

The rheological method proposed by Schermeyer et al. 2016 [218] was used to predict the time dependent stability of GST and Cherry-GST solutions. According to this theory, the shift of the crossover point of G' and G'' along the radial frequency, ω [rad/sec] - ω_{CO} - obtained by frequency sweep measurements, correlates with the phase behavior of the studied protein in aqueous solution. It was observed that the lower the ω_{CO} values, the stronger the protein-protein interactions are in solution. The protein-protein interactions correlate in turn with the agglomeration tendency and hence the colloidal long-term stability of the sample.

In this work GST and Cherry-GST solutions were investigated rheologically under varying buffer conditions and protein concentrations. The ω_{CO} values of all samples were compared to make predictions about the strength of protein-protein interaction, and thereby the stability of the molecules in solution.

In Fig. 8.1 the determined G' and G'' values of four typical samples are plotted against the radial frequency. For CherryGST and GST solutions the G'' values dominate the G' values over a wide frequency range, what implies a weak elasticity for all screened conditions. The curve shape of the studied samples were comparable, with a related difference of the relative position of the ω_{CO} value, which is the crucial parameter for the prediction of protein solution stability in this study.

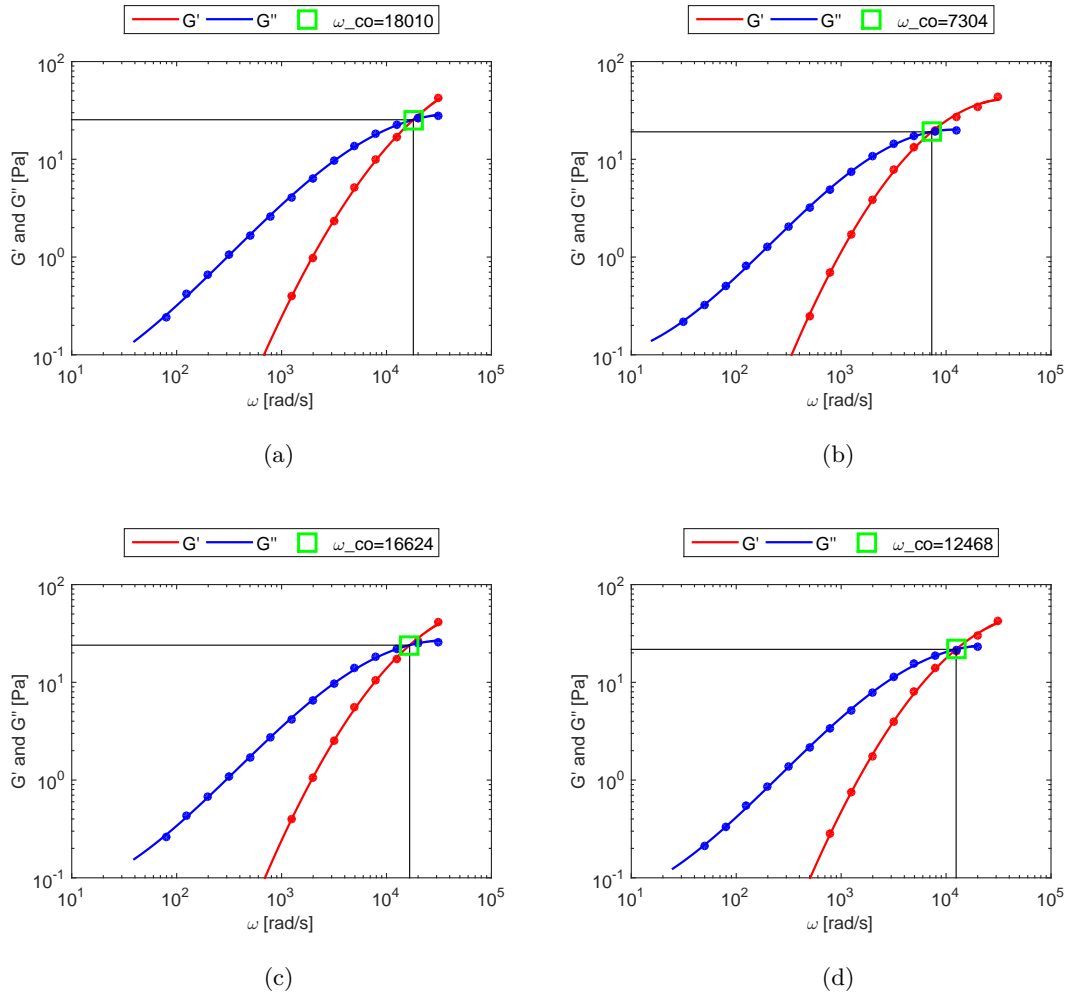


Figure 8.1: Exemplary curve shape of G'' and G' of Cherry-GST and GST under varying solution conditions. Shown is the rheological response of Cherry-GST (a) respectively GST (b) with a concentration of 100 mg/ml, at pH 6 without additives and Cherry-GST (c) respectively GST (d) with a concentration of 80 mg/mL at pH 8 and 400 mM $(NH_4)_2SO_4$. The rheological parameters were recorded at 22 frequency points over a frequency range from 100-40000 rad/sec.

Fig. 8.2 illustrates the influence of the protein concentration, the pH value, as well as the type and concentration of salt on the ω_{CO} values of GST and Cherry-GST samples. The ω_{CO} values are plotted as a colored scale from dark red (high ω_{CO} values) to dark blue

8.3 Results and Discussion

(low ω_{CO} values).

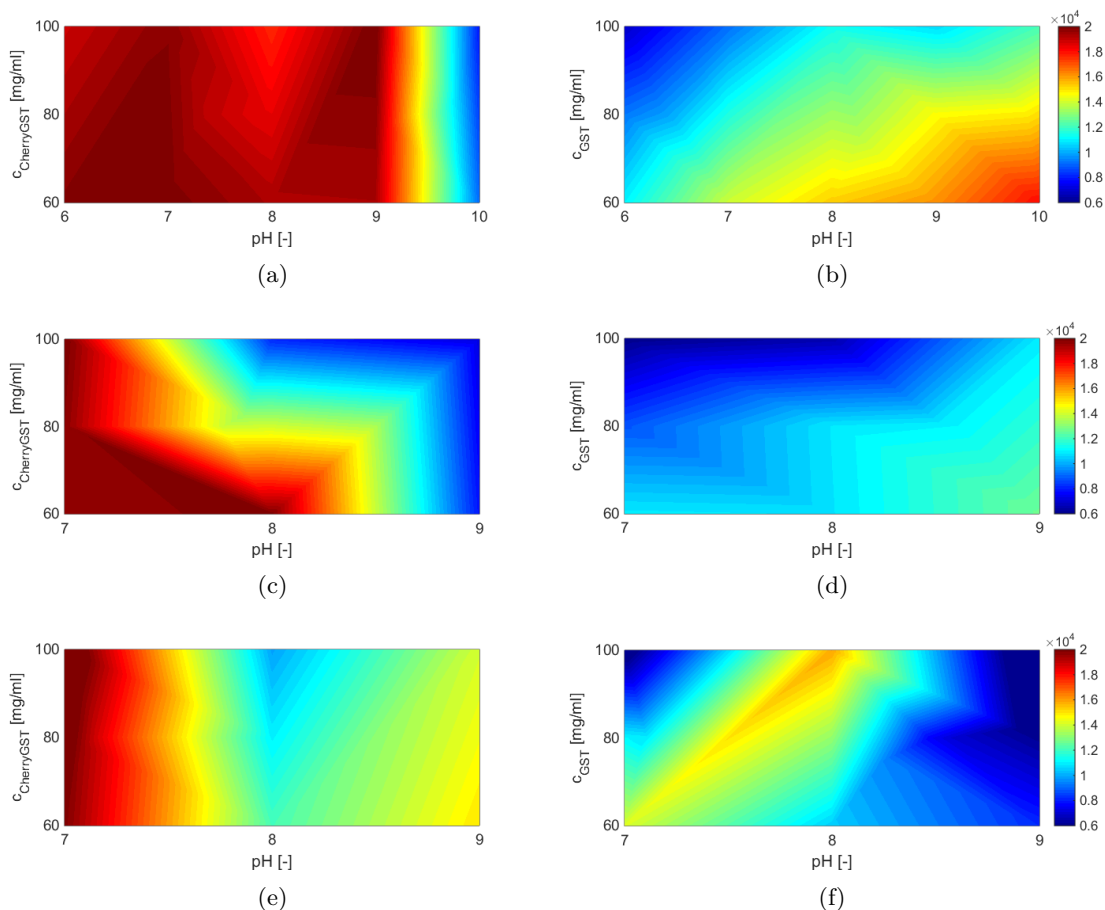


Figure 8.2: Surface plot of ω_{CO} values of Cherry-GST (left hand side) and GST (right hand side) samples in a pH range from 6-10, respectively pH 7-9 and a protein concentration range from 60-100 mg/mL. (a) and (b) without salt, (c) and (d) with $(NH_4)_2SO_4$ and (e) and (f) with $NaCl$. The ω_{CO} values are depicted as a colorbar ranging from 6000 rad/sec (dark blue) to 20000 rad/sec (dark red).

In Fig. 8.2 (a) and (b) the ω_{CO} values of Cherry-GST and GST samples without salt in solution are plotted. From pH 6 to pH 9 the ω_{CO} values of Cherry-GST solutions are comparatively high, and show only a negligible small dependency on the protein concentration (Fig. 8.2 (a)), which indicates that the molecules are flexible and can move freely in solution. It can therefore be concluded that protein-protein interactions of Cherry-GST

without salt in solution are weak, and do not change in the range from pH 6-9 and protein concentrations from 60-100 mg/mL. Using ω_{CO} as a predicting parameter, Cherry-GST at pH 6-9 would be classified as comparatively stable up to a concentration of 100 mg/mL. The stability of Cherry-GST in solution can be explained by repulsive electrostatic interactions of the protein, as the pI of this molecule lies below the tested pH values (pI \leq 5.2). Additionally, the amino acid structure of the attached Cherry-TagTM is in resemblance with the structure of Cytochrome B5. This molecule does have a theoretical pI of 4.3 [238, 239], and thus a negative net charge at tested pH values. Additionally, the linker structure, which covalently binds the Cherry-TagTM to the GST molecule mainly consists of aspartic acid with a theoretical pI of 2.98 [240]. The combination of both structures result in a negative surface charge of the Cherry-TagTM at tested pH values. It is assumed that either the negatively charged Cherry-TagTM shields positively charged or neutral patches on the protein surface or does have a direct impact on the protonation of neighboring groups on the GST surface, what may cause a stronger negative net charge of the whole molecule. At pH 10 the ω_{CO} values of Cherry-GST samples dropped below 10000 rad/sec independent on the protein content in solution. This indicates a limitation of the protein movement and therefore a stronger interacting behavior of the molecules. Similar to samples at pH 6-9 the net charge of the protein surface is negative at pH 10, and should induce repulsive interactions. Thus, the shift of ω_{CO} values to lower frequencies cannot be explained by electrostatic surface interactions alone. The increased viscoelasticity of Cherry-GST at pH 10 may originate from a partly unfolding due to the strong electrostatic repulsion within the molecule. The partly unfolding would lead to an exposition of hydrophobic core groups. It is energetically more favorable to minimize the hydrophobic area in an aqueous solution what would lead to increased protein-protein short-range interactions and thereby to a protein mobility reduction.

The ω_{CO} values of GST samples are dependent on the pH and protein concentration. The ω_{CO} values increased with increasing pH and decreased with increasing protein concentration. At pH 6 and a GST concentration of 100 mg/mL the lowest ω_{CO} value with 6856 rad/sec was calculated. At pH 10 and a GST concentration of 60 mg/mL the highest ω_{CO} value of 18065 rad/sec was determined for this data set. The mobility of GST in solution is less pronounced as the mobility of the Cherry-fusion protein especially at higher protein concentrations. This is bound up with an increase of the deviation from the ideal viscous behavior of GST solutions, and hence an increased propensity of protein network formation. That implies an increase in attractive protein-protein interactions due to forces, which are dependent on the protein concentration, such as short-range interactions [21]. Additionally, GST solutions do have higher ω_{CO} values with increas-

ing distance to the pI, indicating an increased repulsion of the molecules. This repulsive effect was explained earlier by an increasing protein net charge of GST with increasing pH. In contrast to ω_{CO} values of Cherry-GST samples the ω_{CO} values did not decrease abruptly at pH 10, but further increased. That indicates a dominant role of intermolecular repulsive electrostatic forces for GST at pH 10. The fact that solely ω_{CO} values of Cherry-GST drop at pH 10 lead to the conclusion, that the Cherry-TagTM provokes the partly unfolding of the protein due to structural changes or charge multiplication.

Using the ω_{CO} data observed for GST samples as a classification for GST long-term solution stability, samples at high pH values and low GST concentration would be predicted to be stable.

In Fig. 8.2 (c) and (d) the ω_{CO} values of Cherry-GST and GST samples containing 400 mM $(NH_4)_2SO_4$ are plotted in a range from pH 7-9 and a protein concentration range from 60-100 mg/mL.

$(NH_4)_2SO_4$ had an impact on the ω_{CO} values of Cherry-GST and GST. The number of systems where ω_{CO} values dropped below 15000 rad/sec increased for both proteins. That implies that the mobility of the molecules decreased with the addition of $(NH_4)_2SO_4$ dependent on pH, protein concentration and protein type. The impact of $(NH_4)_2SO_4$ on protein-protein interactions is most often explained by the position of the SO_4^- ions in the Hoffmeister Series Dumetz, Snellinger-O'brien, Kaler & Lenhoff [54] and Baldwin [87]. According to this theory $(NH_4)_2SO_4$ is a kosmotropic salt, and hence has a salting out effect on proteins Baumgartner *et al.* [88] and Collins [241]. Kosmotropic salts have the ability to strengthen the structure of water molecules around them. Due to the exclusion of water, which previously surrounded the protein surface, hydrophobic patches on the protein surface are uncovered, what leads to an intensified interaction of the proteins, and therefore a decreased colloidal protein stability. These interactions weaken the mobility of the molecule what induces lower ω_{CO} values. The salting out theory explains the viscoelastic behavior of GST very well. Here, the impact of salt was especially high at high protein concentrations and at pH values close to the pI, where stronger hydrophobic protein-protein interactions are presumed. The theory can not explain the impact of $(NH_4)_2SO_4$ on the viscoelastic behavior of Cherry-GST samples. Here, the salt had mainly an impact on samples at high pH values. The low ω_{CO} values at pH 10 were explained by a partly unfolding of CherryGST due to strong repulsive electrostatic interactions. A shift of the reduced flexibility to lower pH values would imply that $(NH_4)_2SO_4$ has a reinforcing effect on the conformational instability of Cherry-GST. However, SO_4^- ions are known to have a stabilizing impact on the 3D structure of proteins. This theoretical conformational stabilization is inconsistent with the arguments mentioned above. One

explanation for the reduced flexibility of Cherry-GST at pH 9 with $(NH_4)_2SO_4$ in solution could be that the unfolding can not be suppressed by the addition of $(NH_4)_2SO_4$, but that the attraction of the partly unfolded proteins with each other is strengthened by the addition of this salt.

Further, a distinction must be made between GST and Cherry-GST samples containing $(NH_4)_2SO_4$ in relation to the strength and extend of the ω_{CO} drop. For Cherry-GST samples the addition of $(NH_4)_2SO_4$ had only an impact for pH 9 and 100 mg/mL and pH 9. The impact of the salt on the viscoelastic behavior of Cherry-GST at pH 7 and pH 8 (60-80 mg/mL) was negligible small. For GST samples instead, the addition of $(NH_4)_2SO_4$ had a strong impact on each condition tested. Here, all ω_{CO} values decreased below 12562 rad/sec (pH 9, 60 mg/mL). Transferred to the solution stability of the protein, this implies an increased aggregation propensity for GST with the addition of $(NH_4)_2SO_4$ for all tested conditions and an increased aggregation propensity for Cherry-GST samples at pH 8 with a protein concentration of 100 mg/mL as well as for pH 9 with a protein concentration of 60-100 mg/mL.

$NaCl$ had a different impact on the rheological characteristics on both studied proteins in comparison to $(NH_4)_2SO_4$. For Cherry-GST samples $NaCl$ had a decreasing impact on ω_{CO} values solely at pH 8. The lowest ω_{CO} value (9827 rad/sec) was detected at pH 8 and a protein concentration of 100 mg/mL (Fig. 8.2 (e)). At pH 7, the ω_{CO} values were more or less unaffected by the addition of $NaCl$ with values around 19000 rad/sec, similar to ω_{CO} values at pH 9 with values ranging from 13000-14000 rad/sec for the tested protein concentration range.

In comparison, the addition of $NaCl$ had a strong impact on the rheological response of GST samples at all conditions tested (Fig. 8.2 (f)). At pH 8 and a GST concentration of 100 mg/mL the highest ω_{CO} value of 20357 rad/sec was detected. The lowest ω_{CO} values for this screening area were observed at pH 7 and 100 mg/mL (5373 rad/sec) and at pH 9 and 100 mg/mL (4143 rad/sec).

$NaCl$ is classified in the middle of the Hofmeister series. It has neither a strong chaotropic nor kosmotropic character. Nevertheless, only the rheological behavior of Cherry-GST at pH 7 was totally uninfluenced by the addition of $NaCl$. Additional to the salting in and salting out effect preferential interactions between the Na^+ ions and the negatively charged patches of the GST and Cherry-GST surface may occur. This interaction can cause a shielding of the charged surface groups and thus a reduction of protein-protein repulsion. Interestingly, the strongest decreasing impact on ω_{CO} values of Cherry-GST samples was found at pH 8 and a protein content of 100 mg/mL. At this condition $NaCl$ had the least effect on the rheological behavior of GST. $NaCl$ even seemed to stabilize

GST, as the difference between the ω_{CO} values with and without 400 mM *NaCl* is positive with a value of 9850 rad/sec. The surprisingly strong and opposing effect of *NaCl* on GST and CherryGST samples, respectively is difficult to be explained by theoretical considerations. However, it is a further indication that due to the fused tag, the protein behavior in solution changes significantly. After reviewing various studies about the salt impact on different molecule species Curtis et al. concluded that there is no single unified theoretical framework to rationalize the specificity of salt ion effects on protein intermolecular interactions Curtis & Lue [53]. The exact mechanism of *NaCl* on the viscoelastic behavior of GST respectively Cherry-GST under tested conditions seems to be complex and is part of future investigations.

In summary the ω_{CO} values of GST samples are lower in comparison to ω_{CO} values of Cherry-GST samples at similar buffer conditions and protein concentrations, except for samples at pH 10. Without salt in solution the pH (from pH 6-9) and protein concentration had a negligible small impact on the viscoelastic characteristic of Cherry-GST. Per contrast, the rheological behavior of GST changed significantly with changing buffer conditions and protein concentration. Also the tested salts, $(NH_4)_2SO_4$ and *NaCl*, had a differing impact on the rheological response of the solutions dependent on the protein type. Using the rheological measurement and more specifically the ω_{CO} values as a tool to predict protein solution stability, Cherry-GST was assessed as more stable in comparison to GST at tested conditions except for pH 10. The stabilizing effect of the tag is especially rheologically noticeable at higher protein concentrations. Additionally, Cherry-GST is less affected by the addition of salt particularly at pH 7.

For both proteins the measurements were performed under similar buffer and environmental conditions. Therefore, the reasons for the different viscoelastic behavior of GST and Cherry-GST, and the predicted different solution stability, have to be found in the change of protein surface characteristics due to the Cherry-TagTM. It is assumed that a specifically strong negative charge and a shielding character of the tag may be the basis of the predicted stability enhancement. To understand the differing impact of tested salts, pH and protein concentration on GST and Cherry-GST solution viscoelasticity better, the surface characteristics of both molecules were studied *in silico* (see 8.3.3). Prior to the analysis of the protein surface characteristics, the predicted solution stability was validated by long-term colloidal stability tests.

8.3.2 Long-term Colloidal Stability of Cherry-GST and GST Solution

To validate the prediction of the long-term protein solution stability based on rheological results, the long-term colloidal stability of both proteins was investigated by protein phase diagrams. The samples of Cherry-GST and GST were scored after 40 days of incubation in a climate chamber as precipitated, crystallized or discolored, based on optical evaluation. To avoid repetitive text, the listed stability results will only be discussed when a deviation from the already discussed predicted stability of Cherry-GST and GST based on rheological investigations was observed.

In Fig. 8.3 the scoring of GST and Cherry-GST samples are shown. Red full circles symbolize stable samples, samples where aggregation occurred are marked as blue filled squares, gelation is marked as an open diamond and samples where a color shift from red to yellow was observed are symbolized as blue open circles.

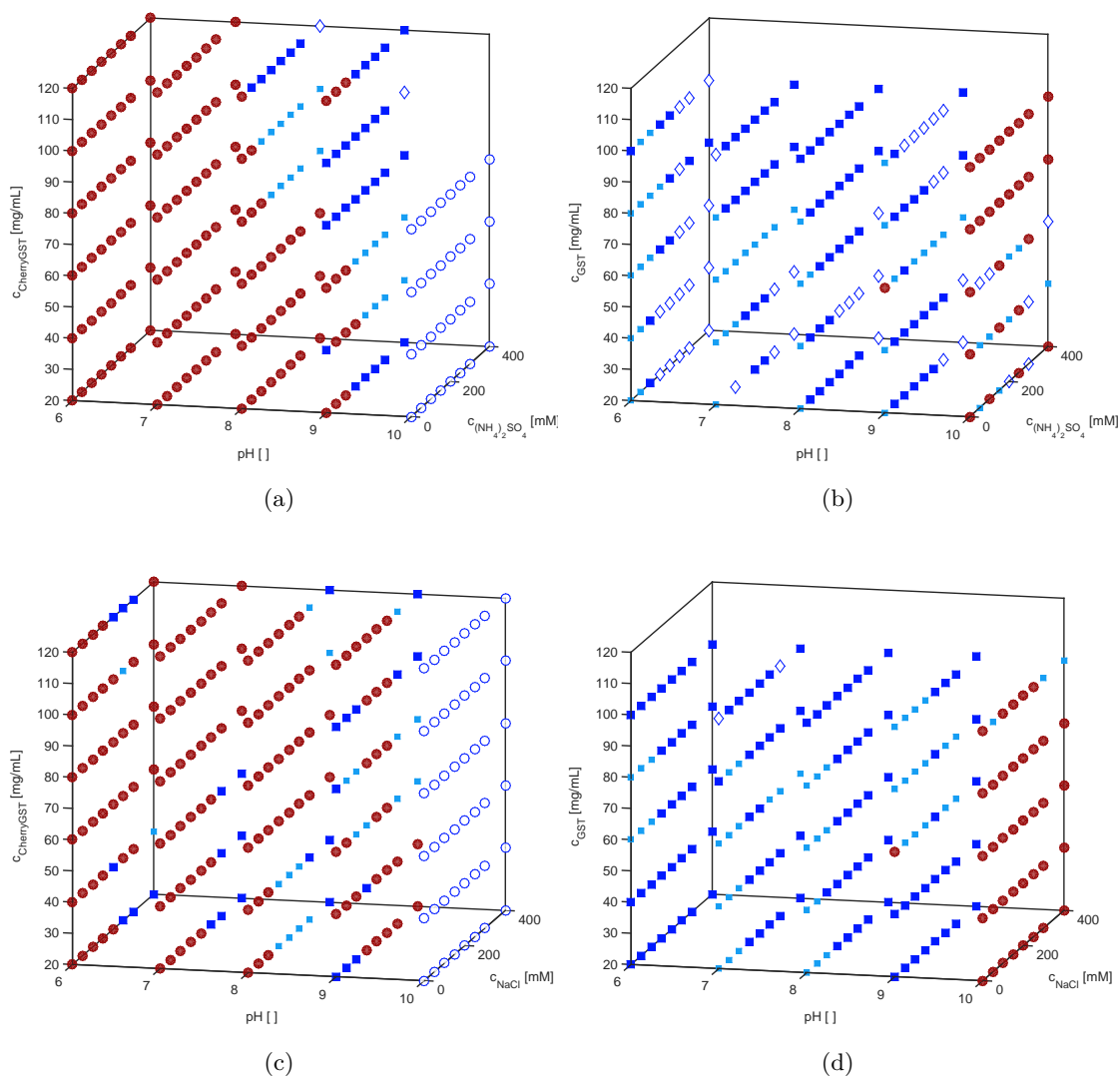


Figure 8.3: Protein phase behavior of Cherry-GST at pH values from 6-10, protein concentrations from 20-120 mg/mL and (a) $(NH_4)_2SO_4$ concentrations from 0-400 mM and (c) $NaCl$ concentrations from 0-400 mM and protein phase behavior of GST at pH values from 6-10, protein concentrations from 20-120 mg/mL and (b) $(NH_4)_2SO_4$ concentrations from 0-400 mM and (d) $NaCl$ concentrations from 0-400 mM. Clear samples are plotted as red filled circles, light precipitated samples as small light blue squares, precipitated samples as blue squares, gel formation as blue diamonds and discolored samples as unfilled blue circles.

Fig. 8.3 (a) displays the scoring of Cherry-GST in a pH range from pH 6-10, a protein concentration range from 20-120 mg/mL, and the addition of 0-400 mM $(NH_4)_2SO_4$. The samples at pH 10 starting at a Cherry-GST concentration of 100 mg/mL could not be scored due to the immediate precipitation of the protein in the preparation process. The protein was colloidal stable at pH 6 and pH 7 over the whole tested protein and $(NH_4)_2SO_4$ concentration range. At pH 8 light precipitation occurred at a Cherry-GST concentration of 80 and 100 mg/mL, starting from a $(NH_4)_2SO_4$ concentration of 150 mM. At pH 8 and a protein concentration of 120 mg/mL the protein precipitated over the whole tested salt concentration range. The unstable region of Cherry-GST increased at pH 9. At pH 10 a color shift from red to yellow was observed for all tested protein and $(NH_4)_2SO_4$ concentrations. The color shift of Cherry-GST was shown to be caused by conformational protein instability [232].

Phase transition was observed for GST samples in a range from pH 6-9 with and without salt in solution (Fig. 8.3 (b)). The strength of precipitation increased with increasing $(NH_4)_2SO_4$ concentration. Additional to strong precipitation, gelation occurred at higher $(NH_4)_2SO_4$ concentrations. At pH 10 GST was stable at protein concentrations of 80 and 100 mg/mL with and without $(NH_4)_2SO_4$ in solution. At lower protein concentrations, GST was destabilized and precipitation and gel formation occurred when $(NH_4)_2SO_4$ was added.

In Fig. 8.3 (c) the phase behavior of Cherry-GST with $NaCl$ as a precipitant is shown. At pH 6 Cherry-GST was stable in a protein concentration range from 20-120 mg/mL and up to a $NaCl$ concentration of 200 mM. At pH 7 precipitation only occurred at Cherry-GST concentrations from 20-60 mg/mL and the addition of 250-400 mM $NaCl$. Similar behavior was observed at pH 8. At pH 9 clear samples were observed with the addition of 150-200 mM $NaCl$ over the whole tested Cherry-GST concentration range. At pH 10 discoloration occurred for the whole tested salt and protein concentration range, similar to the discoloration at pH 10 with $(NH_4)_2SO_4$ as a precipitant (compare Fig. 8.3 (a)). $NaCl$ had a comparable impact on the phase behavior of GST as $(NH_4)_2SO_4$ (Fig. 8.3 (d)). Precipitation occurred at pH 6, pH 7, pH 8 and pH 9 with $NaCl$ as an additive. Only at pH 10 in a protein concentration range from 20-100 mg/mL and the addition of $NaCl$ clear samples were observed. Light precipitate was observed at 100 mg/mL at 250 and 400 mM $NaCl$. In summary, it was found that Cherry-GST had a wider soluble region in comparison to GST under all tested conditions.

For the validation of the rheological measurements as a predicting tool solution conditions, which were rheologically analyzed were correlated directly with the studied phase behavior. To enable an easy comparison of the actual phase behavior and rheological

8.3 Results and Discussion

results the phase state of Cherry-GST (left hand site) and GST (right hand site) is plotted repeatedly in Fig. 8.4 at buffer conditions and protein concentrations as shown in Fig. 8.2.

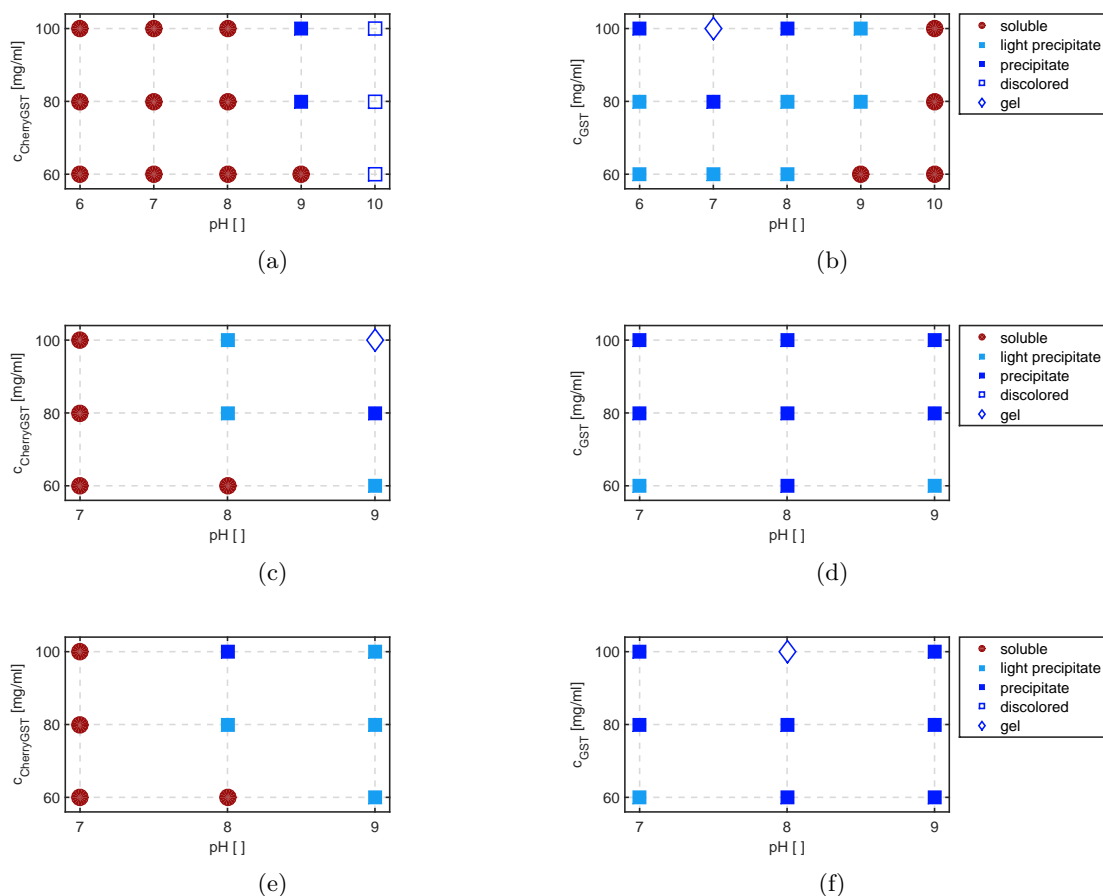


Figure 8.4: Scoring of the phase behavior of Cherry-GST (left hand side) and GST (right hand side) in a pH range from 6-10 respectively pH 7-9 and a protein concentration range from 60-100 mg/mL. (a) and (b) without salt, (c) and (d) with 0-400 mM $(NH_4)_2SO_4$ and (e) and (f) with 0-400 mM $NaCl$. The ω_{CO} values are depicted as a colorbar ranging from 6000 rad/sec (dark blue) to 20000 rad/sec (dark red).

Under stable colloidal conditions, the ω_{CO} values were higher in comparison to conditions where phase transitions occurred. This observation holds true for both proteins at all tested conditions. Also the discoloration, hence the denaturation of Cherry-GST at pH 10 could be reflected by a major drop of the ω_{CO} values below 10000 rad/sec. The

only condition at which the phase transition can not be correlated to a low ω_{CO} value is the sample with a GST content of 100 mg/mL, at pH 8, and 400 mM *NaCl*. At this specific condition gelation occurred but an increase of the ω_{CO} value was observed. An explanation might be that the gelation is formed by a network of native GST molecules induced by specific ionic effects of the *NaCl*. Such network formations were already described for crowded protein solutions [242]. This assumption is hypothetical and the interesting effect of *NaCl* part of future studies.

The predictability of the solution stability of GST and Cherry-GST with the help of rheological measurements was successful. Therefore, the detailed discussion of section 8.3.1 can also be used for the discussion of the actual colloidal stability of Cherry-GST and GST.

To study the conformational stability of the proteins in more detail, additionally to the long-term phase diagrams, thermal stability studies were performed. Here, the melting temperatures (T_m) of discussed samples were determined. As the thermal stability measurements did only show marginal differences under all investigated molecules and buffer conditions, the results can be found in the supplementary material (Figure A2).

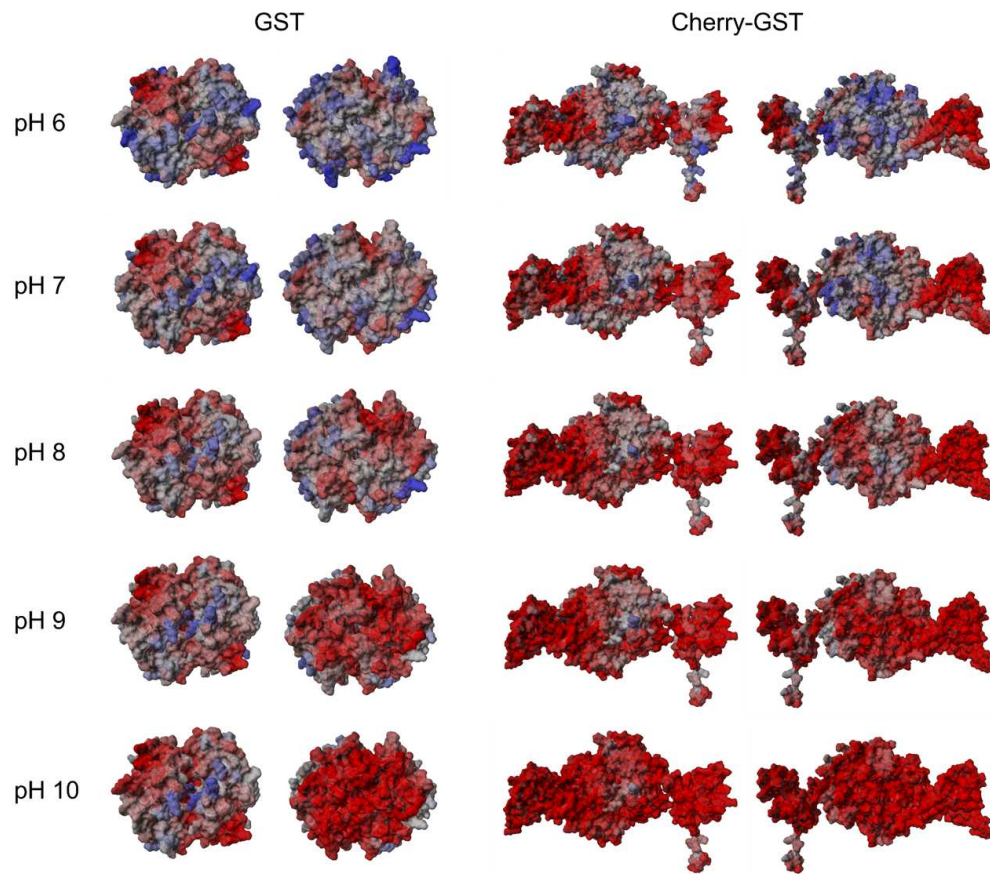
To underline the made assumptions concerning the differing solution stability of GST and Cherry-GST the protein surface characteristics of both proteins were further investigated with the help of MD simulations. The results of the analytical findings are discussed in the next sections.

8.3.3 Molecular Dynamics (MD) Simulations and Molecular Descriptors

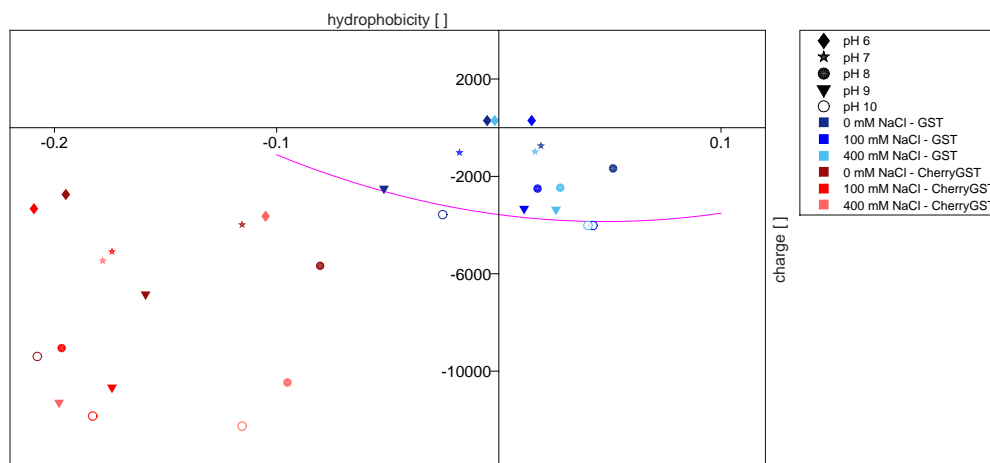
As ζ -potential measurements (data can be found in the supplementary material, Figure A1) are not sufficient to describe the strong enhancement of protein solution stability when adding the Cherry-TagTM, modeling on the molecular level (MD) was performed. The MD approach enables a deeper understanding of molecular properties, including not only electrostatic properties, but also other factors such as shape and surface hydrophobicity on a three-dimensional structure level. Fig. 8.5 (a) illustrates MD models of GST (left) and Cherry-GST (right) under different pH conditions in a range of pH 6 and 10 in 1 pH unit steps. Each of the 3D models is shown from the front side and the back side, respectively. Blue areas represent positively charged molecule patches, and red areas correspond to negatively charged protein surfaces. According to Fig. 8.5 (a) the Cherry-TagTM alone is dominated by negative surface charges in the entire pH range, resulting in an increased negative total surface charge of the fusion protein compared to

8.3 Results and Discussion

GST alone. GST per contrast exhibits a homogenous charge distribution in a pH range of pH 6 to pH 8. Cherry-GST at pH 9 and pH 10 results in a highly negative charged molecule with almost no positively charged residues remaining. Such repulsive forces of equally charged molecules are, however not the only driving effect for enhanced protein solubility.



(a)



(b)

Figure 8.5: (a) MD models of GST (left) and Cherry-GST (right) at pH 6-10. Each 3D model illustrates the front and back side of the protein, whereas blue areas represent positively charged molecule patches, and red areas correspond to negatively charged protein surfaces. (b) Respective total electrostatic potential on the protein surface (sumMapSurfESP), and the total protein surface hydrophobicity (sumMapSurfHyd) of GST and Cherry-GST.

Another factor to be considered is the geometry difference of both molecules. This was investigated by the molecular descriptor `shapeMaxGeo`, which has a value of 1 for ideally spherical shaped proteins, and increasing values for molecules of non-spherical shape. GST results in `shapeMaxGeo` values are in a range of 1.35 to 1.42 for all investigated conditions, whereas Cherry-GST was determined to be in a range of 2.08 to 2.12. Thus, GST is rather compact and of spherical shape and the Cherry-TagTM acts as a steric factor, which might be another stabilizing factor for increasing protein solubility.

Whereas in Fig. 8.5 (a) qualitative values for the electrostatic potential of proteins were discussed only, Fig. 8.5 (b) illustrates the quantitative values of the total electrostatic potential on the protein surface (`sumMapSurfESP`) and the total protein surface hydrophobicity (`sumMapSurfHyd`). Different symbols are used for pH values in a range of pH 6 to 10 with blue colors for GST and red colors for Cherry-GST. The investigated salt concentrations are indicated as color gradients with darker colors for low salt concentrations. All electrostatic and hydrophobic descriptors of GST are situated close to the coordinate origin of the plot, representing a charge homogeneity and moderate hydrophobic character. Per contrast, all system points of Cherry-GST are much more hydrophilic in nature being far left of GST in Fig. 8.5 (b). This is another strong indicator of the distinct phase behavior of both molecules, as proteins of hydrophobic nature are highly instable in water and tend to aggregate. The qualitative trend of total electrostatic potential on the protein surface in Fig. 8.5 (a) is verified by the quantitative values illustrated in Fig. 8.5 (b). Even at the lowest pH of 6 Cherry-GST carries negative charges whereas GST even shows slight cationic behavior. This trend becomes more and more pronounced for higher pH values up to pH 10. The purple line indicates the threshold of solubility determined in the protein phase diagrams. All unstable conditions are found in a cluster close to the coordinate origin, and all stable conditions are of hydrophilic nature with additional charge extremes for electrostatic repulsion. The only exception was found for Cherry-GST at pH 10 where there was no colloidal, but a conformational instability of the protein. This effect might be explained by negative surface charge extremes (Fig. 8.5 (a) - Cherry-GST pH 10) resulting in protein unfolding. The findings of the MD simulations support the assumptions made for interpreting the rheological results and the predicted solution stability of section 8.3.1.

8.4 Conclusions

Engineering and monitoring protein solution stability is an essential task for producing and launching biopharmaceutical products. Whereas established analysis in the field of long-term protein stability still requires time-consuming experimental setups, this screening could demonstrate that new tools can help for predicting and understanding stability attributes within several hours.

We investigated experimental and *in silico* MD tools for fast prediction of protein solution stability under different chemical surroundings and high protein content. Also the protein of interest (GST) was investigated with an additional solubility enhancing Cherry-TagTM fusion.

The rheology measurements indicated a strong enhancement of GST colloidal stability with the additional fusion tag compared to the native protein under all investigated conditions with exception of pH 10. Here, an unfolding of Cherry-GST was identified as a consequence of excess surface charge. The stabilization of Cherry-GST compared to GST was also pronounced under addition of $(NH_4)_2SO_4$ or $NaCl$, though the used concentration range usually leads to a salting out effect. The validation of such short-time predictions based on rheology was performed by long-term stability experiments at identical conditions, leading to comparable results of both methods. Thus, rheology was robust to predict protein solution stability of highly concentrated protein solutions towards changing chemical environment and molecular modifications.

Finally, to understand the solubility enhancing properties of the Cherry-TagTM both proteins were further investigated on the molecular level. The MD simulations clearly indicated that the stabilizing effect of the Cherry-TagTM can be explained by three different effects, namely, the hydrophobicity reduction, the strong negative charge enhancement and additionally a steric geometric effect.

It could be shown that the determination of molecular properties in combination with rheological measurements are strong tools to study the extent and causes of protein long-term stability. With the applied experimental and *in silico* MD tools in hand, buffer optimizations and fast decisions during pharmaceutical process development are possible for ensuring product quality and stability. Also, the stabilizing properties of the Cherry-TagTM might become an approved protein modification by the authorities, analogously to the PEGylation procedures, which are widely employed in industry.

8.5 Acknowledgments

The authors acknowledge the financial support by the German Federal Ministry of Education and Research (BMBF) - funding code 0316071B - and the general support by the industrial partners DelphiGenetics (Belgium) and m2p-Labs (Germany). This research work is part of the project 'ERA Net Euro Trans Bio - 6: Development of an integrated strategy for a high-throughput process development platform on a micro-scale format – FORECAST'. We also highly acknowledge the input by B.Sc. Claudia Weigel. The authors assume the complete responsibility for the contents of this publication and declare no conflict of interest.

Supplementary Material

ζ-potential Measurements

The ζ-potential as an indicator for protein surface charge was determined by Laser Doppler micro-electrophoresis using the Zetasizer Nano ZSP (Malvern Instruments, United Kingdom). The velocity of the molecules is measured when a voltage of 60 mV is applied. With the help of the velocity the ζ-potential of the molecules can be calculated. The ζ-potential represents the electric potential in the interfacial ion double layer of a molecule. It is directly linked to the net surface charge of the molecule and is therefore an important parameter to study protein-protein interactions resulting from electrostatic interactions. In this study the ζ-potential of GST and Cherry-GST with a concentration of 30 mg/mL at pH 6-10 without salt and with 400 mM $(NH_4)_2SO_4$ or $NaCl$ was determined. For the measurement 20 μL of sample was pipetted in a disposable folded capillary cell and measured with the diffusion barrier technique Corbett, Connah & Mattison [243].

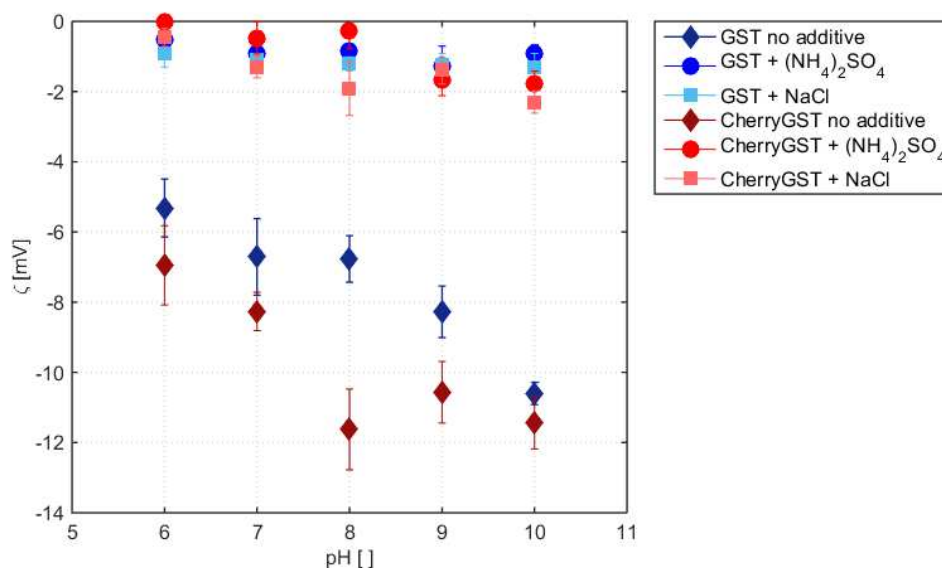


Figure 8.6: ζ -potential values of Cherry-GST and GST at 30 mg/mL, pH 6-10 with and without 400 mM $(NH_4)_2SO_4$ respectively 400 mM $NaCl$ in solution.

Determination of the Protein Melting Temperature (T_m)

To investigate the thermo-stability of GST and Cherry-GST the fluorescence spectra of both proteins were measured over a temperature ramp. The temperature ramp was run to force the protein to unfold. During the temperature ramp the number of exposed fluorescent amino acids from the core increase while the protein unfolds. Due to the increasing amount of detectable amino acids the signal of fluorescent light shifts along the wavelength. This shift can be used to calculate the T_m of the protein. The fluorescence measurements were performed with the UNit acquired from Unchained Labs (Pleasanton, USA). Here 7 μ L of the sample was manually pipetted in a sample carrier containing 12 quartz glass sample tubes. A temperature ramp from 20-90 °C was run and the fluorescence signal was recorded in 0.5 °C steps per minute. Then the shift of the fluorescence signal was plotted against the temperature and the T_m values were calculated at the inflection point of the evolved curve. Investigated samples contained 30 mg/mL of GST or Cherry-GST at pH values of 7, 8, 9 and 10. All conditions were measured without salt and with 400 mM $(NH_4)_2SO_4$ or $NaCl$, respectively.

8.5 Acknowledgments

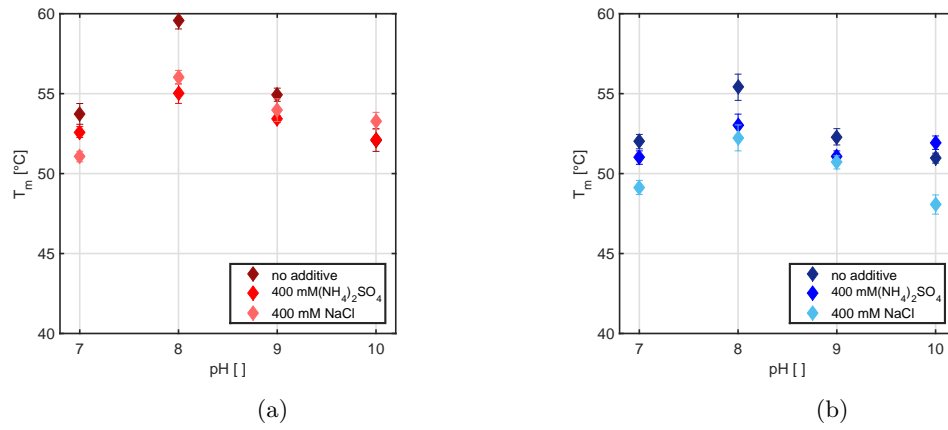


Figure 8.7: T_m values of Cherry-GST, left hand side, and GST, right hand side at pH 7-10 with and without 400 mM $(NH_4)_2SO_4$ respectively 400 mM $NaCl$ in solution.

8.6 References

15. Chari, R., Jerath, K., Badkar, A. V. & Kalonia, D. S. Long- and short-range electrostatic interactions affect the rheology of highly concentrated antibody solutions. *Pharmaceutical research* **26**, 2607–18 (2009).
20. Saluja, A. *et al.* Application of high-frequency rheology measurements for analyzing protein-protein interactions in high protein concentration solutions using a model monoclonal antibody (IgG2). *Journal of Pharmaceutical Sciences* **95** (2006).
21. Kumar, V., Dixit, N., Zhou, L. L. & Fraunhofer, W. Impact of short range hydrophobic interactions and long range electrostatic forces on the aggregation kinetics of a monoclonal antibody and a dual-variable domain immunoglobulin at low and high concentrations. *International Journal of Pharmaceutics*. **421**, 82–93 (2011).
22. Harn, N., Allan, C., Oliver, C. & Middaugh, C. Highly concentrated monoclonal antibody solutions: direct analysis of physical structure and thermal stability. *Journal of Pharmaceutical Sciences* **96**, 532–540 (2007).
27. Chi, E. & Krishnan, S. Physical stability of proteins in aqueous solution: mechanism and driving forces in nonnative protein aggregation. *Pharmaceutical Research* **20**, 1325–1336 (2003).
43. Wang, W. & Roberts, C. J. *Aggregation of therapeutic proteins* 150–151 (Wiley, 2010).
53. Curtis, R. A. & Lue, L. A molecular approach to bioseparations: Protein–protein and protein–salt interactions. *Chemical Engineering Science* **61**, 907–923 (2006).
54. Dumetz, A. C., Snellinger-O’Brien, A. M., Kaler, E. W. & Lenhoff, A. M. Patterns of protein protein interactions in salt solutions and implications for protein crystallization. *Protein science : a publication of the Protein Society* **16**, 1867–77 (2007).
61. Kyte, J. & Doolittle, R. F. A simple method for displaying the hydrophobic character of a protein. *Journal of Molecular Biology* **157**, 105–132 (1982).
87. Baldwin, R. L. How Hofmeister ion interactions affect protein stability. *Biophysical journal* **71**, 2056–63 (1996).

88. Baumgartner, K. *et al.* Determination of protein phase diagrams by microbatch experiments: Exploring the influence of precipitants and pH. *International Journal of Pharmaceutics* **479**, 28–40 (2015).
105. Wilson, W. Light scattering as a diagnostic for protein crystal growth—A practical approach. *Journal of Structural Biology* **142**, 56–65 (2003).
107. Goldberg, D. S., Bishop, S. M., Shah, A. U. & Sathish, H. A. Formulation Development of Therapeutic Monoclonal Antibodies Using High-Throughput Fluorescence and Static Light Scattering Techniques: Role of Conformational and Colloidal Stability. *Journal of Pharmaceutical Sciences* **100**, 1306–1315 (2011).
120. George, A. & Wilson, W. W. Predicting protein crystallization from a dilute solution property. *Acta crystallographica. Section D, Biological crystallography* **50**, 361–5 (1994).
127. Saluja, A. *et al.* Ultrasonic storage modulus as a novel parameter for analyzing protein-protein interactions in high protein concentration solutions: correlation with static and dynamic light scattering measurements. *Biophysical journal* (2007).
138. Kirschenmann, L. *Aufbau zweier piezoelektrischer Sonden (PRV/PAV zur Messung der viskoelastischen Eigenschaften weicher Substanzen im Frequenzbereich* PhD thesis (Universitaet Ulm, 2003).
161. Hansen, C. L., Sommer, M. O. A. & Quake, S. R. Systematic investigation of protein phase behavior with a microfluidic formulator. *Proceedings of the National Academy of Sciences of the United States of America* **101**, 14431–14436 (2004).
162. Rakel, N., Baum, M. & Hubbuch, J. Moving through three-dimensional phase diagrams of monoclonal antibodies. *Biotechnology Progress* **30**, 1103–1113 (2014).
184. Liu, J., Nguyen, M. D. H., Andya, J. D. & Shire, S. J. Reversible self-association increases the viscosity of a concentrated monoclonal antibody in aqueous solution. *Journal of Pharmaceutical Sciences* **94**, 1928–40 (2005).
188. Rosenbaum, D. F. & Zukoski, C. F. Protein interactions and crystallization. *Journal of Crystal Growth* **169**, 752–758 (1996).
190. Rakel, N., Galm, L., Bauer, K. & Hubbuch, J. From osmotic second virial coefficient (B₂₂) to phase behavior of a monoclonal antibody. *Biotechnological Process* **31**, 438–451 (2015).
204. Macosko, C. W. *Rheology: Principles, Measurements, and Applications* (Wiley-VCH, 1994).

208. Venkataramani, S., Truntzer, J. & Coleman, D. R. Thermal stability of high concentration lysozyme across varying pH: A Fourier Transform Infrared study. *Journal of Pharmacy & Bioallied Sciences* **5**, 148–53 (2013).
216. Skoulakis, S. & Goodfellow, J. M. The pH-dependent stability of wild-type and mutant transthyretin oligomers. *Biophysical Journal* **84**, 2795–2804 (2003).
217. Ma, B. & Nussinov, R. Simulations as analytical tools to understand protein aggregation and predict amyloid conformation. *Current Opinion in Chemical Biology* **10**, 445–452 (2006).
218. Schermeyer, M.-T. *et al.* Squeeze flow rheometry as a novel tool for the characterization of highly concentrated protein solutions. *Biotechnol. Bioeng.* **113**, 576–587 (2016).
219. Krishnan, S. *et al.* Aggregation of granulocyte colony stimulating factor under physiological conditions: Characterization and thermodynamic inhibition. *Biochemistry* **41**, 6422–6431 (2002).
220. Grigsby, J. J., Blanch, H. W. & Prausnitz, J. M. Cloud-point temperatures for lysozyme in electrolyte solutions: Effect of salt type, salt concentration and pH. *Biophysical Chemistry* **91**, 231–243 (2001).
221. Rodríguez-Martínez, J. A. *et al.* Stabilization of α -chymotrypsin upon PEGylation correlates with reduced structural dynamics. *Biotechnology and Bioengineering* **101**, 1142–1149 (2008).
222. Nie, Y., Zhang, X., Wang, X. & Chen, J. Preparation and stability of N-terminal mono-PEGylated recombinant human endostatin. *Bioconjugate Chemistry* **17**, 995–999 (2006).
223. Basu, A. *et al.* Structure-Function Engineering of Interferon- β -1b for Improving Stability, Solubility, Potency, Immunogenicity, and Pharmacokinetic Properties by Site-Selective Mono-PEGylation. *Bioconjugate Chemistry* **17**, 618–630 (2006).
224. Kapust, B. R. & Waugh, S. D. Escherichia coli maltose-binding protein is uncommonly effective at promoting the solubility of polypeptides to which it is fused. *Protein Science* **8**, 1668–1674 (1999).
225. Esposito, D. & Chatterjee, D. K. Enhancement of soluble protein expression through the use of fusion tags. *Current Opinion in Biotechnology* **17**, 353–358 (2006).

226. Zhang, Y. B. *et al.* Protein aggregation during overexpression limited by peptide extensions with large net negative charge. *Protein Expression and Purification* **36**, 207–216 (2004).
227. Baumann, P., Baumgartner, K. & Hubbuch, J. Influence of binding pH and protein solubility on the dynamic binding capacity in hydrophobic interaction chromatography. *Journal of Chromatography A* **1396**, 77–85 (2015).
228. Mohan Padmanabha Das, K. *et al.* A Novel Thermostability Conferring Property of Cherry Tag and its Application in Purification of Fusion Proteins. *Journal of Microbial & Biochemical Technology* **01**, 059–063 (2009).
229. Azhar, M. & Somashekhar, R. Cloning , expression and purification of human and bovine Enterokinase light chain with Cherry tag and their activity comparison. *Indian Journal of Applied and Pure Biology* **29**, 125–132 (2014).
230. Consortium, U. UniProt: a hub for protein information. *Nucleic Acids Research* **43**, 204–212 (2015).
231. Wilkins, M. R. *et al.* Protein identification and analysis tools in the ExPASy server. *Methods in Molecular Biology* **112**, 531–52 (1999).
232. Baumann, P. *et al.* Integrated development of up- and downstream processes supported by the Cherry-Tag[®],c for real-time tracking of stability and solubility of proteins. *Journal of Biotechnology*. **200**, 27–37 (2015).
233. Pechhold, W., Kirschenmann, L. & Groß, T. *Offenlegungsschrift DE 101 62 838 A1* 2003.
234. Berman, H. M. The Protein Data Bank. *Nucleic Acids Research* **28**, 235–242 (2000).
235. Krieger, E., Koraimann, G. & Vriend, G. Increasing the precision of comparative models with YASARA NOVA-a self-parameterizing force field. *Proteins: Structure, Function, and Bioinformatics* **47**, 393–402 (2002).
236. Duan, Y. *et al.* A point-charge force field for molecular mechanics simulations of proteins based on condensed-phase quantum mechanical calculations. *Journal of Computational Chemistry* **24**, 1999–2012 (2003).
237. Anandakrishnan, R., Aguilar, B. & Onufriev, A. V. H++ 3.0: automating pK prediction and the preparation of biomolecular structures for atomistic molecular modeling and simulations. *Nucleic Acids Research* **40**, W537–W541 (2012).

238. Abe, K. & Sugita, Y. Properties of Cytochrome b5, and Methemoglobin Reduction in Human Erythrocytes. *European Journal of Biochemistry* **101**, 423–428 (1979).
239. Kuwada, M., Hasumi, H. & Furuse, Y. Purification of Cytochrome b5 from Pig Testis Microsomes by Isoelectric Focusing in an Immobilized pH Gradient. *Protein Expression and Purification* **12**, 420–424 (1998).
240. Brown, W. H. *Organic chemistry* (Brooks/Cole Cengage Learning, 2009).
241. Collins, K. D. Ions from the Hofmeister series and osmolytes: effects on proteins in solution and in the crystallization process. *Methods* **34**, 300–311 (2004).
242. Miklos, A., Sarkar, M., Wang, Y. & Pielak, G. Protein Crowding Tunes Protein Stability. *Journal of the American Chemical Society* **133**, 7116–7120 (2011).
243. Corbett, J. C. W., Connah, M. T. & Mattison, K. Advances in the measurement of protein mobility using laser Doppler electrophoresis - the diffusion barrier technique. *Electrophoresis* **32**, 1787–94 (2011).
254. Ahamed, T. *et al.* Phase behavior of an intact monoclonal antibody. *Biophysical Journal* **93**, 610–619 (2007).

Characterization of highly concentrated antibody solution -
A toolbox for the description of protein long-term solution
stability

Marie-Therese Schermeyer¹, Anna K. Wöll¹, Bas Kokke², Michel Eppink² and Jürgen Hubbuch¹

¹*Institute of Engineering in Life Sciences, Section IV: Biomolecular Separation Science, Karlsruhe Institute of Technology (KIT), 76131 Karlsruhe, Germany*

²*Synthon Biopharmaceuticals B.V., Microweg 22, 6545 CM Nijmegen, The Netherlands*

Abstract

High protein titers gain increasing significance for the biopharmaceutical industry. A major challenge in the development of highly concentrated mAb solutions is their long-term stability and often incalculable viscosity. The complexity of the molecule itself as well as the various molecular interactions make it difficult to describe their solution behavior. To study the formulation stability long and short-range interactions as well as the formation of complex network structures have to be taken into account. For a better understanding of highly concentrated solutions, this work combines established and novel analytical tools to characterize the impact of solution properties on the stability of highly concentrated mAb formulations. In this study monoclonal antibody solutions in a concentration range of 50 - 200 mg/ml at pH 5 - 9 with and without glycine, PEG4000 and Na_2SO_4 were analyzed. To determine the monomer content analytical SEC runs were performed. ζ -potential measurements were conducted to analyse the electrophoretic properties within different solutions. The melting and aggregation temperatures were determined with the help of fluorescence and static light scattering measurements. Additionally, rheological measurements were conducted to study the solution viscosity and the viscoelastic behavior of the mAb solutions. The so determined analytical parameters were scored and merged as an analytical toolbox. The resulting scoring was then successfully correlated with long-term storage (40 days of incubation) experiments. The study indicates that the sensitivity of complex rheological measurements in combination with the applied techniques allow reliable statements about the impact of solution properties such as protein concentration, ionic strength and pH shift on the strength of protein-protein interaction and solution colloidal stability.

Keywords: *monoclonal antibodies; conformational and colloidal stability; zeta potential; viscosity; viscoelasticity; thermal stability; phase diagrams*

9.1 Introduction

Antibodies are used for a wide range of pharmaceutical treatments. Particularly for cancer or autoimmune diseases they are indispensable as specifically effective drugs [244, 245]. New therapeutic forms and mode of administrations demand an ever increasing molecule titer of the monoclonal antibodies in the final formulation [246]. The molecular density in solution cause new challenges for the biopharmaceutical process development, formulation and application. Especially the colloidal and conformational long-term stability of the molecules are considered as a bottleneck [16].

The stability of highly concentrated mAb solutions is influenced by various forces. These forces can be divided into long-range and short-range interactions. Long-range interactions do have an impact on proteins in ideal dilute solutions whereas the impact of short-range interactions increase with increasing protein titer. So that at highly concentrated conditions an interplay of short- and long-range interactions occur. Following the DLVO theory, electrostatic forces do have the longest reach and are classified as repulsive long-range interactions [247]. The stronger the net charge of the molecular surface, the more likely the molecules of the same kind will repel each other and the weaker is the aggregation tendency of the proteins in the respective solution [15]. However, it was found that when exceeding a certain charge value the protein starts to unfold. In this case the intramolecular repulsive interactions are so strong that the chemical bonds stabilizing the protein 3D structure are destroyed [207, 248, 249]. Due to the progress of MD simulations and the advancements of analytical techniques, the charge distribution on the protein surface and its influence on the solution stability is well understood [21, 250]. An established method to experimentally characterize the net surface charge of a protein is the determination of the ζ -potential. The ζ -potential describes the electric ion potential of the interfacial double layer and can for example be determined with the help of laser-doppler-mikro-elektrophoresis [251]. The determination of the ζ -potential provide insights into the kind and strength of electrostatic forces which may lead to protein agglomeration and unfolding.

According to the DLVO theory, Van der Waals forces are classified as short-range interactions. They can be described as universal weak attractive interactions of electromagnetic origin which are induced by dipole moments [55]. The forces between two polarized molecules only have a short range, so that they only have a measurable effect within the molecule and in highly concentrated protein solutions. In the last decades the DLVO theory was extended by taking hydrophobic forces, specific ion effects and the impact of the

hydration layer into account when discussing protein-protein interactions. Comparable to van der Waals forces they can be classified as attractive short-range interactions. They are known to have a significant impact on the native structure of a protein and protein-protein interactions in the highly concentrated regime [21]. The experimental detection of the type and strength of short-range interactions is comparable difficult due to their weak individual effects.

Both, the character and strength of short and long-range interactions are influenced by the amino acid sequence and molecular structure of the protein as well as the pH, ionic strength and co-solutes of the surrounding solution [67, 252]. The complex interplay of the listed forces and their individual dependency on varying solution conditions makes it so difficult to describe and predict protein long-term stability in the highly concentrated regime.

Because of the complexity of the interactions involved, not the forces themselves are analyzed in industry, but rather their effects on the molecular stability and the protein phase behavior. For this purpose, the target molecule is solved in relevant solutions and, after the equilibrium has been established, its phase state and/or 3D structure is determined. In order to be able to compare the actual behavior of the molecules in solution, without having to wait for the equilibrium condition, the process can be accelerated by energy input in form of increased temperature conditions. The increased temperature induces the agglomeration and chemical degradation of the protein in a short time period and can therefore accelerate long-term stability tests. Weiss, Young & Roberts [99] and He *et al.* [108] could show that an increase of the so depicted melting temperature values (T_m) correlate with an increased long-term stability of studied proteins. As this method is high throughput compatible and has a working volume in μL scale, the temperature induced phase transition is widely used, especially in the pre-selection of buffer components and molecule main candidates.

Although these methods provide information on the behavior of the proteins in solution, they merely provide a glimpse of the full picture of protein solution stability. In order to widen the view and thus to predict the long-term stability of antibodies in solution it is necessary to clarify the underlying causes, which is why a lot of research has been done in this area in recent years [100, 126, 253]. What is needed is a lump parameter accounting for all the different influencing parameters. For a long time the B_{22} value was thought to be such a key parameter [105, 120, 188, 254]. However, this approach has not delivered regarding concentrated protein solutions [20, 162]. An approach where multidimensional interactions, occurring only at high protein concentrations, are taken into account, is the measure of protein solution viscosity. The solution viscosity, hereafter called viscosity, is

the resistance of a fluid to gradual deformation. The rheological parameter was shown to correlate with the aggregation tendency of biopharmaceutical molecules, especially in the highly concentrated regime [115, 184]. Additionally to the good comparability with protein stability, the viscosity itself is of high importance for processing and formulation. When the viscosity exceeds the processability or syringability of the solution to be handled it can not be manufactured as a liquid application, which is the favored formulation for the very difficult to crystallize antibodies. It is for this reason that the study of the long-term stability of a protein solution and the resulting selection of main candidates and buffer conditions should always take viscosity investigations into account.

A further promising application of rheology with regard to protein solution stability is the study of the viscoelastic behavior of protein solutions.

Protein solutions behave viscoelastic. That implies that the protein solutions exhibit both viscous and elastic characteristics when undergoing deformation [204]. The viscous behavior can be described by the loss modulus, G'' and the elastic behavior by the storage modulus, G' . The characteristic viscoelastic response of the samples provides insights into the strength of protein-protein interaction and the development of protein networks. The behavior of proteins considering their interactions with other proteins or co-solutes as well as their molecular flexibility can be depicted without the manipulation of the sample, also in the highly concentrated regime [204].

Saluja *et al.* [20] introduced a viscoelastic parameter which has the potential to be correlated directly with the protein long-term stability. In the published work highly concentrated antibody solutions were characterized with ultrasonic shear rheology. Saluja *et al.* determined G' of given solutions at a set frequency value. The determined G' values were used to correlate the viscoelastic characteristics of protein solutions with the aggregation tendency of different antibodies. The work of Schermeyer *et al.* [218] is based on these findings. Here, frequency sweep measurements were applied to be able to calculate G' as well as G'' over a wide frequency range. When measuring viscoelastic substance the values of G' and G'' plotted over the radial frequency show a characteristic curve shape with a crossover point. It was shown that dependent on the molecule interactions and molecular flexibility the crossover point shifts along the frequency axis [131, 218]. The frequency value of this crossover point, ω_{CO} could be successfully correlated to the long-term phase behavior of the model protein lysozyme at concentrations ranging from 100 - 225 mg/ml. The study of the viscoelastic characteristic was also applied to describe the stability enhancing effect of the Cherry-Tag[®] which was fused to Glutathion-S-Transferase. Here, the rheological study in combination with molecular dynamics simulation could not only be used for the description of the colloidal solution stability but also the conformational

stability of the fused protein [252].

Unfortunately none of the presented novel or established methods is FDA approved to predict the long-term stability of antibody solutions, yet [100, 109]. The parameters which have an impact on the molecular conformational and colloidal stability are so complex that decision-makers hesitate to recommend one single predicting analytical method. So that in industry, every formulation has to be stored at least 12 - 24 months to prove the long-term stability of the target molecule, which is time and therefore cost-intensive.

To address this challenge, an analytical toolbox is presented in this work. The toolbox includes the intelligent combination of established and novel analytical techniques for the description and prediction of protein long-term solution stability. As strong orthogonal analytical techniques SEC measurements, ζ -potential and viscosity measurements, thermal stability tests as well as complex rheological measurements are performed in a wide screening range. The solution conditions were selected on the basis of pre-stability tests, with the aim of being able to investigate a wide range of positive and negative influencing physico-chemical mechanisms. The impact of three types of co-solutes, namely polyethylene glycol (PEG), sodium sulfate (Na_2SO_4) and glycine, on the mAb solution stability were investigated. The large-scale screening allows the investigation of the antibody stability behavior under various conditions and also reveals the limits of the individual analytical methods applied. Furthermore, the results of the measurements are scored and merged in a last step. The scoring values are directly compared to long-term stability tests. The combined scoring values conduce as a valid and safe toolbox for the description and prediction of the mAb long-term solution stability.

9.2 Materials and Methods

9.2.1 Materials

The humanized monoclonal antibody (mAb) used in this study has a molecular weight of 145.5 kDa and a theoretical pI of 8.7. It was kindly provided by Synthon Biopharmaceuticals B.V.. The mAb was delivered with a monomer content of above 98 % at pH 5.5 and a protein concentration of ca. 30 mg/ml (hereinafter: stock solution). For this study multi component buffer systems containing CABS (Santa Cruz Biotechnology), CHES (AppliChem), MES and TAPS (AppliChem), sodium acetate trihydrate (Fulka), sodium dihydrogen phosphate monohydrate (Merck) and TAPSO (Sigma-Aldrich) were used. The ionic strength of the buffer solutions was 10 mM. Glycine (Sigma), PEG4000

and Na_2SO_4 (Merck) were used as additives. Ultrapure water (ISO3696) was used to prepare all solutions. For buffer exchange and concentration of the samples 20 ml and 40 ml Vivaspin ultrafiltration spin columns (Sartorius) with a molecular weight cut off of 60000 Da were employed. To prepare protein phase diagrams 96-well microbatch crystallization plates from Greiner Bio-One were used.

9.2.2 Experimental Setup

9.2.2.1 Buffer and mAb Preparation

For the experiments multicomponent buffers were prepared following the description of Kröner & Hubbuch [255]. Buffers used in this study were adjusted with sodium chloride to an ionic strength of 6.7 mS/cm using the conductivity-electrode CDM 230 (Radiometer Analytical). The mAb stock solution was buffer exchanged and concentrated up to 250 mg/ml with Vivaspin columns and a rotational speed of 12300 g (fixed angle rotor, Eppendorf centrifuge 5810R). Subsequently, a protein dilution series with the corresponding buffer was prepared, so that after the addition of the second component, either a high salt or low salt buffer in a ratio of 1:5 (buffer:protein solution) the required final protein concentration could be achieved. The second component was added manually. After the components were mixed, an equilibration time of 15 min was kept before the analytical measurements were started. All analytical runs were performed at 20°C and at least in duplicate.

9.2.2.2 Size Exclusion Chromatography

To study the mAb monomer content, the amount of high molecular weight species (HMW) and low molecular weight species (LMW) size exclusion chromatography (SEC) runs were performed directly after sample preparation. The SEC measurements were done with an UHPLC system (Agilent) using an Acquity PLC BEH200 SEC column. The samples were diluted with 100 mM phosphate buffer (pH 7.5) to a mAb concentration of 1 mg/ml. This buffer was also used as running buffer for all chromatography runs. The measurements were done with a flowrate of 0.3 ml/min and an injection volume of 2.5 μ L. The UV signal at 280 nm was detected and processed by the Chromeleon 7.1 chromatography data system. The mass ratio of monomer, HMW and LMW was calculated based on the areas of the detected peaks.

9.2.2.3 ζ -potential Measurements

To study the surface potential of the target molecule the ζ -potential was determined by Laser Doppler micro-electrophoresis using the Zetasizer Nano ZSP (Malvern Instruments). According to the manufacturer the sensitivity of this measurement tool is ± 2 mV. A voltage of 60 mV was applied to calculate the ζ -potential over the velocity of the molecules. The voltage was set to limit the current to a maximum of ± 5 mA and the number of runs were limited to 10. To determine the ζ -potential disposable folded capillary cells and the diffusion barrier technique were used to reduce the sample volume to 20 μ L. In this study the ζ -potential of mAb solutions with a concentration of 10 mg/ml in a pH range from pH 5-11 without additives, with 15 mM glycine, 0.2 (m/V)% PEG4000 respectively 16 mM Na_2SO_4 was determined. The mAb and additive concentration was reduced 10 fold to avoid interference of electro osmosis which may occur at samples with an ionic strength greater than 150 mM [111].

9.2.2.4 Viscosity Measurements

The viscosity was measured with the Viscosizer (Malvern Instruments) using Poiseuille flow. Here, the sample is automatically pumped through a microcapillary under constant drive pressure. The time (Δt_s) the sample needs to pass a set pathlength is measured and referenced against the time (Δt_r) taken for a fluid of known viscosity. The relative viscosity values of mAb samples with 120 and 180 mg/ml protein content at pH 5, with and without 50-150 mM glycine, pH 7 with and without 50-150 mM glycine, 100-160 mM Na_2SO_4 and pH 9 with and without 50-150 mM glycine respectively 0.4-4 (m/V)% PEG4000 in solution were determined.

9.2.2.5 Thermal Colloidal and Conformational Stability

To study the conformational and colloidal thermo stability of the mAb under varying conditions a temperature ramp was run to force the protein to aggregate or/and to unfold. The measurements were performed with the UNit (Unchained Labs) where T_m and T_{agg} of 48 samples can be measured simultaneously. The T_m values were calculated at the inflection point of the curve developed when plotting the shift of the fluorescence signal over the applied temperature. For some samples two inflection points could be calculated. For this reason the parameter was additionally indexed with 1 for the first inflection

point (T_{m1}) and 2 for the second inflection point (T_{m2}). The T_{agg} values were calculated based on the steepest slope which evolved when plotting the static light scattering signal over the applied temperature. The temperature ramp started at 20°C, ended at 90°C and had a step width of 1 °C/*min*. In this study samples with a mAb concentration of 5-180 mg/ml at pH 7 without additives and samples with a mAb concentration of 120 mg/ml and 180 mg/ml at pH 5, 7 and 9 with 50, 100 and 150 mM glycine, mAb concentration of 120 mg/ml and 180 mg/ml at pH 7 and 100, 140 and 160 mM Na_2SO_4 and mAb concentration of 120 mg/ml and 180 mg/ml at pH 9 with 0.4, 1.2 and 2 (m/V)% PEG4000 were screened.

9.2.2.6 Determination of Protein Solution Viscoelasticity

To determine the storage modulus (G') and the loss modulus (G'') frequency sweep measurements in a frequency range of 100-60000 rad/sec were performed with the Piezo Axial Vibrator (PAV). The applied frequency range also defines the detection limit of the measurement tool. Following the publication of Schermeyer *et al.* [218] the frequency value of the crossover point of G' and G'' , ω_{CO} was used to compare the viscoelastic response of studied samples. The calculated ω_{CO} values also conducted as a predictive parameter. A description of the measurement tool and the derivation of G' and G'' can be found elsewhere [138, 139, 218]. The height of the measuring chamber was 15 μ m. For the measurement 35 μ L of sample was pipetted on the measurement head. The measurement head was closed with a force of 2 Nm. In this study mAb solution with concentrations of 50, 120, 180 and 200 mg/ml at pH 5, 7 and 9 without additives, with concentrations of 50, 120, 180 and 200 mg/ml at pH 5, 7 and 9 with 150 mM glycine, 2 (m/V)% PEG4000 respectively 160 mM Na_2SO_4 were conducted.

9.2.2.7 Preparation of Protein Phase Diagrams

To study the colloidal long-term solution stability of the mAb protein phase diagrams were prepared. Therefore, a robotic liquid handling station (Tecan) was used following the method described by Baumgartner *et al.* [88]. To achieve 96 conditions on one plate, four buffer troughs were prepared including two low salt and two buffers with one of the selected additives in a high concentration. A buffer plate was prepared with these solutions to achieve six additive concentrations ranging from 0-2.5 M glycine, 0-1.6 M Na_2SO_4 and 0-20 (m/V)% PEG4000. These conditions were then mixed with manually

prepared mAb samples ranging from 0-250 mg/ml in a ratio of 1:5 resulting in a sample volume of 24 μ L. One crystallization plate consisted of two pH values ranging from pH 5-9, mAb concentrations ranging from 120-225 mg/ml and additive concentrations ranging from 0-200 mM glycine, 0-160 mM Na_2SO_4 respectively 0-2 (m/V)% PEG4000. After preparation the plates were centrifuged for 1 min at 1540 g to reduce air bubble content and covered using optically clear and UV compatible sealing tape (Duck Brands). The plates were then placed in an automated high resolution imaging system (Rock Imager, Formulatrix). Every single well was photographed in specific time intervals. After 40 days the samples were visually scored as colloidal stable, low precipitated or precipitated. Additionally, Fourier transform infrared spectroscopy (FTIR) measurements were performed to study the long-term conformational stability of the antibody under varying conditions. The results revealed that the 2D structure of the antibody did not change at studied conditions after 40 days of incubation, wherefore the results are not shown here.

9.3 Results and Discussion

9.3.1 Preliminary Selection of Additives

In this study the predictive properties of different analytical methods on the solution stability of highly concentrated mAb solutions is investigated. The protein solution stability is substantially dependent on the solution additives. Attention was paid that the used additives have either positive or negative effects on the mAb solution stability and that the impact is triggered by different physico-chemical mechanisms. Therefore, the selection followed the results of pre-tests, where the impact of several additive types and concentrations on the mAb solution stability was tested qualitatively with dynamic light scattering (DLS) measurements. The methodology of the DLS measurement, conditions tested and results can be found in the supplementary material (see section A1). Three types of additives, namely salts, polymers and osmolytes were tested. In the following section, possible physico-chemical mechanisms of these co-solutes on the antibody solution stability and thus the reasoning for their selection are shortly discussed.

The effect of salts on the protein solution stability is mainly dependent on their concentration and type. At low ionic strengths salts primarily have a stabilizing impact, due to nonspecific electrostatic interactions. This stabilizing effect was found to be independent on salt type and is mostly pronounced close to the pI of proteins [256]. With increasing

salt content, the impact of salt type becomes more pronounced. The stabilizing effect at low salt concentrations can be reversed to a destabilizing effect, also known as salting-out [85]. The Hofmeister series divides the salts according to their salting-out character. Salts with a strong salting-out character are classified as kosmotropes and salts with a predominantly salting-in character are classified as chaotropes. In several studies it was shown that antibody solution behavior follows this theory [257]. Strongly hydrated ions (kosmotropes) do have a negative impact on the hydration shell of proteins, increasing the hydrophobic protein-protein interactions and therefore have a negative impact on the protein colloidal stability (e.g. Na_2SO_4) [84, 256, 258, 259]. The strengthening of inner molecular hydrophobic interactions on the other hand lead to an increased conformational protein stability. Chaotropic salts, like potassium iodide, decrease hydrophobic interactions by destroying the water structure around solvated molecules. They have a denaturing effect on proteins but may increase the colloidal stability at low to moderate concentrations. As the interactions of salt ions with the protein are mainly based on electrostatic interactions, the impact of salt is pH dependent and dependent on the amino acid sequence of the molecule tested. Specific interactions of salt ions with amino acid residues are not totally understood, especially at higher protein concentrations. So that modulations on protein-protein interactions by salt ions and their implications for protein solution behavior cannot be completely rationalized [53]. The impact of the kosmotropic salt Na_2SO_4 on the mAb solution stability will be studied in this context.

In contrast to salt ions polymers are uncharged, hydrophilic molecules whose effect on proteins is mainly dependent on their chain length. Attractive protein-protein interactions can be strengthened when adding long chain polymers by depletion attraction. The depletion attraction arises from an increase in osmotic pressure of the surrounding solution when the proteins in solution get close enough such that the excluded co-solutes cannot fit in between them [260, 261]. Based on this theory, the comparatively large hydrophilic polyethylene glycol (PEG) molecules exclude a certain amount of volume from the solution which is then inaccessible to other molecules [262]. Thereby, the mAb molecules are sterically excluded from the volume of PEG and concentrate in the remaining volume. The so increased mAb concentration may lead to stronger short-range protein interactions which may cause agglomeration or unfolding of the molecules.

Short-chain polymers, on the other hand, can increase protein stability by preventing protein-protein interactions due to sterical hindrance. Additionally it was found that the OH group of polyethylene glycol can interact with positively charged amino acid residues of proteins [263]. This specific binding changes the net charge of the protein and may have a negative impact on the protein colloidal stability below the pI. In this study a

comparatively large PEG with a molecular weight of 4000 Da will be investigated. Osmolytes including polyols, certain amino acids and methylamines are mainly used as stabilizing additives. The stabilizing effect of osmolytes is most often explained by the preferential exclusion of these small molecules from the protein surrounding. The preferential exclusion implies that the concentration of the osmolyte in the immediate volume element surrounding the protein is lower, than its concentration in the bulk phase. That increases the water volume and its structured orientation around the protein, resulting in a colloidal stabilization [83, 95]. The theory of protein surface hydration and the accompanying increase of surface tension is also known as the cavity theory. Several studies on protein colloidal and conformational stability support the cavity theory and the stabilizing character of osmolytes [264–267]. The impact of glycine on the mAb solution behavior will be studied in this work.

9.3.2 Analytical Characterization of mAb Solution

To be able to describe the colloidal and conformational long-term stability of the mAb solutions, various analytical methods were applied. The analytics focused on pH 5, pH 7 and pH 9 and mAb concentrations of 120 and 180 mg/ml. The impact of 50, 100 and 150 mM glycine was tested for all pH values. The effect of 0.4, 1.2 and 2.0 (m/V)% PEG4000 was studied at pH 9. The impact of 100 - 160 mM Na_2SO_4 was tested at pH 7. To evaluate the monomer, HMW and LMW content of the mAb in the stock solution, as well as before and after sample preparation (buffer exchange and concentration) SEC runs were conducted. The impact of electrostatic interactions were studied by ζ -potential measurements. To get to know the conformational and colloidal thermal stability of selected mAb samples T_m and T_{agg} values were determined. The focus here was to evaluate the comparability of thermal and time induced phase transitions of the mAb. Additionally, rheological measurements were performed to study the impact of varying solution conditions on the viscosity and to correlate the viscoelastic behavior of the mAb molecules with the long-term stability. The listed analytics shall give a detailed picture of the micro and macroscopic antibody behavior and should, as a combination of strong orthogonal tools, enable a precise description of the long-term stability. The applied analytics are discussed separately.

9.3.2.1 Initial Solution Characteristics: Size Exclusion Chromatography

A description of the influence of preparation procedure, pH and additives on the initial solution characteristics at t_0 was performed using SEC measurements upfront of the analytical assays chosen in this study.

The evaluation of the chromatograms, namely the setting of the peak limits and the area calculation of the respective peaks, were always carried out according to the same methodology and by the same operator, so that a very small mean standard deviation of 0.04 % could be achieved. The mAb stock solution had a monomer content of 98 %, 0.33 % HMW and a LMW content of 0.98 %.

In general the tested mAb is relatively stable against buffer exchange and concentration in relation to the monomer content determined by analytical SEC chromatography. The monomer content in all tested samples was higher than 94.8 %. In Figure 1 (a) the monomer, LMW and HMW content of samples after buffer exchange and original concentrations of 120 mg/ml and 180 mg/ml are plotted. The antibody concentration had a small decreasing impact on the monomer content of the antibody with or without additive in solution. The monomer decrease may be caused by the strengthening of mAb-mAb interactions due to the reduced distance of the molecules with increasing mAb concentration.

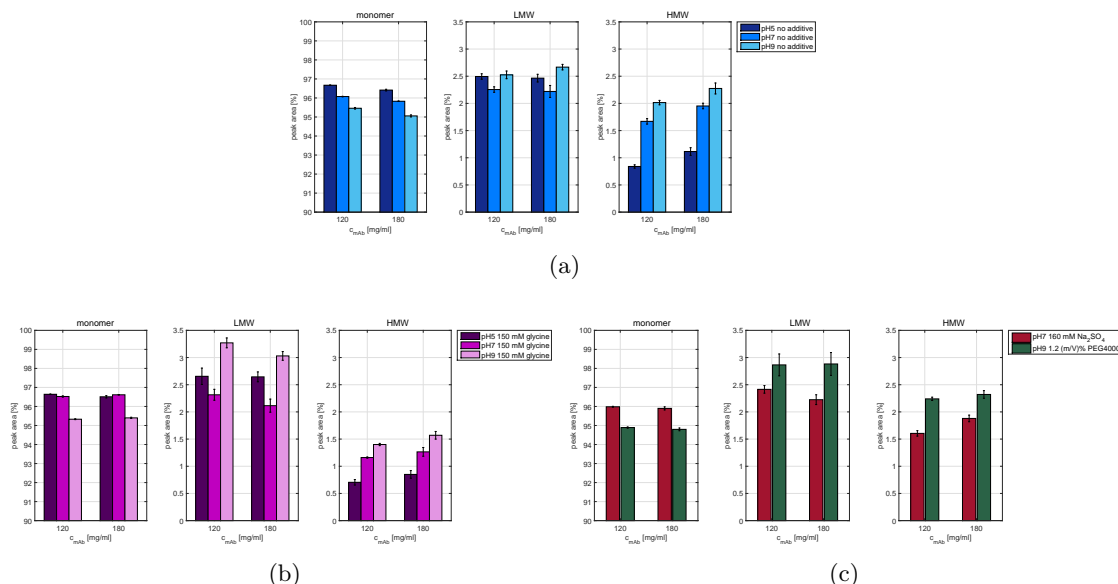


Figure 9.1: Monomer, HMW and LMW content of the tested antibody determined with the help of size exclusion chromatography. Plotted are conditions after buffer exchange with an original mAb concentration of 120 and 180 mg/ml, at pH 5, pH 7 and pH 9 without additive (a) and with 150 mM glycine (b), as well as samples at pH 7 and 160 mM Na_2SO_4 and samples at pH 9 containing 1.2 (m/V)% PEG4000 (c).

The pH had a more pronounced impact on the monomer content in solution in comparison to the mAb concentration. The monomer content decreased by 2 - 3.6 % comparing results of samples at pH 5 with samples at pH 9. The decrease of the monomer content with increasing protein concentration or increasing pH resulted in an increase of HMW content. At pH 9, the HMW content increased by 1.69 % for samples with a mAb concentration of 120 mg/ml and 1.95 % for samples with a mAb concentration of 180 mg/ml in comparison to the stock solution. The decrease in monomer content with increasing pH could be a sign of the destabilization of the antibody solution due to the shift of the buffer pH towards the theoretical pI of the molecule at 8.7. The resulting reduction of repulsive electrostatic interaction may increase the aggregation tendency of the mAb molecules and therefore the HMW content in solution. Even if this effect is weak at t_0 it may be an indication of a decreased long-term colloidal stability of the mAb at pH 7 and pH 9 in comparison to pH 5.

Without additive in solution, the LMW content increased by 1.5 % for pH 5 and pH 9 and 1.2 % for pH 7 in comparison to the LMW content of the stock solution. The LMW

content did not change with changing pH so that a conformational destabilization due to the pH shift can be excluded.

The addition of glycine decreased the HMW content at all tested pH conditions (Figure 1 (b)). Especially at pH 9 this amino acid seemed to have a positive impact on the colloidal solution stability and is therefore considered as a stabilizing additive in this study. The positive impact of glycine follows the general positive effect of osmolytes on the colloidal stability of protein solutions (see section 9.3.1). The osmolyte further increased the LMW content at pH 5, pH 7 and pH 9. At pH 7 and a mAb concentration of 180 mg/ml a slight decrease of LMW content was observed.

The polymer PEG4000 increased the HMW content at pH 9. This was especially pronounced at 120 mg/ml (Figure 1 (c)). The increase in HMW content with PEG4000 in solution can be explained with the depletion attraction theory. A detailed discussion of this theory can be found in section 9.3.1. The LMW content increased by 0.34 % with PEG4000 in solution and a mAb concentration of 120 mg/ml, respectively 0.21 % with a mAb concentration of 180 mg/ml.

Na_2SO_4 had a small decreasing impact on the HMW content of the studied mAb at pH 7 (Figure 1 (c)). The decrease was within the calculated standard deviation and is therefore negligible. Na_2SO_4 slightly increased the LMW content solely at pH 7 and 120 mg/ml. The reduction of monomer content of around 2 - 3 % could also partly be caused by the mechanical stress during centrifugation. To evaluate this hypothesis SEC runs were performed with samples which were transferred into a buffer similar to the stock solution buffer. Here a monomer loss of 1.6 % was determined. The observed monomer loss was mainly due to the defragmentation of the antibody, which is reflected by a 0.9 % increase in LMW species. Thus, the change in LMW content of the tested mAb solutions can be attributed mainly to mechanical stress and a change in the HMW content correlated to the varying environmental conditions.

9.3.2.2 Electrostatic Interactions: ζ -potential Measurements

In Figure 2 the ζ -potential of mAb solutions with a protein concentration of 10 mg/ml, in a pH range from 5 - 11, without additive, 15 mM glycine, 16 mM Na_2SO_4 and 0.2 (m/V)% PEG4000, respectively is shown.

The determined ζ -potential values are discussed with regard to protein-protein interactions which may be induced by the surface net charge of mAb molecules dependent on the surrounding solution. As it was assumed, based on the theoretical pI of 8.7, the monoclonal antibody did have a positive net surface charge at pH 5 with a value of 5.7 mV and a negative net surface charge at pH 10 and pH 11 with a value of -3.56 mV. The ζ -potential values followed the expected ζ -potential curve of proteins [268]. In a pH range between pH 7 and pH 9 the mAb molecules possessed a relatively low effective charge. Here, repulsive electrostatic protein-protein interactions are weak so that the inter-separation distance of the molecules decreases [269]. This induces positive short-range protein-protein interactions, including dipole mediated and hydrophobic interactions [270]. These attractive interactions may increase the aggregation propensity of the antibody. The results underline the findings of the SEC analytics where an increase of HMW species at pH 7 and pH 9 in comparison to pH 5 was determined.

With the selected additives in solution the ζ -potential values scattered around zero. This leads to the assumption that glycine, PEG4000 and Na_2SO_4 reduce the electrostatic repulsion of the mAb molecules at all tested pH values. The reduction of the mAb surface charge by Na_2SO_4 and the zwitter ion glycine can be explained by attractive electrostatic interactions between the charged additives and charged amino acid residues on the mAb surface. PEG, on the other hand, is an uncharged molecule. A possible explanation for the reduced ζ -potential due to PEG4000, is the interaction of the OH group of the PEG molecule with charged amino acid side chains (see section 9.3.1). Another explanation could be the steric hindrance of protein movement in the electric field by the long chain

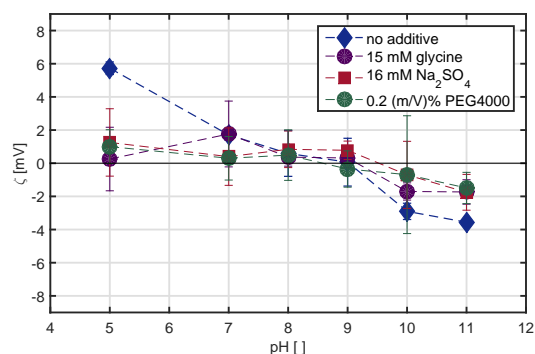


Figure 9.2: ζ -potential values of mAb at 10 mg/ml, pH 5-11 with and without 150 mM glycine, 2 (m/V)% PEG4000 respectively 160 mM Na_2SO_4 in solution determined by Laser Doppler microelectrophoresis.

polymer.

In comparison to the ζ -potential results the SEC measurements revealed mAb solution stability differences dependent on the additive type. Either the additives do have an additional impact on the protein-protein interactions which can not be described solely by ζ -potential measurements, or the electrophoretic measurements are not sensitive enough to depict the differing impact of glycine, PEG4000 and Na_2SO_4 on the protein-protein interactions. When discussing these results it should be considered that the ζ -potential measurements had to be conducted at relatively low ionic strength to gain stable results. To keep the additive-protein ratio similar to other measurements, also the protein concentration had to be reduced for these measurements to 10 mg/ml. Thus, a direct comparison to analytic results gained at high protein concentrations and higher additive content should be handled with care.

9.3.2.3 Protein Mobility: Viscosity Measurements

The study of viscosity is crucial for the processability as well as the formulation of mAb solutions and can give insights into the strength and causes of protein-protein interactions. The viscosity of mAb solutions at pH 5, pH 7 and pH 9 was tested for samples with mAb concentrations of 120 mg/ml and 180 mg/ml. Additionally, the impact of glycine, PEG4000 and Na_2SO_4 was tested at selected conditions (see Figure 3). The reproducibility of the measurements were very high with an average standard deviation of 0.6 %, except of conditions at 180 mg/ml and the addition of PEG4000 with an average standard deviation of 10.2 %. The high standard deviations may be due to the local formation of a two-phase system or the instability of the mAb at these conditions. A change in the viscosity by 1 mPas and a change greater than the calculated standard deviation was classified as significant.

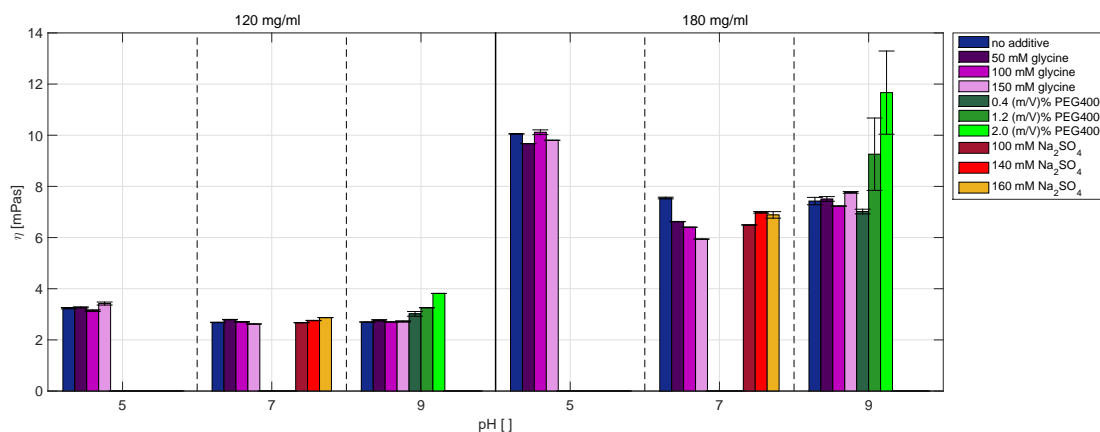


Figure 9.3: Comparison of the viscosity values of samples with a mAb concentration of 120 and 180 mg/ml at pH 5, pH 7 and pH 9 with and without additive in solution.

In this study the mAb concentration had the main impact on the viscosity. The viscosity values at a protein concentration of 180 mg/ml were higher than viscosity values determined at 120 mg/ml, independent on pH or additive tested. The impact was mostly pronounced at pH 5. Here a difference of around 7 mPas between 120 mg/ml and 180 mg/ml was detected. The concentration dependent increase of viscosity is a function of the ability of the mAb to self-associate and must therefore arise from protein-protein interactions induced by charge, hydrophobicity or dipole moments [184]. Based on the viscosity investigations it is assumed that up to a concentration of 120 mg/ml, where relatively low viscosity values were observed, repulsive long-range protein-protein interactions dominate weak attractive short range interactions. At higher concentrations the attractive short-range interactions gain increasing impact on the viscosity due to the reduced distance between the mAb molecules resulting in a viscosity increase [15].

With the change of mainly long-range mAb-mAb interactions to short-range interactions, also the impact of pH on the viscosity increases. The pH dependency of protein solution viscosity can not be described without invoking protein surface hydration. Water molecules that are structured around the protein surface are less mobile than bulk water molecules [271]. Thus, the viscosity depends on the strength of the hydration layer, which in turn is directly related to the pH and the surface properties of the protein.

The viscosity values determined at pH 5 were higher compared to viscosity values at pH 7 and pH 9. pH 5 is farthest away from the pI of the studied mAb and based on ζ -potential measurements it is presumed that the surface charge of the molecule is stronger at pH 5

compared to pH 7 and pH 9. With this knowledge the viscosity increase at pH 5 might be explained by the electroviscous effect [272]. The electroviscous effect considers three kinds of contribution which may affect the viscosity. The primary effect describes the resistance of the diffusive double layer surrounding the molecule. The secondary effect takes the intermolecular repulsion between the double layer into account. When the intermolecular repulsion is so strong that it affects the molecular shape it is described as the tertiary effect [210]. Based on these assumptions the viscosity increases with an increase of molecular charge and is minimal at the pI. This theory can explain the results of this study and has already been successfully applied for several other molecules [272–274] and also for highly concentrated IgG1 solutions [275]. But this theory is contrary to the general understanding that the viscosity is greatest near the pI. Saluja *et al.* [20] also studied the viscosity of highly concentrated antibody formulations under varying pH conditions. They stated that at higher concentrations viscosity can not only be described by the electroviscous effect. Connolly *et al.* [276] supports this observation by a viscosity screening of 29 different mAbs. The screening resulted in a very low comparability of mAb effective charge and viscosity what contradicts the theory of the electroviscous effect. The listed publications and the findings of this study demonstrate that no general statements about parameters which influence the viscosity of monoclonal antibodies can be made and that the effect of ionic strength can not be generalized, especially in the highly concentration regime. Based on the assumption that protein-protein interaction do have an impact on solution viscosity the significant differences obtained in the behavior of viscosity caused by relatively similar antibody molecules may be explained by mAb aggregation studies. Here, it could be demonstrated that mAb self-association is largely due to Fab-Fab interactions [184]. The Fab region has the highest variability and is thus unique for each antibody which may explain the differing viscosity behavior.

Following the generally accepted hypothesis that an increased viscosity also implicates a decreased mAb solution stability, pH 5 at first sight would be considered as the least favorable solution pH. Therefore, at high concentration solutions viscosity measurements might pose an opposite statement on optimal buffer pH selection when compared to the SEC analytics and ζ -potential determinations.

Glycine only had a weak impact on the viscosity. At pH 7 and 180 mg/ml a decrease of the viscosity due to the addition of glycine occurred. The viscosity dropped from 7.55 mPas without additive in solution to 5.94 mPas with 150 mM glycine in solution. A decreasing impact of glycine on the viscosity could already be described by Wang *et al.* [277]. Glycine is a hydrophilic amino acid and preferentially hydrate molecules in solution which may reduce mAb-mAb interactions and thus the viscosity.

An increase of the viscosity was caused by PEG4000 at pH 9. Especially at 180 mg/ml the viscosity increased significantly up to a value of 11.67 mPas, which was the maximal viscosity value detected in this screening range. Simultaneously, with the increase of PEG4000 content the reproducibility of the measurement weakened which resulted in a standard deviation of up to 15 %. The increase in viscosity by the addition of PEG can be attributed to two effects. On the one hand, PEG with a molecular weight of 4000 Da is a relatively large long-chain molecule which increases the viscosity per se due to sterical hindrance. On the other hand, it is known that high molecular weight PEGs induce attractive protein-protein interactions by excluding volume from the environment of the proteins which could also increase the mAb solution viscosity (see section 9.3.1).

Na_2SO_4 had a weak increasing impact on the viscosity values. This can be explained by the kosmotropic character of Na_2SO_4 (see section 9.3.1). This kosmotropic effect strengthens the mAb-mAb interactions, which reduces the protein mobility resulting in an increased viscosity.

9.3.2.4 Thermal Colloidal and Conformational Stability

The accelerated temperature study provides information on the colloidal and conformational stability of the mAb under stressed conditions. Based on published thermal stability studies a difference of 1°C was considered as a significant result and is assumed to be caused by a stabilizing or destabilizing effect on the protein structure or protein monodispersity [100, 278–280].

The thermal colloidal and conformational stability of the mAb was tested as a function of protein concentration, pH, additive type and concentration. In the chosen screening area one T_{agg} value and dependent on the condition one (T_{m1}) or two T_m (T_{m1} and T_{m2}) values could be detected for each sample. The exact T_m and T_{agg} values can be looked up in Table 2a and Table 2b in the supplementary materials.

In the first part of this section the thermal conformational stability (T_m) of the antibody is discussed. The T_m values which have been calculated can be directly correlated with the thermal conformational stability of the antibody. The higher the T_m value, the higher the energy input required to unfold the protein (see section 9.1). The standard deviations of the measurements did not exceed 1°C. Except at pH 5 and 120 mg/ml with and without glycine in solution and at pH 9 and 120 mg/ml with PEG4000 in solution. The high standard deviations at pH 5 and 120 mg/ml with and without glycine in solution could be due to the comparatively low intrinsic fluorescence of the antibody. With increasing mAb concentration, the standard deviations decreased due to the stronger fluorescence signal. The pH dependency of the signal strength may be due to a changing flexibility of the molecule, which causes the exposition of more or less detectable fluorescence amino acids on the mAb surface. The high standard deviations observed for samples with PEG in solution may be due to the UV scattering of PEG itself as it is a comparable big molecule and its UV signal may overlay the scattering of the protein of interest.

To study the impact of mAb concentration the calculated T_{m1} , T_{m2} and T_{agg} values are plotted as a function of the protein concentration in Figure 4. The detected T_{agg} values are similar for all tested mAb concentrations with a value of about 70°C. They dominate the T_{m1} values up to a protein concentration of 60 mg/ml. At conditions with mAb concentrations of up to 60 mg/mL two fluorescence shifts were detected so that a second T_m value, T_{m2} could be calculated. T_{m2} values do have similar values as T_{m1} values detected at higher mAb concentrations. The second shift of the fluorescence signal indicates that the mAb concentration had an impact on the unfolding pathway of the protein. The second shift implies a two step unfolding of the protein [278]. A monoclonal antibody consists of four polypeptide chains which have a differing stability against heat [281]. Assuming that the studied antibody does have a comparable thermal stability behavior as other monoclonal antibodies, the Fab fragment of the mAb is most sensitive to heat treatment and denatures first. Underlining this assumption, the measured T_{m1} values of

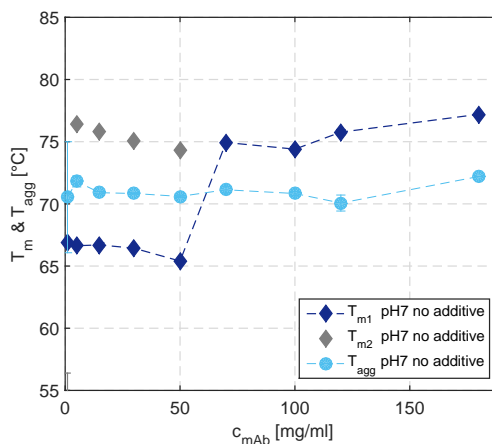


Figure 9.4: T_{m1} , T_{m2} and T_{agg} values of mAb samples in a concentration range from 1-180 mg/ml at pH 7 without additive in solution determined over a temperature ramp ranging from 20 – 90°C.

66°C are close to T_m values of single domain Fab analysis by Menzen [282]. A partly unfolding of the variable region of the mAb did not take place at mAb concentrations higher than 60 mg/ml. The increased mAb concentration seemed to conformationally stabilize this region.

In Figure 5 (a) the impact of protein concentration (120 mg/ml and 180 mg/ml), pH, additive type and concentration on the T_{m1} values is depicted. At these conditions no second fluorescence shift occurred. The impact of mAb concentration from 120 - 180 mg/ml on the thermal stability was found to be dependent on the pH. At pH 5 the T_m values are lower compared to pH 7 and pH 9 and decrease with increasing antibody concentration by 6°C. pH 5 is the condition farthest away from the pI of the mAb. It was already found that the increased net charge of the amino acids result in a reduced density of a protein due to innermolecular repulsive electrostatic interactions [283]. The less compact protein leads to a decrease of the T_m values. It is conceivable that the conformational change at pH 5 is accelerated with increasing mAb concentration due to additional attractive short-range interactions at 180 mg/ml. At pH 7 and pH 9 the increase of protein concentration in between 120 and 180 mg/ml only had a small impact on the thermal conformational stability of the mAb molecules. It is inferred that the innermolecular forces which have an impact on the 3D structure of the molecule are not affected by a concentration of the antibody at these pH values. That supports the assumption that electrostatic forces induce the conformational change at pH 5. At pH 7 slightly higher T_m values were detected in comparison to samples at pH 9. This underlines the findings of Razvi & Scholtz [284] who stated that the highest protein thermodynamic stability can be found at physiological conditions. That implies that antibodies are most conformationally stable at conditions similar to the extracellular matrix (pH 7.3) where they show the highest activity.

The impact of additives on the thermal conformational stability were dependent on additive type (Figure 5 (a)). Glycine and Na_2SO_4 had a slightly positive impact, whereas PEG4000 had a predominantly negative impact on the determined T_m values. The increase of T_m of around 4% indicates that glycine and Na_2SO_4 stabilize the 3D structure of the mAb under high temperature conditions. Glycine is an osmolyte, which are known to have the ability to preferentially hydrate molecules (see also section 9.3.1). The sulfate ions of Na_2SO_4 do have a kosmotropic character [269]. Kosmotropic salts are known to suppress protein denaturation up to a protein specific salt concentration [88] (see also section 9.3.1).

With PEG4000 the antibody solutions became opaque at concentrations higher than 120 mg/ml. Due to the high scattering signal the determination of T_m was not possible with a mAb concentration of 180 mg/ml. Therefore, only the T_m values determined

9.3 Results and Discussion

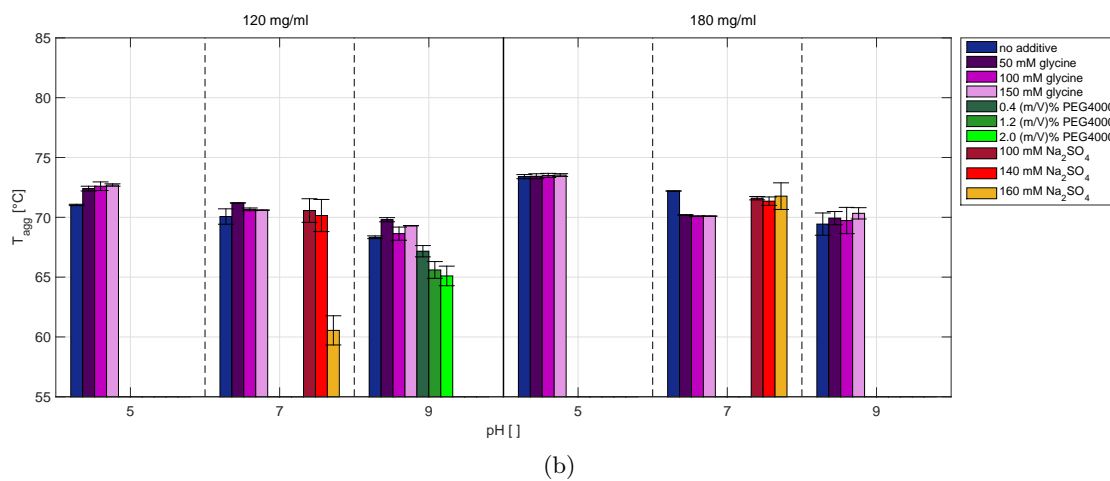
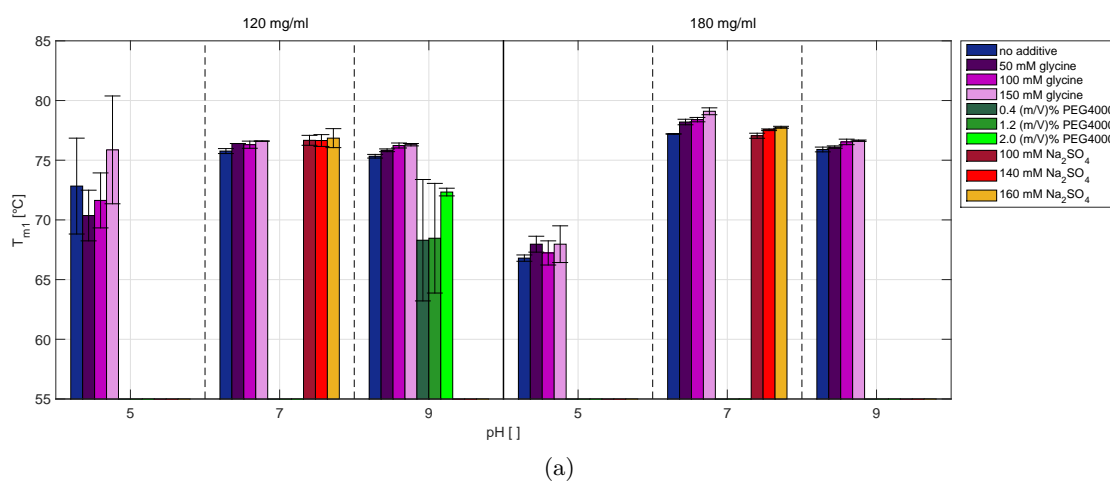


Figure 9.5: Comparison of T_{m1} (a) and T_{agg} (b) values of samples with a mAb concentration of 120 and 180 mg/ml at pH 5, pH 7 and pH 9 with and without selected additives.

at 120 mg/ml and PEG4000 in solution can be discussed. The polymer had a negative impact on the conformational stability of the mAb molecules resulting in a T_m decrease of up to 9°C at pH 9. The decreased thermostability of the protein due to the PEG molecules can be explained by the depletion attraction theory and an accompanied increased osmotic pressure, already discussed in section 9.3.1.

The next section discusses the thermal colloidal stability of the mAb solution by comparing the T_{agg} values of tested conditions. The T_{agg} values indicate an increase in light scattering and can thus be correlated directly with the agglomeration of the molecules in solution at accelerated temperatures. A high T_{agg} value stands for a high thermal colloidal stability.

The T_{agg} values were constant in a concentration range from 1-120 mg/ml (Figure 4). Interestingly, the partly unfolded state of the antibody, which was detected by fluorescence measurements, did not have an impact on the T_{agg} values. This implies that the amino acids exposed by the partial unfolding do not influence the colloidal stability of the antibody. From 120-180 mg/ml the T_{agg} values increased for all pH values tested (Figure 5). This phenomenon may be explained by a reduced movement of the molecules due to sterical hindrance at 180 mg/ml. The reduced number of molecule collisions implies a deceleration of the aggregation kinetic.

At pH 5 higher T_{agg} values were detected in comparison to pH 7 and pH 9. The above discussed stronger net charge of the protein at pH 5 may lead to a weaker thermal conformational stability but increases the thermal colloidal stability by repulsive electrostatic interactions.

Glycine increased the T_{agg} values of samples at pH 5 and pH 7 with a protein concentration of 120 mg/ml. Also at pH 9 at 120 and 180 mg/ml an increasing trend of T_{agg} due to the addition of glycine could be observed. However, the changes were within experimental error and are therefore not discussed. At pH 7 and a mAb concentration of 180 mg/ml glycine decreased the T_{agg} by 2°C.

PEG4000 had a decreasing impact on the determined T_{agg} values. With increasing PEG4000 concentration the T_{agg} values decreased by 5°C. A major drop of T_{agg} values with PEG4000 in solution indicates an increase of mAb-mAb interactions due to the polymer. It is assumed that the reduced colloidal thermal stability is caused by similar mechanisms, such as the reduced conformational stability.

Na_2SO_4 is a kosmotropic salt and therefore stabilizes the 3D structure but is also known to destabilize the colloidal stability of proteins [88]. Thus, the temperature induced unfolding should be reduced but the aggregation of mAb molecules intensified by the ad-

dition of Na_2SO_4 . Decreased T_{agg} values could only be observed for samples at pH 7, a Na_2SO_4 concentration of 160 mM and a mAb concentration of 120 mg/ml with a reduction of 12°C. Here, the kosmotropic salt seemed to strengthen the hydrophobic protein-protein interactions, resulting in an increased aggregation propensity [258]. At higher protein concentrations or lower salt concentration the salt-protein-ratio is lower, resulting in a lower impact of the kosmotropic salt and therefore no change of the measured T_{agg} values. This assumption could be validated by rising the salt concentration at a mAb concentration of 180 mg/ml to 260 mM. Here also a certain drop of the T_{agg} values could be observed, similar to the T_{agg} decrease observed for a mAb concentration of 120 mg/ml (data not shown).

Important information also provides the location of T_{agg} and T_m in relation to each other. If T_{agg} is higher than T_m , it can be assumed that even under isothermic conditions, the molecule unfolds first and then aggregates and vice versa. Only at pH 7 and low mAb concentrations (1-60 mg/ml) (Figure 4) and at pH 5 and mAb concentrations up to 180 mg/ml (Figure 5) the T_{agg} values dominate the T_m values. But, the discussed partly unfolding of the antibody at low concentration conditions did not have an impact on the thermal colloidal stability.

At pH 7 and pH 9 and mAb concentrations of 120 and 180 mg/ml the T_m values dominate the T_{agg} values. At these conditions the aggregation kinetic is therefore faster than the unfolding kinetic. Summarizing these observations, the colloidal stability is lower at pH 7 and pH 9 in comparison to pH 5 but a conformational destabilization at pH 5 due to repulsive innermolecular interactions should be included for optimal buffer selection.

9.3.2.5 A Comprehensive View: Determination of Protein Solution Viscoelasticity

To study the complex rheological behavior of the mAb solutions the rheological parameters G' and G'' were determined over a set frequency range. The value of these parameters, more specifically their ratio at the different frequency points provide insights into the relaxation behavior of the proteins in solution [158]. The relaxation behavior in turn is influenced by spatial limitations and the strength of molecule-molecule interaction. The measurable relaxation behavior of the protein solution is thus directly linked to the solution stability of the protein samples tested [218]. Stronger protein-protein interactions increase the relaxation time and therefore result in a higher solution viscoelasticity. This relation can be precisely described by the frequency value of the crossover point of G' and G'' , ω_{CO} . The higher the rigidity of the system due to attractive interactions is the

lower the ω_{CO} values. Additional to the strength of protein-protein interactions, the ω_{CO} value is dependent on the size and structure of the protein itself. Under conditions where the protein-protein interactions of two proteins are equally pronounced, a small, globular protein exhibits higher ω_{CO} values than a larger, structurally more complex protein. The threshold value ω_{limit} can be used as a reference point. Above ω_{limit} protein solutions are expected to be stable, below this value samples are expected to be colloidal unstable. The ω_{limit} for lysozyme is 20000 rad/sec [218]. Since the antibody of this study has a ten fold higher molecular mass as lysozyme and is not spherically shaped, the ω_{limit} value of the mAb is expected to be lower. Additionally, liquid formulations which exhibit ω_{CO} values below 1000 rad/sec are generally expected to be unstable.

The standard deviations of the viscoelastic measurements were in between 0.06 - 4 % except for conditions with PEG4000 in solution. Here, standard deviations of up to 30 % were observed. This decreased reproducibility may be due to the additional viscoelastic response of the PEG molecules. The calculated ω_{CO} values of this screening varied in relation to the studied protein concentration, pH as well as the additive type. The shift of the ω_{CO} values in relation to the changing solution conditions are discussed in the next section.

In Figure 6 the impact of mAb concentration and pH without additives (a) and the impact of mAb concentration and additive in solution at pH 5 (b), pH 7 (c) and pH 9 (d) on the rheological response is shown.

The highest ω_{CO} values were detected for low mAb concentrations at pH 5 with a value of 24043 rad/sec. The lowest ω_{CO} values for samples without additive in solution were calculated for pH 7 ranging from 21770 rad/sec at 50 mg/ml and 607 rad/sec at 200 mg/ml.

9.3 Results and Discussion

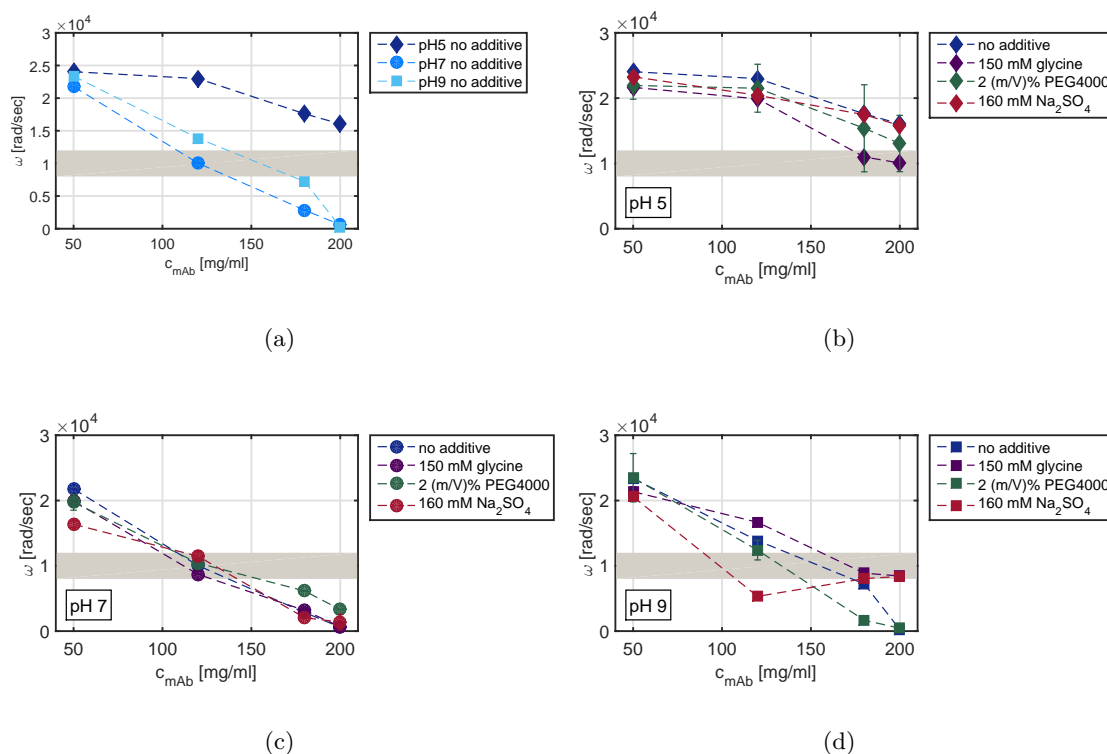


Figure 9.6: Viscoelastic response of mAb samples without additive in solution dependent on protein concentration and pH (a). Impact of pH with additive in solution, namely 160 mM glycine (b), 150 mM Na_2SO_4 (c) and 2 (m/V)% PEG4000 (d) on the viscoelastic response. The grey area symbolizes the critical ω_{CO} region. Above this region the viscoelastic response indicates stable mAb solutions. ω_{CO} values below this region indicate samples which might undergo phase transition.

With increasing protein concentration the ω_{CO} values decreased (see Figure 6 (a)). The increased viscoelasticity, indicated by an ω_{CO} decrease, of the samples can be explained by the concomitant shortened distance between the individual molecules. At low concentrations, electrostatic forces dominate, which are repulsive with similarly charged molecules. In the case of a concentration increase, the influence of the short-range interactions, which have attractive properties, and thus limit the mobility of the molecules in solution, is increased. This mobility constraint is associated with an increase in solution elasticity and thus with a reduction of the ω_{CO} values. The decrease of the ω_{CO} values with increasing protein concentration depended on the pH value of samples tested. The drop of the ω_{CO} was more pronounced at pH 7 and pH 9 in comparison to samples at pH 5. For samples

at pH 5 the ω_{CO} decreased by 33 % comparing samples with a protein concentration of 50 mg/ml and 200 mg/ml. At pH 5 the molecules in solution could follow the applied movement up to high frequency values also at higher mAb concentrations. That implies that even at high mAb concentrations the molecules could move along each other without strong resistance due to the strong repulsive interactions, triggered by similar net surface charge of the molecules. At pH 7 and pH 9 a decrease of 97 % and 98 %, respectively occurred, resulting in a ω_{CO} values below 1000 rad/sec for samples with a mAb concentration of 200 mg/ml. The strong decrease of ω_{CO} values with increasing protein concentration implies that the type and strength of protein-protein or protein-solvent interactions changed when increasing the protein concentration at pH values close to the pI. It is assumed that short-range interactions which occur in the highly concentration regime have a bigger impact on samples at pH 7 and pH 9 in comparison to pH 5. As the impact of pH on the viscoelastic behavior is comparable to the impact on orthogonal analytical parameters a detailed argumentation can be found in section 9.3.2.1 and section 9.3.2.4.

To emphasize the impact of the pH on the viscoelastic response in Figure 6 (b)-(d) the differences of the ω_{CO} values at pH 5, pH 7 and pH 9 with 150 mM glycine, 2 (m/V)% PEG4000 as well as 160 mM Na_2SO_4 and the ω_{CO} values without additive in solution are plotted against the protein concentration. At a mAb concentration of 50 mg/ml the impact of the additives on the rheological response was comparatively low. At pH 5 and pH 9 the ω_{CO} values with and without additive and a mAb concentration of 50 mg/ml are within experimental error (Figure 6 (b) and (d)). At pH 7 the used additives had a comparatively small impact at all mAb concentrations tested (Figure 6 (c)).

The following discussion is structured based on the additive studied.

The impact of glycine on the viscoelastic behavior of mAb samples depended on the pH. At pH 5 (Figure 6 (b)) glycine decreased the ω_{CO} values at all mAb concentrations tested and therefore strengthened the viscoelasticity of the protein solution. Glycine is a zwitter ion and has the ability to interact with the protein surface with both its negative and positive charged groups [285]. The mAb molecule has a positive net charge at pH 5. The electrostatic repulsive interactions of the molecules could thus be reduced due to the specific interaction of glycine ions with positively charged surface groups of the mAb molecules. Additionally it was shown that glycine can also interact with the peptide backbone of proteins which plays an important role in protein stabilization.[92, 286, 287]. The impact of glycine on the ω_{CO} values changed with increasing pH value and increasing mAb concentration. The negative impact of glycine on the ω_{CO} values decreased comparing samples at pH 5 and pH 7 with each other (Figure 6 (c)). At pH 9

(Figure 6 (d)) glycine even increased the ω_{CO} values of the mAb solution significantly in a concentration range from 100 - 200 mg/ml by 20 to > 100%. It is assumed that close to the pI of the molecule, the specific electrostatic interaction of negatively charged glycine ions and positively charged patches on the mAb surface are dominated by the competition for water between the protein and the co-solute. This leads to the preferential exclusion of glycine from the protein surrounding and thus to an increased protein solubility (see also section 9.3.1). This observation matches the findings of the thermal stability enhancement discussed in the previous section (section 9.3.2.4). It has to be emphasized that glycine decreased the ω_{CO} values at pH 5 but only down to 10000 rad/sec. This value is still above ω_{CO} values calculated for samples at pH 7 and pH 9. Additionally, the decrease of ω_{CO} values due to the addition of glycine at pH 5 was low compared to the impact of PEG4000 and Na_2SO_4 .

At pH 5 the impact of PEG4000 (Figure 6 (b)) on the ω_{CO} values strengthened with increasing protein concentration. The polymer seemed to decrease the repulsive effect of the positively charged groups on the mAb surface. As already described in section 9.3.2.3 the polymer may hinder the molecular movement due to sterical hindrance or due to the destruction of the protecting hydration shell of the mAb molecules [288]. The same effect can be seen for samples at pH 9 (Figure 6 (d)). The impact was most pronounced at 180 mg/ml with a ω_{CO} difference of -5600 rad/sec compared to samples without PEG in solution. It is assumed that a further decrease of the ω_{CO} values at pH 9 and 200 mg/ml with PEG4000 could not be seen because the ω_{CO} values without PEG4000 and similar conditions were already below 200 rad/sec, which is close to the lower detection limit of the instrument used (100 rad/sec) [138]. At pH 7 (Figure 6 (b)) in comparison, the PEG4000 molecules seemed to have a positive impact on the flow behavior in a concentration range from 150 - 200 mg/ml. The strong viscoelasticity (low ω_{CO} values) which was detected for samples at pH 7 could be reduced with the addition of PEG4000. The decreasing elastic behavior of mAb solutions at these conditions may be explained by a decrease of short-range interactions caused by a specific binding of the non polar PEG molecules on the molecular surface [260, 289]. The impact of PEG4000 on mAb solution viscoelasticity is complex and can be interpreted in terms of several opposing factors which depend on the solution pH and the ratio of PEG and protein molecules in solution. This balance of opposing factors has already been described by Arakawa & Timasheff [256] who studied the impact of PEG concentration and molecular mass on the conformational and colloidal stability of β -Lactoglobulin.

Na_2SO_4 as an additive had a decreasing impact on the ω_{CO} values of mAb samples in a concentration range from 50-150 mg/ml at pH 9 (Figure 6 (d)). Here, the addition of the

kosmotropic salt leveled the ω_{CO} values down to 8000 rad/sec with an ω_{CO} difference of -8500 rad/sec in comparison to samples without Na_2SO_4 in solution. The sulfate ions strengthen the hydrophobic interactions of the anyhow low charged proteins. In this way the movement of the individual molecules was hindered which leads to a significant decrease of ω_{CO} . It is assumed that the salt at pH 7 had a similar effect on the interactions of the mAb molecules as at pH 9. However, the adjusted pH value had such a strong influence on the rheological response of the samples that the effect of the salt on the solution viscoelasticity was overlaid by the pH effect. At pH 5 where the mAb molecules have a stronger net surface charge, the concentration of sulfate ions was too low to induce strong hydrophobic interaction and thus a drop of the ω_{CO} values.

At pH 9 and higher protein concentrations the salt seemed to have an opposite effect on the viscoelasticity of mAb samples (Figure 6 (d)). At 200 mg/ml the ω_{CO} values with salt in solution were higher compared to samples without salt in solution. Here an ω_{CO} increase of +8100 rad/sec was observed. That implies that the strength of protein-protein interaction decreased due to the addition of Na_2SO_4 starting at a mAb concentration of 200 mg/ml. Du & Klivanov [290] assumed that in highly concentrated protein solutions kosmotropic salts do not induce hydrophobic protein-protein interactions but may compete with hydrophobic protein-protein interactions which are assumed to be the dominant stability decreasing factor at pH 9. Additionally, in this study the concentration of the salt was kept constant while the mAb concentration increased, therefore the protein-salt ratio varied with increasing protein concentration. A reason for the differing impact of Na_2SO_4 with increasing protein concentration could thus also be found in the changing protein-salt ratio. It is assumed that at low mAb concentrations up to 150 mg/ml, the salting-out effect was dominant what causes an increased elasticity and therefore lower ω_{CO} values. At high protein-salt ratios the salting-in effect might be dominant. Here, the salt interacts favorable with charged residues and stabilized the protein in solution (see section 9.3.1). The mAb concentration dependent impact of Na_2SO_4 supports the assumption that the type of protein-protein interaction changes with increasing protein concentration.

In summary, the pH value had the main impact on the viscoelastic response of the mAb samples tested. A clear differentiation between the viscoelastic behavior at pH 7, pH 9 and pH 5 could be made. The impact of the additives depended on the additive type, pH value and also the protein concentration.

Based on the correlation of the ω_{CO} values with the long-term stability tests (section 9.3.3) a critical range could be defined were the mAb solution is assumed to undergo phase transition. This area is marked in grey in Figure 6. Above an ω_{CO} value of 10000 rad/sec

the mAb molecules are predicted to be colloidal stable below this limit, aggregation of the mAb molecules can be expected. This knowledge enables the description of mAb phase behavior based on one single rheological measurement.

9.3.3 Long-term Solution Stability

To be able to correlate the analytical investigations with mAb solution stability mAb phase diagrams were studied. The prepared protein phase diagrams were visually scored after 40 days of incubation following the method of Baumgartner *et al.* [88]. Consequently, long-term stability is equated with 40 days of incubation in this study. The results of the long-term solution stability results are only discussed when a deviation from the described analytical results occurred (see section 9.3.2). In Figure 7 (a)-(c) the visual scoring of the mAb phase diagrams made after 40 days of incubation (t_{40}) are plotted. The long-term colloidal stability of the mAb in a pH range from pH 5 - 9, with a protein concentration of 120 - 225 mg/ml and the additives glycine, PEG4000 and Na_2SO_4 was tested. The first area symbolizes conditions without additive in solution at all three subplots.

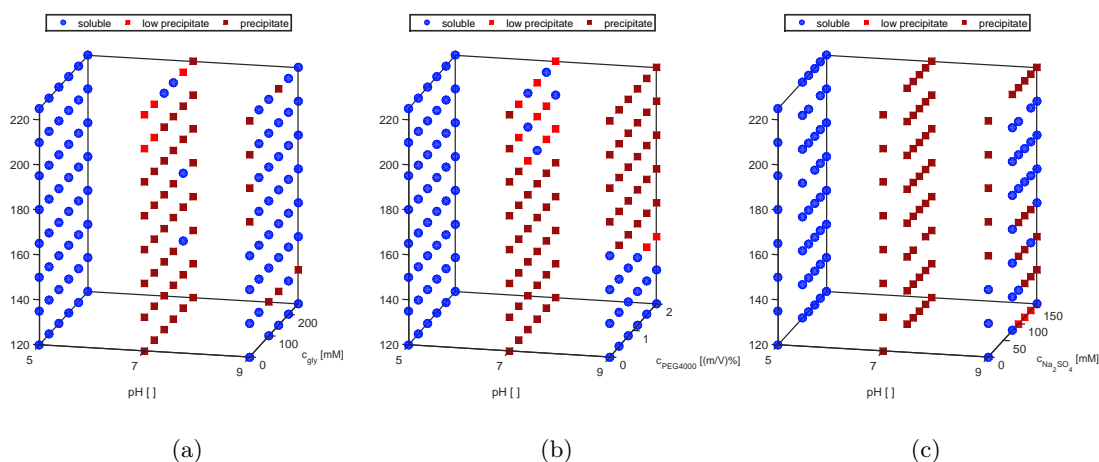


Figure 9.7: Scoring of the phase behavior of mAb in a pH range from 5-11, a protein concentration range from 120-225 mg/mL and (a) 0-250 mM glycine, (b) 0-2 (m/V)% PEG4000 and (c) 0-200 mM Na_2SO_4 visualized as 3D plots. The scoring was done after 40 days of incubation at a constant temperature of 20°C based on the visual evaluation of the pictures taken by the Rock Imager. The blue round symbols stand for samples containing soluble mAb molecules, the small light red squares symbolize light precipitation in the middle of the well and the dark red squares symbolize heavy precipitation.

The mAb colloidal long-term stability was mainly dependent on pH and additive type. At pH 5 the mAb molecules were soluble at all tested conditions. It is assumed that mainly repulsive electrostatic forces hinder the antibody to form aggregates also in the highly concentrated regime. At pH 7 the mAb was least stable. Precipitation occurred over the whole tested mAb concentration range. It is assumed that strong hydrophobic and dipole induced interactions are responsible for this instability. Interestingly, the region where the mAb is colloidal stable increases at pH 9 in comparison to pH 7. The theoretical pI of the mAb molecules is 8.7. Theoretically, that implies that repulsive interactions are further reduced when shifting the pH from pH 7 to pH 9. The decrease of repulsive electrostatic forces allows the reduction of the molecular distance and thus an enhancement of the attractive hydrophobic and dipole induced short-range forces. Therefore, a reduced colloidal stability at pH 9 would have been expected. An explanation for the higher stability of the antibody at pH 9 could be found in the charge distribution of the mAb surface which may differ between pH 7 and pH 9. The charge distribution can have a substantial impact on the attractive forces between the molecules [291]. In order to be able to examine the charge distribution in more detail, molecular dynamics simulations

have to be carried out, which are part of future studies.

In Figure 7 (a) the scoring of the phase diagrams with glycine as an additive is shown. At pH 7 precipitates were detected at almost all samples. At pH 9 precipitation occurred with a protein content of 135 mg/ml and glycine concentrations from 100 - 250 mM. At higher mAb concentrations glycine seemed to stabilize the protein. In comparison PEG4000 destabilized the molecule at pH 9 (see Figure 7 (b)). Here precipitation occurred starting at mAb concentrations of 150 mg/ml. PEG4000 seemed to have a stabilizing character at pH 7 starting at protein concentrations of 195 mg/ml and PEG4000 concentrations of 0.8 (m/V)%. At these conditions only low precipitation in the middle of the well or soluble samples were detected. Na_2SO_4 did have a stabilizing character on the tested mAb at pH 9 in a mAb concentration range from 180 - 225 mg/ml with 75 - 200 mM Na_2SO_4 , and destabilized the mAb at lower protein concentrations (see Figure 7 (c)). At pH 7 strong precipitation occurred for all samples containing Na_2SO_4 .

A detailed discussion of the impact of pH on the mAb colloidal stability as well as the impact of used additives can be found in section 9.3.1 and section 9.3.2).

9.3.4 Comparison of Analytical Methods and Protein Long-term Stability

In this section the analytical methods which were applied in this study are combined to describe the long-term solution stability of the mAb samples screened. Therefore, a scoring had to be introduced, which is able to classify the analytical results concerning their statement about protein stability. The correlation presented here has its focus on the descriptiveness of the colloidal antibody stability under tested conditions.

To keep it simple all analytical results were normalized and a scoring from 0 to 10 defined. Whereby 10 is a result indicating a high colloidal stability and 0 an analytical result indicating a weak solution stability of the screened mAb. For the SEC analytics a score of 10 was set for the maximal monomer content (96.7%) and a score of 0 was set for the lowest monomer content (94.8%) observed, as it is assumed that a high monomer content at t_0 is an indicator for a high long-term colloidal stability. A ζ -potential of 0 (scoring value 0) indicates weak electrostatic repulsion and therefore an increased aggregation propensity. The maximum ζ -potential of this study with a value of 5.7 mV was normalized to 10. A high viscosity is unfavorable for liquid formulations and may be correlated to strong protein-protein interactions, therefore the maximum viscosity value of this screening (11.7 mPa/s) was normalized to 0, the minimum value (2.6 mPa/sec) to 10. Temperature ramps are commonly used to fasten up the degradation and aggre-

gation process of protein solutions and were successfully correlated to long-term stability [100, 292, 293]. It was shown that the melting temperature is only predictive in cases where degradation is linked to unfolded protein structure [282, 294, 295]. In this study the aggregation kinetic was not dependent on the unfolding kinetic. Wherefore, the T_{agg} and not the T_m values of this study were used to describe the solution stability of the antibody. The maximal T_{agg} value (74 °C) was normalized to 10 and the minimal T_{agg} value (61 °C) was normalized to 0. Furthermore, it could be shown that the viscoelastic characteristic of a molecule in solution directly correlates with the long-term solution stability [218]. The characteristic ω_{CO} value determined by frequency sweep measurements is maximal (24043 rad/sec) at minimal aggregation propensity (score=10) and minimal (256 rad/sec) at maximal aggregation propensity (score=0). The so determined scoring values were weighted equally, summed and divided by the amount of scores used for the specific sample. The scoring values can be found in the supplementary materials (Table 3).

The scoring results are visualized with the help of a surface plot to ensure an easy comparison with the long-term stability results (see Figure 8 (a)). To simplify the comparison the long-term stability scoring of similar samples is plotted next to the analytical scoring (see Figure 8 (b)). The red areas in Figure 8 (a) mark conditions where the mAb is predicted to be unstable. Blue areas symbolize conditions where the mAb is predicted to be stable. The surface plot enables an easy detection of conditions which are predicted to be stable and robust (in blue) as well as screening points which may be sensitive towards slight changes of the molecular surrounding (e.g. pH 9, 180 mg/ml, 160 mM Na_2SO_4).

9.3 Results and Discussion

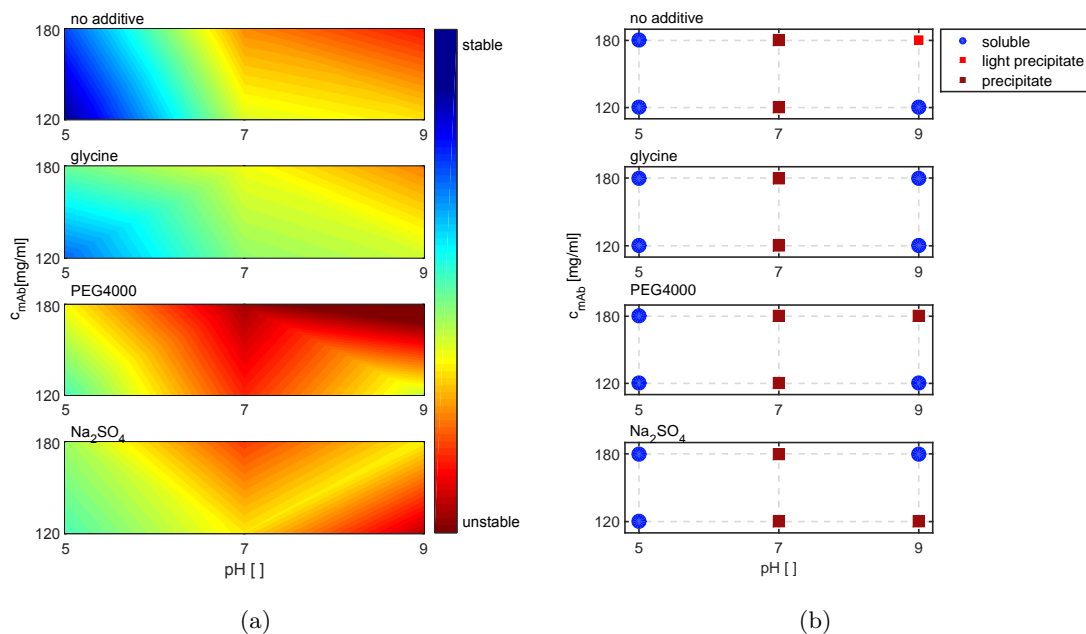


Figure 9.8: Scoring of analytical results is shown in relation to their statement about the long-term colloidal stability. The scoring of the phase behavior at t_{40} of similar samples is depicted on the right hand side for an easier comparison.

The colloidal stability of the mAb is predicted to be dependent on protein concentration, pH and additive type. The most stable region was predicted to be at pH 5 without additive in solution at 120 mg/ml. For mAb samples at pH 9, a mAb concentration of 180 mg/ml with the addition of PEG4000 the smallest scoring value was calculated.

In general, the colloidal solution stability could be described very well with the help of the analytical toolbox and the defined scoring. The prediction, that samples at pH 5 are most stable, glycine does have a stabilizing character on mAb samples, Na_2SO_4 and PEG4000 do have a destabilizing effect dependent on pH and mAb concentration, could be confirmed with long-term stability tests. It is particularly to be emphasized, that the stabilizing character of Na_2SO_4 at pH 9 and 180 mg/ml and the strong destabilizing effect due to the addition of PEG4000 at similar conditions could be described correctly. However, not sufficiently visible is the precipitation of the antibody at pH 7 with and without additive in solution. The scoring was pushed to values around 4 due to the impact on the scoring of low viscosity values measured at these conditions. At pH 7 and 120 mg/ml with and without additive in solution the viscosity was even lower than for samples at pH 5, what resulted in viscosity scoring values above 9. The viscosity dif-

ferences between pH 5, pH 7 and pH 9 were explained by the electroviscous effect (see section 9.3.2.3). This effect may be helpful to explain the solution fluidity but may not have an impact on the long-term colloidal stability, especially at mAb concentrations equal or below 120 mg/ml. Here, the repulsive interactions at pH 5 expand the molecular size and therefore increase viscosity but on the other hand increase the colloidal stability due to strong electrostatic repulsion. SEC measurements, thermal stability test, ζ -potential measurements and the study of mAb viscoelasticity described the instability of mAb solutions at pH 7 correctly, whereby the wrong description based on viscosity measurements could be partly compensated.

The protein concentration dependent impact of the additives Na_2SO_4 and PEG4000 was described correctly but the effect was damped due to the insensitivity of ζ -potential and thermal stability tests. In this study, the ζ -potential results contained important information at conditions where electrostatic interactions dominated the repulsive or attractive forces of solvated proteins in solution, this means at ideal dilute conditions and without additives in solution. At higher protein concentrations and with the addition of additives the influencing factors on the protein solution stability become more complex and cannot be depicted by protein surface charge characterization alone. The results of thermal stability tests were more or less unaffected in relation to the changing impact of the additives. Here, it becomes clear that different processes can occur at isothermal long-term stability tests in comparison to accelerated temperature tests. The discrepancies between thermal and isothermal long-term stability tests were already described [100, 252] but so far there is no explanation why and when the discrepancy occurs. Therefore, it is important especially in the highly concentrated regime to combine the thermal stability tests and ζ -potential measurements with other biophysical characterization techniques to overcome these insensitivities. The viscoelastic characterization of the mAb solutions was found to be a reliable tool to describe the behavior of the mAb molecules in the solution. Whereby the impact of protein concentration on the colloidal stability of the antibody was slightly overestimated. This overestimation may be due to the formation of structured mAb networks, which would increase the elastic portion of the probe and result in lower ω_{CO} values but would have a positive impact on the long-term colloidal stability [296, 297].

The listed results illustrate the limits of used analytical techniques and the importance of the combined use of orthogonal tools to be able to describe the long-term solution stability at varying conditions correctly.

9.4 Conclusions

The work presented here proposes the use of an analytical toolbox to describe the long-term stability of highly concentrated antibody solutions. The evaluation of protein mobility, rheology and the thermal stability studies of mAb solutions revealed a sensitivity of the studied antibody towards mAb concentration, pH, additive type and concentration with regard to the colloidal solution stability. At pH 5 the antibody solution stability was described to be highest. Here the molecule was resistant against colloidal instability up to protein concentrations of 200 mg/ml and also unaffected by the addition of PEG4000 and Na_2SO_4 . Glycine was described to further stabilize the molecule also at pH 7 and pH 9. PEG4000 and Na_2SO_4 were described to have a destabilizing impact on the antibody, except of pH 9 at high protein concentrations, where Na_2SO_4 was assumed to have a stabilizing impact on the molecule.

The scoring of the novel and established techniques could be correlated successfully with long-term stability experiments. Not only the description of the protein behavior became possible but also a detailed characterization of the extend and type of protein-protein interaction. Furthermore, the study demonstrates the strength and weaknesses of the different techniques applied and that the description of the mAb phase behavior could only be achieved by a combination of these techniques. The SEC chromatography results were a good starting point to make first rough assumptions about the long-term stability of the antibody solutions based on soluble aggregates formed immediately after preparation. ζ -potential measurements localized correctly the pH range where only weak electrostatic interactions induce repulsive forces. However, with the study of the surface net charge it was not possible to differentiate between stabilizing and destabilizing effects of studied additives. It was shown that an increase of viscosity does not always correlates with antibody long-term stability. Reasons for the increased viscosity at pH 5, where the antibody was found to be most stable, were discussed and explained with the electroviscous effect. The colloidal and conformational thermal stability of the antibody revealed insights into the unfolding and aggregation kinetics. Most conditions where the additives did have an impact on the antibody solution stability were described correctly by this high throughput compatible method. Here, only the sensitivity towards concentration dependent interactions of co-solutes with the antibody surface could not be depicted sufficiently. The sensitivity towards the pH and protein concentration dependent impact of studied co-solutes could be achieved by characterizing the viscoelastic behavior of the antibody solution. The ω_{CO} values could be correlated directly with the

observed antibody phase behavior after forty days of incubation.

The combined statement of the applied techniques resulted in a precise characterization of the antibody behavior and a very good description of the long-term solution stability under tested conditions. Further studies are required (e.g. study of the surface hydrophobicity) to refine the scoring of the applied analytical techniques for an even more precise description. Additionally, the development of a high throughput compatible setup of the used analytical tools is part of future work to enable an easy and fast description of protein solution stability. Despite the potential of further development the presented and evaluated analytical toolbox is a very important step towards an easier main candidate selection and strategic buffer optimization so that product stability can be ensured.

9.5 Acknowledgments

We would like to acknowledge Synthon Biopharmaceuticals B.V. for the delivery of the mAb stock solution and the opportunity to carry out part of the experiments at the company site in Nijmegen. We gratefully acknowledge instrumental support by Norbert Willenbacher, head of the Department of Applied Mechanics, Institute of Mechanical Process Engineering and Mechanics, KIT. The authors would like to acknowledge the financial support by the Federal Ministry of Education and Research (BMBF) - funding code 0316071B.

Supplementary Material

A1-Preliminary Experiments

In order to be able to select additives, which have an impact on the mAb solution stability, DLS measurements were carried out. With the help of the DLS measurements and the Stokes-Einstein equation, the hydrodynamic radius (r_h) of the antibody was determined as well as higher molecular weight species detected. The increase of the r_h of the mAb and the detection of higher molecular weight species indicate a colloidal destabilization of the mAb [115, 298]. A reduction of r_h as well as the complete elimination of higher molecular weight species indicate a stabilizing character of the tested additive. Additives with a visual pH and concentration dependent impact will be selected for the actual study. First, the reference value of the antibody without additives was determined at pH 5, 7 and 9. The additive was then added to this solution in the lowest concentration and measured after an hour of waiting time. This procedure was repeated with increasing additive concentration. Glycine decreased the r_h of the mAb at pH 7 and pH 9 with in-

Table 9.1: Type and concentration of additives used for pre-tests.

additive	$c_{additive}$ [M]
glycine	0.05 0.1 0.15 0.2 0.25 0.3
glycerol	0.01 0.02 0.03 0.04
D-sorbitol	0.02 0.04 0.06 0.08
PEG4000	0.002 0.004 0.006 0.008 0.01
Na_2SO_4	0.06 0.08 0.1 0.12 0.14 0.16
NaI	0.025 0.05 0.1 0.15 0.2 0.4 0.8

creasing glycine concentration. At pH 5 the r_h decreased with the addition of glycine but was not glycine concentration dependent. With glycine in solution no higher molecular weight species could be detected. Glycerol and D-sorbitol had a comparable impact on the antibody tested. At pH 5 and pH 7 a slight increase of the r_h of the mAb was observed whereas at pH 7 a slight decrease appeared. The impact of osmolyte concentration was not as pronounced as for glycine. PEG4000 had a strong increasing impact on the r_h of the mAb and also on the development of higher molecular weight species for all pH values tested. The effect was mostly pronounced at higher PEG concentrations and at pH 7. With the addition of Na_2SO_4 the r_h of the mAb molecules increased. This effect was Na_2SO_4 concentration dependent at all pH values tested. NaI had an increasing impact on the r_h at pH 5 comparable to Na_2SO_4 . At pH 7 instead low NaI concentrations had a strong increasing impact on the r_h of the mAb. This effect decreased with increasing

NaI concentration to a marginal small effect at the maximal NaI concentration (800 mM) tested. At pH 9 the impact of NaI as a n additive on the mAb r_h could not be tested due to immediate precipitation.

A2-Results Thermal Stability

Table A2a: Results of the thermal stability test. Listed are average values (duplicate measurement) of T_{m1} , T_{m2} and T_{agg} of all samples tested.

Thermal stability results 1						
pH	mAb conc	additive	additive conc	T_{m1}	T_{m2}	T_{agg}
[]	[mg/ml]		[]	[°C]	[°C]	[°C]
5	120	no add	-	72.83	-	71.03
5	180	no add	-	66.80	-	73.40
7	1	no add	-	66.87	54.77	70.53
7	5	no add	-	66.63	76.43	71.80
7	15	no add	-	66.70	75.83	70.90
7	30	no add	-	66.43	75.03	70.83
7	50	no add	-	65.40	74.30	70.60
7	70	no add	-	74.93	-	71.13
7	100	no add	-	74.40	-	70.83
7	120	no add	-	75.77	-	70.07
7	180	no add	-	77.20	-	72.20
9	100	no add	-	74.57	-	67.90
9	120	no add	-	75.33	-	68.33
9	180	no add	-	75.90	-	69.43
[]	[mg/ml]		[mM]	[°C]	[°C]	[°C]
5	120	glycine	50	70.37	-	72.40
5	120	glycine	100	71.63	-	72.60
5	120	glycine	150	75.87	-	72.70
5	180	glycine	50	67.97	-	73.43
5	180	glycine	100	67.23	-	73.50
5	180	glycine	150	67.97	-	73.53
7	120	glycine	50	76.40	-	71.20
7	120	glycine	100	76.30	-	70.67
7	120	glycine	150	76.60	-	70.60
7	180	glycine	50	78.20	-	70.20
7	180	glycine	100	78.40	-	70.10
7	180	glycine	150	79.10	-	70.10
9	120	glycine	50	75.83	-	69.80
9	120	glycine	100	76.23	-	68.63
9	120	glycine	150	76.30	-	69.30
9	180	glycine	50	76.10	-	69.93
9	180	glycine	100	76.53	-	69.73
9	180	glycine	150	76.63	-	70.33

9.5 Acknowledgments

Table A2b: Results of the thermal stability test. Listed are average values (duplicate measurement) of T_{m1} , T_{m2} and T_{agg} of all samples tested.

Thermal stability results 2						
pH	mAb conc	additive	additive conc	T_{m1}	T_{m2}	T_{agg}
[]	[mg/ml]		[(m/V)%]	[°C]	[°C]	[°C]
9	120	PEG4000	0.4	68.30	-	67.17
9	120	PEG4000	1.2	68.47	-	65.60
9	120	PEG4000	2.0	72.33	-	65.10
[]	[mg/ml]		[mM]	[°C]	[°C]	[°C]
7	120	Na ₂ SO ₄	100	76.67	-	70.57
7	120	Na ₂ SO ₄	140	76.65	-	70.15
7	120	Na ₂ SO ₄	160	76.85	-	60.55
7	180	Na ₂ SO ₄	100	77.05	-	71.60
7	180	Na ₂ SO ₄	140	77.55	-	71.35
7	180	Na ₂ SO ₄	160	77.76	-	71.77

A3-Scoring Values Analytical Toolbox

Table A3: Scoring values of the analytical methods applied. The raw analytical results were normalized and a scoring from 0 to 10 defined. Whereby 10 is a result indicating a high colloidal stability and 0 an analytical result indicating a weak solution stability of the screened mAb.

scoring - no additive							
analytical method	parameter	pH 5		pH 7		pH 9	
		120 mg/ml	180 mg/ml	120 mg/ml	180 mg/ml	120 mg/ml	180 mg/ml
SEC	monomer	10.00	8.64	1.47	0.15	3.53	1.38
thermal stability	T _{agg}	5.20	9.75	3.34	7.44	0.01	2.12
viscosity	η	9.31	1.79	9.93	4.56	9.92	4.69
charge	ζ-potential	10.00	10.00	2.98	2.98	0.11	0.11
viscoelasticity	ω _{CO}	10.00	7.47	3.93	0.55	5.72	2.61
AVERAGE VALUE		8.90	7.53	4.33	3.14	3.86	2.18

scoring - glycine							
analytical method	parameter	pH 5		pH 7		pH 9	
		120 mg/ml	180 mg/ml	120 mg/ml	180 mg/ml	120 mg/ml	180 mg/ml
SEC	monomer	9.84	9.14	3.88	4.36	2.83	3.21
thermal stability	T _{agg}	8.40	10.01	4.37	6.29	1.87	3.85
viscosity	η	9.12	2.06	10.00	6.33	9.89	4.31
charge	ζ-potential	0.44	0.44	3.08	3.08	0.55	0.55
viscoelasticity	ω _{CO}	8.55	4.37	3.30	0.70	7.03	3.38
AVERAGE VALUE		7.27	5.21	4.92	4.15	4.43	3.06

scoring - PEG4000							
analytical method	parameter	pH 5		pH 7		pH 9	
		120 mg/ml	180 mg/ml	120 mg/ml	180 mg/ml	120 mg/ml	180 mg/ml
SEC	monomer	-	-	-	-	0.48	0.05
thermal stability	T _{agg}	-	-	-	-	7.63	-
viscosity	η	-	-	-	-	8.68	0.45
charge	ζ-potential	1.75	1.75	0.52	0.52	0.61	0.61
viscoelasticity	ω _{CO}	9.31	6.43	4.10	2.10	5.03	0.00
AVERAGE VALUE		5.53	4.09	2.31	1.31	4.49	0.15

scoring - Na ₂ SO ₄							
analytical method	parameter	pH 5		pH 7		pH 9	
		120 mg/ml	180 mg/ml	120 mg/ml	180 mg/ml	120 mg/ml	180 mg/ml
SEC	monomer	-	-	0.99	0.53	-	-
thermal stability	T _{agg}	-	-	3.40	5.81	-	-
viscosity	η	-	-	9.72	5.29	-	-
charge	ζ-potential	2.19	2.19	0.69	0.69	1.36	1.36
viscoelasticity	ω _{CO}	8.80	7.41	4.60	0.18	1.71	4.58
AVERAGE VALUE		5.49	4.80	3.88	2.50	1.54	2.97

9.6 References

15. Chari, R., Jerath, K., Badkar, A. V. & Kalonia, D. S. Long- and short-range electrostatic interactions affect the rheology of highly concentrated antibody solutions. *Pharmaceutical research* **26**, 2607–18 (2009).
16. Pindrus, M. *et al.* Solubility Challenges in High Concentration Monoclonal Antibody Formulations: Relationship with Amino Acid Sequence and Intermolecular Interactions. *Molecular Pharmaceutics* **12**, 3896–3907 (2015).
20. Saluja, A. *et al.* Application of high-frequency rheology measurements for analyzing protein-protein interactions in high protein concentration solutions using a model monoclonal antibody (IgG2). *Journal of Pharmaceutical Sciences* **95** (2006).
21. Kumar, V., Dixit, N., Zhou, L. L. & Fraunhofer, W. Impact of short range hydrophobic interactions and long range electrostatic forces on the aggregation kinetics of a monoclonal antibody and a dual-variable domain immunoglobulin at low and high concentrations. *International Journal of Pharmaceutics*. **421**, 82–93 (2011).
53. Curtis, R. A. & Lue, L. A molecular approach to bioseparations: Protein–protein and protein–salt interactions. *Chemical Engineering Science* **61**, 907–923 (2006).
58. Amrhein, S., Oelmeier, S. A., Dismer, F. & Hubbuch, J. Molecular dynamics simulations approach for the characterization of peptides with respect to hydrophobicity. *Journal of Physical Chemistry B* **118**, 1707–1714 (2014).
67. Muramatsu, N. & Minton, A. P. Tracer diffusion of globular proteins in concentrated protein solutions. *Proceedings of the National Academy of Sciences of the United States of America* **85**, 2984–8 (1988).
69. Minton, A. P. Implications of macromolecular crowding for protein assembly. *Current opinion in structural biology* **10**, 34–9 (2000).
82. Damodaran, S. & Kinsella, J. E. The effects of neutral salts on the stability of macromolecules. A new approach using a protein-ligand binding system. *The Journal of biological chemistry* **256**, 3394–8 (1981).
83. Arakawa, T. & Timasheff, S. N. Preferential interactions of proteins with solvent components in aqueous amino acid solutions. *Archives of Biochemistry and Biophysics* **224**, 169–177 (1983).

84. Melander, W. & Horváth, C. Salt effect on hydrophobic interactions in precipitation and chromatography of proteins: an interpretation of the lyotropic series. *Arch. Biochem. Biophys.* **183**, 200–15 (1977).
85. Arakawa, T. & Timasheff, S. Mechanism of protein salting in and salting out by divalent cation salts: balance between hydration and salt binding. *Biochemistry*, 5912–5923 (1984).
86. Majumdar, R. *et al.* Effects of Salts from the Hofmeister Series on the Conformational Stability, Aggregation Propensity, and Local Flexibility of an IgG1 Monoclonal Antibody. *Biochemistry* **52**, 3376–3389 (2013).
87. Baldwin, R. L. How Hofmeister ion interactions affect protein stability. *Biophysical journal* **71**, 2056–63 (1996).
88. Baumgartner, K. *et al.* Determination of protein phase diagrams by microbatch experiments: Exploring the influence of precipitants and pH. *International Journal of Pharmaceutics* **479**, 28–40 (2015).
92. Liu, Y. & Bolen, D. W. The Peptide Backbone Plays a Dominant Role in Protein Stabilization by Naturally Occurring Osmolytes. *Biochemistry* **34**, 12884–12891 (1995).
95. Bruździak, P., Panuszko, A. & Stangret, J. Influence of Osmolytes on Protein and Water Structure: A Step To Understanding the Mechanism of Protein Stabilization. *The Journal of Physical Chemistry B* **117**, 11502–11508 (2013).
99. Weiss, W. 4., Young, T. & Roberts, C. Principles, approaches, and challenges for predicting protein aggregation rates and shelf life. *Journal of Pharmaceutical Sciences* (2009).
100. Thiagarajan, G. *et al.* A comparison of biophysical characterization techniques in predicting monoclonal antibody stability. *mAbs* (2016).
105. Wilson, W. Light scattering as a diagnostic for protein crystal growth—A practical approach. *Journal of Structural Biology* **142**, 56–65 (2003).
108. He, F. *et al.* Screening of monoclonal antibody formulations based on high-throughput thermostability and viscosity measurements: Design of experiment and statistical analysis. *Journal of Pharmaceutical Sciences* **100**, 1330–1340 (2011).
109. Webster, S. Predicting Long-Term Storage Stability of Therapeutic Proteins. *PharmTech* **37** (2013).

111. Clogston, J. D. & Patri, A. K. Zeta potential measurement. *Methods in molecular biology (Clifton, N.J.)* **697**, 63–70 (2011).
112. Galm, L., Amrhein, S. & Hubbuch, J. Predictive approach for protein aggregation: Correlation of protein surface characteristics and conformational flexibility to protein aggregation propensity. *Biotechnology and bioengineering* (2016).
115. Bauer, K. C. *et al.* Concentration-dependent changes in apparent diffusion coefficients as indicator for colloidal stability of protein solutions. *International Journal of Pharmaceutics* **511**, 276–287 (2016).
120. George, A. & Wilson, W. W. Predicting protein crystallization from a dilute solution property. *Acta crystallographica. Section D, Biological crystallography* **50**, 361–5 (1994).
126. Scherer, T. M., Liu, J., Shire, S. J. & Minton, A. P. Intermolecular interactions of IgG1 monoclonal antibodies at high concentrations characterized by light scattering. *Journal of Physical Chemistry B* **114** (2010).
127. Saluja, A. *et al.* Ultrasonic storage modulus as a novel parameter for analyzing protein-protein interactions in high protein concentration solutions: correlation with static and dynamic light scattering measurements. *Biophysical journal* (2007).
131. Metzger, T. G. *Das Rheologiehandbuch* 4th ed., 138–216 (Vincentz Network, Hannover, 2011).
138. Kirschenmann, L. *Aufbau zweier piezoelektrischer Sonden (PRV/PAV zur Messung der viskoelastischen Eigenschaften weicher Substanzen im Frequenzbereich* PhD thesis (Universitaet Ulm, 2003).
139. Crassous, J. & Régisser, R. Characterization of the viscoelastic behavior of complex fluids using the piezoelastic axial vibrator. *Journal of Rheology* **49(4)**, 851–864 (2005).
150. Rao, M. A. in *Food Rheology and Structure* 1–26 (2014).
162. Rakel, N., Baum, M. & Hubbuch, J. Moving through three-dimensional phase diagrams of monoclonal antibodies. *Biotechnology Progress* **30**, 1103–1113 (2014).
163. Neal, B., Asthagiri, D. & Lenhoff, A. Molecular Origins of Osmotic Second Virial Coefficients of Proteins. *Biophysical Journal* **75**, 2469–2477 (1998).
164. Saluja, A. & Kalonia, D. S. Nature and consequences of protein-protein interactions in high protein concentration solutions. *International journal of pharmaceutics* **358**, 1–15 (2008).

184. Liu, J., Nguyen, M. D. H., Andya, J. D. & Shire, S. J. Reversible self-association increases the viscosity of a concentrated monoclonal antibody in aqueous solution. *Journal of Pharmaceutical Sciences* **94**, 1928–40 (2005).
186. Teeter, M. M. Water protein interactions : Theory and Experiment. *Annual Review of Biophysics and Biophysical Chemistry* **20**, 577–600 (1991).
188. Rosenbaum, D. F. & Zukoski, C. F. Protein interactions and crystallization. *Journal of Crystal Growth* **169**, 752–758 (1996).
195. Abegg, J.-L., Boiteux, J.-P. & Hourseau, C. US3958581 A (1976).
204. Macosko, C. W. *Rheology: Principles, Measurements, and Applications* (Wiley-VCH, 1994).
207. Haezebrouck, P. *et al.* An equilibrium partially folded state of human lysozyme at low pH. *Journal of molecular biology* **246**, 382–387 (1995).
210. Harding, S. in *Functional properties of food macromolecules* (eds Hill, S., Ledward, D. & Mitchel, J.) 2nd ed., 10–15 (Aspen, 1998).
215. Brummitt, R. K., Nesta, D. P. & Roberts, C. J. Predicting accelerated aggregation rates for monoclonal antibody formulations, and challenges for low-temperature predictions. *Journal of Pharmaceutical Sciences* **100**, 4234–4243 (2011).
218. Schermeyer, M.-T. *et al.* Squeeze flow rheometry as a novel tool for the characterization of highly concentrated protein solutions. *Biotechnol. Bioeng.* **113**, 576–587 (2016).
244. Scott, A., Wolchok, J. & Old, L. Antibody therapy of cancer. *Nature Reviews Cancer* **12**, 14 (2012).
245. Rosman, Z., Shoenfeld, Y. & Zandmann-Goddard, G. Biologic therapy for autoimmune diseases: an update. *BMC Medicine* **11**, 88 (2013).
246. Shire, S. J., Shahrokh, Z. & Liu, J. Challenges in the development of high protein concentration formulations. *J. Pharm. Sci.* **93**, 1390–402 (2004).
247. Leckband, D. & Sivasankar, S. Forces controlling protein interactions: theory and experiment. *Colloids and Surfaces B: Biointerfaces* **14**, 83–97 (1999).
248. Monahan, F. J., German, J. B. & Kinsella, J. E. Effect of pH and temperature on protein unfolding and thiol/disulfide interchange reactions during heat-induced gelation of whey proteins. *Journal of Agricultural and Food Chemistry* **43**, 46–52 (1995).

249. Dill, K. A. Dominant forces in protein folding. *Biochemistry* **29**, 7133–7155 (1990).
251. Lehermayr, C., Mahler, H. C., Mäder, K. & Fischer, S. Assessment of net charge and protein-protein interactions of different monoclonal antibodies. *Journal of Pharmaceutical Sciences* **100**, 2551–2562 (2011).
252. Prediction and characterization of the stability enhancing effect of the Cherry-Tag in highly concentrated protein solutions by complex rheological measurements and MD simulations, Author = Baumann, Pascal and Schermeyer, Marie-Therese and Burghardt, Hannah and Dürr, Cathrin and Hubbuch, J. *International Journal of Pharmaceutics*. submitted (2016).
253. Thakkar, S. V. *et al.* An Application of Ultraviolet Spectroscopy to Study Interactions in Proteins Solutions at High Concentrations. *Journal of Pharmaceutical Sciences* **101**, 3051–3061 (09/2012).
254. Ahamed, T. *et al.* Phase behavior of an intact monoclonal antibody. *Biophysical Journal* **93**, 610–619 (2007).
255. Kröner, F. & Hubbuch, J. Systematic generation of buffer systems for pH gradient ion exchange chromatography and their application. *Journal of Chromatography A* **1285**, 78–87 (2013).
256. Arakawa, T. & Timasheff, S. N. Theory of protein solubility. *Methods in enzymology* **114**, 49–77 (1985).
257. Mason, B. *et al.* Liquid-liquid phase separation of a monoclonal antibody and nonmonotonic influence of Hofmeister anions. *Biophysical journal* **99**, 3792–800 (2010).
258. Wu, S. L. & Karger, B. L. Hydrophobic interaction chromatography of proteins. *Methods in enzymology* **270**, 27–47 (1996).
259. Arakawa, T., Bhat, R. & Timasheff, S. N. Preferential interactions determine protein solubility in three-component solutions: the MgCl₂ system. *Biochemistry* **29**, 1914–23 (02/1990).
260. Tardieu, A., Bonneté, F., Finet, S. & Vivarès, D. Understanding salt or PEG induced attractive interactions to crystallize biological macromolecules. *Acta Crystallographica Section D Biological Crystallography* **58**, 1549–1553 (2002).
261. Pusey, P. N., Poon, W. C. K., Ilett, S. M. & Bartlett, P. Phase behaviour and structure of colloidal suspensions. *Journal of Physics: Condensed Matter* **6**, A29–A36 (1994).

262. Hill, T. L. *An introduction to statistical thermodynamics* 508 (Dover Publications, 1986).
263. Luangtana-Anan, M. *et al.* Polyethylene glycol on stability of chitosan microparticulate carrier for protein. *AAPS PharmSciTech* **11**, 1376–82 (2010).
264. Arakawa, T. & Timasheff, S. N. Abnormal solubility behavior of beta-lactoglobulin: salting-in by glycine and sodium chloride. *Biochemistry* **26**, 5147–5153 (1987).
265. Zhang, M. Z., Wen, J., Arakawa, T. & Prestrelski, S. J. A new strategy for enhancing the stability of lyophilized protein: the effect of the reconstitution medium on keratinocyte growth factor. *Pharmaceutical research* **12**, 1447–52 (1995).
266. Chen, B.-L. & Arakawa, T. Stabilization of Recombinant Human Keratinocyte Growth Factor by Osmolytes and Salts. *Journal of Pharmaceutical Sciences* **85**, 419–422 (1996).
267. Arakawa, T. *et al.* Biotechnology applications of amino acids in protein purification and formulations. *Amino acids* **33**, 587–605 (2007).
268. Jiskoot, W. & Crommelin, D. *Methods for Structural Analysis of Protein Pharmaceuticals* (ed Jiskoot, W.) (Springer Science & Business Media, 2005).
269. Laurance, J. S. & Middaugh, C. R. *Aggregation of therapeutic proteins* (eds Wang, W. & Roberts, C. J.) (Wiley, 2010).
270. Piazza, R. Protein interactions and association: an open challenge for colloid. *Current Opinion in Colloid & Interface Science* **8**, 515–522 (2004).
271. Halle, B. Protein hydration dynamics in solution: a critical survey. *Philosophical transactions of the Royal Society of London. Series B, Biological sciences* **359**, 1207–23 (2004).
272. Booth, F. The Electroviscous Effect for Suspensions of Solid Spherical Particles. *Proceedings of the Royal Society of London A: Mathematical, Physical and Engineering Sciences* **203** (1950).
273. Tanford, C. & Buzzell, J. G. The Viscosity of Aqueous Solutions of Bovine Serum Albumin between pH 4.3 and 10.5. *The Journal of Physical Chemistry* **60**, 225–231 (1956).
274. Buzzell, J. G. & Tanford, C. The Effect of Charge and Ionic Strength on the Viscosity of Ribonuclease. *The Journal of Physical Chemistry* **60**, 1204–1207 (1956).

275. Salinas, B. A. *et al.* Understanding and modulating opalescence and viscosity in a monoclonal antibody formulation. *Journal of pharmaceutical sciences* **99**, 82–93 (2010).
276. Connolly, B. D. *et al.* Weak Interactions Govern the Viscosity of Concentrated Antibody Solutions: High-Throughput Analysis Using the Diffusion Interaction Parameter. *Biophysical Journal* **103**, 69–78 (2012).
277. Wang, S. *et al.* Viscosity-Lowering Effect of Amino Acids and Salts on Highly Concentrated Solutions of Two IgG1 Monoclonal Antibodies. *Molecular Pharmaceutics* **12**, 4478–4487 (2015).
278. Vermeer, A. W. & Norde, W. The thermal stability of immunoglobulin: unfolding and aggregation of a multi-domain protein. *Biophysical journal* **78**, 394–404 (2000).
279. Nicoud, L. *et al.* Effect of polyol sugars on the stabilization of monoclonal antibodies. *Biophysical Chemistry* **197**, 40–46 (2015).
280. Ladbroke, B. & Chapman, D. Thermal analysis of lipids, proteins and biological membranes - A review and summary of some recent studies. *Chemistry and Physics of Lipids* **3** (1969).
281. Nicoud, L. *et al.* Role of Cosolutes in the Aggregation Kinetics of Monoclonal Antibodies. *The Journal of Physical Chemistry B* **118**, 11921–11930 (2014).
282. Menzen, T. A. *Temperature-Induced Unfolding, Aggregation, and Interaction of Therapeutic Monoclonal Antibodies* PhD thesis (2014).
283. Wen, J., Jiang, Y. & Nahri, L. Effect of carbohydrate on thermal stability of antibodies. *American Pharmaceutical Review* **11**, 1–6 (2008).
284. Razvi, A. & Scholtz, J. M. Lessons in stability from thermophilic proteins. *Protein science: a publication of the Protein Society* **15**, 1569–78 (2006).
285. Bye, J. W. & Falconer, R. J. Three Stages of Lysozyme Thermal Stabilization by High and Medium Charge Density Anions. *The Journal of Physical Chemistry B* **118**, 4282–4286 (2014).
286. Street, T. O., Bolen, D. W. & Rose, G. D. A molecular mechanism for osmolyte-induced protein stability. *Proceedings of the National Academy of Sciences of the United States of America* **103**, 13997–4002 (2006).
287. Platts, L. & Falconer, R. J. Controlling protein stability: Mechanisms revealed using formulations of arginine, glycine and guanidinium HCl with three globular proteins. *International journal of pharmaceutics* **486**, 131–5 (2015).

288. Arakawa, T. & Timasheff, S. N. Mechanism of polyethylene glycol interaction with proteins. *Biochemistry* **24**, 6756–6762 (1985).
289. Ingham, K. C. Polyethylene glycol in aqueous solution: Solvent perturbation and gel filtration studies. *Archives of Biochemistry and Biophysics* **184**, 59–68 (1977).
290. Du, W. & Klibanov, A. M. Hydrophobic salts markedly diminish viscosity of concentrated protein solutions. *Biotechnology and Bioengineering* **108**, 632–636 (2011).
291. Wada, A. & Nakamura, H. Nature of the charge distribution in proteins. *Nature* **293**, 757–758 (1981).
293. Hussack, G. *et al.* Engineered Single-Domain Antibodies with High Protease Resistance and Thermal Stability. *PLoS ONE* **6** (2011).
294. Youssef, A. M. & Winter, G. A critical evaluation of microcalorimetry as a predictive tool for long term stability of liquid protein formulations: Granulocyte Colony Stimulating Factor (GCSF). *European Journal of Pharmaceutics and Biopharmaceutics* **84**, 145–155 (2013).
295. Arakawa, T. & Tsumoto, K. The effects of arginine on refolding of aggregated proteins: not facilitate refolding, but suppress aggregation. *Biochemical and biophysical research communications* **304**, 148–52 (2003).
296. Minton, A. P. Influence of macromolecular crowding upon the stability and state of association of proteins: predictions and observations. *Journal of pharmaceutical sciences* **94**, 1668–75 (08/2005).
297. Charlton, L. M. *et al.* Residue-Level Interrogation of Macromolecular Crowding Effects on Protein Stability. *Journal of the American Chemical Society* **130**, 6826–6830 (2008).
298. Hanlon, A., Larkin, M. & Reddick, R. Free-solution, label-free protein-protein interactions characterized by dynamic light scattering. *Biophysical journal* **98**, 297–304 (2010).

Impact of polymer surface characteristics on the
microrheological measurement quality of protein solutions -
a tracer particle screening

Katharina C. Bauer¹, Marie-Therese Schermeyer¹, Jonathan Seidel and Jürgen Hubbuch

*Institute of Engineering in Life Sciences, Section IV: Biomolecular Separation Science,
Karlsruhe Institute of Technology (KIT), 76131 Karlsruhe, Germany*

¹ *These authors contributed equally to this work.*

Abstract

Microrheological measurements prove to be suitable to identify rheological parameters of biopharmaceutical solutions. These give information about the flow characteristics but also about the interactions and network structures in protein solutions. For the microrheological measurement tracer particles are required. Due to their specific surface characteristic not all are suitable for reliable measurement results in biopharmaceutical systems. In the present work a screening of melamine, PMMA, polystyrene and surface modified polystyrene as tracer particles were investigated at various protein solution conditions. The surface characteristics of the screened tracer particles were evaluated by zeta potential measurements. Furthermore each tracer particle was used to determine the dynamic viscosity of lysozyme solutions by microrheology and compared to a standard. The results indicate that the selection of the tracer particle had a strong impact on the quality of the microrheological measurement dependent on pH and additive type. Surface modified polystyrene was the only tracer particle that yielded good microrheological results for all tested conditions. The study indicated that the electrostatic surface charge of the tracer particle had a minor impact than its hydrophobicity. This characteristic was the crucial surface property that needs to be considered for the selection of a suitable tracer particle to achieve high measurement accuracy.

Keywords: *Microrheology; Polymer Protein Interaction; Dynamic Viscosity; Hydrophobicity; Tracer Particle*

10.1 Introduction

With the trend towards concentrated biotherapeutics flow characteristics gain increasing relevance for the pharmaceutical process and formulation development. One key issue is the increasing viscosity of these concentrated protein solutions, which affects the outcome of different processing steps like filtration and formulation [246]. For filtration the viscous solutions are more difficult to pump and can even clog filtration membranes [299]. For formulation the high viscosity of a solution hinders a subcutaneous delivery by syringe [300].

With the help of rheological measurements information about the flow characteristics of protein solutions can be obtained to prevent, predict and manipulate high viscosity. Besides the basic information about the dynamic viscosity of the solution these measurement methods enable the determination of complex rheological parameters like storage and loss modulus, G' and G'' , which can be used to interpret the interactions and structures formed between the proteins [127, 301]. In comparison to other complex systems, like polymer solutions, pharmaceutically relevant protein solutions show a weak network formation and therefore the existing elastic behavior is difficult to detect. Hence rheological methods that are able to characterize low elastic behavior are required. Aggravating for the downstream process and formulation development the available protein volumes are very low and therefore expensive. So only small samples can be used for the analytical screenings of highly concentrated solutions. Conventional measurement methods like cone-plate, plate-plate rheometers or capillary viscometers often do not meet these requirements [20]. Methods with the possibility to measure in the high frequency region and require low sample volumes are high frequency rheological [202, 302] or microrheological measurements. High frequency rheological measurements are based on devices, which are able to create frequencies in the kilohertz region. They have already been established for the investigation of proteins Saluja *et al.* [20] and Schermeyer *et al.* [218]. Yet there are only few suitable devices, which all represent prototypes and never got into production [127, 142]. In contrast to the high frequency rheological measurements, microrheological measurements can be performed by common dynamic light scattering (DLS) or diffusing-wave spectroscopy (DWS) devices. This analytical technique is already established in the biopharmaceutical process development. The principle of this method is based on the diffusion of a particle D dependent on its hydrodynamic radius r_h , the thermal energy

kT and the network structure of the surrounding environment. For the determination of the dynamic viscosity η the Stokes-Einstein equation can be applied

$$D = \frac{kT}{6\pi r_h \eta}. \quad (10.1)$$

For the determination of the complex moduli G' and G'' a more complex analysis needs to be performed [147]. In both cases tracer particles of known size are necessary to determine microrheological parameters. These particles are required to be considerably larger than the size of the studied molecule and should not interact with the surrounding solution. Tracer particles smaller in size would not accurately measure the bulk properties. Interactions caused by the surface characteristics of the particle would falsify the measurement data and therefore the rheological information [147, 303]. Currently tracer particles of different material are used to perform microrheological measurements of protein solutions. They consist of materials such as melamine [146], Poly(methyl methacrylate) (PMMA) [304], polystyrene (PS) [148] or surface modified polymers [305]. Amin, Rega & Jankevics [146], Valentine *et al.* [305] and Gilroy, Hicks, Smith & Rodger [306] found that the selection of the tracer particles has an impact on the microrheological measurement quality for protein solutions. One material, which is often reported to interact with its surrounding or with itself, is polystyrene [303, 307]. The reason could be found in its surface characteristics. By modification of the surface these particles showed less interaction [308, 309]. Looking at these findings good microrheological practice is based on a thorough selection of tracer particles. Knowledge to evaluate the functionality are required.

In order to fill this gap we performed a screening of four different tracer particles for microrheological measurements of lysozyme solutions, used as a model system. Melamine, PMMA, polystyrene and surface modified polystyrene, namely PEG-PS, were selected to find out about their surface characteristics and hence their impact on measurement quality at various system conditions. These conditions were represented by the different lysozyme concentrations, pH-values, plus varying additives. At these conditions the surface characteristics of the tracer particles were studied by zeta potential measurements. The change in the electrostatic potential allowed conclusions about possible interactions in solution. To identify its actual impact on the microrheological measurements the dynamic viscosity of the selected solutions was determined. The results gained with the different tracer particles were compared to results of high frequency rheological measurements. This measurement method was already successfully implemented by several scientific groups [20, 202, 218, 302] and is therefor used as a standard.

10.2 Materials and Methods

10.2.1 Chemicals and Supplies

The tracer particles used in this study were melamine, polymethylmethacrylate (PMMA), polystyrene and surface modified polystyrene (PEG-PS). Analogous to Amin, Rega & Jankevics [146] and Waigh [147], their size was carefully chosen in a size range, which should exceed the microstructural length scale of the lysozyme network, because this protein has a comparatively small size of 1.7 nm [310]. Polystyrene with a diameter of 0.2 μm and melamine with a diameter of 0.3 μm were both purchased by Alfa Aesar GmbH & Co. KG (Karlsruhe, Germany). PMMA with a diameter of 0.2 μm was purchased by micro particles GmbH (Berlin, Germany). For the surface modified particles with a diameter of 0.22 μm the blank polystyrene particles, described above, were covered with a layer of short length polyethylene glycol (PEG) molecules. Further particle specifications are listed in Table 10.1.

Table 10.1: Particle specifications.

Name	Company	Size	Functional groups	Lot
Polystyrene	Alfa Aesar	0.2 μm	Slight anionic charge from surface sulfate groups	T11A024
PMMA	Micro particles GmbH	0.2 μm	-	F-KM255
Melamine	Micro particles GmbH	0.3 μm	-	MF-F-S1902
Pluronic F-127	Sigma Life Sciences	12600 g/mol	-	BCBK9787V

The modification of the polystyrene particles followed the PEGylation script of Kim et al. [311]. Instead of Pluronic F115 Pluronic F127 (Sigma-Aldrich, St. Louis, USA) was used. The stability of the PEG coating was verified by analytical SEC runs and regular size measurement for each screened buffer condition (data not shown). When using orthogonal PEGylation methods [312], the achieved PEG density, which may influence the microrheological measurements, has to be considered. The model protein used in this study was lysozyme from chicken egg white (Hampton Research, Aliso Viejo, CA, USA). It was supplied as a lyophilized powder. The protein has a molecular size of 14.5 kDa, a theoretical pI of 10.7 [313] and an experimentally determined mass extinction coefficient $E1\%(280\text{ nm})$ of 22 L/(g·cm). The buffer components acetic acid,

citric acid, trisodium citrate were purchased from Merck KGaA (Darmstadt, Germany), sodium acetate from Sigma-Aldrich (St. Louis, MO, USA), BisTris propane (1,3-bis-(tris(hydroxymethyl)methylamino)propane) from MOLEKULA (München, Germany), MOPSO (β -Hydroxy-4-morpholinepropanesulfonic acid) from AppliChem GmbH (Darmstadt, Germany). Sodium hydroxide and hydrochloric acid for pH-titration and the additives NaCl, $(\text{NH}_4)_2\text{SO}_4$ came from Merck KGaA, the remaining additives polyethylenglycol (PEG) 300 and 1000 from Sigma-Aldrich. Their specific characteristics are further specified in Table 10.2.

Table 10.2: PEG characteristics.

characteristic	PEG 400	PEG 1000
vapor density	> 1 (vs air)	> 1 (vs air)
vapor pressure	< 0.01 mmHg (20°C)	< 0.01 mmHg (20°C)
autoignition temp.	581 °F	581 °F
mol wt	380-420	950-1050
refractive index	n ₂₀ /D 1.467	
viscosity	~ 120 mPas (20°C)	

Ultrapure water (ISO3696) was used to prepare all solutions. Buffers were filtered with 0.2 μm cellulose acetate membranes (Sartorius, Göttingen, Germany). Protein solutions were filtered with syringe filters with cellulose acetate membrane (VWR, Radnor, PA, USA). To reduce the residual salt content of the lyophilized lysozyme solution a size exclusion chromatography (SEC) was conducted with SephadexTM resin from GE Healthcare (Buckinghamshire, Great Britain). The column was manually packed with a diameter of 2.5 cm and a bed height of 23 cm. For the concentration of the protein 20 mL Vivaspin[®] ultra filtration spin columns (Sartorius) with a molecular weight cut off of 3000 Da were used. For the viscosity measurements ZEN2112 quartz glass cuvettes (Hellma, Müllheim, Germany) were utilized. The zeta potential measurements were performed with folded disposable capillary cells (Malvern Instruments, Malvern, UK) equipped with two electrodes.

10.2.2 Instrumentation

The buffer exchange was conducted with an ÄKTAprimeTM plus system from GE Healthcare. The protein concentration of the lysozyme solutions was determined with the NanoDropTM 2000c UV-Vis spectrophotometer (Thermo Fisher Scientific, Waltham, MA, USA). Zetapotential and microrheological measurements were conducted with the Ze-

tasizer Nano ZSP (Malvern Instruments, Malvern, UK) using dynamic light scattering. With the Non-Invasive Backscatter (NIBS™) optics even turbid samples can be measured without double scattering. The rheological results were compared to results obtained with a squeeze flow rheometer, the Piezo Axial Vibrator (PAV). This instrument was chosen due to its high reproducibility and therefore functions as the standard for this study. The accuracy of this measurement tool could be proven in various publications [139, 141, 202, 203].

10.2.3 Sample Preparation

Buffers used in this study all had an ionic strength of 100 mM. For the experiments buffers with pH values of 3, 5, 7, and 9 were prepared. The respective buffer components were citric acid and trisodium citrate for pH 3, acetic acid and sodium acetate for pH 5, MOPSO for pH 7 and BisTris Propane for pH 9. Lysozyme of chicken egg white was dissolved in the respective buffer with a starting concentration of 150 mg/mL. To remove residual salts a SEC method followed. Here 5 mL of lysozyme solution with a concentration of 150 mg/mL was purified with a Sephadex™ adsorber. This was packed with a constant flow method. The protein was fractioned in 10 mL Falcon tubes and the concentration measured with an extinction coefficient $E_{1\%}(280\text{ nm})$ of 22 L/(g·cm). The concentration of the diluted protein solution to 200 mg/mL was performed in Vivaspins® and a rotational speed of 8000 rad/sec. To have neglectable impact on the studied system tracer particle solutions of 5 w% were induced in a ratio of 1:200 (V(particle solution):V(protein solution)) for the microrheological measurement.

10.2.4 Zeta Potential Measurements

Depending on the pH and buffer components molecules do have a characteristic surface net charge. This charged surface results in an increased concentration of counter ions close to the particle's surface. The zeta potential is defined as the potential at the boundary, inside which the ions and particles form a stable entity, when the particles move due to an applied electric field. The method used here is based on electrophoretic light scattering. In this case the velocity of particles moving in the electric field is determined by the frequency change of the scattered laser light [314, 315]. The zeta potential measurements were performed at 25°C for tracer particles dissolved in buffer and lysozyme solution

under conditions mentioned above. A sample volume of 20 μL was pipetted in a disposable cuvettes and measured with the diffusion barrier technique [243]. With the correlation to the microrheological results a change of the measurement quality due to electrostatic interactions could be studied.

10.2.5 Determination of the Dynamic Viscosity and Complex Moduli using Microrheology

In this study passive microrheology was applied. This method extracts rheological properties from the motion of particles undergoing thermal fluctuations. The motion of the particles is measured by dynamic light scattering.

For the calculation of the dynamic viscosity η measured by microrheology the Stokes-Einstein equation, listed as equation 10.1 in this study, was applied. The two unknown parameters r_h and D of the respective tracer particle were determined by two dynamic light scattering measurements. First, r_h of the respective tracer particle was determined in buffer with an estimated viscosity of water at 25°C. Second, D of the respective tracer particle was determined in lysozyme solution. Considering this approach the dynamic viscosity of protein solutions with melamine, PMMA, polystyrene and PEG-PS as tracer particles was determined using the Zetsizer Nano ZS. The concentration of protein solution was varied within the range of 30 - 200 mg/mL, the pH was shifted from 3-9. Additionally the influence of additive type, namely NaCl, $(\text{NH}_4)_2\text{SO}_4$, PEG 300 and PEG 1000 on the accuracy of the dynamic viscosity determination was studied. A volume of 40 μL of the sample with the addition of tracer particles in the ratio of 1:200 was directly pipetted into the quartz cuvette and measured at a stable temperature of 25°C. Microrheological measurements with good results for the dynamic viscosity were further investigated by determination of the complex moduli G' and G'' . The frequency dependence of the storage (G') and loss modulus (G'') were obtained from a thermal energy balance and the measured mean square displacement [316]. G' and G'' were determined over a frequency range of 10 to 100000 rad/sec.

10.2.5.1 Determination of the Dynamic Viscosity Using High Frequency Rheology

The high frequency rheological measurements were performed with a squeeze flow rheometer, namely the Piezo Axial Vibrator (PAV), performing a frequency sweep. With frequency sweep measurements one can obtain complex rheological parameters, like the

complex storage modulus G' and loss modulus G'' as well as the complex viscosity η^* . The complex viscosity can be extrapolated to the zero shear viscosity η_0 . The zero shear viscosity obtained with oscillatory measurements can be equated with the dynamic viscosity determined by microrheological measurements, following the Cox-Merz Rule [131, 317]. All measurements were conducted at a temperature of 25°C and a sample volume of 30 μL . The sample was directly pipetted on the measuring head and closed with a thick stainless steel top plate leaving a circular gap with a height of 15 μm in the measurement chamber. A detailed operation of the appliance and a derivation of the required rheological parameters is described in the doctoral thesis of L. Kirschenmann Kirschenmann [138].

10.3 Results

The measurement quality of microrheological measurements strongly depends on the tracer particles and their specific surface properties in solution. To find the key characteristics of a suitable tracer particle different materials, namely melamine, Poly(methyl methacrylate) (PMMA), polystyrene (PS) and PEGylated polystyrene (PEG-PS) were tested at various conditions. To determine the impact of pH and additives on the electrostatic surface characteristics the zeta potential was determined. Its consequences for the quality of the microrheological measurements were evaluated by the comparison of the determined dynamic viscosity with results of high frequency rheological measurements.

10.3.1 Impact of pH and Additives on the Zeta Potential of the Studied Tracer Particles

Tracer particle surface characteristics are one of the main issues for the quality of a microrheological measurement. These characteristics can induce interactions with the proteins in solution. To better understand the impact of the electrostatic surface characteristics on possible interactions the zeta potential of the respective particle was determined under varying solution conditions. Therefore the influence of pH on the zeta potential of the tracer particles in buffer solution was determined. These results were compared to the same conditions with a constant lysozyme concentration of 150 mg/mL in solution. The deviation of these two values of zeta potential is given by $\delta\zeta$. Analog to this procedure the impact of additives on protein-particle interactions was studied at

pH 3. Here the zeta potential determined for samples with protein in solution were compared to the zeta potential determined for samples with protein and additive in solution. Figure 10.1(a) displays the zeta potential of melamine, PMMA, polystyrene and PEG-PS tracer particles at pH 3, 5, 7 and 9 in the respective buffer solution. For melamine the surface potential was positive over the studied pH range. At pH 3 and 9 the zeta potential was 11 mV. The highest zeta potential was found at pH 5 with 20 mV, the lowest value at pH 7 with 6 mV. PMMA and polystyrene are both negatively charged and show the same progression of zeta potential over pH. From pH 3 to 7 the zeta potential decreased to a minimum of -25 mV for PMMA and -27 mV for polystyrene. At pH 9 the zeta potential increased to a value around -18 mV for both materials. In comparison to PMMA polystyrene showed high standard deviations for pH 3, 5 and 7. The zeta potential of PEG-PS was determined close to zero for pH 3, 5 and 7. For pH 9 the surface potential decreased to a slightly negative value of -4 mV.

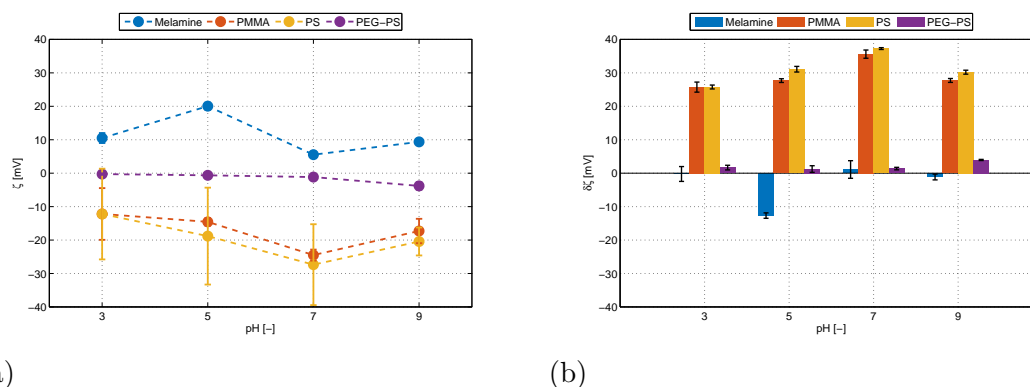


Figure 10.1: (a) Zetapotential and calculated standard deviations of the tracer particles melamine, PMMA, polystyrene and PEG-PS in buffer and (b) difference between the zetapotential of the tracer particles in buffer and in lysozyme solution at a constant concentration of 150 mg/mL at pH 3, 5, 7 and 9. The depicted standard deviation are calculated for the determined zeta potential in lysozyme solution.

With addition of lysozyme the zeta potential of the tracer particles changed depending on tracer particle type and pH value studied. Figure 10.1(b) shows $\delta\zeta$ for melamine, PMMA, polystyrene and PEG-PS. The zeta potential of melamine stayed constant with addition of lysozyme at pH 3, 7 and 9. At pH 5 the determined zeta potential of the particle decreased. The zeta potential of PMMA and polystyrene increased with addition of lysozyme by a $\delta\zeta > 20$ mV and led to a positive overall surface potential for the studied

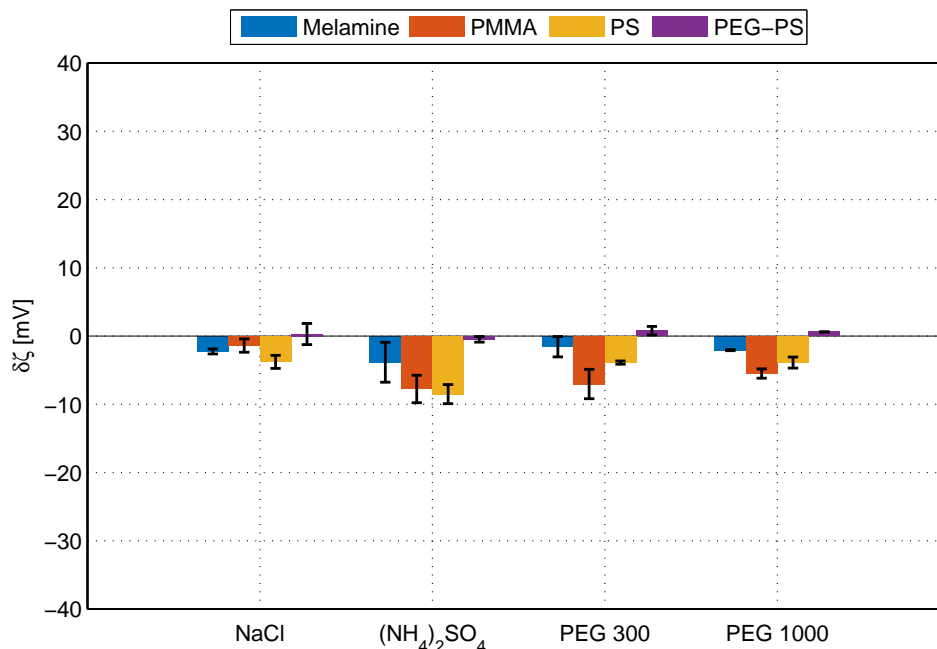


Figure 10.2: Differences of the zeta potential of melamine, PMMA, polystyrene (PS) and PEG-PS in a lysozyme solution with and without addition of NaCl, $(\text{NH}_4)_2\text{SO}_4$, PEG 300 and PEG 1000 at pH 3.

pH range. In comparison to these two particles the $\delta\zeta$ for PEG-PS was relatively small with the highest value of 3.9 mV at pH 9. This increase led to a neutral surface potential. In Figure 10.2 the difference of the zeta potential $\delta\zeta$ of the tracer particles in a lysozyme solution with and without additive at pH 3 are shown. This pH-value was chosen due to its low impact on the microrheological measurement accuracy in comparison to pH 5, 7, and 9 (Figure 10.4). At this condition a predominating impact of the additives is expected.

In comparison to changes in pH, the chosen additives had a minor impact on the determined zeta potential of the different tracer particles. In general they decreased the zeta potential by a maximum value of 8.5 mV. This value was found for polystyrene with $(\text{NH}_4)_2\text{SO}_4$ as additive. For PEG-PS $\delta\zeta$ stayed constant with addition of the studied additives. As already observed for the impact of pH in Figure 10.1 the surface potential for this tracer particle is close to 0.

10.3.2 Impact of the Tracer Particles on the Microrheological Measurement Quality

The following results show the dynamic viscosity of lysozyme solution measured with microrheology in comparison to the results gained by squeeze flow rheology used as standard. Protein concentration, pH and additive type had varying impact on the tracer particles used in this study.

Figure 10.3(a) shows the dynamic viscosity determined by microrheological measurements with tracer particles consisting of melamine, PMMA, polystyrene, PEG-PS and high frequency measurements conducted with the PAV dependent on lysozyme concentration at pH 3. For every measured system the dynamic viscosity increased with increasing concentration. In comparison to the dynamic viscosity determined with the PAV the viscosity derived by microrheological measurements with polystyrene as tracer particle were overestimated for every studied protein concentration. The results for systems with melamine and PMMA were underestimated. The dynamic viscosity determined with PEG-PS was closest to the values of the chosen standard and had the same progression up to 150 mg/mL.

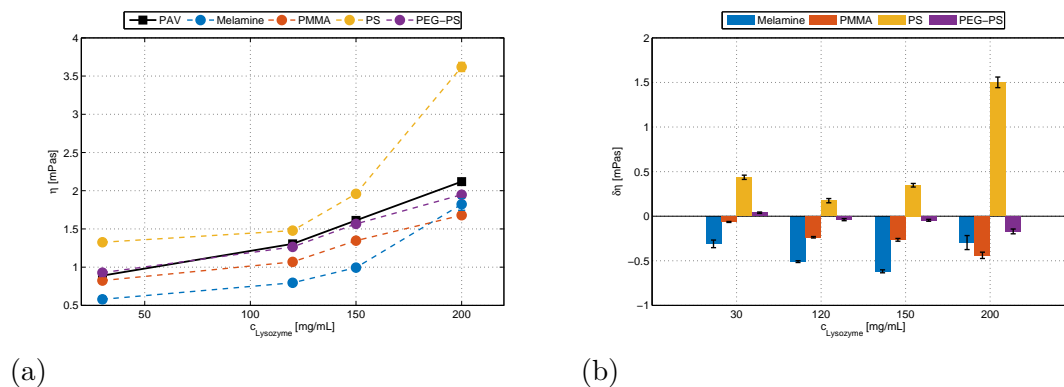


Figure 10.3: (a) Dynamic viscosity of a lysozyme solutions determined with the PAV (standard) and microrheological measurements conducted with different tracer particles dependent on concentration at pH 3. (b) Difference to the gold standard for each tracer particle dependent on the lysozyme concentration at pH 3.

The difference between the viscosity measured by microrheological measurements and the viscosity determined with the PAV $\delta\eta$ and the standard deviations of the microrheological measurements are shown in Figure 10.3(b). In general the differences increase with

increasing protein concentration for all tested particles. The highest $\delta\eta$ was found for polystyrene at a lysozyme concentration of 200 mg/mL. The results for PEG-PS showed high consistency with the PAV. For melamine at a lysozyme concentration of 200 mg/mL $\delta\eta$ decreased, but the standard deviation of the microrheological measurement increased to 7.8 mPas. This was also the highest value of standard deviation determined for this measurement series.

Figure 10.4 demonstrates the influence of pH on the difference between the dynamic viscosity determined by microrheological measurements and the standard method at a constant lysozyme concentration of 120 mg/mL. Additionally the standard deviations of the microrheological measurements are displayed.

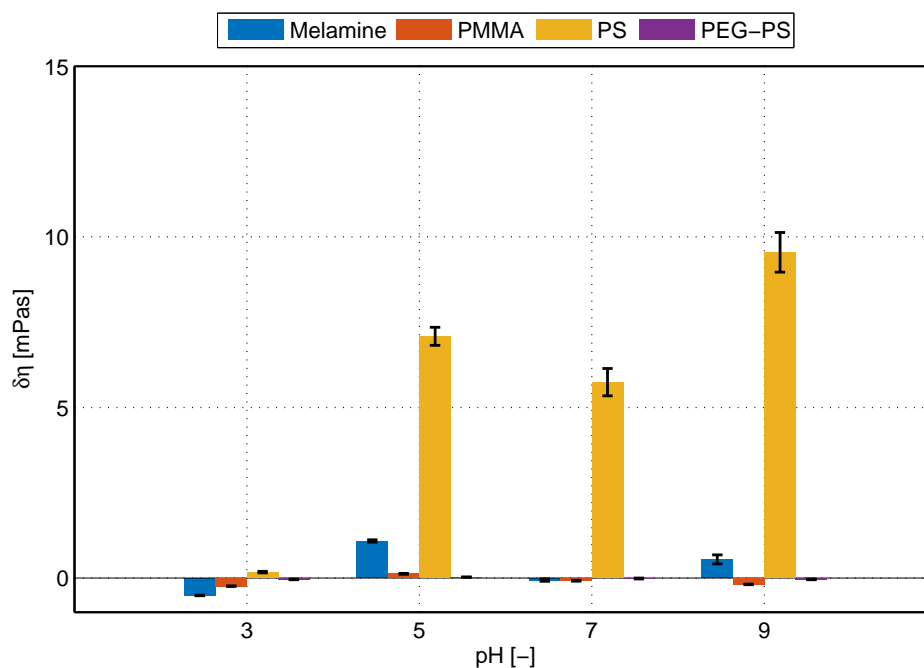


Figure 10.4: Difference to the standard $\delta\eta$ and the standard deviation of the microrheological measurement for each tracer particle dependent on pH at a constant lysozyme concentration of 120 mg/mL.

The values of $\delta\eta$ determined with melamine, PMMA and polystyrene were sensitive to pH. In case of the measurements with melamine no clear trend could be observed. The dynamic viscosity determined for pH 3 and pH 7 was underestimated and thus $\delta\eta$ negative, for pH 5 and pH 9 the dynamic viscosity was overestimated and thus $\delta\eta$ positive. The highest difference for melamine could be found for pH 5 with a value of 1.09 mPas.

For PMMA the smallest difference to the standard was detected at pH 7. With a decrease or increase of pH from this point the dynamic viscosity got underestimated and the modulus of $\delta\eta$ increased up to a value of 0.19 mPas. The highest values of $\delta\eta$ as well as the highest standard deviations were determined for polystyrene. For pH 5, pH 7 and pH 9 the dynamic viscosity of the protein solution was overestimated by more than 5 mPas. The standard deviations increased from 0.024 mPas at pH 3 to 0.58 mPas at pH 9. The influence of the pH on PEG-PS was negligibly small and the $\delta\eta$ did not exceeded a modulus of 0.039 mPas.

Also the complex moduli G' and G'' determined with PEG-PS particles in triplicate showed a comparable course to the results of the standard. Figure 10.5 shows the raw data of the microrheological measurements and of the PAV as well as its fit by Fourier transformation of second order.

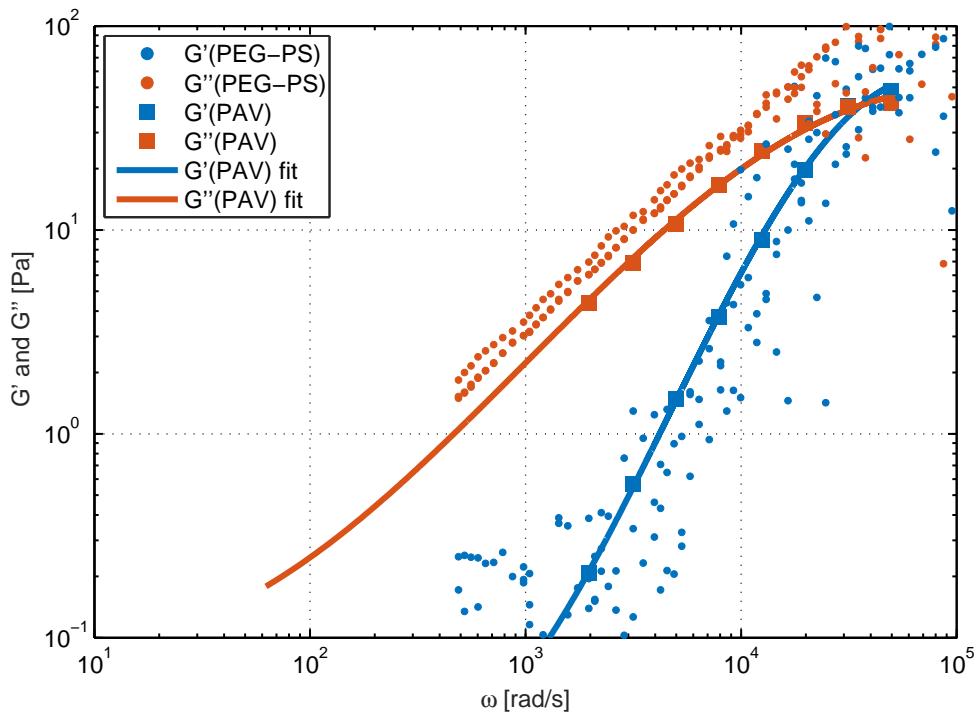


Figure 10.5: Triplicate microrheological measurement with modified polystyrene particles (PEG-PS) of the complex storage and loss modulus (G' and G'') in comparison to the standard (PAV) plus its fit [218] at pH 7 and a lysozyme concentration of 150 mg/mL.

The impact of additives on the dynamic viscosity measured with the different tracer particles can be found in Figure 10.6.

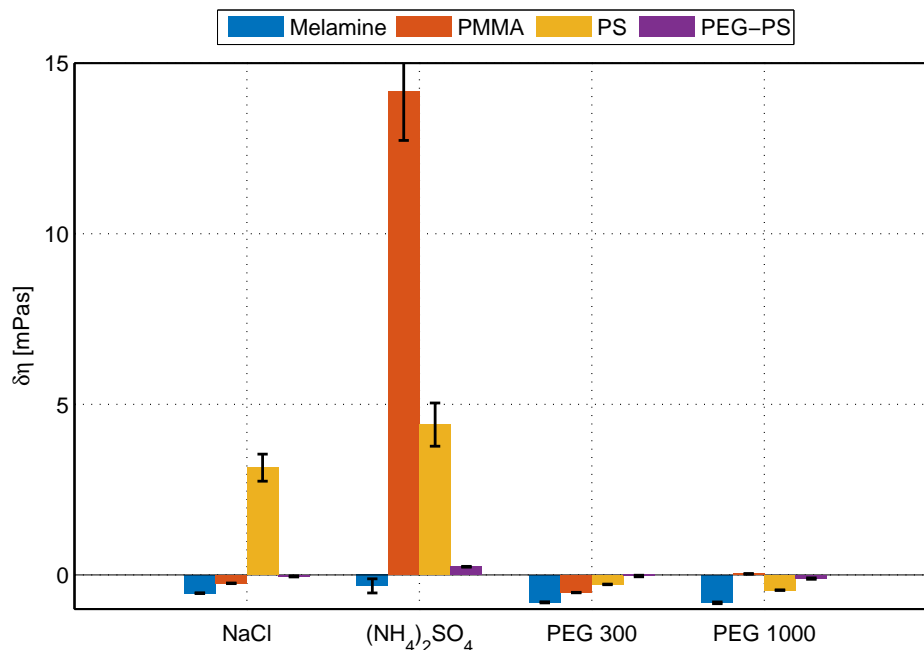


Figure 10.6: Difference to the standard for each tracer particle and the standard deviation of the microrheological measurement dependent on the additives NaCl, $(\text{NH}_4)_2\text{SO}_4$, PEG 300 and PEG 1000 at pH 3 and lysozyme concentration of 120 mg/mL.

Here the differences between the microrheological measurements and the standard induced by added salts and PEG molecules are shown. Two salt types, NaCl and $(\text{NH}_4)_2\text{SO}_4$, and two PEG molecules of different molecular weight, PEG 300 and PEG 1000, were investigated in this study. Dependent on tracer particle and additive type the measurement quality varied. The dynamic viscosity determined with melamine particles was underestimated with every additive type in solution. The standard deviation calculated for samples containing $(\text{NH}_4)_2\text{SO}_4$ and melamine as tracer particle in solution was higher than the resulting $\delta\eta$. The difference to the standard $\delta\eta$ with PMMA as tracer particle was negative with sodium chloride and PEG 300 in solution. The addition of $(\text{NH}_4)_2\text{SO}_4$ resulted in a positive $\delta\eta$. In comparison to the standard the determined viscosity was 13 times higher. PEG 1000 had no significant impact on the measurement accuracy with PMMA as tracer particle. For the microrheological measurements with polystyrene and the two studied salts $\delta\eta$ values were higher than 3 mPas. The addition of PEG revealed a lower

determined viscosity. In comparison with the other tracer particles the influence of the chosen additives on the measurement quality with PEG-PS was low. The viscosity was underestimated with addition of sodium chloride, PEG 300 and PEG 1000. $(\text{NH}_4)_2\text{SO}_4$ resulted in a positive $\delta\eta$ of 0.24 mPas, the highest difference to the standard for this particle.

10.4 Discussion

In this work we investigated the suitability of different tracer particles, namely melamine, PMMA, polystyrene and PEG-PS, for microrheological measurements under various conditions. The results of this investigation showed that the specific particle surface properties dependent on solution conditions like protein concentration, pH as well as the addition of additives had an impact on the measurement quality. The changes on the tracer particle surface and the consequences for the microrheological measurement accuracy are discussed in the following sections.

10.4.1 Impact of pH and Additives on the Zeta Potential of the Studied Tracer Particles

To investigate the electrostatic surface characteristics and its possible influence on the microrheological measurement quality the zeta potential of the tracer particles melamine, PMMA, polystyrene and PEG-PS was determined under varying conditions. In the following section the impact of pH and additives are discussed.

For the studied pH range the sign of the measured net charge stayed the same for all tested tracer particles. Melamine had a positive zeta potential. This observed surface character is mainly governed by the partial positively charged amine groups, which is in accordance with literature [318]. With addition of lysozyme the observed variance of charge with changing pH is compensated to a constant value of 10 mV. This change in zeta potential for pH 5 implies an interaction of the tracer particles with lysozyme. As both particles are positive in net charge this effect has to be based on hydrophobic interactions with the hydrocarbon segments of the melamine surface [319]. For PMMA a negative zeta potential was determined due to the ionized carboxyl groups Baptista *et al.* [320]. This finding is in good agreement to literature, which reviewed and determined zeta potential data of unmodified PMMA [321, 322]. At pH 3 comparatively high

standard deviation was observed, which could be attributed to its pKa at 4.5. Below this pH-value the carboxyl groups are not ionized. This could lead to a destabilization of the particles. In lysozyme solution the zeta potential of PMMA became positive, which is due to electrostatic protein-particle interactions between the positively charged protein surface and the negatively charged tracer particle surface. As PMMA polystyrene had a negative zeta potential from pH 3 to 9, which was also seen for the measurements conducted by Ohsawa et al. Ohsawa, Murata & Ohshima [323]. In comparison to PMMA the $\delta\zeta$ of polystyrene in protein solution were even higher. This behavior could be explained by the strong hydrophobic character of polystyrene [324]. Another argument for the strong hydrophobic character are the high standard deviations for the zeta potential measurements, shown in Figure 10.1. The hypothesis, that the polystyrene particles did not reach equilibrium could not be confirmed by repeated measurements after zero, three, and ten hours (data not shown). Here, the motion in the electric field could be influenced by the hydrophobic forces. This may also lead to aggregation of the poorly stabilized polystyrene particles. By addition of lysozyme the strong hydrophobic impact on the standard deviation decreases. This decrease can be explained by the adsorption of lysozyme to the polystyrene surface, which shields the hydrophobic surface patches. In contrast to the other tracer particles the zeta potential of PEG-PS was close to zero for the tested pH range. This implies a uncharged particle surface. As the PEG-PS surface is neither charged nor hydrophobic no protein-particle interactions are anticipated. The determination of the zeta potential with lysozyme in solution confirms this assumption, because only a small $\delta\zeta$ was observed.

The addition of salts or PEGs had less impact than the change in pH on the determined zeta potential of the tracer particles in lysozyme solution. For melamine, PMMA and polystyrene the additives decreased the zeta potential and hereby the surface charge. Regardless if the tracer particle was positively or negatively charged the additives shield the electrostatic groups on the surface. Comparing the two salt types $(\text{NH}_4)_2\text{SO}_4$ had a higher shielding effect than NaCl due to its higher electron valence [325]. The different polymer length of PEG 300 and PEG 1000 did not seem to have an impact on the modulus of $\delta\zeta$. The zeta potential of PEG-PS is not influenced by the studied additives due to its uncharged surface.

10.4.2 Impact of Tracer Particle Surface on the Microrheological Measurement Quality

The observed changes in surface characteristics discussed in the section before are evaluated regarding their impact on the quality of the microrheological measurements dependent on lysozyme concentration, pH and additives. The possible interactions of tracer particles in protein solution, which cause these deviations from the ideal value, are also taken into account.

Compared to pH and addition of additives the influence of lysozyme concentration on the microrheological measurement quality at pH 3 was low independent on the tracer particle type used. The maximum value of $\delta\eta$ with changing lysozyme concentration was 1.5 mPas for the measurement with polystyrene as tracer particle. In general $\delta\eta$ increased with increasing protein concentration. This effect is due to the decreasing molecule distances, which promote increasing interactions [164]. Only exceptions were the measurement values of polystyrene at 30 mg/mL of lysozyme and melamine at 200 mg/mL of lysozyme. Whereas this value for polystyrene could be assessed as an outlier the determined value for melamine could be explained by the different ranges of electrostatic and hydrophobic interactions. Melamine is protonated at pH 3, which causes a positive surface charge. This can be seen in the measured zeta potential in Figure 10.1. This positive charge of the particle and the positive charge of lysozyme at pH 3 (pI of 10.7) lead to repulsive electrostatic interactions and result in an lower determined viscosity. This state seems to apply for lysozyme concentrations up to 150 mg/mL. At higher concentrations shorter distances between the particles and the proteins allow the formation of additional short-range interactions like attractive hydrophobic interactions and hydration forces [191, 326], which could decrease $\delta\eta$. Like for melamine the viscosity values of the lysozyme solutions measured with PMMA as tracer particle were underestimated, although this particle had a contrary charge in comparison to melamine at pH 3. One possible reason could be the adsorption of protein on the particle surface. As shown in Figure 10.1 (b) the surface potential of PMMA with addition of lysozyme became positive. This shift could be explained by the formation of an adsorption equilibrium of lysozyme molecules on the PMMA surface. This change in particle surface leads to repulsive interactions with the positively charged lysozyme molecules in solution and thus to a negative $\delta\eta$. In comparison to melamine and PMMA the determined viscosity with polystyrene as tracer particle was overestimated for all lysozyme concentrations. This particle has the same surface potential as PMMA, but also a strongly hydrophobic character. Thus the particle is poorly hydrated, which leads to a bad dispersability in aqueous solutions. For

this reason one can expect strong particle-particle and particle-protein interactions [327]. Both effects might lead to higher determined viscosity values. Short-range hydrophobic interactions between lysozyme and polystyrene intensify with increasing protein concentrations, which might cause the highest $\delta\eta$ of 1.5 mPas at 200 mg/mL of lysozyme for the studied influence of concentration at pH 3. In case of PEG-PS the hydrophobic surface groups of polystyrene are shielded with neutral and hydrophilic PEG molecules. This modification results in a good accordance of the determined viscosity values with the standard, which does not change with addition of lysozyme (Figure 10.1). Due to the neutral surface potential and hydrophilic character of PEG-PS $\delta\eta$ is below $|0.17|$ mPas for the whole measurement range. To summarize the impact of lysozyme concentration on the measured dynamic viscosity values all tracer particles showed the right trend of increasing viscosity with protein concentration. The measurements with PEG-PS showed the highest accuracy.

The pH-value has an impact on the microrheological measurement quality depending on the type of tracer particle used. In comparison to the impact of lysozyme concentration the impact of different pH values on $\delta\eta$ was up to five times higher. The strongest impact could be found for polystyrene at pH 5, 7 and 9. This unacceptably high difference in viscosity and high standard deviations might be due to hydrophobic interactions of the polystyrene particles with each other respectively interactions of the polystyrene particles with lysozyme [328]. These interactions may cause aggregation of the particles and adsorption of lysozyme to the particle surface. Both phenomena increase the observed hydrodynamic radius of the tracer particles and therefore lead to inadequate measurement results and calculations. The adsorption of the protein was already observed in a minor dimension with the increase of lysozyme concentration at pH 3 in section 10.4.2. One could explain the high deviations for pH 5, 7 and 9 with an adsorption of proteins to the surface, but also a denaturing effect of the strongly hydrophobic polystyrene on the proteins. This property is already used by several research groups to investigate protein unfolding in solution [329]. As well as for polystyrene hydrophobic interactions could cause differences of the determined dynamic viscosity with melamine as a tracer particle. This claim can be explained by the comparison of the zeta potential values for melamine in buffer, shown in Figure 10.1, and lysozyme in solution at pH 5. At this condition melamine and lysozyme both have a positive surface potential. Thus, the observed change of the zeta potential of melamine in lysozyme solution in Figure 10.1 (b) can not be explained by electrostatics. In this case hydrophobic interactions must cause an adsorption of lysozyme to the particle, which partially shields the positively charged groups of the melamine surface. In comparison to pH 5 $\delta\eta$ is smaller for pH 3 and 9

and no changes in zeta potential were observed. With this considerations one expects hydrophobic interactions but no shielding at these pH values. For PMMA and PEG-PS the impact of pH can be neglected. All values calculated for $\delta\eta$ are below a value of 0.25 mPas. The best accuracy over the investigated pH range was determined for PEG-PS with $\delta\eta < 0.04$ mPas according to a percentage deviation of 3 %. Therefore those two tracer particles are suitable for microrheological measurements in the tested pH range without additive in solution. For PEG-PS this is due to the fact that the particles' surface is uncharged, which is depicted in Figure 10.1. The good accordance of rheological results obtained with PEG-PS with the standard holds true for the determination of complex viscoelastic moduli. Figure 10.5 demonstrates that the course of G' and G'' obtained with PEG-PS are in acceptable agreement with values obtained with the PAV. The scattering of the G' values and thus a limited reproducibility of the complex moduli are due to not optimized measurement settings and have to be improved for future measurements. For this optimization the impact of particle size is of special interest. In contrast to the zero zeta potential of PEG-PS the measurements conducted with PMMA reveal a negative zeta potential within the tested pH range. With the assumptions made so far one would expect a deviation in the determined dynamic viscosity for this tracer particle. Yet the discussed deviations of the dynamic viscosity for melamine and polystyrene had their cause in hydrophobic interactions. PMMA is more hydrophilic in character [330, 331]. This characteristic seems to dominate the quality of microrheological measurements. The changes in electrostatic character, detected by the zeta potential measurements, have a minor impact on the quality of the microrheological measurements. With this knowledge the determination of hydrophobicity should be prioritized over the determination of electrostatic surface characteristics.

Compared to the impact of pH the addition of the selected additives had a minor influence on the measurement quality. The highest deviation could be found for the viscosity determined with PMMA in a 120 mg/mL lysozyme solution with 150 mM $(\text{NH}_4)_2\text{SO}_4$. Poor solubility of this tracer particle in buffer solution containing additives seem to be the only plausible reason. Conducted size measurements of PMMA revealed aggregation caused by the addition of the studied additives in buffer (Data not shown). For NaCl, PEG 300 and PEG 1000 this impact could be suppressed by the addition of lysozyme. For $(\text{NH}_4)_2\text{SO}_4$, which is a common precipitating agent for protein solutions [332, 333], the aggregation was enhanced. Further deviations were found for measurements with polystyrene and the selected salts. As described before the zeta potential of the polystyrene particles in these two systems shifts to a positive value with addition of lysozyme. This positive zeta potential is reduced by the interaction with the negatively charged salt ions. This re-

duction in electrostatics promotes the already present hydrophobic interactions between particles and proteins. This increase in attractive interactions results in an increase in $\delta\eta$. The different impact of the two salt types could be explained analog to the change in zeta potential in Figure 10.2 with the different valence of the salt ions. Consequently, polystyrene and PMMA are unsuitable for microrheological measurement with salt as an additive. For melamine and PEG-PS additional salt does not have an influence on the measurement accuracy, which makes them suitable tracer particles for these specific conditions. With an alteration of conditions this observation would need to be reexamined. In comparison to salt the microrheological measurements with PEG 300 and PEG 1000 in solution resulted in adequate viscosity values independent of PEG type and tracer particle used.

10.5 Conclusions

Taken all influences on tracer surface characteristics and their impact on the microrheological measurement quality into account PEG-PS was the only suitable tracer particle in this study. It resulted in good agreement for the dynamic viscosity as well as first promising results for the complex moduli. The key factors were its hydrophilic character and uncharged surface. Although PMMA was oppositely charged to lysozyme it showed exclusively high deviations of measurement quality with the addition of $(\text{NH}_4)_2\text{SO}_4$. The measurement accuracy for melamine was insufficient for high protein concentrations and changes in pH. These deviations could be explained by its charged and hydrophobic character. However, this study was conducted with respect to the pharmaceutically relevant bioproducts. Here the accuracy of analytical measurements is very important. If costs for PEG-PS exceed investigation budget and measurements in ideal, solute solutions are performed, then melamine could be considered as an alternative. The highest deviations to the standard were determined with polystyrene as tracer particle for every varied parameter in this study. The reason could be found in its charged but mainly hydrophobic character. In principle these results reinforce the observations from other publications, which stated that the selection of a suitable tracer particle is one of the key requirements for the accuracy of a microrheological measurement. Our work reveals that electrostatic interactions due to the charged surface of the tracer particles and the protein molecules seems to have a minor impact on the measurement quality of this screening. It suggests that the hydrophobicity of the tracer particle has the major impact on the microrheological measurement quality. This surface property can cause strong interactions with the

protein molecules in solution, especially at high concentrations. Consequently this characteristic is the crucial surface property that needs to be considered for the selection of a suitable tracer particle to achieve high measurement accuracy. This allows a better analysis of biopharmaceutical solutions in the early process and formulation development.

10.6 Acknowledgments

Thanks to Michèle Delbé and Michael Wörner for their valuable pieces of advice during the development of this article. We thank Kristina Schleining for performing some of the experimental work.

This research work is part of the projects 'Proteinaggregation bei der Herstellung moderner Biopharmazeutika' (0315342B) and 'EuroTransBio' (0316071B), both funded by the German Federal Ministry of Education and Research (BMBF).

10.7 References

20. Saluja, A. *et al.* Application of high-frequency rheology measurements for analyzing protein-protein interactions in high protein concentration solutions using a model monoclonal antibody (IgG2). *Journal of Pharmaceutical Sciences* **95** (2006).
68. Minton, A. P. Influence of excluded volume upon macromolecular structure and associations in a crowded media. *Current Opinion in Biotechnology* **8**, 65–69 (1997).
69. Minton, A. P. Implications of macromolecular crowding for protein assembly. *Current opinion in structural biology* **10**, 34–9 (2000).
84. Melander, W. & Horváth, C. Salt effect on hydrophobic interactions in precipitation and chromatography of proteins: an interpretation of the lyotropic series. *Arch. Biochem. Biophys.* **183**, 200–15 (1977).
127. Saluja, A. *et al.* Ultrasonic storage modulus as a novel parameter for analyzing protein-protein interactions in high protein concentration solutions: correlation with static and dynamic light scattering measurements. *Biophysical journal* (2007).
131. Metzger, T. G. *Das Rheologiehandbuch* 4th ed., 138–216 (Vincentz Network, Hannover, 2011).

138. Kirschenmann, L. *Aufbau zweier piezoelektrischer Sonden (PRV/PAV zur Messung der viskoelastischen Eigenschaften weicher Substanzen im Frequenzbereich* PhD thesis (Universitaet Ulm, 2003).
139. Crassous, J. & Régisser, R. Characterization of the viscoelastic behavior of complex fluids using the piezoelastic axial vibrator. *Journal of Rheology* **49**(4), 851–864 (2005).
141. Vadillo, D. & Tuladhar, T. The rheological characterization of linear viscoelasticity for ink jet fluids using piezo axial vibrator and torsion resonator rheometers. *Journal of Rheology* **54**, 781–795 (2010).
142. Willenbacher, N. & Oelschlaeger, C. Dynamics and structure of complex fluids from high frequency mechanical and optical rheometry. *Curr. Opin. Colloid Interface Sci.* **12**, 43–49 (2007).
146. Amin, S., Rega, C. A. & Jankevics, H. Detection of Viscoelasticity in Aggregating Dilute Protein Solutions through Dynamic Light Scattering-Based Optical Microrheology. *Rheol Acta* **51**, 329–342 (2012).
147. Waigh, T. A. Microrheology of complex fluids. en. *Rep. Prog. Phys.* **68**, 685–742 (2005).
148. He, F. *et al.* High-throughput dynamic light scattering method for measuring viscosity of concentrated protein solutions. *Anal. Biochem.* **399**, 141–3 (2010).
164. Saluja, A. & Kalonia, D. S. Nature and consequences of protein-protein interactions in high protein concentration solutions. *International journal of pharmaceutics* **358**, 1–15 (2008).
166. Winzor, D. J. & Wills, P. R. Molecular crowding effects of linear polymers in protein solutions. *Biophysical chemistry* **119**, 186–95 (2006).
191. Ellis, R. J. Macromolecular crowding : obvious but under appreciated. *TRENDS in Biochemical Sciences* **26**, 597–604 (2001).
202. Fritz, G., Pechhold, W., Willenbacher, N. & Wagner, N. J. Characterizing complex fluids with high frequency rheology using torsional resonators at multiple frequencies. *Journal of Rheology* **47**, 303 (02/2003).
203. Pawelzyk, P., Herrmann, H. & Willenbacher, N. Mechanics of intermediate filament networks assembled from keratins K8 and K18. *Soft Matter* **9**, 8871 (2013).
207. Haezebrouck, P. *et al.* An equilibrium partially folded state of human lysozyme at low pH. *Journal of molecular biology* **246**, 382–387 (1995).

208. Venkataramani, S., Truntzer, J. & Coleman, D. R. Thermal stability of high concentration lysozyme across varying pH: A Fourier Transform Infrared study. *Journal of Pharmacy & Bioallied Sciences* **5**, 148–53 (2013).
218. Schermeyer, M.-T. *et al.* Squeeze flow rheometry as a novel tool for the characterization of highly concentrated protein solutions. *Biotechnol. Bioeng.* **113**, 576–587 (2016).
243. Corbett, J. C. W., Connah, M. T. & Mattison, K. Advances in the measurement of protein mobility using laser Doppler electrophoresis - the diffusion barrier technique. *Electrophoresis* **32**, 1787–94 (2011).
246. Shire, S. J., Shahrokh, Z. & Liu, J. Challenges in the development of high protein concentration formulations. *J. Pharm. Sci.* **93**, 1390–402 (2004).
250. Kramer, R. M. *et al.* Toward a molecular understanding of protein solubility: increased negative surface charge correlates with increased solubility. *Biophys. J.* **102**, 1907–15 (2012).
296. Minton, A. P. Influence of macromolecular crowding upon the stability and state of association of proteins: predictions and observations. *Journal of pharmaceutical sciences* **94**, 1668–75 (08/2005).
299. Rosenberg, E., Hepbildikler, S., Kuhne, W. & Winter, G. Ultrafiltration concentration of monoclonal antibody solutions: Development of an optimized method minimizing aggregation. *J. Membr. Sci.* **342**, 50–59 (2009).
300. Burckbuchler, V. *et al.* Rheological and syringeability properties of highly concentrated human polyclonal immunoglobulin solutions. *Eur. J. Pharm. Biopharm.* **76**, 351–356 (2010).
301. Jezek, J., Rides, M. & Derham, B. Viscosity of concentrated therapeutic protein compositions. *Advanced drug delivery ...* (2011).
302. Fritz, G., Maranzano, B., Wagner, N. & Willenbacher, N. High frequency rheology of hard sphere colloidal dispersions measured with a torsional resonator. *J. Nonnewton. Fluid Mech.* **102**, 149–156 (2002).
303. Breedveld, V. & Pine, D. J. Microrheology as a tool for high-throughput screening. *J. Mater. Sci.* **38**, 4461–4470 (2003).
304. Lazzari, S. *et al.* Colloidal stability of polymeric nanoparticles in biological fluids. *J. Nanopart. Res.* **14** (2012).

305. Valentine, M. *et al.* Colloid Surface Chemistry Critically Affects Multiple Particle Tracking Measurements of Biomaterials. *Biophys. J.* **86**, 4004–4014 (2004).
306. Gilroy, E. L., Hicks, M. R., Smith, D. J. & Rodger, A. Viscosity of aqueous DNA solutions determined using dynamic light scattering. *Analyst (Cambridge, U. K.)* **136**, 4159 (2011).
307. Gisler, T. & Weitz, D. A. Tracer microrheology in complex fluids. *Curr. Opin. Colloid Interface Sci.* **3**, 586–592 (1998).
308. Cassidy, O. E. *et al.* Surface modification and electrostatic charge of polystyrene particles. *Int. J. Pharm. (Amsterdam, Neth.)* **182**, 199–211 (1999).
309. Ter Veen, R., Fromell, K. & Caldwell, K. D. Shifts in polystyrene particle surface charge upon adsorption of the Pluronic F108 surfactant. *J. Colloid Interface Sci.* **288**, 124–128 (2005).
310. Stradner, A., Cardinaux, F. & Schurtenberger, P. A Small-Angle Scattering Study on Equilibrium Clusters in Lysozyme Solutions. *J. Phys. Chem. B* **110**, 21222–21231 (2006).
311. Kim, A. J., Manoharan, V. N. & Crocker, J. C. Swelling-based method for preparing stable, functionalized polymer colloids. *J. Am. Chem. Soc.* **127**, 1592–3 (2005).
312. Nance, E. A. *et al.* NIH Public Access. **4** (2013).
313. Naidu, A. S. *Natural Food Antimicrobial Systems* (ed Naidu, A.) 382 (CRC Press, 2000).
314. Blake, R. C., Shute, E. A. & Howard, G. T. Solubilization of minerals by bacteria: Electrophoretic mobility of *Thiobacillus ferrooxidans* in the presence of iron, pyrite, and sulfur. *Appl. Environ. Microbiol.* **60**, 3349–3357 (1994).
315. Winzor, D. J. Determination of the net charge (valence) of a protein: a fundamental but elusive parameter. *Anal. Biochem.* **325**, 1–20 (2004).
316. Dasgupta, B. R. *et al.* Microrheology of polyethylene oxide using diffusing wave spectroscopy and single scattering. *Phys. Rev. E: Stat., Nonlinear, Soft Matter Phys.* **65**, 051505 (2002).
317. Kulicke, W. M. & Porter, R. S. Relation between steady shear flow and dynamic rheology. *Rheol. Acta* **19**, 601–605 (1980).
318. Olmsted, J. & Williams, G. *Chemistry: The Molecular Science* 1189 (Learning, Jones & Bartlett, 1997).

319. Deryło-Marczewska, A. *et al.* Characterization of Melamine-Formaldehyde Resins by XPS, SAXS, and Sorption Techniques. *Langmuir* **18**, 7538–7543 (2002).
320. Baptista, R. P. *et al.* Activity, conformation and dynamics of cutinase adsorbed on poly(methyl methacrylate) latex particles. *J. Biotechnol.* **102**, 241–249 (2003).
321. Kirby, B. J. & Hasselbrink, E. F. Zeta potential of microfluidic substrates: 2. Data for polymers. *Electrophoresis* **25**, 203–213 (2004).
322. Falahati, H. *et al.* The zeta potential of PMMA in contact with electrolytes of various conditions: Theoretical and experimental investigation. *Electrophoresis* **35**, 870–882 (2014).
323. Ohsawa, K., Murata, M. & Ohshima, H. Zeta potential and surface charge density of polystyrene-latex; comparison with synaptic vesicle and brush border membrane vesicle. *Colloid Polym. Sci.* **264**, 1005–1009 (2005).
324. Kumar, N., Parajuli, O., Gupta, A. & Hahn, J. I. Elucidation of protein adsorption behavior on polymeric surfaces: Toward high-density, high-payload protein templates. *Langmuir* **24**, 2688–2694 (2008).
325. Broide, M. L., Tominc, T. M. & Saxowsky, M. D. Using phase transitions to investigate the effect of salts on protein interactions. *Phys. Rev. E: Stat., Nonlinear, Soft Matter Phys.* **53**, 6325–6335 (1996).
326. Beretta, S., Chirico, G. & Baldini, G. Short-Range Interactions of Globular Proteins at High Ionic Strengths. *Macromolecules* **33**, 8663–8670 (2000).
327. Rosenberg, M. Bacterial adherence to polystyrene: a replica method of screening for bacterial hydrophobicity. *Appl. Envir. Microbiol.* **42**, 375–377 (1981).
328. Onwu, F. K. & Ogah, S. Adsorption of lysozyme unto silica and polystyrene surfaces in aqueous medium. *Afr. J. Biotechnol.* **10**, 3014–3021 (2011).
329. Miriani, M. *et al.* Unfolding of beta-lactoglobulin on the surface of polystyrene nanoparticles: Experimental and computational approaches. *Proteins: Struct., Funct., Bioinf.* **82**, 1272–1282 (2014).
330. Ochoa, N. Effect of hydrophilicity on fouling of an emulsified oil wastewater with PVDF/PMMA membranes. *J. Membr. Sci.* **226**, 203–211 (2003).
331. Feldman, K., Tervoort, T., Smith, P. & Spencer, N. D. Toward a Force Spectroscopy of Polymer Surfaces. *Langmuir* **14**, 372–378 (1998).
332. Duong-Ly, K. C. & Gabelli, S. B. Salting out of proteins using ammonium sulfate precipitation. *Methods Enzymol.* **541**, 85–94 (2014).

10.7 References

333. Shih, Y. C., Prausnitz, J. M. & Blanch, H. W. Some characteristics of protein precipitation by salts. *Biotechnol. Bioeng.* **40**, 1155–1164 (1992).

Conclusion and Outlook

This doctoral thesis was centered on developing novel methodologies to enable a better description and prediction of the protein solution stability in the highly concentrated regime. For this purpose, rheological methods have been successfully applied in this work. In addition, a rheological parameter, ω_{CO} has been established, which has the potential to accurately predict the long-term stability of highly concentrated protein solutions.

This work required the handling of highly viscous solutions and the processing of a high number of samples with complex flow properties. In order to ensure accurate experiments, a device was developed which allows the automated determination of the protein concentration in the highly concentrated regime in a 96-well microscale format. The accuracy, repeatability and linearity of the introduced device as well as the applicability could be proven in this work.

In addition, the preparation of phase diagrams, for the study of colloidal and conformational protein stability, was successfully adapted to highly concentrated protein solutions. The automated methodology allows to screen a variety of solution conditions. The phase diagrams produced in this way served as the basis for the correlation to the rheological measurements.

After realization of the preparatory projects, rheological screenings of highly concentrated protein solutions were conducted. First, the viscoelastic properties of the model protein lysozyme were systematically investigated with a mechanical rheometer. As a rheological standard analysis, frequency sweep measurements were performed in the high-frequency range in order to determine the rheological parameters G' and G'' in the linear viscoelastic range. The large-scale screening demonstrated that viscoelasticity is sensitive to factors that influence protein stability, such as pH, ionic strength or protein concentration. For the correlation of the viscoelastic behavior with the long-term stability of the investigated protein solutions, the crossover point of G' and G'' was defined as a key parameter. The

frequency value of this intersection, ω_{CO} could be successfully correlated with the long-term phase behavior of the model protein. Furthermore a solubility limit for lysozyme based on the ω_{CO} values could be defined. With that knowledge one can make specific statements about the agglomeration tendency of the model protein, immediately after sample preparation.

As a next step, the established rheological methodology was successfully applied to more complex biomolecules. The rheological approach enabled the description of the solubility enhancing effect of a fusion protein in comparison to the native form. The study demonstrated that the rheological approach is predictive regarding the colloidal and conformational stability of GST and Cherry-GST solutions. The combination of the rheological measurements with MD simulations allowed the exact prediction as well as the description of the causes for the solubility enhancing effect of the Cherry-TagTM fusion.

Finally, an analytical toolbox was established in which the rheological methodology was combined with established analytical methods for the description of protein-protein interactions. This toolbox has been successfully applied to precisely describe and predict the long-term stability of antibody solutions under process and formulation-relevant conditions. The study demonstrated the strengths and weaknesses of the orthogonal techniques applied and that a correct description of the complex monoclonal antibody phase behavior could only be achieved by a combination of these techniques. The toolbox is considered as a very important step towards an easier main candidate selection and strategic process buffer and formulation optimization.

In addition to the rheological characterization of highly concentrated protein solutions a key aspect of this thesis was to optimize alternative rheological measurement methods. Microrheology was identified as a potential technique for the rheological characterization of protein solutions. A high measurement quality can only be achieved if the tracer particles, required for this measuring method, are inert. To ensure this, the surface properties of various tracers were investigated and their suitability for microrheological measurements of protein solutions evaluated. Our work reveals that tracer surface hydrophobicity is the crucial surface property that needs to be considered for the selection of a suitable tracer particle to achieve high measurement accuracy. In addition, with the help of the systematic screening, specific recommendations for the selection of the tracers can be given. In order to promote the establishment of this promising methodology, future studies should focus on the optimization of further measurement-relevant parameters, such as tracer size, tracer protein ratio and measurement time.

In conclusion, the doctoral thesis has shown that the viscoelastic response of a protein solution contains important information on the strength of protein-protein interactions

and protein network formation. In addition, it could be demonstrated that the rheological characterization has the potential to precisely predict the long-term stability of highly concentrated protein solutions. For this reason, we are working on the establishment of the introduced rheological technique as a standard analysis in biopharmaceutical laboratories. Furthermore, the aim of current research is to identify the link between the measurable rheological properties and the forces acting in highly concentrated protein solutions. With the resulting database the investigations of rheological properties of one molecule class could be transferred to further molecule classes. It would thus be possible to determine the solution stability of highly concentrated protein solutions with only one rheological measurement.

Comprehensive Reference List

1. Ereky, K. *Biotechnologie der Fleisch-, Fett-, und Milcherzeugung im landwirtschaftlichen Grossbetriebe: für naturwissenschaftlich gebildete Landwirte verfasst* (ed Ereky, K.) 84 (P. Parey, 1919).
2. Verma, A. S., Agrahari, S., Rastogi, S. & Singh, A. Biotechnology in the realm of history. *Journal of pharmacy and bioallied sciences* (2011).
3. Rosano, G. L. & Ceccarelli, E. Recombinant protein expression in Escherichia coli: advances and challenges. *Frontiers in Microbiology* **5**, 172 (2014).
4. De Marco, A. Recombinant antibody production evolves into multiple options aimed at yielding reagents suitable for application-specific needs. *Microbial Cell Factories* **14**, 125 (2015).
5. Dahm, R. Friedrich Miescher and the discovery of DNA. *Developmental Biology* **278**, 274–288 (2005).
6. Berg, P. *et al.* Summary statement of the Asilomar conference on recombinant DNA molecules. *Proceedings of the National Academy of Sciences of the United States of America* **72**, 1981–1984 (1975).
7. Demain, A. L. & Vaishnav, P. Production of recombinant proteins by microbes and higher organisms. *Biotechnology Advances* **27** (2009).
8. Schein, C. H. Production of Soluble Recombinant Proteins in Bacteria. *Nature Biotechnology* **7**, 1141–1149 (1989).
9. Ullrich, A. *et al.* Genetic variation in the human insulin gene. *Science* **209**, 612–615 (1980).
10. Dimov, D. & Martin de Holan, P. Firm Experience and Market Entry by Venture Capital Firms (1962–2004). *Journal of Management Studies* **47**, 130–161 (2010).

11. Zucker, L., Darby, M. & Brewer, M. *Intellectual Capital and the Birth of U.S. Biotechnology Enterprises* tech. rep. (National Bureau of Economic Research, Cambridge, MA, 1994).
12. Ecker, D. M., Jones, S. D. & Levine, H. L. The therapeutic monoclonal antibody market. *mAbs* **7**, 9–14 (2015).
13. Rader, R. A. FDA biopharmaceutical product approvals and trends in 2012. *Bio-Process International* **11**, 18–27 (2013).
14. Foo, F. *et al.* Biopharmaceutical process development: Part I, Information from the first product generation. *Pharmaceutical Technology Europe* **13**, 876–882 (2001).
15. Chari, R., Jerath, K., Badkar, A. V. & Kalonia, D. S. Long- and short-range electrostatic interactions affect the rheology of highly concentrated antibody solutions. *Pharmaceutical research* **26**, 2607–18 (2009).
16. Pindrus, M. *et al.* Solubility Challenges in High Concentration Monoclonal Antibody Formulations: Relationship with Amino Acid Sequence and Intermolecular Interactions. *Molecular Pharmaceutics* **12**, 3896–3907 (2015).
17. Ahrer, K., Buchacher, A., Iberer, G. & Jungbauer, A. Effects of ultra-/diafiltration conditions on present aggregates in human immunoglobulin G preparations. *Journal of Membrane Science* **274** (2006).
18. Manning, M. C. *et al.* Stability of Protein Pharmaceuticals: An Update. *Pharmaceutical Research* **27**, 544–575 (2009).
19. Sukumar, M., Doyle, B. L., Combs, J. L. & Pekar, A. H. Opalescent appearance of an IgG1 antibody at high concentrations and its relationship to noncovalent association. *Pharmaceutical research* **21**, 1087–93 (2004).
20. Saluja, A. *et al.* Application of high-frequency rheology measurements for analyzing protein-protein interactions in high protein concentration solutions using a model monoclonal antibody (IgG2). *Journal of Pharmaceutical Sciences* **95** (2006).
21. Kumar, V., Dixit, N., Zhou, L. L. & Fraunhofer, W. Impact of short range hydrophobic interactions and long range electrostatic forces on the aggregation kinetics of a monoclonal antibody and a dual-variable domain immunoglobulin at low and high concentrations. *International Journal of Pharmaceutics*. **421**, 82–93 (2011).

-
22. Harn, N., Allan, C., Oliver, C. & Middaugh, C. Highly concentrated monoclonal antibody solutions: direct analysis of physical structure and thermal stability. *Journal of Pharmaceutical Sciences* **96**, 532–540 (2007).
 23. Koch, M. *Pat applied in biopharmaceutical process development and manufacturing: an enabling tool for quality-by-design* (ed Koch, M.) (CRC Press, 2011).
 24. Chow, S.-C. Pharmaceutical Validation and Process Controls in Drug Development. *Therapeutic Innovation & Regulatory Science* **31**, 1195–1201 (1997).
 25. Tyers, M. & Mann, M. From genomics to proteomics. *Nature* **422**, 193–197 (2003).
 26. Moroder, L. in *Methods of Organic Chemistry* (eds Büchel, K., Falbe, J., Hagemann, H. & Hanack, M.) 4th ed., 17–18 (Georg Thieme Verlag, New York, 2004).
 27. Chi, E. & Krishnan, S. Physical stability of proteins in aqueous solution: mechanism and driving forces in nonnative protein aggregation. *Pharmaceutical Research* **20**, 1325–1336 (2003).
 28. Pace, C. Conformational stability of globular proteins. *Trends in Biochemical Sciences* **15**, 14–17 (1990).
 29. Bekard, I. B., Asimakis, P., Bertolini, J. & Dunstan, D. E. The effects of shear flow on protein structure and function. *Biopolymers* **95** (2011).
 30. Gething, M.-J. & Sambrook, J. Protein folding in the cell. *Nature* **355**, 33–45 (1992).
 31. Cheung, J. Protein folding mediated by solvation: water expulsion and formation of the hydrophobic core occur after the structural collapse. *PNAS* **99**, 685–690 (2002).
 32. Khmelnitsky, Y. L., Belova, A. B., Levashov, A. V. & Mozhaev, V. V. Relationship between surface hydrophilicity of a protein and its stability against denaturation by organic solvents. *FEBS Letters* **284**, 267–269 (1991).
 33. Damodaran, S. in *Fennema's Food Chemistry* (eds Damodaran, S., Parkin, K. & Fennema, O. R.) 4th ed., 219–323 (CRC Press, New York, 2007).
 34. Palmer, K. J., Ballantyne, M. & Galvin, J. A. The Molecular Weight of Lysozyme Determined by the X-Ray Diffraction Method. *Journal of the American Chemical Society* **70**, 906–908 (1948).
 35. Duan, Y. & Kollman, P. A. Pathways to a Protein Folding Intermediate Observed in a 1-Microsecond Simulation in Aqueous Solution. *Science* **282** (1998).

36. Murphy, K. P. & Gill, S. J. Solid model compounds and the thermodynamics of protein unfolding. *Journal of Molecular Biology* **222**, 699–709 (1991).
37. Pfeil, W. in *Thermodynamic Data for Biochemistry and Biotechnology* 349–376 (Springer Berlin Heidelberg, Berlin, Heidelberg, 1986).
38. Wright, C. F., Lindorff-Larsen, K., Randles, L. G. & Clarke, J. Parallel protein-unfolding pathways revealed and mapped. *Nature Structural Biology* **10**, 658–662 (2003).
39. Daggett, V. & Levitt, M. Protein Unfolding Pathways Explored Through Molecular Dynamics Simulations. *Journal of Molecular Biology* **232** (1993).
40. Kuwajima, K. The molten globule state as a clue for understanding the folding and cooperativity of globular-protein structure. *Proteins: Structure, Function, and Genetics* **6**, 87–103 (1989).
41. Mark, A. E. & van Gunsteren, W. F. Simulation of the thermal denaturation of hen egg white lysozyme: trapping the molten globule state. *Biochemistry* **31**, 7745–8 (1992).
42. Morozova, L. A. *et al.* Structural basis of the stability of a lysozyme molten globule. *Nature Structural Biology* **2**, 871–875 (1995).
43. Wang, W. & Roberts, C. J. *Aggregation of therapeutic proteins* 150–151 (Wiley, 2010).
44. Mahler, H.-C., Friess, W., Grauschopf, U. & Kiese, S. Protein aggregation: Pathways, induction factors and analysis. *Journal of Pharmaceutical Sciences* **98**, 2909–2934 (2009).
45. Chiti, F. & Dobson, C. M. Amyloid formation by globular proteins under native conditions. *Nature Chemical Biology* **5**, 15–22 (2009).
46. Maas, C. *et al.* A Role for Protein Misfolding in Immunogenicity of Biopharmaceuticals. *Journal of Biological Chemistry* **282**, 2229–2236 (2007).
47. Kahn, S. E., Andrikopoulos, S. & Verchere, C. B. Islet amyloid: a long-recognized but underappreciated pathological feature of type 2 diabetes. *Diabetes* **48**, 241–53 (1999).
48. Cromwell, M. E. M., Hilario, E. & Jacobson, F. Protein aggregation and bioprocessing. *The AAPS Journal* **8**, E572–E579 (2006).

-
49. Necula, M., Kayed, R., Milton, S. & Glabe, C. G. Small Molecule Inhibitors of Aggregation Indicate That Amyloid beta Oligomerization and Fibrillization Pathways Are Independent and Distinct. *Journal of Biological Chemistry* **282**, 10311–10324 (2007).
 50. Ecroyd, H. & Carver, J. A. The effect of small molecules in modulating the chaperone activity of α B-crystallin against ordered and disordered protein aggregation. *FEBS Journal* **275**, 935–947 (2008).
 51. Murphy, K. P., Bhakuni, V., Xie, D. & Freire, E. Molecular basis of co-operativity in protein folding: III. Structural identification of cooperative folding units and folding intermediates. *Journal of Molecular Biology* **227**, 293–306 (1992).
 52. Espargaró, A., Castillo, V., de Groot, N. S. & Ventura, S. The in Vivo and in Vitro Aggregation Properties of Globular Proteins Correlate With Their Conformational Stability: The SH3 Case. *Journal of Molecular Biology* **378**, 1116–1131 (2008).
 53. Curtis, R. A. & Lue, L. A molecular approach to bioseparations: Protein–protein and protein–salt interactions. *Chemical Engineering Science* **61**, 907–923 (2006).
 54. Dumetz, A. C., Snellinger-O’Brien, A. M., Kaler, E. W. & Lenhoff, A. M. Patterns of protein protein interactions in salt solutions and implications for protein crystallization. *Protein science : a publication of the Protein Society* **16**, 1867–77 (2007).
 55. Parsegian, A. V. *Van der Waals Forces: A Handbook for Biologists, Chemists, Engineers, and Physicists* (ed Parsegian, A. V.) (Cambridge University Press, Cambridge, 2006).
 56. Pace, C. N. *et al.* Contribution of hydrogen bonds to protein stability. *Protein science : a publication of the Protein Society* **23**, 652–61 (2014).
 57. Israelachvili, J. & Wennerström, H. Role of hydration and water structure in biological and colloidal interactions. *Nature* **379**, 219–225 (1996).
 58. Amrhein, S., Oelmeier, S. A., Dismar, F. & Hubbuch, J. Molecular dynamics simulations approach for the characterization of peptides with respect to hydrophobicity. *Journal of Physical Chemistry B* **118**, 1707–1714 (2014).
 59. Privalov, P. L. & Gill, S. J. Stability of Protein Structure and Hydrophobic Interaction. *Advances in Protein Chemistry* **39**, 191–234 (1988).
 60. Kauzmann, W. Some factors in the interpretation of protein denaturation. *Advances in Protein Chemistry* **14**, 63 (1959).

61. Kyte, J. & Doolittle, R. F. A simple method for displaying the hydrophatic character of a protein. *Journal of Molecular Biology* **157**, 105–132 (1982).
62. Abraham, D. J. & Leo, A. J. Extension of the fragment method to calculate amino acid zwitterion and side chain partition coefficients. *Proteins: Structure, Function, and Genetics* **2**, 130–152 (1987).
63. Gilson, M. K., Rashin, A., Fine, R. & Honig, B. On the calculation of electrostatic interactions in proteins. *Journal of Molecular Biology* **184**, 503–516 (1985).
64. Honig, B. & Nicholls, A. Classical electrostatics in biology and chemistry. *Science (New York, N.Y.)* **268**, 1144–9 (1995).
65. Verwey, E. J. W. Theory of the Stability of Lyophobic Colloids. *The Journal of Physical and Colloid Chemistry* **51**, 631–636 (1947).
66. Tavares, F. W., Bratko, D., Blanch, H. W. & Prausnitz, J. Ion-Specific Effects in the Colloid–Colloid or Protein–Protein Potential of Mean Force: Role of Salt–Macroion van der Waals Interactions. *The Journal of Physical Chemistry B* (2004).
67. Muramatsu, N. & Minton, A. P. Tracer diffusion of globular proteins in concentrated protein solutions. *Proceedings of the National Academy of Sciences of the United States of America* **85**, 2984–8 (1988).
68. Minton, A. P. Influence of excluded volume upon macromolecular structure and associations in a crowded media. *Current Opinion in Biotechnology* **8**, 65–69 (1997).
69. Minton, A. P. Implications of macromolecular crowding for protein assembly. *Current opinion in structural biology* **10**, 34–9 (2000).
70. Asherie, N. Protein crystallization and phase diagrams. *Methods* **34**, 266–272 (2004).
71. Frokjaer, S. & Otzen, D. E. Protein drug stability: a formulation challenge. *Nature Reviews Drug Discovery* **4**, 298–306 (2005).
72. Amin, S. *et al.* Protein aggregation, particle formation, characterization & rheology. *Current Opinion in Colloid & Interface Science* **19**, 438–449 (2014).
73. Patro, S. & Przybycien, T. Simulations of reversible protein aggregate and crystal structure. *Biophysical Journal* **70**, 2888–2902 (1996).
74. Sapir, L. & Harries, D. Macromolecular Stabilization by Excluded Cosolutes: Mean Field Theory of Crowded Solutions. *Journal of Chemical Theory and Computation* **11**, 3478–3490 (2015).

-
75. Buck, P. M., Chaudhri, A., Kumar, S. & Singh, S. K. Highly Viscous Antibody Solutions Are a Consequence of Network Formation Caused by Domain-Domain Electrostatic Complementarities: Insights from Coarse-Grained Simulations. *Molecular Pharmaceutics* **12**, 127–139 (2015).
 76. Khechinashvili, N., Janin, J. & Rodier, F. Thermodynamics of the temperature-induced unfolding of globular proteins. *Protein Science* **4**, 1315–1324 (1995).
 77. Brandts, J. F. & Hunt, L. Thermodynamics of protein denaturation. III. Denaturation of ribonuclease in water and in aqueous urea and aqueous ethanol mixtures. *Journal of the American Chemical Society* **89**, 4826–4838 (1967).
 78. Privalov, P. L. Cold Denaturation of Protein. *Critical Reviews in Biochemistry and Molecular Biology* **25**, 281–306 (1990).
 79. Perrin, D. D., Dempsey, B. & Serjeant, E. P. in *pK a Prediction for Organic Acids and Bases* 1–11 (Springer Netherlands, Dordrecht, 1981).
 80. Albertson, P., Sasakawa, S. & Walter, H. Cross Partition and Isoelectric Points of Proteins. *Nature* **228**, 1329–1330 (1970).
 81. Tanford, C. *Physical chemistry of macromolecules* (Wiley, New York, 1962).
 82. Damodaran, S. & Kinsella, J. E. The effects of neutral salts on the stability of macromolecules. A new approach using a protein-ligand binding system. *The Journal of biological chemistry* **256**, 3394–8 (1981).
 83. Arakawa, T. & Timasheff, S. N. Preferential interactions of proteins with solvent components in aqueous amino acid solutions. *Archives of Biochemistry and Biophysics* **224**, 169–177 (1983).
 84. Melander, W. & Horváth, C. Salt effect on hydrophobic interactions in precipitation and chromatography of proteins: an interpretation of the lyotropic series. *Arch. Biochem. Biophys.* **183**, 200–15 (1977).
 85. Arakawa, T. & Timasheff, S. Mechanism of protein salting in and salting out by divalent cation salts: balance between hydration and salt binding. *Biochemistry*, 5912–5923 (1984).
 86. Majumdar, R. *et al.* Effects of Salts from the Hofmeister Series on the Conformational Stability, Aggregation Propensity, and Local Flexibility of an IgG1 Monoclonal Antibody. *Biochemistry* **52**, 3376–3389 (2013).
 87. Baldwin, R. L. How Hofmeister ion interactions affect protein stability. *Biophysical journal* **71**, 2056–63 (1996).

88. Baumgartner, K. *et al.* Determination of protein phase diagrams by microbatch experiments: Exploring the influence of precipitants and pH. *International Journal of Pharmaceutics* **479**, 28–40 (2015).
89. Lekkerkerker, H. *et al.* Phase-behavior of colloid plus Polymer mixtures. *Europhysics Letters* **20**, 559–564 (1992).
90. Kulkarni, A. M., Chatterjee, A. P., Schweizer, K. S. & Zukoski, C. F. Effects of polyethylene glycol on protein interactions. *The Journal of Chemical Physics* (2000).
91. Tardieu, A., Finet, S. & Bonneté, F. Structure of the macromolecular solutions that generate crystals. *Journal of Crystal Growth* **232**, 1–9 (2001).
92. Liu, Y. & Bolen, D. W. The Peptide Backbone Plays a Dominant Role in Protein Stabilization by Naturally Occurring Osmolytes. *Biochemistry* **34**, 12884–12891 (1995).
93. Schellman, J. A. Protein stability in mixed solvents: a balance of contact interaction and excluded volume. *Biophysical journal* **85**, 108–25 (2003).
94. Bolen, D. & Baskakov, I. V. The osmophobic effect: natural selection of a thermodynamic force in protein folding. *Journal of Molecular Biology* **310**, 955–963 (2001).
95. Bruździak, P., Panuszko, A. & Stangret, J. Influence of Osmolytes on Protein and Water Structure: A Step To Understanding the Mechanism of Protein Stabilization. *The Journal of Physical Chemistry B* **117**, 11502–11508 (2013).
96. Yancey, P. H. *et al.* Living with water stress: evolution of osmolyte systems. *Science (New York, N.Y.)* **217**, 1214–22 (1982).
97. Timasheff, S. N. The Control of Protein Stability and Association by Weak Interactions with Water: How Do Solvents Affect These Processes? *Annual Review of Biophysics and Biomolecular Structure* **22**, 67–97 (1993).
98. Harries, D. & Rösgen, J. A practical guide on how osmolytes modulate macromolecular properties. *Methods in cell biology* **84** (2008).
99. Weiss, W. 4., Young, T. & Roberts, C. Principles, approaches, and challenges for predicting protein aggregation rates and shelf life. *Journal of Pharmaceutical Sciences* (2009).
100. Thiagarajan, G. *et al.* A comparison of biophysical characterization techniques in predicting monoclonal antibody stability. *mAbs* (2016).

-
101. Ghebremichael, K. A. *et al.* A simple purification and activity assay of the coagulant protein from *Moringa oleifera* seed. *Water Research* **39**, 2338–2344 (2005).
 102. Wirth, S. J. & Wolf, G. A. Dye-labelled substrates for the assay and detection of chitinase and lysozyme activity. *Journal of Microbiological Methods* **12**, 197–205 (1990).
 103. Kong, J. & Yu, S. Fourier Transform Infrared Spectroscopic Analysis of Protein Secondary Structures. *Acta Biochimica et Biophysica Sinica* **39**, 549–559 (2007).
 104. Singh, S. & Singh, J. Effect of polyols on the conformational stability and biological activity of a model protein lysozyme. *AAPS PharmSciTech* **4**, 101–109 (2003).
 105. Wilson, W. Light scattering as a diagnostic for protein crystal growth—A practical approach. *Journal of Structural Biology* **142**, 56–65 (2003).
 106. Jachimska, B., Wasilewska, M. & Adamczyk, Z. Characterization of Globular Protein Solutions by Dynamic Light Scattering, Electrophoretic Mobility, and Viscosity Measurements. *Langmuir* **24**, 6866–6872 (2008).
 107. Goldberg, D. S., Bishop, S. M., Shah, A. U. & Sathish, H. A. Formulation Development of Therapeutic Monoclonal Antibodies Using High-Throughput Fluorescence and Static Light Scattering Techniques: Role of Conformational and Colloidal Stability. *Journal of Pharmaceutical Sciences* **100**, 1306–1315 (2011).
 108. He, F. *et al.* Screening of monoclonal antibody formulations based on high-throughput thermostability and viscosity measurements: Design of experiment and statistical analysis. *Journal of Pharmaceutical Sciences* **100**, 1330–1340 (2011).
 109. Webster, S. Predicting Long-Term Storage Stability of Therapeutic Proteins. *PharmTech* **37** (2013).
 110. *Thermal ramp experiments measure protein conformational stability and propensity to aggregate* tech. rep. (Pleasanton, 2015), 1–5.
 111. Clogston, J. D. & Patri, A. K. Zeta potential measurement. *Methods in molecular biology (Clifton, N.J.)* **697**, 63–70 (2011).
 112. Galm, L., Amrhein, S. & Hubbuch, J. Predictive approach for protein aggregation: Correlation of protein surface characteristics and conformational flexibility to protein aggregation propensity. *Biotechnology and bioengineering* (2016).
 113. Alonso, H. & Bliznyuk A. A.A. Bliznyuk, A. Combining docking and molecular dynamic simulations in drug design. *Medicinal Research Reviews* **26**, 531–568 (2006).

114. Lindorff-Larsen, K. *et al.* Simultaneous determination of protein structure and dynamics. *Nature* **433**, 128–132 (2005).
115. Bauer, K. C. *et al.* Concentration-dependent changes in apparent diffusion coefficients as indicator for colloidal stability of protein solutions. *International Journal of Pharmaceutics* **511**, 276–287 (2016).
116. Terdale, S. S., Dagade, D. H. & Patil, K. J. Thermodynamic Studies of Molecular Interactions in Aqueous Alpha-Cyclodextrin Solutions: Application of McMillan Mayer and Kirkwood Buff Theories. *The Journal of Physical Chemistry B* **110**, 18583–18593 (2006).
117. Gaigalas, A. *et al.* A non-perturbative relation between the mutual diffusion coefficient, suspension viscosity, and osmotic compressibility: Application to concentrated protein solutions. *Chemical Engineering Science* **50**, 1107–1114 (1995).
118. Quigley, A. & Williams, D. The second virial coefficient as a predictor of protein aggregation propensity: A self-interaction chromatography study. *European Journal of Pharmaceutics and Biopharmaceutics* **96**, 282–290 (2015).
119. Tessier, P. M. *et al.* Predictive crystallization of ribonuclease A via rapid screening of osmotic second virial coefficients. *Proteins: Structure, Function, and Bioinformatics* **50**, 303–311 (2002).
120. George, A. & Wilson, W. W. Predicting protein crystallization from a dilute solution property. *Acta crystallographica. Section D, Biological crystallography* **50**, 361–5 (1994).
121. George, A. *et al.* Second virial coefficient as predictor in protein crystal growth. *Methods in Enzymology* **276**, 100–110 (1997).
122. Le Brun, V. *et al.* A critical evaluation of self-interaction chromatography as a predictive tool for the assessment of protein–protein interactions in protein formulation development: A case study of a therapeutic monoclonal antibody. *European Journal of Pharmaceutics and Biopharmaceutics* **75**, 16–25 (2010).
123. Chou, D. K. *et al.* Physical Stability of Albinterferon-alpha2b in Aqueous Solution: Effects of Conformational Stability and Colloidal Stability on Aggregation. *Journal of Pharmaceutical Sciences* **101**, 2702–2719 (2012).
124. Bajaj, H. *et al.* Protein Structural Conformation and Not Second Virial Coefficient Relates to Long-Term Irreversible Aggregation of a Monoclonal Antibody and Ovalbumin in Solution. *Pharmaceutical Research* **23**, 1382–1394 (2006).

-
125. Saito, S. *et al.* Behavior of Monoclonal Antibodies: Relation Between the Second Virial Coefficient (B 2) at Low Concentrations and Aggregation Propensity and Viscosity at High Concentrations. *Pharmaceutical Research* **29**, 397–410 (2012).
 126. Scherer, T. M., Liu, J., Shire, S. J. & Minton, A. P. Intermolecular interactions of IgG1 monoclonal antibodies at high concentrations characterized by light scattering. *Journal of Physical Chemistry B* **114** (2010).
 127. Saluja, A. *et al.* Ultrasonic storage modulus as a novel parameter for analyzing protein-protein interactions in high protein concentration solutions: correlation with static and dynamic light scattering measurements. *Biophysical journal* (2007).
 128. Morrison, F. A. *Understanding rheology* (ed Morrison, F. A.) 545 (Oxford University Press, 2001).
 129. Furukawa, J. in (eds Schäfer, F. P., Toennies, J. P. & Zingth, W.) 72nd ed., 278 pp. (Kodansha, Tokyo, 2003).
 130. Sworn, G. *Rheology of Biological Soft Matter* (2017).
 131. Metzger, T. G. *Das Rheologiehandbuch* 4th ed., 138–216 (Vincentz Network, Hannover, 2011).
 132. Sharma, V., Jaishankar, A., Wang, Y.-C. & McKinley, G. H. Rheology of globular proteins: apparent yield stress, high shear rate viscosity and interfacial viscoelasticity of bovine serum albumin solutions. *Soft Matter* **7**, 5150 (2011).
 133. Winter, H. H. & Chambon, F. Analysis of Linear Viscoelasticity of a Crosslinking Polymer at the Gel Point. *Journal of Rheology* **30**, 367–382 (1986).
 134. Steffe, J. F. *Rheological Methods in Food Process Engineering* 2nd ed. (ed Steffe, J. F.) (Freeman Press, East Lansing, 1992).
 135. Ferry, J. D. *Viscoelastic Properties of Polymers* 3rd ed. (ed Ferry, J. D.) (John Wiley and Sons, New York, 1980).
 136. Saluja, A. & Kalonia, D. S. Application of ultrasonic shear rheometer to characterize rheological properties of high protein concentration solutions at microliter volume. *Journal of pharmaceutical sciences* **94**, 1161–8 (2005).
 137. Meeten, G. H. Yield stress of structured fluids measured by squeeze flow. *Rheologica Acta* **39**, 399–408 (2000).
 138. Kirschenmann, L. *Aufbau zweier piezoelektrischer Sonden (PRV/PAV zur Messung der viskoelastischen Eigenschaften weicher Substanzen im Frequenzbereich* PhD thesis (Universitaet Ulm, 2003).

139. Crassous, J. & Régisser, R. Characterization of the viscoelastic behavior of complex fluids using the piezoelastic axial vibrator. *Journal of Rheology* **49**(4), 851–864 (2005).
140. Schuppe, Z. *et al.* *The Piezo Axial Vibrator - new perspectives for on-line viscosity measurements on polymers* tech. rep. (Karlsruhe, 2006).
141. Vadillo, D. & Tuladhar, T. The rheological characterization of linear viscoelasticity for ink jet fluids using piezo axial vibrator and torsion resonator rheometers. *Journal of Rheology* **54**, 781–795 (2010).
142. Willenbacher, N. & Oelschlaeger, C. Dynamics and structure of complex fluids from high frequency mechanical and optical rheometry. *Curr. Opin. Colloid Interface Sci.* **12**, 43–49 (2007).
143. Scheffold, F. *et al.* in *Trends in Colloid and Interface Science XVI* 141–146 (Springer Berlin Heidelberg, Berlin, Heidelberg, 2004).
144. Mansel, B. W. *et al.* A Practical Review of Microrheological Techniques. *Rheology - New Concepts, Applications and Methods* **2**, 1–21 (2013).
145. Dasgupta, B. R. *Microrheology and Dynamic Light Scattering Studies of Polymer Solutions* PhD thesis (2004).
146. Amin, S., Rega, C. A. & Jankevics, H. Detection of Viscoelasticity in Aggregating Dilute Protein Solutions through Dynamic Light Scattering-Based Optical Microrheology. *Rheol Acta* **51**, 329–342 (2012).
147. Waigh, T. A. Microrheology of complex fluids. en. *Rep. Prog. Phys.* **68**, 685–742 (2005).
148. He, F. *et al.* High-throughput dynamic light scattering method for measuring viscosity of concentrated protein solutions. *Anal. Biochem.* **399**, 141–3 (2010).
149. Tabilo-Munizaga, G. & Barbosa-Cánovas, G. V. Rheology for the food industry. *Journal of Food Engineering* **67**, 147–156 (2005).
150. Rao, M. A. in *Food Rheology and Structure* 1–26 (2014).
151. Awad, T. *et al.* Applications of ultrasound in analysis, processing and quality control of food: A review. *Food Research International* **48**, 410–427 (2012).
152. Tadros, T. Application of rheology for assessment and prediction of the long-term physical stability of emulsions. *Advances in Colloid and Interface Science* **108**, 227–258 (2004).

-
153. Guaratini, T., Gianeti, M. D. & Campos, P. M. Stability of cosmetic formulations containing esters of vitamins E and A: chemical and physical aspects. *International journal of pharmaceutics* **327**, 12–16 (2006).
 154. Brust, M. *et al.* Rheology of Human Blood Plasma: Viscoelastic Versus Newtonian Behavior. *Physical Review Letters* **110** (2013).
 155. Inoue, H. & Matsumoto, T. Viscoelastic characterization of solid-like structure in aqueous colloids of globular proteins. *Colloids and Surfaces A: Physicochemical and Engineering Aspects* **109**, 89–96 (1996).
 156. Matsumoto, T. & Inoue, H. Colloidal structure and properties of bovine serum globulin aqueous systems using SAXS and rheological measurements. *Chemical Physics* **207**, 167–172 (1996).
 157. Ikeda, S. & Nishinari, K. Solid-like mechanical behaviors of ovalbumin aqueous solutions. *International Journal of Biological Macromolecules* **28**, 315–320 (2001).
 158. Yadav, S. *et al.* Establishing a Link Between Amino Acid Sequences and Self-Associating and Viscoelastic Behavior of Two Closely Related Monoclonal Antibodies. *Pharmaceutical Research* **28**, 1750–1764 (2011).
 159. Neergaard, M. & Kalonia, D. Viscosity of high concentration protein formulations of monoclonal antibodies of the IgG1 and IgG4 subclass—Prediction of viscosity through protein–protein interaction. *European Journal of Pharmaceutical Sciences* **49**, 400–410 (2013).
 160. Karplus, M. & McCammon, J. A. Molecular dynamics simulations of biomolecules. *Nature Structural Biology* **9**, 646–652 (2002).
 161. Hansen, C. L., Sommer, M. O. A. & Quake, S. R. Systematic investigation of protein phase behavior with a microfluidic formulator. *Proceedings of the National Academy of Sciences of the United States of America* **101**, 14431–14436 (2004).
 162. Rakel, N., Baum, M. & Hubbuch, J. Moving through three-dimensional phase diagrams of monoclonal antibodies. *Biotechnology Progress* **30**, 1103–1113 (2014).
 163. Neal, B., Asthagiri, D. & Lenhoff, A. Molecular Origins of Osmotic Second Virial Coefficients of Proteins. *Biophysical Journal* **75**, 2469–2477 (1998).
 164. Saluja, A. & Kalonia, D. S. Nature and consequences of protein–protein interactions in high protein concentration solutions. *International journal of pharmaceutics* **358**, 1–15 (2008).

165. Mason, T. G. & Weitz, D. A. Optical Measurements of Frequency-Dependent Linear Viscoelastic Moduli of Complex Fluids. *Physical Review Letters* **74**, 1250–1253 (1995).
166. Winzor, D. J. & Wills, P. R. Molecular crowding effects of linear polymers in protein solutions. *Biophysical chemistry* **119**, 186–95 (2006).
167. Clark, A. *Functional Properties of Food Macromolecules* (eds Hill, S., Ledward, D. A. & Mitchell, J.) 77–138 (Springer Science & Business Media, 1998).
168. Walsh, G. Biopharmaceutical benchmarks 2014. *Nature Biotechnology* **32**, 992–1000 (2014).
169. Lowe, C. R., Lowe, A. R. & Gupta, G. New developments in affinity chromatography with potential application in the production of biopharmaceuticals. *Journal of Biochemical and Biophysical Methods* **49**, 561–574 (2001).
170. Nfor, B. K. *et al.* Rational and systematic protein purification process development: the next generation. *Trends in Biotechnology* **27**, 673–679 (2009).
171. Bhambure, R., Kumar, K. & Rathore, A. S. High-throughput process development for biopharmaceutical drug substances. *Trends in Biotechnology* **29**, 127–135 (2011).
172. Hertzberg, R. P. & Pope, A. J. High-throughput screening: new technology for the 21st century. *Current Opinion in Chemical Biology* **4**, 445–451 (2000).
173. Nfor, B. K. *et al.* Design strategies for integrated protein purification processes: challenges, progress and outlook. *Journal of Chemical Technology & Biotechnology* **83**, 124–132 (2008).
174. Bensch, M., Schulze Wierling, P., von Lieres, E. & Hubbuch, J. High Throughput Screening of Chromatographic Phases for Rapid Process Development. *Chemical Engineering & Technology* **28**, 1274–1284 (2005).
175. Wiendahl, M. *et al.* A novel method to evaluate protein solubility using a high throughput screening approach. *Chemical Engineering Science* **64**, 3778–3788 (2009).
176. Robertson, C. US6628382 B2 (2003).
177. Wiendahl, M. *et al.* High Throughput Screening for the Design and Optimization of Chromatographic Processes – Miniaturization, Automation and Parallelization of Breakthrough and Elution Studies. *Chemical Engineering & Technology* **31**, 893–903 (2008).

-
178. Waldbaur, A., Kittelmann, J., Radtke, C. P. & Hubbuch, J. Microfluidics on liquid handling stations (μ F-on-LHS): an industry compatible chip interface between microfluidics and automated liquid handling stations. *Lab on a Chip* **13**, 2337–2343 (2013).
 179. McGown, E. L. & Hafeman, D. G. *Multichannel Pipettor Performance Verified by Measuring Pathlength of Reagent Dispensed into a Microplate* 1998.
 180. Lampinen, J. *et al.* Microplate Based Pathlength Correction Method for Photometric DNA Quantification Assay (1993).
 181. Hansen, S. K., Skibsted, E., Staby, A. & Hubbuch, J. A label-free methodology for selective protein quantification by means of absorption measurements. *Biotechnology and bioengineering* **108**, 2661–2669 (11/2011).
 182. Hansen, S. K., Jamali, B. & Hubbuch, J. Selective high throughput protein quantification based on UV absorption spectra. *Biotechnology and Bioengineering* **110**, 448–460 (02/2013).
 183. Pelegrine, D. & Gasparetto, C. Whey proteins solubility as function of temperature and pH. *LWT - Food Science and Technology* **38**, 77–80 (02/2005).
 184. Liu, J., Nguyen, M. D. H., Andya, J. D. & Shire, S. J. Reversible self-association increases the viscosity of a concentrated monoclonal antibody in aqueous solution. *Journal of Pharmaceutical Sciences* **94**, 1928–40 (2005).
 185. Cleland, J. L., Powell, M. F. & Shire, S. J. The development of stable protein formulations: a close look at protein aggregation, deamidation, and oxidation. en. *Critical reviews in therapeutic drug carrier systems* **10**, 307–77 (1993).
 186. Teeter, M. M. Water protein interactions : Theory and Experiment. *Annual Review of Biophysics and Biophysical Chemistry* **20**, 577–600 (1991).
 187. Naveed, H. & Han, J. J. Structure-based protein-protein interaction networks and drug design. *Quantitative Biology* **1**, 183–191 (2013).
 188. Rosenbaum, D. F. & Zukoski, C. F. Protein interactions and crystallization. *Journal of Crystal Growth* **169**, 752–758 (1996).
 189. Ruppert, S., Sandler, S. I. & Lenhoff, a. M. Correlation between the osmotic second virial coefficient and the solubility of proteins. *Biotechnology progress* **17**, 182–7 (2001).

190. Rakel, N., Galm, L., Bauer, K. & Hubbuch, J. From osmotic second virial coefficient (B₂₂) to phase behavior of a monoclonal antibody. *Biotechnological Process* **31**, 438–451 (2015).
191. Ellis, R. J. Macromolecular crowding : obvious but under appreciated. *TRENDS in Biochemical Sciences* **26**, 597–604 (2001).
192. Davis, S. S. Rheological Properties of Semi Solute Food Stuff - Elasticity and its Role in Quality Control. *Journal of Texture Studies* **4**, 15–40 (1973).
193. Brummer, R. & Godersky, S. Rheological studies to objectify sensations occurring when cosmetic emulsions are applied to the skin. *Colloids and Surfaces A: Physicochemical and Engineering Aspects* **152**, 89–94 (1999).
194. Brummer, R. *Rheology Essentials of Cosmetic and Food Emulsions* 81–124 (2006).
195. Abegg, J.-L., Boiteux, J.-P. & Hourseau, C. US3958581 A (1976).
196. Winnik, F. M. Elements of Polymer Science, 1–50 (1999).
197. Goddard, D. E. & Gruber, J. V. *Principles of Polymer Science and Technology in Cosmetics and Personal Care* 230–434 (Marcel Dekker AG, 1999).
198. Liu, R. C. W., Morishima, Y. & Winnik, F. M. Rheological Properties of Mixtures of Oppositely Charged Polyelectrolytes. A Study of the Interactions between a Cationic Cellulose Ether and a Hydrophobically Modified Poly[sodium 2-(acrylamido)-2-methylpropanesulfonate]. *Polymer Journal* **34**, 340–346 (05/2002).
199. Kanai, S., Liu, J., Patapoff, T. W. & Shire, S. J. Reversible self-association of a concentrated monoclonal antibody solution mediated by Fab-Fab interaction that impacts solution viscosity. *Journal of pharmaceutical sciences* **97**, 4219–27 (10/2008).
200. Huopalahti, R., López-Fandiño, R., Anton, M. & Schade, R. in *Bioactive Egg Compounds* 298 (Springer Science & Business Media, 2007).
201. Abeyrathne, E., Lee, H. & Ahn, D. Sequential separation of lysozyme, ovomucin, ovotransferrin, and ovalbumin from egg white. *Poultry Science* **93**, 1001–1009 (2014).
202. Fritz, G., Pechhold, W., Willenbacher, N. & Wagner, N. J. Characterizing complex fluids with high frequency rheology using torsional resonators at multiple frequencies. *Journal of Rheology* **47**, 303 (02/2003).
203. Pawelzyk, P., Herrmann, H. & Willenbacher, N. Mechanics of intermediate filament networks assembled from keratins K8 and K18. *Soft Matter* **9**, 8871 (2013).

-
204. Macosko, C. W. *Rheology: Principles, Measurements, and Applications* (Wiley-VCH, 1994).
205. Larson, R. *The structure and rheology of complex fluids*. 105–258 (Oxford University Press, New York, 1999).
206. Mewis, J. & Wagner, N. in *Cambridge Series in Chemical Engineering* 36–62 (Cambridge University Press, Cambridge, 2012).
207. Haezebrouck, P. *et al.* An equilibrium partially folded state of human lysozyme at low pH. *Journal of molecular biology* **246**, 382–387 (1995).
208. Venkataramani, S., Truntzer, J. & Coleman, D. R. Thermal stability of high concentration lysozyme across varying pH: A Fourier Transform Infrared study. *Journal of Pharmacy & Bioallied Sciences* **5**, 148–53 (2013).
209. Muschol, M. & Rosenberger, F. Liquid-liquid phase separation in supersaturated lysozyme solutions and associated precipitate formation/crystallization. *The Journal of Chemical Physics* **107**, 1953 (08/1997).
210. Harding, S. in *Functional properties of food macromolecules* (eds Hill, S., Ledward, D. & Mitchel, J.) 2nd ed., 10–15 (Aspen, 1998).
211. Shadwick, R. Mechanical design in arteries. *J. Exp. Biol.* **202**, 3305–3313 (1999).
212. Hjortdal, J. O. Regional elastic performance of the human cornea. *Journal of biomechanics* **29**, 931–42 (1996).
213. Moretti, J. J., Sandler, S. I. & Lenhoff, A. M. Phase equilibria in the lysozyme-ammonium sulfate-water system. en. *Biotechnology and bioengineering* **70**, 498–506 (12/2000).
214. Curtis, R. a. *et al.* Protein-protein interactions in concentrated electrolyte solutions. *Biotechnology and bioengineering* **79**, 367–80 (2002).
215. Brummitt, R. K., Nesta, D. P. & Roberts, C. J. Predicting accelerated aggregation rates for monoclonal antibody formulations, and challenges for low-temperature predictions. *Journal of Pharmaceutical Sciences* **100**, 4234–4243 (2011).
216. Skoulakis, S. & Goodfellow, J. M. The pH-dependent stability of wild-type and mutant transthyretin oligomers. *Biophysical Journal* **84**, 2795–2804 (2003).
217. Ma, B. & Nussinov, R. Simulations as analytical tools to understand protein aggregation and predict amyloid conformation. *Current Opinion in Chemical Biology* **10**, 445–452 (2006).

218. Schermeyer, M.-T. *et al.* Squeeze flow rheometry as a novel tool for the characterization of highly concentrated protein solutions. *Biotechnol. Bioeng.* **113**, 576–587 (2016).
219. Krishnan, S. *et al.* Aggregation of granulocyte colony stimulating factor under physiological conditions: Characterization and thermodynamic inhibition. *Biochemistry* **41**, 6422–6431 (2002).
220. Grigsby, J. J., Blanch, H. W. & Prausnitz, J. M. Cloud-point temperatures for lysozyme in electrolyte solutions: Effect of salt type, salt concentration and pH. *Biophysical Chemistry* **91**, 231–243 (2001).
221. Rodríguez-Martínez, J. A. *et al.* Stabilization of α -chymotrypsin upon PEGylation correlates with reduced structural dynamics. *Biotechnology and Bioengineering* **101**, 1142–1149 (2008).
222. Nie, Y., Zhang, X., Wang, X. & Chen, J. Preparation and stability of N-terminal mono-PEGylated recombinant human endostatin. *Bioconjugate Chemistry* **17**, 995–999 (2006).
223. Basu, A. *et al.* Structure-Function Engineering of Interferon- β -1b for Improving Stability, Solubility, Potency, Immunogenicity, and Pharmacokinetic Properties by Site-Selective Mono-PEGylation. *Bioconjugate Chemistry* **17**, 618–630 (2006).
224. Kapust, B. R. & Waugh, S. D. Escherichia coli maltose-binding protein is uncommonly effective at promoting the solubility of polypeptides to which it is fused. *Protein Science* **8**, 1668–1674 (1999).
225. Esposito, D. & Chatterjee, D. K. Enhancement of soluble protein expression through the use of fusion tags. *Current Opinion in Biotechnology* **17**, 353–358 (2006).
226. Zhang, Y. B. *et al.* Protein aggregation during overexpression limited by peptide extensions with large net negative charge. *Protein Expression and Purification* **36**, 207–216 (2004).
227. Baumann, P., Baumgartner, K. & Hubbuch, J. Influence of binding pH and protein solubility on the dynamic binding capacity in hydrophobic interaction chromatography. *Journal of Chromatography A* **1396**, 77–85 (2015).
228. Mohan Padmanabha Das, K. *et al.* A Novel Thermostability Conferring Property of Cherry Tag and its Application in Purification of Fusion Proteins. *Journal of Microbial & Biochemical Technology* **01**, 059–063 (2009).

-
229. Azhar, M. & Somashekhar, R. Cloning , expression and purification of human and bovine Enterokinase light chain with Cherry tag and their activity comparison. *Indian Journal of Applied and Pure Biology* **29**, 125–132 (2014).
230. Consortium, U. UniProt: a hub for protein information. *Nucleic Acids Research* **43**, 204–212 (2015).
231. Wilkins, M. R. *et al.* Protein identification and analysis tools in the ExPASy server. *Methods in Molecular Biology* **112**, 531–52 (1999).
232. Baumann, P. *et al.* Integrated development of up- and downstream processes supported by the Cherry-Tag²,³ for real-time tracking of stability and solubility of proteins. *Journal of Biotechnology*. **200**, 27–37 (2015).
233. Pechhold, W., Kirschenmann, L. & Groß, T. *Offenlegungsschrift DE 101 62 838 A1* 2003.
234. Berman, H. M. The Protein Data Bank. *Nucleic Acids Research* **28**, 235–242 (2000).
235. Krieger, E., Koraimann, G. & Vriend, G. Increasing the precision of comparative models with YASARA NOVA—a self-parameterizing force field. *Proteins: Structure, Function, and Bioinformatics* **47**, 393–402 (2002).
236. Duan, Y. *et al.* A point-charge force field for molecular mechanics simulations of proteins based on condensed-phase quantum mechanical calculations. *Journal of Computational Chemistry* **24**, 1999–2012 (2003).
237. Anandkrishnan, R., Aguilar, B. & Onufriev, A. V. H++ 3.0: automating pK prediction and the preparation of biomolecular structures for atomistic molecular modeling and simulations. *Nucleic Acids Research* **40**, W537–W541 (2012).
238. Abe, K. & Sugita, Y. Properties of Cytochrome b5, and Methemoglobin Reduction in Human Erythrocytes. *European Journal of Biochemistry* **101**, 423–428 (1979).
239. Kuwada, M., Hasumi, H. & Furuse, Y. Purification of Cytochrome b5 from Pig Testis Microsomes by Isoelectric Focusing in an Immobiline pH Gradient. *Protein Expression and Purification* **12**, 420–424 (1998).
240. Brown, W. H. *Organic chemistry* (Brooks/Cole Cengage Learning, 2009).
241. Collins, K. D. Ions from the Hofmeister series and osmolytes: effects on proteins in solution and in the crystallization process. *Methods* **34**, 300–311 (2004).
242. Miklos, A., Sarkar, M., Wang, Y. & Pielak, G. Protein Crowding Tunes Protein Stability. *Journal of the American Chemical Society* **133**, 7116–7120 (2011).

243. Corbett, J. C. W., Connah, M. T. & Mattison, K. Advances in the measurement of protein mobility using laser Doppler electrophoresis - the diffusion barrier technique. *Electrophoresis* **32**, 1787–94 (2011).
244. Scott, A., Wolchok, J. & Old, L. Antibody therapy of cancer. *Nature Reviews Cancer* **12**, 14 (2012).
245. Rosman, Z., Shoenfeld, Y. & Zandmann-Goddard, G. Biologic therapy for autoimmune diseases: an update. *BMC Medicine* **11**, 88 (2013).
246. Shire, S. J., Shahrokh, Z. & Liu, J. Challenges in the development of high protein concentration formulations. *J. Pharm. Sci.* **93**, 1390–402 (2004).
247. Leckband, D. & Sivasankar, S. Forces controlling protein interactions: theory and experiment. *Colloids and Surfaces B: Biointerfaces* **14**, 83–97 (1999).
248. Monahan, F. J., German, J. B. & Kinsella, J. E. Effect of pH and temperature on protein unfolding and thiol/disulfide interchange reactions during heat-induced gelation of whey proteins. *Journal of Agricultural and Food Chemistry* **43**, 46–52 (1995).
249. Dill, K. A. Dominant forces in protein folding. *Biochemistry* **29**, 7133–7155 (1990).
250. Kramer, R. M. *et al.* Toward a molecular understanding of protein solubility: increased negative surface charge correlates with increased solubility. *Biophys. J.* **102**, 1907–15 (2012).
251. Lehermayr, C., Mahler, H. C., Mäder, K. & Fischer, S. Assessment of net charge and protein-protein interactions of different monoclonal antibodies. *Journal of Pharmaceutical Sciences* **100**, 2551–2562 (2011).
252. Prediction and characterization of the stability enhancing effect of the Cherry-Tag in highly concentrated protein solutions by complex rheological measurements and MD simulations, Author = Baumann, Pascal and Schermeyer, Marie-Therese and Burghardt, Hannah and Dürr, Cathrin and Hubbuch, J. *International Journal of Pharmaceutics*. submitted (2016).
253. Thakkar, S. V. *et al.* An Application of Ultraviolet Spectroscopy to Study Interactions in Proteins Solutions at High Concentrations. *Journal of Pharmaceutical Sciences* **101**, 3051–3061 (09/2012).
254. Ahamed, T. *et al.* Phase behavior of an intact monoclonal antibody. *Biophysical Journal* **93**, 610–619 (2007).

-
255. Kröner, F. & Hubbuch, J. Systematic generation of buffer systems for pH gradient ion exchange chromatography and their application. *Journal of Chromatography A* **1285**, 78–87 (2013).
256. Arakawa, T. & Timasheff, S. N. Theory of protein solubility. *Methods in enzymology* **114**, 49–77 (1985).
257. Mason, B. *et al.* Liquid-liquid phase separation of a monoclonal antibody and nonmonotonic influence of Hofmeister anions. *Biophysical journal* **99**, 3792–800 (2010).
258. Wu, S. L. & Karger, B. L. Hydrophobic interaction chromatography of proteins. *Methods in enzymology* **270**, 27–47 (1996).
259. Arakawa, T., Bhat, R. & Timasheff, S. N. Preferential interactions determine protein solubility in three-component solutions: the MgCl₂ system. *Biochemistry* **29**, 1914–23 (02/1990).
260. Tardieu, A., Bonneté, F., Finet, S. & Vivarès, D. Understanding salt or PEG induced attractive interactions to crystallize biological macromolecules. *Acta Crystallographica Section D Biological Crystallography* **58**, 1549–1553 (2002).
261. Pusey, P. N., Poon, W. C. K., Ilett, S. M. & Bartlett, P. Phase behaviour and structure of colloidal suspensions. *Journal of Physics: Condensed Matter* **6**, A29–A36 (1994).
262. Hill, T. L. *An introduction to statistical thermodynamics* 508 (Dover Publications, 1986).
263. Luangtana-Anan, M. *et al.* Polyethylene glycol on stability of chitosan microparticulate carrier for protein. *AAPS PharmSciTech* **11**, 1376–82 (2010).
264. Arakawa, T. & Timasheff, S. N. Abnormal solubility behavior of beta-lactoglobulin: salting-in by glycine and sodium chloride. *Biochemistry* **26**, 5147–5153 (1987).
265. Zhang, M. Z., Wen, J., Arakawa, T. & Prestrelski, S. J. A new strategy for enhancing the stability of lyophilized protein: the effect of the reconstitution medium on keratinocyte growth factor. *Pharmaceutical research* **12**, 1447–52 (1995).
266. Chen, B.-L. & Arakawa, T. Stabilization of Recombinant Human Keratinocyte Growth Factor by Osmolytes and Salts. *Journal of Pharmaceutical Sciences* **85**, 419–422 (1996).
267. Arakawa, T. *et al.* Biotechnology applications of amino acids in protein purification and formulations. *Amino acids* **33**, 587–605 (2007).

268. Jiskoot, W. & Crommelin, D. *Methods for Structural Analysis of Protein Pharmaceuticals* (ed Jiskoot, W.) (Springer Science & Business Media, 2005).
269. Laurance, J. S. & Middaugh, C. R. *Aggregation of therapeutic proteins* (eds Wang, W. & Roberts, C. J.) (Wiley, 2010).
270. Piazza, R. Protein interactions and association: an open challenge for colloid. *Current Opinion in Colloid & Interface Science* **8**, 515–522 (2004).
271. Halle, B. Protein hydration dynamics in solution: a critical survey. *Philosophical transactions of the Royal Society of London. Series B, Biological sciences* **359**, 1207–23 (2004).
272. Booth, F. The Electroviscous Effect for Suspensions of Solid Spherical Particles. *Proceedings of the Royal Society of London A: Mathematical, Physical and Engineering Sciences* **203** (1950).
273. Tanford, C. & Buzzell, J. G. The Viscosity of Aqueous Solutions of Bovine Serum Albumin between pH 4.3 and 10.5. *The Journal of Physical Chemistry* **60**, 225–231 (1956).
274. Buzzell, J. G. & Tanford, C. The Effect of Charge and Ionic Strength on the Viscosity of Ribonuclease. *The Journal of Physical Chemistry* **60**, 1204–1207 (1956).
275. Salinas, B. A. *et al.* Understanding and modulating opalescence and viscosity in a monoclonal antibody formulation. *Journal of pharmaceutical sciences* **99**, 82–93 (2010).
276. Connolly, B. D. *et al.* Weak Interactions Govern the Viscosity of Concentrated Antibody Solutions: High-Throughput Analysis Using the Diffusion Interaction Parameter. *Biophysical Journal* **103**, 69–78 (2012).
277. Wang, S. *et al.* Viscosity-Lowering Effect of Amino Acids and Salts on Highly Concentrated Solutions of Two IgG1 Monoclonal Antibodies. *Molecular Pharmaceutics* **12**, 4478–4487 (2015).
278. Vermeer, A. W. & Norde, W. The thermal stability of immunoglobulin: unfolding and aggregation of a multi-domain protein. *Biophysical journal* **78**, 394–404 (2000).
279. Nicoud, L. *et al.* Effect of polyol sugars on the stabilization of monoclonal antibodies. *Biophysical Chemistry* **197**, 40–46 (2015).
280. Ladbrooke, B. & Chapman, D. Thermal analysis of lipids, proteins and biological membranes - A review and summary of some recent studies. *Chemistry and Physics of Lipids* **3** (1969).

-
281. Nicoud, L. *et al.* Role of Cosolutes in the Aggregation Kinetics of Monoclonal Antibodies. *The Journal of Physical Chemistry B* **118**, 11921–11930 (2014).
282. Menzen, T. A. *Temperature-Induced Unfolding, Aggregation, and Interaction of Therapeutic Monoclonal Antibodies* PhD thesis (2014).
283. Wen, J., Jiang, Y. & Nahri, L. Effect of carbohydrate on thermal stability of antibodies. *American Pharmaceutical Review* **11**, 1–6 (2008).
284. Razvi, A. & Scholtz, J. M. Lessons in stability from thermophilic proteins. *Protein science: a publication of the Protein Society* **15**, 1569–78 (2006).
285. Bye, J. W. & Falconer, R. J. Three Stages of Lysozyme Thermal Stabilization by High and Medium Charge Density Anions. *The Journal of Physical Chemistry B* **118**, 4282–4286 (2014).
286. Street, T. O., Bolen, D. W. & Rose, G. D. A molecular mechanism for osmolyte-induced protein stability. *Proceedings of the National Academy of Sciences of the United States of America* **103**, 13997–4002 (2006).
287. Platts, L. & Falconer, R. J. Controlling protein stability: Mechanisms revealed using formulations of arginine, glycine and guanidinium HCl with three globular proteins. *International journal of pharmaceutics* **486**, 131–5 (2015).
288. Arakawa, T. & Timasheff, S. N. Mechanism of polyethylene glycol interaction with proteins. *Biochemistry* **24**, 6756–6762 (1985).
289. Ingham, K. C. Polyethylene glycol in aqueous solution: Solvent perturbation and gel filtration studies. *Archives of Biochemistry and Biophysics* **184**, 59–68 (1977).
290. Du, W. & Klibanov, A. M. Hydrophobic salts markedly diminish viscosity of concentrated protein solutions. *Biotechnology and Bioengineering* **108**, 632–636 (2011).
291. Wada, A. & Nakamura, H. Nature of the charge distribution in proteins. *Nature* **293**, 757–758 (1981).
292. Wang, Y. & Annunziata, O. Comparison between ProteinâPolyethylene Glycol (PEG) Interactions and the Effect of PEG on ProteinâProtein Interactions Using the LiquidâLiquid Phase Transition. *The Journal of Physical Chemistry B* **111**, 1222–1230 (2007).
293. Hussack, G. *et al.* Engineered Single-Domain Antibodies with High Protease Resistance and Thermal Stability. *PLoS ONE* **6** (2011).

-
294. Youssef, A. M. & Winter, G. A critical evaluation of microcalorimetry as a predictive tool for long term stability of liquid protein formulations: Granulocyte Colony Stimulating Factor (GCSF). *European Journal of Pharmaceutics and Biopharmaceutics* **84**, 145–155 (2013).
295. Arakawa, T. & Tsumoto, K. The effects of arginine on refolding of aggregated proteins: not facilitate refolding, but suppress aggregation. *Biochemical and biophysical research communications* **304**, 148–52 (2003).
296. Minton, A. P. Influence of macromolecular crowding upon the stability and state of association of proteins: predictions and observations. *Journal of pharmaceutical sciences* **94**, 1668–75 (08/2005).
297. Charlton, L. M. *et al.* Residue-Level Interrogation of Macromolecular Crowding Effects on Protein Stability. *Journal of the American Chemical Society* **130**, 6826–6830 (2008).
298. Hanlon, A., Larkin, M. & Reddick, R. Free-solution, label-free protein-protein interactions characterized by dynamic light scattering. *Biophysical journal* **98**, 297–304 (2010).
299. Rosenberg, E., Hepbildikler, S., Kuhne, W. & Winter, G. Ultrafiltration concentration of monoclonal antibody solutions: Development of an optimized method minimizing aggregation. *J. Membr. Sci.* **342**, 50–59 (2009).
300. Burckbuchler, V. *et al.* Rheological and syringeability properties of highly concentrated human polyclonal immunoglobulin solutions. *Eur. J. Pharm. Biopharm.* **76**, 351–356 (2010).
301. Jezek, J., Rides, M. & Derham, B. Viscosity of concentrated therapeutic protein compositions. *Advanced drug delivery ...* (2011).
302. Fritz, G., Maranzano, B., Wagner, N. & Willenbacher, N. High frequency rheology of hard sphere colloidal dispersions measured with a torsional resonator. *J. Nonnewton. Fluid Mech.* **102**, 149–156 (2002).
303. Breedveld, V. & Pine, D. J. Microrheology as a tool for high-throughput screening. *J. Mater. Sci.* **38**, 4461–4470 (2003).
304. Lazzari, S. *et al.* Colloidal stability of polymeric nanoparticles in biological fluids. *J. Nanopart. Res.* **14** (2012).
305. Valentine, M. *et al.* Colloid Surface Chemistry Critically Affects Multiple Particle Tracking Measurements of Biomaterials. *Biophys. J.* **86**, 4004–4014 (2004).

-
306. Gilroy, E. L., Hicks, M. R., Smith, D. J. & Rodger, A. Viscosity of aqueous DNA solutions determined using dynamic light scattering. *Analyst (Cambridge, U. K.)* **136**, 4159 (2011).
307. Gisler, T. & Weitz, D. A. Tracer microrheology in complex fluids. *Curr. Opin. Colloid Interface Sci.* **3**, 586–592 (1998).
308. Cassidy, O. E. *et al.* Surface modification and electrostatic charge of polystyrene particles. *Int. J. Pharm. (Amsterdam, Neth.)* **182**, 199–211 (1999).
309. Ter Veen, R., Fromell, K. & Caldwell, K. D. Shifts in polystyrene particle surface charge upon adsorption of the Pluronic F108 surfactant. *J. Colloid Interface Sci.* **288**, 124–128 (2005).
310. Stradner, A., Cardinaux, F. & Schurtenberger, P. A Small-Angle Scattering Study on Equilibrium Clusters in Lysozyme Solutions. *J. Phys. Chem. B* **110**, 21222–21231 (2006).
311. Kim, A. J., Manoharan, V. N. & Crocker, J. C. Swelling-based method for preparing stable, functionalized polymer colloids. *J. Am. Chem. Soc.* **127**, 1592–3 (2005).
312. Nance, E. A. *et al.* NIH Public Access. **4** (2013).
313. Naidu, A. S. *Natural Food Antimicrobial Systems* (ed Naidu, A.) 382 (CRC Press, 2000).
314. Blake, R. C., Shute, E. A. & Howard, G. T. Solubilization of minerals by bacteria: Electrophoretic mobility of *Thiobacillus ferrooxidans* in the presence of iron, pyrite, and sulfur. *Appl. Environ. Microbiol.* **60**, 3349–3357 (1994).
315. Winzor, D. J. Determination of the net charge (valence) of a protein: a fundamental but elusive parameter. *Anal. Biochem.* **325**, 1–20 (2004).
316. Dasgupta, B. R. *et al.* Microrheology of polyethylene oxide using diffusing wave spectroscopy and single scattering. *Phys. Rev. E: Stat., Nonlinear, Soft Matter Phys.* **65**, 051505 (2002).
317. Kulicke, W. M. & Porter, R. S. Relation between steady shear flow and dynamic rheology. *Rheol. Acta* **19**, 601–605 (1980).
318. Olmsted, J. & Williams, G. *Chemistry: The Molecular Science* 1189 (Learning, Jones & Bartlett, 1997).
319. Deryło-Marczewska, A. *et al.* Characterization of Melamine-Formaldehyde Resins by XPS, SAXS, and Sorption Techniques. *Langmuir* **18**, 7538–7543 (2002).

320. Baptista, R. P. *et al.* Activity, conformation and dynamics of cutinase adsorbed on poly(methyl methacrylate) latex particles. *J. Biotechnol.* **102**, 241–249 (2003).
321. Kirby, B. J. & Hasselbrink, E. F. Zeta potential of microfluidic substrates: 2. Data for polymers. *Electrophoresis* **25**, 203–213 (2004).
322. Falahati, H. *et al.* The zeta potential of PMMA in contact with electrolytes of various conditions: Theoretical and experimental investigation. *Electrophoresis* **35**, 870–882 (2014).
323. Ohsawa, K., Murata, M. & Ohshima, H. Zeta potential and surface charge density of polystyrene-latex; comparison with synaptic vesicle and brush border membrane vesicle. *Colloid Polym. Sci.* **264**, 1005–1009 (2005).
324. Kumar, N., Parajuli, O., Gupta, A. & Hahm, J. I. Elucidation of protein adsorption behavior on polymeric surfaces: Toward high-density, high-payload protein templates. *Langmuir* **24**, 2688–2694 (2008).
325. Broide, M. L., Tominc, T. M. & Saxowsky, M. D. Using phase transitions to investigate the effect of salts on protein interactions. *Phys. Rev. E: Stat., Nonlinear, Soft Matter Phys.* **53**, 6325–6335 (1996).
326. Beretta, S., Chirico, G. & Baldini, G. Short-Range Interactions of Globular Proteins at High Ionic Strengths. *Macromolecules* **33**, 8663–8670 (2000).
327. Rosenberg, M. Bacterial adherence to polystyrene: a replica method of screening for bacterial hydrophobicity. *Appl. Environ. Microbiol.* **42**, 375–377 (1981).
328. Onwu, F. K. & Ogah, S. Adsorption of lysozyme unto silica and polystyrene surfaces in aqueous medium. *Afr. J. Biotechnol.* **10**, 3014–3021 (2011).
329. Miriani, M. *et al.* Unfolding of beta-lactoglobulin on the surface of polystyrene nanoparticles: Experimental and computational approaches. *Proteins: Struct., Funct., Bioinf.* **82**, 1272–1282 (2014).
330. Ochoa, N. Effect of hydrophilicity on fouling of an emulsified oil wastewater with PVDF/PMMA membranes. *J. Membr. Sci.* **226**, 203–211 (2003).
331. Feldman, K., Tervoort, T., Smith, P. & Spencer, N. D. Toward a Force Spectroscopy of Polymer Surfaces. *Langmuir* **14**, 372–378 (1998).
332. Duong-Ly, K. C. & Gabelli, S. B. Salting out of proteins using ammonium sulfate precipitation. *Methods Enzymol.* **541**, 85–94 (2014).
333. Shih, Y. C., Prausnitz, J. M. & Blanch, H. W. Some characteristics of protein precipitation by salts. *Biotechnol. Bioeng.* **40**, 1155–1164 (1992).

Abbreviations

2D	two-dimensional
3D	three-dimensional
ACF	autocorrelation function
CEX	cation exchange chromatography
Cherry-GST	Glutathione-S-Transferase fused with the Cherry-Tag technology TM
CytC	Cytochrome C
DNA	Deoxyribonucleic acid
DLVO	theory named after Derjaguin, Landau, Verwey and Overbeek
DWP	deep well plate
DWS	diffusive wave spectroscopy
G-CSF	Granulocyte colony-stimulating factor
GST	Glutathion-S-Transferase
HTE	high throughput experimentation
ICH	International Council for Harmonisation
IgG1	subclass of Immunoglobulin G
LHS	liquid handling station
mAb	monoclonal antibody
MC	Monte Carlo
MD	molecular dynamics
μ F	microfluidic
MSD	mean square displacement
MTP	microtiter plate
OD	optical density
PAV	Piezo Axial Vibrator
PEG	polyethylene glycol

pH	potential of hydrogen
pI	pH value where the protein surface net charge is 0
PMMA	Poly(methyl methacrylate)
QSAR	quantitative structure activity relationship
RNA	Ribonucleic acid
SEC	size exclusion chromatography
UV	ultraviolet

Parameter

B_{22}	second virial coefficient
η	solution viscosity
G'	storage modulus
G''	loss modulus
T_{agg}	aggregation temperature
T_m	melting temperature
ω_{CO}	crossover point frequency of G' and G''
ζ -potential	zeta-potential

Curriculum Vitae

Curriculum Vitae

Marie-Therese Schermeyer

Education

- 07/2013–present **PhD**, Karlsruhe Institute of Technology (KIT), Institute of Engineering in Life Sciences (IBLT), Section IV: Biomolecular Separation Engineering (MAB), Characterization and Prediction of Protein Solution Stability by Rheological Methods.
Karlsruhe, Germany
- 11/2007–04/2013 **Study of Bioprocess Engineering**, KIT, Final Degree: Diploma in Bioprocess Engineering, special subjects: Bioprocess Technology and Purification and Mechanical Process Engineering.
Karlsruhe, Germany
- 09/2003–03/2007 **Carpentry Apprenticeship**, Gymnasium Kloster Wald, Journeyman Carpenter.
Wald, Germany
- 09/1997–06/2006 **Grammar School**, Gymnasium Kloster Wald, Final Degree: Abitur.
Wald, Germany

Practical Experience

- 11/2012–04/2013 **Student Research Project**, KIT, IBLT, Section IV: MAB, Diploma Thesis - Investigations on the binding orientation of model proteins on Mixed-Mode chromatography adsorbers..
Karlsruhe, Germany
- 12/2011–05/2012 **Student Research Project**, BASF & KIT, Institute of Product Engineering, Adaption of an institution's internal product development tool (iPEM) to the biotech industry.
Karlsruhe, Germany
- 10/2010–04/2011 **Co-op**, Genentech, Study on the influence of cell culture conditions and antibody composition on host cell protein purification during proA affinity chromatography.
San Francisco, USA
- 04/2010–08/2010 **Research Assistant**, KIT, IBLT, Section IV: MAB, Method development for the characterization of protein interactions in solution..
Karlsruhe, Germany
- 10/2008–04/2010 **Research Assistant**, KIT, Institute of Product Engineering, Development and Innovation Management.
Karlsruhe, Germany

✉ marie-therese.schermeyer@kit.edu

03/2007–04/2007 **Intern**, Hug Engineering, Development of catalyst coatings.
Winterthur, Switzerland

Publications

Articles **Characterization of highly concentrated antibody solution - A toolbox for the description of long-term solution stability**, Marie-Therese Schermeyer, Anna K. Wöll, Bas Kokke, Michel Eppink and Jürgen Hubbuch, *mAbs*, (2017): accepted.

Prediction and characterization of the stability enhancing effect of the Cherry-TagTM in highly concentrated protein solutions by complex rheological measurements and MD simulations, Pascal Baumann¹, Marie-Therese Schermeyer¹, Hannah Burghardt, Cathrin Dürr, Jonas Gärtner and Jürgen Hubbuch, *International Journal of Pharmaceutics*, (2017): submitted manuscript.

¹ contributed equally to this work.

Implementation of an analytical microfluidic device for the quantification of protein concentrations in a high-throughput format, Carsten Philipp Radtke¹, Marie-Therese Schermeyer¹, Yün Claudia Zhai, Jacqueline Göpper and Jürgen Hubbuch, *Engineering in Life Sciences*, 16 (2016): 515-524.

¹ contributed equally to this work.

Concentration-dependent changes in apparent diffusion coefficients as indicator for colloidal stability of protein solutions, Katharina C. Bauer, Matthias Göbel, Marie-Luise Schwab, Marie-Therese Schermeyer and Jürgen Hubbuch, *International Journal of Pharmaceutics*, 511 (2016): 276-287.

Impact of polymer surface characteristics on the microrheological measurement quality of protein solutions – a tracer particle screening, Katharina C. Bauer¹, Marie-Therese Schermeyer¹, Jonathan Seidel and Jürgen Hubbuch, *International Journal of Pharmaceutics*, 505 (2016): 246-254.

¹ contributed equally to this work.

Squeeze flow rheometry as a novel tool for the characterization of highly concentrated protein solutions, Marie-Therese Schermeyer, Heike Sigloch, Katharina C. Bauer, Claude Oelschlaeger and Jürgen Hubbuch, *Biotechnology and Bioengineering*, 113 (2016): 576-587.

Talks **Toolbox of experimental and *in silico* methods to predict protein long-term stability**, Marie-Therese Schermeyer, Pascal Baumann and Jürgen Hubbuch, 252nd American Chemical Society National Meeting & Exposition (ACS), San Francisco, USA, April 2017.

Characterization of highly concentrated mAb solution, Marie-Therese Schermeyer, Anna K. Wöll, Bas Kokke and Jürgen Hubbuch, *International Symposium on the Separation of Proteins, Peptides and Polynucleotides (ISPPP)*, Salzburg, Austria, November 2016.

Correlation of complex rheology with protein phase behavior - One step towards the predictability of protein long term stability, Marie-Therese Schermeyer, Katharina C. Bauer, Anna K. Wöll, Kristina Schleining and Jürgen Hubbuch, Industry lecture at Merck MSD Sharp & Dohme GmbH (Kenilworth, USA), Pfizer (Andover, USA) and Biogen (Boston, USA), July-August 2016.

Impact of polymer protein interactions on the quality of microrheological measurements, Marie-Therese Schermeyer, Katharina C. Bauer, Jonathan Seidel and Jürgen Hubbuch, PARTEC International Conference on Particle Technology, Nürnberg, Germany, April 2016.

Characterization of highly concentrated mAb solution – One step towards the prediction of long-term stability, Marie-Therese Schermeyer, Anna K. Wöll, Bas Kokke and Jürgen Hubbuch, 251st American Chemical Society National Meeting & Exposition (ACS), San Diego, USA, March 2016.

Characterization and Prediction of Protein Phase Behavior by means of Squeeze Flow Rheometry, Marie-Therese Schermeyer, Katharina C. Bauer, Marie-Luise Schwab, Stefan Oelmeier and Jürgen Hubbuch, Biological and Pharmaceutical Complex Fluids II: Novel Trends in Characterizing Interactions, Microstructure and Rheology, Durham, USA. July 2014.

Predictive Approaches for Protein Phase Behavior, Sven Amrhein¹, Katharina C. Bauer¹, Lara Galm¹, Marie-Therese Schermeyer¹ and Jürgen Hubbuch, Recovery of Biological Products Conference XVI, Rostock, Germany. July 2014.

¹ contributed equally to this work.

Posters **Squeeze Flow Rheometry as a Predicting Tool – Correlation of rheological key parameters with protein phase behavior**, Marie-Therese Schermeyer, Anna K. Wöll, Bas Kokke and Jürgen Hubbuch, 3rd European Congress of Applied Biotechnology (ECAB 3), Nizze, France. October 2015.

Formulation Studies on Cherry-Tagged Proteins (ISPPP Poster Award), Marie-Therese Schermeyer, Pascal Baumann, Hannah Burghardt and Jürgen Hubbuch, International Symposium on the Separation of Proteins, Peptides and Polynucleotides (ISPPP), Würzburg, Germany. November 2014.